NASA Conference Publication 10195

1996 Coolant Flow Management Workshop

Proceedings of a conference held at the
Ohio Aerospace Institute
NASA Lewis Research Center
Cleveland, Ohio
December 12–13, 1996

NASA Conference Publication 10195

1996 Coolant Flow Management Workshop

Proceedings of the conference
held at the Ohio Aerospace Institute
cosponsored by NASA Lewis Research Center
and the Ohio Aerospace Institute
Cleveland, Ohio
December 12–13, 1996

National Aeronautics and
Space Administration

Office of Management

**Scientific and Technical
Information Program**

1997

PREFACE

The following compilation of documents includes a list of the 66 attendees, a copy of the viewgraphs presented, and a summary of the discussions held after each session at the 1996 Coolant Flow Management Workshop held at the Ohio Aerospace Institute, adjacent to the NASA Lewis Research Center, Cleveland, Ohio on December 12-13, 1996. The workshop was organized by H. Joseph Gladden and Steven A. Hippensteele of NASA Lewis Research Center. Participants in this workshop included Coolant Flow Management team members from the NASA Lewis, their support service contractors, the turbine engine companies, and the universities.

The NASA Lewis Coolant Flow Management Team began their process in response to the 1993 Turbomachinery Peer Review committee suggestion and after visiting several aircraft engine manufacturers and discussing what was of interest to industry (ref. NASA TM 107161, "Research Strategy for Modeling the Complexities of Turbine Heat Transfer" by Robert J. Simoneau, March, 1996). Three areas of turbine study developed: (1) details of the internal passages, (2) computational film cooling capabilities, and (3) the effects of heat transfer on both sides. Several research projects, contracts, and grants have resulted. Also mentioned in this reference, this workshop was planned to keep the team focused and to assess the progress of the work.

The purpose of the workshop was to assemble the team members, along with others who work in gas turbine cooling research, to discuss needed research and recommend approaches that can be incorporated into the Center's Coolant Flow Management Program. The workshop was divided into three sessions: (I) Internal Coolant Passage Presentations, (II) Film Cooling Presentations, and (III) Coolant Flow Integration & Optimization. Following each session there was a group discussion period.

Steven A. Hippensteele
Workshop Organizer and Editor

TABLE OF CONTENTS

Session III. Coolant Flow Integration & Optimization

*Presented at the conference by Yong Kim, AlliedSignal Aerospace.
†Presented at the conference by Joe Gladden, NASA Lewis Research Center.

COOLANT FLOW MANAGEMENT WORKSHOP

Thursday 12 December 1996

8:00 Welcome and Opening Remarks — Larry Diehl

8:05 Introductory Remarks — Louis Povinelli

8:15 Overview — Joe Gladden

8:30 Session I: Internal Coolant Passage Heat Transfer

1:10 Session II: Film Cooling Heat Transfer

Friday 13 December 1996

8:30 Session III: Integration & Optimization

Overview

1996 COOLANT FLOW MANAGEMENT WORKSHOP

Joe Gladden
NASA Lewis Research Center

Welcome to the first annual Coolant Flow Management Workshop. The purpose of the workshop is to review the status of work accomplished to date on a number of research efforts and to assess the planned work effort. The coolant flow management program is a response to the 1993 Turbomachinery Peer Review committee suggestion that LeRC pursue coupling of the internal coolant passage flow and heat transfer with the external gas path of the high pressure turbine through the blade/vane film cooling holes.

This program evolved through a series of meetings with designers and heat transfer researchers in industry in 1994 and 1995. Modeling, turbulence models, validation data and grid generation were identified as topics that needed to be addressed for both internal passage heat transfer and film cooling. In addition, the capability to integrate the internal and external heat transfer solutions and optimize the results was identified as a long term goal.

The workshop will cover three discreet topics: Internal Coolant Passage Heat Transfer, Film Cooling Heat Transfer, and Coolant Flow Integration and Optimization. Each session will present a combination of analytical and experimental research and will present both current results and future plans. There will be a group discussion at the end of each session for clarification of the material presented and to assess the needs for future research.

NASA LeRC is developing robust multi-block schemes and multi-block merging techniques to improve the accuracy of the computation of heat transfer in serpentine passages while decreasing the time required to generate computational models. Turbulence models are also being assessed. Prof. Lau (Texas A & M) has been experimentally studying serpentine passage geometry with turbulence generating ribs at LeRC to provide validation data. This geometry will be modified to include bleed effects representing film cooling holes. Mr. Wagner (PE/UTRC) and Dr. Tse (SRA) have experimentally studied heat transfer in rotating serpentine passages.

A similar effort is underway on external film cooling with the same emphasis on understanding the flow field around the film cooling hole and its effect on film effectiveness. Dr. Garg (LeRC/AYT) has developed computational techniques to compute the film cooling effects over the entire airfoil surface starting at the hole exit plane. Prof. Simon (U of Minn.) and Prof. Acharya (LSU) are studying the fundamental flow phenomena around the entrance to the film cooling holes to improve turbulence modeling. Dr. Ames (Allison) has just completed an experimental film cooling study using a cascade of airfoils in a high turbulence flow field.

The ability to couple and optimize the internal coolant flow and the external film cooling for turbine airfoils is the goal. Research is underway at Arizona State University, AlliedSignal Engine Co., Ohio State University, General Electric and Penn State University to accomplish this goal. These programs are designed to incorporate the best computational tools and methodologies available and to provide validation data.

You will be hearing about progress toward these goals during the next day and a half.

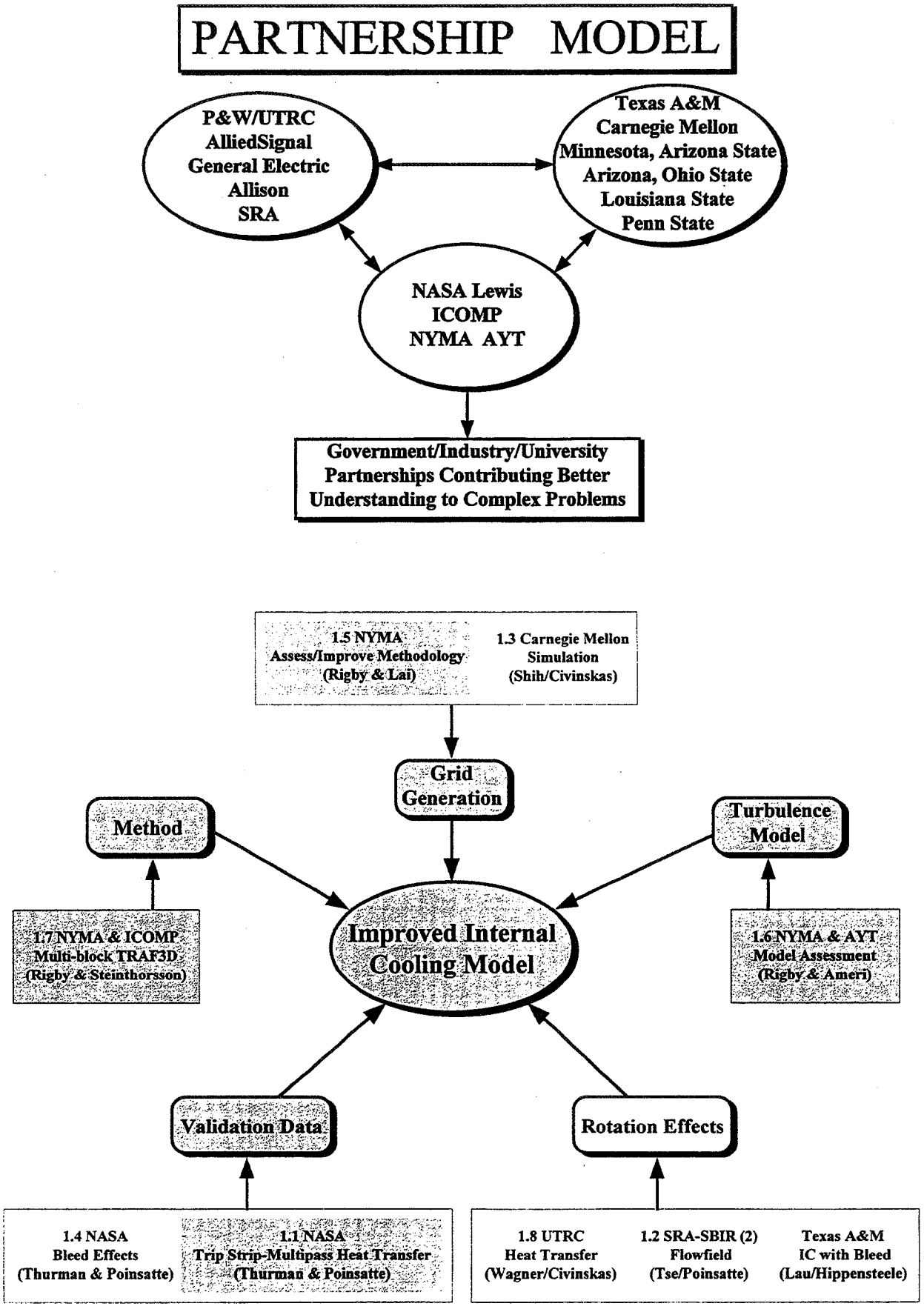
PARTNERSHIP MODEL
P&W/UTRC
AlliedSignal
General Electric
Allison
SRA
Texas A&M
Carnegie Mellon
Minnesota, Arizona State
Arizona, Ohio State
Louisiana State
Penn State
NASA Lewis
ICOMP
NYMA AYT
Government/Industry/University
Partnerships Contributing Better
Understanding to Complex Problems
1.5 NYMA
Assess/Improve Methodology
(Rigby & Lai)
1.3 Carnegie Mellon
Simulation
(Shih/Civinskas)
Grid
Generation
Method
Turbulence
Model
1.7 NYMA & ICOMP
Multi-block TRAF3D
(Rigby & Steinthorsson)
Improved Internal
Cooling Model
1.6 NYMA & AYT
Model Assessment
(Rigby & Ameri)
Validation Data
Rotation Effects
1.4 NASA
Bleed Effects
(Thurman & Poinsatte)
1.1 NASA
Trip Strip-Multipass Heat Transfer
(Thurman & Poinsatte)
1.8 UTRC
Heat Transfer
(Wagner/Civinskas)
1.2 SRA-SBIR (2)
Flowfield
(Tse/Poinsatte)
Texas A&M
IC with Bleed
(Lau/Hippensteele)

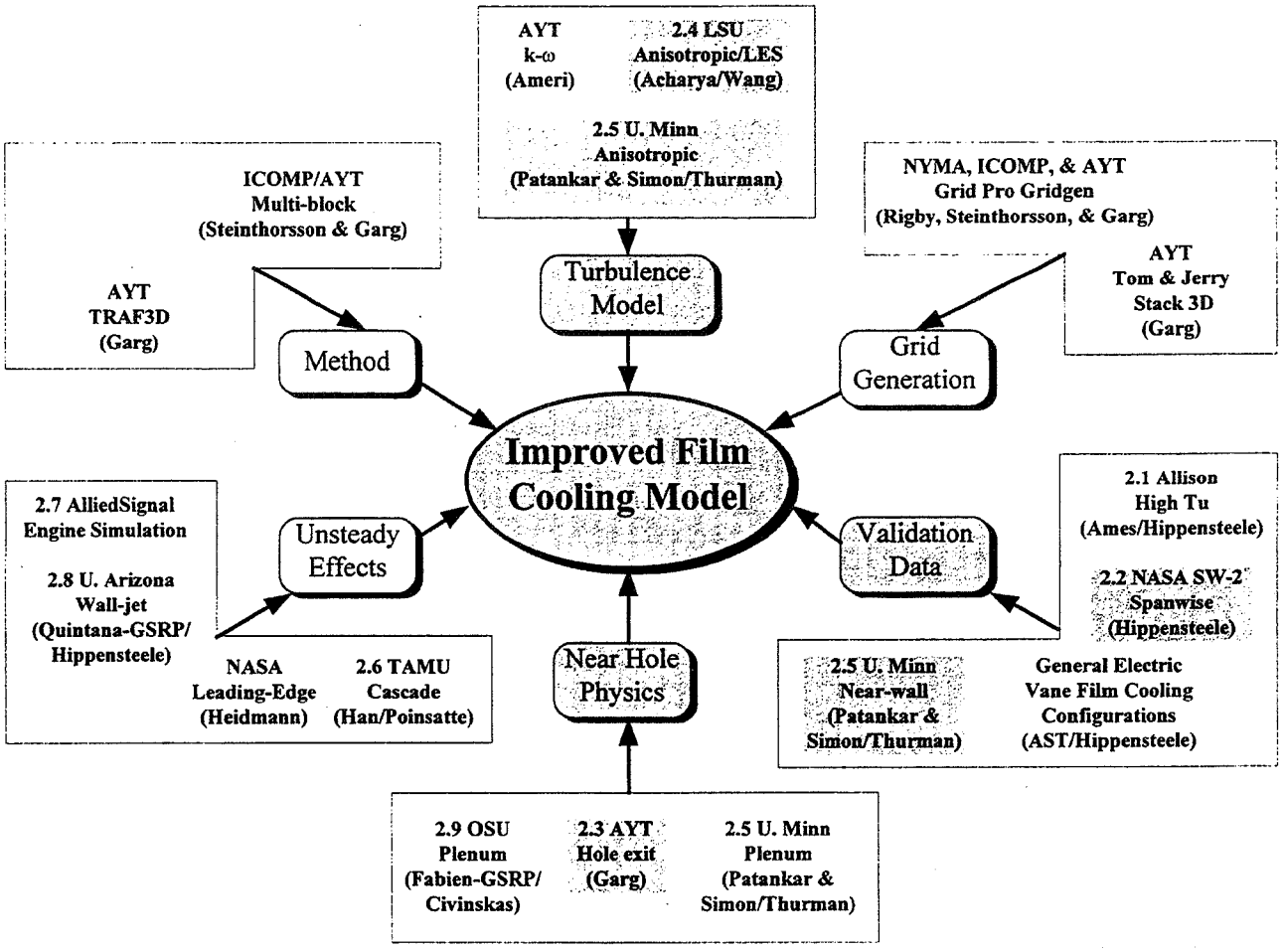
AYT
k-ω
(Ameri)
2.4 LSU
Anisotropic/LES
(Acharya/Wang)
2.5 U. Minn
Anisotropic
(Patankar & Simon/Thurman)
Turbulence Model
ICOMP/AYT
Multi-block
(Steinthorsson & Garg)
AYT
TRAF3D
(Garg)
Method
NYMA, ICOMP, & AYT
Grid Pro Gridgen
(Rigby, Steinthorsson, & Garg)
AYT
Tom & Jerry
Stack 3D
(Garg)
Grid Generation
Improved Film Cooling Model
2.7 AlliedSignal
Engine Simulation
2.8 U. Arizona
Wall-jet
(Quintana-GSRP/
Hippensteele)
Unsteady Effects
NASA
Leading-Edge
(Heidmann)
2.6 TAMU
Cascade
(Han/Poinsatte)
2.1 Allison
High Tu
(Ames/Hippensteele)
2.2 NASA SW-2
Spanwise
(Hippensteele)
Validation Data
2.5 U. Minn
Near-wall
(Patankar &
Simon/Thurman)
General Electric
Vane Film Cooling
Configurations
(AST/Hippensteele)
Near Hole Physics
2.9 OSU
Plenum
(Fabien-GSRP/
Civinskas)
2.3 AYT
Hole exit
(Garg)
2.5 U. Minn
Plenum
(Patankar &
Simon/Thurman)

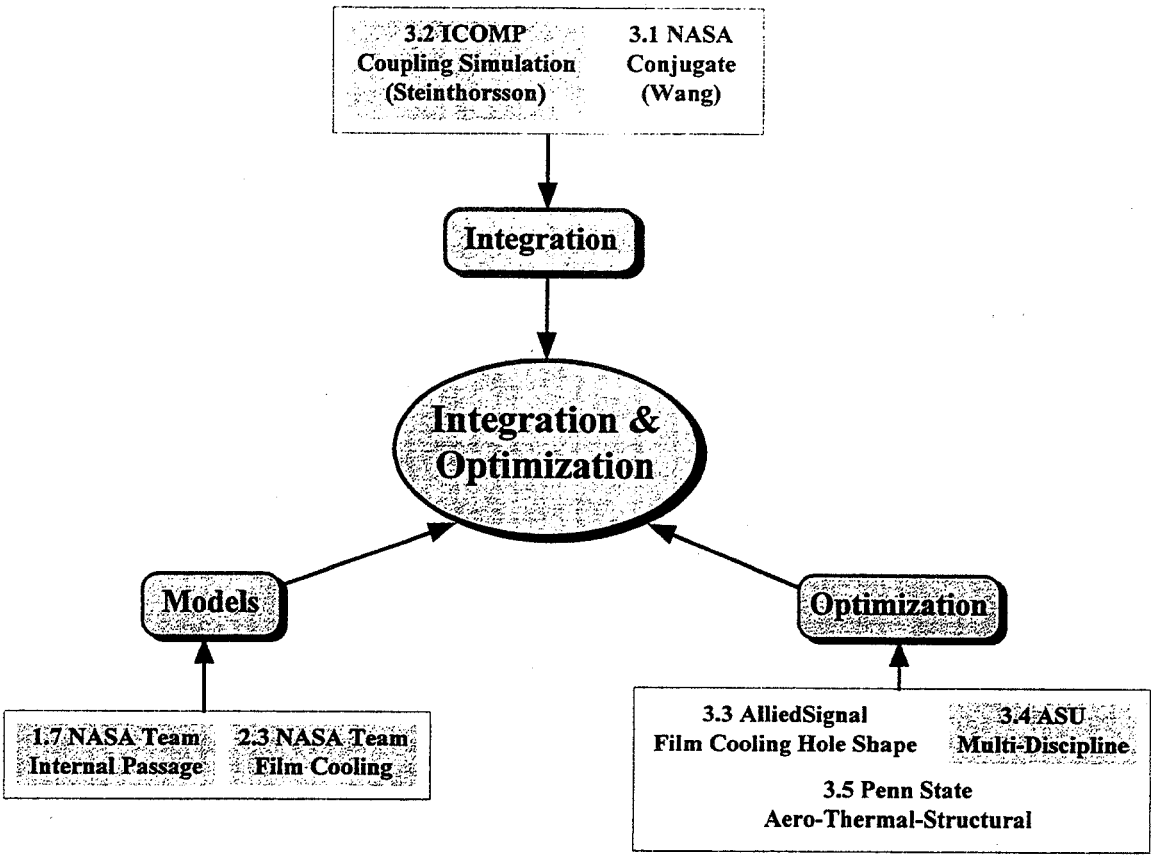
3.2 ICOMP
Coupling Simulation
(Steinthorsson)
3.1 NASA
Conjugate
(Wang)
Integration
Integration &
Optimization
Models
Optimization
1.7 NASA Team
Internal Passage
2.3 NASA Team
Film Cooling
3.3 AlliedSignal
Film Cooling Hole Shape
3.4 ASU
Multi-Discipline
3.5 Penn State
Aero-Thermal-Structural

GOAL STATEMENT

Provide an integrated enabling technology base of understanding and tools useful to making design decisions for the management of turbine coolant flow.

References:

"The review team strongly feels that NASA should have a leadership role in multi-disciplinary analysis methods. Two specific examples ... (ii) system that couples the internal cooling system through the film cooling holes to the external aerodynamics.

- Turbomachinery Peer Review Report, Sept 22, 1993
- Industrial Contacts, 1994 & 1995
- SAE Aerospace Atlantic Conference, 1996

NASA / INDUSTRY IDENTIFIED NEEDS

Internal Passage Cooling:

- Modeling - wall function, NS technique
- Turbulence - wall independent
- Validation Data - with & w/o bleed
- Grid Generation - Multi-block
- Rotation Effects -

Film-Cooling:

- Methodology - code type, near-wall model
- Turbulence Model - anisotropic, k-ω
- Validation Data - near-wall, LES, spanwise effect, high Tu
- Unsteady Effects - leading edge, wall jet, cascade
- Boundary Conditions - plenum effect, hole exit, conjugate problem
- Grid Generation - Gridgen

Coolant Flow Integration & Optimization:

- Integration Modeling - Conjugate, NS technique
- Optimization Modeling - MDO, hole/location optimization
- Film-Cooling & Internal Passage Models

RESOURCES

MILESTONES - Thru FY 1998/99

Effects of Bleed Experimentally Demonstrated on Internal Passage Heat Transfer and Coupling Effects on Film Cooling

Advanced Film Cooling Model Demonstrated in a Navier-Stokes Code

Demonstrated Capability to Predict Internal Passage Heat Transfer

Provide CFD Based Integration-Optimization Methodologies for Airfoil Coolant Flow

RESOURCES

Item FY	1994	1995	1996	1997	1998	1999	Total
In-House	$300K	$600K	$485K	$445K	$460K	$475K	$2,765K
Grants	40K	238K	238K	303K	97K	93K	1,009K
Contracts	203K	260K	180K	459K	516K	183K	1,801K
Total	$543K	$1,098K	$903K	$1,207K	$1,073K	$751K	$5,575K

Overview
Session I: Internal Coolant Passage Heat Transfer

8:30 On the Use of Structured Multi-Block Grids for Internal Coolant Flow Calculations — David Rigby, NYMA

8:50 Numerical Simulation of Turbine Blade Cooling — Tom Shih, CMU

9:10 Flow in Serpentine Coolant Passages with Trip Strips — David Tse, SRA

9:30 Experimental Heat Transfer in Turn Regions of Rotating Coolant Passages — Joel Wagner, UTRC

9:50 Experimental Multipass Heat Transfer with Trips & Bleed — Douglas Thurman, LeRC

10:10 Rotating Multipass Coolant Passages with Bleed — Sai Lau, Texas A&M

Break

10:50 Group Discussion

HEAT TRANSFER PREDICTION IN INTERNAL COOLANT CHANNELS

David Rigby, NYMA, Inc.

Objective

- Improve heat transfer prediction capability in internal coolant passages.
- Advance technology in this area to bring higher fidelity prediction into the design stage.

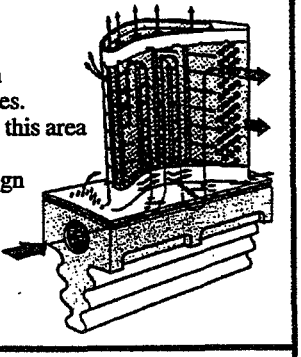

Approach

- Multi-block approach currently being investigated.
- Multi-block grid generation currently able to handle complex geometries.
- Structured flow solver maximizes computational efficiency
- Wilcox k-ω turbulence model which does not require a reference to the distance from a wall is used.

Results

- Flow in a channel with both ribs and bleed holes has been completed.
- Comparison of numerical heat transfer results to experimental data is good.

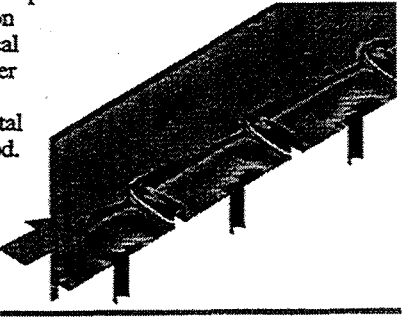

Future

- Additional turbulence models will be investigated.
- Progressively more complex geometries will be attempted.
- Rotation effects will also be studied.
- Grid generation and turbulence modeling remain the largest obstacles, followed by computational requirements.

Numerical Simulation of Turbine Blade Cooling

Tom I-P. Shih, Mark A. Stephens, and Yu-Liang Lin
Department of Mechanical Engineering, Carnegie Mellon University

OBJECTIVE

- Develop, adapt, and validate CFD codes for studying internal and film cooling of turbine blades.
- Apply validated CFD codes to obtain understanding of fluid mechanics and heat transfer processes relevant to internal and film cooling and how they are affected by design and operating parameters.
- Develop design strategies for more effective cooling based on understanding of basic flow physics.

APPROACH

- Internal coolant passages are currently modeled as two straight ducts with and without ribs connected by a tightly wound 180° bend under rotating and non-rotating conditions.
- Film cooling is modelled by a semi-cylindrical leading edge with a flat afterbody with rows of compound-angle holes drilled through it. Computations resolve flow over leading edge and afterbody as well as flow in film-cooling holes and the internal coolant passage from which the cooling flow emerges.
- Formulation is the ensemble-averaged conservation equations of mass, momentum (full compressible Navier-Stokes), and total energy closed by a "low-Reynolds number" k-ω model. Wall functions are not used!
- Grid systems are multi-block structured grids – perfectly patched, arbitrarily patched, and overlapped.
- Numerical method of solution utilizes flux-difference splitting of Roe with limiters for inviscid flux vectors, central for viscous vectors, and a diagonalized ADI scheme with multigrid for relaxation to steady state.
- Codes used are CFL3D, MAGGIE, and RONNIE.
- Validation is based on comparison with available experimental data.

RESULTS

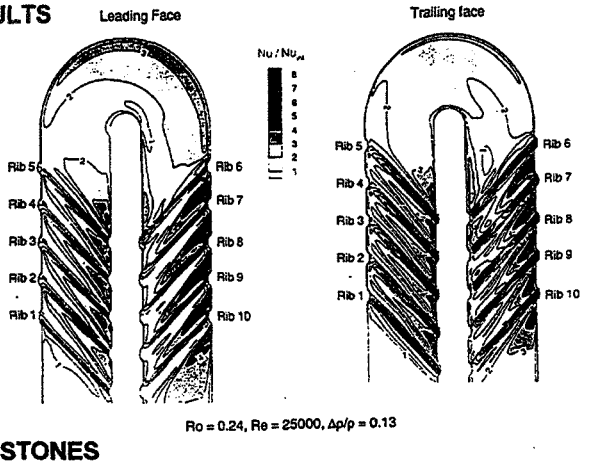

Ro = 0.24, Re = 25000, Δp/p = 0.13

MILESTONES

- Showed that for a given Reynolds and Rotation number, an infinite number of angular speeds are possible. To fix the angular speed, must specify Mach number as well.
- Showed angular speed to have significant effects on pressure and density variations along an internal coolant passage. Actual angular speeds must be simulated in order to capture centrifugal buoyancy correctly.
- Showed how flow separation induced by centrifugal buoyancy causes the formation of additional vortical structures beyond the traditional two from Coriolis force.
- Studied how secondary flows induced by Coriolis force, centrifugal buoyancy, 180° bend, and ribs affect each other and the heat transfer characteristics.
- Studied leading-edge film cooling with injection through staggered rows of compound-angle discrete holes.

Flow in Serpentine Coolant Passages with Skewed Trips.

David Tse, Scientific Research Assoc., Inc.

OBJECTIVES

- Measure, assess and analyze the flow in serpentine coolant passages having skewed trips.
- Perform computational studies on the influence of Coriolis and buoyancy effects on the flow characteristics and heat transfer.
- Analyze the velocity data in relation to the heat transfer measurements of Johnson, et al (1994).
- Examine the influence of trip orientation on the flow characteristics and the heat transfer.

APPROACH

Experimental - (SRA)

- Three components of velocity were obtained under stationary and rotating conditions by laser velocimetry with the aid of refractive-index-matching (RIM).

Computational - (P&W)

- The flow characteristics and heat transfer were examined using periodically fully-developed "conveyor-belt" boundary conditions.
- Boundary conditions at the exit of the computational domain were used to create the inlet conditions.

RESULTS

- Skewed trips generate strong secondary flows and induce considerable streamwise development of the primary flow.
- Rotation and skewed trips produce a swirling vortex and a corner recirculation zone in the straight passage.
- Trips skewed at -45° in the outward flow passage and trips skewed at +45° in the inward flow passage maximize heat transfer.
- The velocity measurements explain the heat transfer phenomena reported in Johnson, et al (1994).

MILESTONES

- RIM and laser velocimetry can produce highly detailed maps of flow field in a serpentine coolant passage.
- RIM requires an isothermal flow field and can not include buoyancy forces. However, it does quantify the effect of the interacting Coriolis and trip driven secondary flows.
- The overall agreement between the velocity data and CFD calculations is very good.
- Flow, temperature and pressure fields can be assumed to be periodic over a streamwise repeating geometric pattern in a ribbed-wall passage.

HEAT TRANSFER IN TURNS, LET - Task 30

Joel Wagner, United Technologies Research Center

Objective:	Results:
Experimentally measure, assess, and analyze the heat transfer within the internal cooling configuration of a serpentine coolant passage for comparison with CFD and numerical heat transfer prediction codes.	Thermocouple results show significant increases in heat transfer in the tip and root turn regions. Liquid crystal results show variation in heat transfer distribution in turns due to flow and thermal conditions.
Approach:	Milestones:
Conduct experiments using rotating models employing previously developed measurement techniques, including a transient heat transfer technique and liquid crystals to determine the heat transfer distribution throughout the model coolant passage.	•Design and Fabrication •H(0.5) Model Tests •H(2.0) Model Tests •Turn Model Tests •Analysis and Final Report

Experimental Multipass Heat Transfer with Trips and Bleed

Doug Thurman, Phil Poinsatte, NASA

Objectives: *To obtain simple geometry surface heat transfer data for internal channels with trips and bleed for use in validating models*	Facility: *SW-6*
Approach: *Transient liquid crystal technique*	Milestones: *Rib data, turn data, bleed data*

LOCAL HEAT TRANSFER DISTRIBUTIONS IN ROTATING MULTIPASS CHANNELS WITH BLEED

Sai Lou, Texas A & M University

OBJECTIVES:

Make detailed local experimental measurements with rotating multipass channel models

- to enhance understanding of effects of rotation, sharp turns channel geometry, and rib turbulators.
- to help improve the design of these cooling passages.

APPROACH:

- Naphtalene sublimation experiments in rotating multipass channels.

FACILITY/RESULTS:

The facility consists of a rotational test rig, and open flow loop and mass transfer measurement equipment. The results include normalized Nusselt and Sherwood number distributions.

MILESTONES:

- 10/99 Complete experiments with two-pass and three-pass channels to determine effect of coolant bleed.

Overview
Session II: Film Cooling Heat Transfer

1:10 Film Cooling with Anisotropic Diffusion and Hole Entry Effects: Experiments and Computations — Terry Simon, U of Minn

1:30 Large Eddy Simulation and Improved Turbulence Modeling of Film Cooling — Sumanta Acharya, LSU

1:50 Heat Transfer in Film-Cooled Turbine Blades — Vijay Garg, AYT

2:10 Effect of Tabs on a Jet in Cross Flow — Khairul Zaman, LeRC

2:30 Film Cooling Heat Transfer Measurements Using Liquid Crystals — Steve Hippensteele, LeRC

2:50 Turbine Vane Heat Transfer, Film Cooling, and Turbulence Experiments — Forrest Ames, Allison Engine Co

3:10 Break

3:30 Investigation of Rotor Wake Effects on Film Cooling — Jim Heidmann, LeRC

4:10 Unsteady High Tu Effects on Turbine Blade Film Cooling Heat Transfer Using Liquid Crystals — J. C. Han, Texas A & M

4:30 Group Discussion

5:30 Social

6:30 Dinner

FILM COOLING LATERAL DIFFUSION AND HOLE ENTRY EFFECTS

Terry Simon, University of Minnesota

OBJECTIVES:

To support the continued improvement of film cooling modeling and design by better describing the effects on film cooling performance of (1) anisotropic eddy transport in the mixing zone where freestream flow and film cooling flow interact and (2) the geometry of the plenum from which the film cooling flow enters the holes. The former will lead to more accurate computation of design models and the latter will aid in the assessment of film cooling data in the literature and will assist in the selection of supply plenum geometric features. Since detailed measurements are taken within the flowfield and on the film-cooled surface, the study lends a valuable glimpse into the physics of this complex flow.

APPROACH:

Experiments are conducted which simulate many features of the actual film cooling flow situation. In these tests, the freestream turbulence intensity and scale are simulated, as are the hole and supply plenum geometries. Measurements are with high-resolution traversing of fine thermocouple and hot-wire probes throughout the flowfield. Film cooling effectiveness values are found by traversing the thermocouple probe from the freestream down into the near-wall adiabatic zone to first measure the freestream temperature, then to deduce the adiabatic wall temperature. Computation is with the finite-volume numerical model with k-ε turbulence closure modeling.

FACILITIES:

The facility is a flat plate with a single row of 35°, streamwise-oriented, round film cooling holes spaced laterally at 3D and of 2.3D long. The delivery flow issues from an unheated combustor simulator section. The film cooling flow can be heated slightly for film cooling effectiveness measurements.

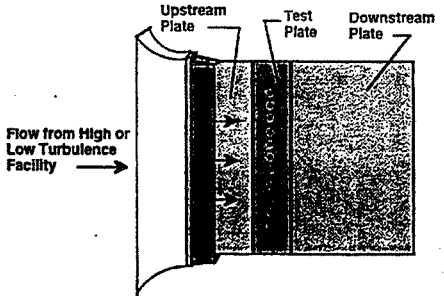

MILESTONES:

In HTD-Vol. 327, measurements are presented of the lateral and wall-normal, turbulent eddy diffusivities. These are used to compute the anisotropy ratio, $\varepsilon_{m,z} \div \varepsilon_{m,y}$. In 96-WA/HT-7, measurements of streamwise velocity are presented to show the effects on the flowfield in the interaction zone of hole length, freestream turbulence level, and blowing ratio. In 96-WA/HT-8, computational results were presented to show the effect of plenum geometry on film cooling performance. In a paper submitted to the 97-IGTC, measurements are presented which show the effects on the flow in the interaction zone of the means by which the flow to the film cooling holes is channeled to the supply plenum. Presently, measurements are being taken with laterally-oriented holes and a test plate has been fabricated for compound-angle injection. Upcoming plans include the evaluation of performance with shaped holes and we are preparing to take heat transfer coefficient data.

TIME- AND SPACE- ACCURATE SIMULATIONS OF A FILM-COOLING JET FLOW

Sumanta Acharya
Louisiana State University

OBJECTIVES

- To perform Direct Numerical Simulations (DNS) and Large Eddy Simulations for a Film Cooling Jet Flow to better understand the large scale dynamics, their effects on surface heat transfer and to guide model development.

APPROACH

- Higher order finite-differences for DNS code
- Smagorinsky and Dynamic sub-grid scale stress models
- Non-linear and other improved turbulence models

RESULTS

- Time-and space-accurate simulations reveal the important flow structures

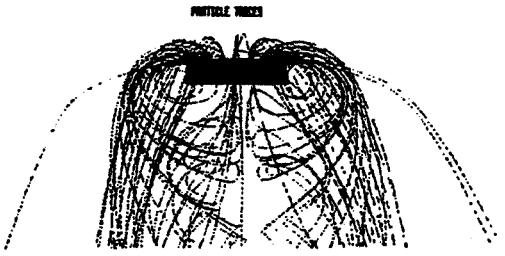

MILESTONES

- Codes developed for DNS, LES and RANS simulations
- DNS code can handle multi-block domains and curvilinear grids
- Film cooling flow and heat transfer simulations ongoing

HEAT TRANSFER IN FILM-COOLED TURBINE BLADES

Vijay Garg, AYT Corp.

OBJECTIVE

- TO DEVELOP TOOLS & MODELS TO ACCURATELY PREDICT HOT GAS SIDE HEAT TRANSFER TO A FILM-COOLED TURBINE BLADE
- TO MINIMIZE THE INJECTED MASS FLOW FOR A GIVEN COOLING EFFICIENCY
- TO DECREASE AERODYNAMIC LOSSES INDUCED BY THE JET-SECONDARY FLOW INTERACTION

APPROACH

- 3-D COMPRESSIBLE NAVIER-STOKES EQUATIONS
- VARIOUS TURBULENCE MODELS (Baldwin-Lomax with Mayle's transition criterion, k-ε, q-ω, k-ω); ($y^+ < 1$ near walls)
- EXIT AREA OF EACH HOLE DISTRIBUTED OVER SEVERAL CONTROL VOLUMES
- DIFFERENT VELOCITY & TEMPERATURE PROFILES SPECIFIED AT THE HOLE EXIT
- MULTI-GRID, CELL-CENTERED FINITE VOLUME CODE WITH FOUR-STAGE RUNGE-KUTTA TIME STEPPING SCHEME, 3-D EIGENVALUE SCALING OF ARTIFICIAL DISSIPATION & RESIDUAL SMOOTHING

RESULTS

- LARGE CHANGE IN HEAT TRANSFER COEFFICIENT AT THE BLADE SURFACE CAUSED BY DIFFERENT VELOCITY & TEMPERATURE PROFILES AT THE HOLE EXIT
- DIFEFRENT EFFECTS OBSERVED ON THE SUCTION AND PRESSURE SURFACE DEPENDING UPON THE BLADE & HOLE SHAPE AND HOLE LOCATION
- BLADE ROTATION HAS A SIGNIFICANT EFFECT ON THE FILM COOLING EFFECTIVENESS
- BALDWIN-LOMAX TURBULENCE MODEL SEEMS TO BE AS GOOD AS ANY TWO-EQUATION MODEL, AND IS 40-50% LESS EXPENSIVE

FUTURE DIRECTIONS

- DETAILS OF IN-HOLE AND NEAR-HOLE PHYSICS REQUIRED UNDER CONDITIONS RELEVANT TO THE GAS TURBINE (DENSITY RATIO, CURVATURE EFFECTS, HIGH Tu, etc.)
- EXPERIMENTAL DATA ON ROTATING FILM-COOLED BLADES REQUIRED
- INCORPORATE HOLE-EXIT PROFILES BASED ON RECENT EXPERIMENTAL DATA IN THE CODE
- USE A MULTI-BLOCK CODE TO DEVELOP HOLE-EXIT PROFILES ON A ROTATING BLADE
- INCORPORATE SIMPLIFIED FILM-COOLING MODEL TO SPEED-UP THE CODE

THE EFFECTS OF TABS ON A JET IN A CROSS-FLOW

Khairul Zaman, NASA

Objective:

A tab placed on the leeward side of the nozzle was expected to increase jet penetration into the cross-flow. An experiment at UTRC showed insignificant effect. The primary objective of the present study was to confirm and explain the ineffectiveness.

Approach:

- Experiments in a low speed wind tunnel.
- Conduct hot-wire measurements for mean velocity and streamwise vorticity fields.

Results:

- Ineffectiveness of tab, when placed on leeward side, is confirmed.
- Static pressure distribution around the nozzle provides an explanation for the ineffectiveness.
- Tab placed on the windward side of the nozzle is found to reduce the jet penetration.

Milestones:

- 5/97 Experiments to optimize tab geomery for maximum reduction in jet penetration.
- 5/98 Active control for increasing jet penetration and mixing.

Film Cooling Heat Transfer w/Liquid Crystals

2-D Film-Cooling Heat-Transfer on AlliedSignal Vane

Steven A. Hippensteele, NASA

Objective:

- Provide 2-D, high-resolution heat transfer map for model validation.

Approach:

- Linear vane cascade
- Transient Liquid Crystals
- Match: M, Re, c/g Den.
- H T Coef. and F C Effect.

Results:

- A-S design data recd
- Scaled design points done
- Cascade design started
- Tests and Results remain

Milestones:

- 1Q98-Init. HT Data
- 1Q99-Final HT Data

Film Cooling Heat Transfer w/Liquid Crystals

Effects of Tab Vortex Generators on Surface Heat-Transfer Downstream of a Jet in Crossflow

Steven A. Hippensteele, NASA

Objective:

- Provide 2-D, high-resolution heat transfer maps for investigation.

Approach:

- Modified Sq. Duct Tunnel
- Transient Liquid Crystals
- Compare jets & FC holes; w/ & w/o tabs
- H T Coefficient Maps

Results:

- Jet tests started
- F C hole tests next
- Variation Tests and Results remain

Milestones:

- 2Q97-Init. HT Data
- 3Q97-Final HT Data

Turbine Vane Heat Transfer, Film Cooling, and Turbulence Experiments

Forrest Ames, Allison Engine Company

OBJECTIVES

- Determine the influence of high inlet turbulence on vane film cooling
- Document the influence of vane film cooling on local heat transfer rates in the presence of high inlet turbulence

APPROACH

- Four vane ambient cascade rig
- Mock combustor turbulence generator
- Thin foil heat transfer technique with finite element analysis
- Adiabatic effectiveness corrected for conduction
- Hot wire boundary layer, turbulence and spectra measurements
- Total pressure exit loss measurements with film cooling

RESULTS

- Suction surface film cooling results correlated well with flat plate data but the influence of turbulence gradually reduced film cooling protection
- Suction surface heat transfer was increased in the near hole region. Two rows had higher augmentation than one
- Pressure surface film cooling protection was strongly dissipated by the high turbulence
- Heat transfer was substantially enhanced by the film cooling and increased with blowing ratio and with the number of rows
- Single wire velocity profiles showed good spanwise uniformity by an X/d of 10 for the high turbulence case for both the single and double row cases.

MILESTONES

- All milestones for the contract have been completed and the final report has been published

Investigation of Rotor Wake Effects on Film Cooling

Jim Heidmann, NASA

OBJECTIVES:

- use CFD to understand 3D flow physics
- measure local film effectiveness and Nusselt number values
- resolve chordwise, spanwise, and temporal variations
- vary blowing ratio, density ratio, and Strouhal number
- develop model accounting for wake–passing effects

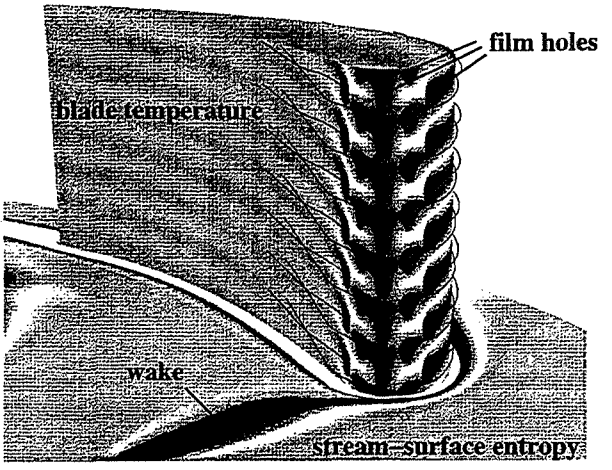

APPROACH:

- modify 3D Navier–Stokes solver for unsteady film cooling
- perform computations for experimental conditions
- use film–cooled blade in annular turbine cascade
- model wake passing with rotating row of cylindrical rods
- measure blade temperatures with thin–film gauges

MILESTONES:

- completed unsteady computations (3rd Q '95)
- completed test matrix (2nd Q '96)
- completed data reduction (3rd Q '96)
- completed matrix of steady computations (4th Q '96)
- developed wake–affected film cooling model (4th Q '96)

UNSTEADY HIGH TURBULENCE EFFECT ON TURBINE BLADE FILM COOLING HEAT TRANSFER PERFORMANCE USING A TRANSIENT LIQUID CRYSTAL TECHNIQUE

J. C. Han, *Turbine Heat Transfer Laboratory, Texas A&M University*

OBJECTIVES

To study detailed distributions of heat transfer coefficients and film effectiveness for a gas turbine blade, including film cooling hole region, under the effects of upstream flow conditions:

- Free stream turbulence
- Unsteady wakes
- Unsteady wakes with trailing edge coolant ejections

and the effects of film cooling injections with air and CO_2 as coolants:

- Blowing ratios
- Coolant-to-mainstream density ratios
- Advanced film hole shapes.

RESULTS

- Nusselt numbers increase with an increase in free-stream turbulence level, and also increase with the addition of unsteady wakes. Adding grid-generated turbulence to unsteady wakes further increases Nusselt numbers on the downstream blade surface.
- The trailing edge ejection is to increase Nusselt numbers on the front parts of both the blade suction and pressure surfaces.
- Film injection promotes earlier laminar to turbulent boundary layer transition on the suction surface and also greatly enhances local Nusselt numbers.
- Unsteady wakes slightly enhance Nusselt numbers but significantly reduce film effectiveness on a film-cooled blade compared with a film-cooled blade without unsteady wakes.
- An increase in blowing ratio increases Nusselt numbers for both coolants. Film effectiveness is highest at a blowing ratio of 0.8 for air injection and at a blowing ratio of 1.2 for CO_2 injection.

APPROACH

A transient liquid crystal technique has been developed for this study. In the experiments, the liquid crystal coated blade is heated to a uniform temperature, and then suddenly exposed to a pre-set mainstream flow condition. A Color Frame Grabber system, through the RGB cameras, is used to record the time of the color change of the liquid crystal on the blade surface. The color change times are related to heat transfer coefficients and film effectiveness based on the solution of a 1-D semi-infinite transient conduction model with a convective boundary conditions.

MILESTONE

The effects of upstream flow conditions and film cooling injections have been studied. The tasks for the coming year are:

- To design and fabricate a test blade with several rows of shaped film holes. These advanced film hole shape designs will be decided after consulting with GE for the optimum shapes.
- To measure detailed heat transfer coefficients and film effectiveness for the blade with shaped film cooling holes under the combined effects of free-stream turbulence, unsteady wake and unsteady wake with coolant ejection.

Overview
Session III: Coolant Flow Integration & Optimization

8:30 Multi-Disciplinary Optimization of Cooled Turbine Design Using 3-D CFD Analysis — Yong Kim, AlliedSignal

8:50 CFD/Experiment to Optimize Film-Cooling Hole Shape — Yong Kim

9:10 Film Cooling Flow and Heat Transfer Design — Robert Bergholz, GE

9:30 An Initial Multi-Domain Modeling of an Actively Cooled Structure — Erlendur Steinthorsson, ICOMP

9:50 Aero-Thermo-Structural Optimization — Joe Gladden, NASA LeRC for George Dulikravich, Penn State Univ

10:10 Break

10:30 Group Discussion

11:30 Adjourn

MULTI-DISCIPLINARY OPTIMIZATION OF COOLED TURBINE DESIGN

Aditi Chattopadhyay, Arizona State University
Presented by Yong Kim, AlliedSignal Aerospace

Objective:

- Minimize turbine blade temperature and optimize coolant flow using Multiobjective, Multidisciplinary Optimization Procedure.

Approach:

- CFD flow field analysis
- FE heat transfer analysis (blade)
- Multiobjective, Multidisciplinary Optimization procedure
  - Kreisselmeier-Steinhauser function
  - Multilevel format

Design Variables:

- Blade Chord
- Surface geometry
- Film cooling parameters
  - -Hole position
  - - Shape/size of hole
  - - Injection angle
  - - Injection rate

Milestones:

- FY98 Develop MDO procedure
- FY98 2-D turbine design
- FY99 3-D aero opt (inviscid)
- FY99 Extend to viscous effects

CFD/EXPERIMENTS TO OPTIMIZE FILM-COOLING HOLE SHAPE DESIGN TOOLS

Yong Kim, AlliedSignal Aerospace

OBJECTIVE

Develop efficient hole shape design method that will help achieve the contract goal of increasing TRIT of regional aircraft engines by 150 to 200°F without counterproductive increases in cooling flow

RESULTS

- CFD can be used as an effective design tool
- Promising new hole shape was identified

APPROACH

- CFD as main design tool
- Code calibration against experiment
- Develop new hole shape
- Hole manufacturing trial
- Validation test in 2D cascade rig

MILESTONES

- CFD hole shape design efforts
  - 95% complete
- 2D cascade tests
  - Starts in 1 st quarter of '97
- Hole shape and CFD design tool validation
  - Starts in 2 nd quarter of '98

Turbine Airfoil Film Cooling - Design Integration

Robert F. Bergholz

Objectives

- Maximize coolant heat capacity utilization.
- Focus on overall heat flux management via film and thermal barrier technologies to control structural thermal gradients.
- Optimize overall film effectiveness distribution.
- Customize film hole geometries for improved effectiveness with lower blowing ratios.

Results

- GEAE Single-Passage Cascade
  - Gas concentration / mass-transfer method.
  - η_f results for several airfoil geometries.
- GE CR&D Transient Cascade
  - Both η_f and **h** measurement capability.
  - Data acquired for full-scale vane geometries.
- GE CR&D Water Tunnel
  - PLIF measurement technique.
  - Full-coverage, discrete-hole film cooling applicable to combustor liners.

Approach

- Acquire film effectiveness and external heat transfer coefficient data on promising film cooling configurations.
- Apply optimization and computational DOE methods to quantify and rank design payoffs.
- Use unstructured grid CFD tools to predict film hole and external flowfields, local heat transfer effects, and customized film hole geometries.

Milestones

- **1996**
  - Single-Passage Cascade
    - Engine airfoil support tests.
  - Transient Cascade
    - GEAE / CR&D IR&D film tests.
- **1997 - 99**
  - Single-Passage Cascade
    - Engine blade / vane, showerhead, ...
  - Transient Cascade
    - AST film tests.

AN INITIAL MULTI-DOMAIN MODELING OF AN ACTIVELY COOLED STRUCTURE

Erlendur Steinthorsson, ICOMP

Objective

- Develop a capability for detailed simulations of flow and heat transfer in turbomachinery.
- Prepare a platform for testing and evaluating turbulence models, film-cooling flow models and other possible models for turbine cooling flows.

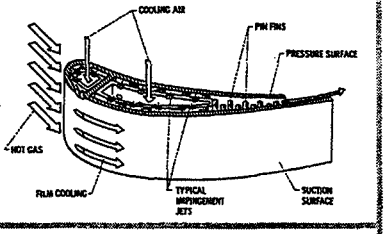

Approach

- Multi-block grid systems for complex geometries:
  - Globally unstructured for flexibility
  - Locally structured for efficiency and accuracy.
- Finite volume discretization of the governing equations.
- Multigrid convergence acceleration for high computational efficiency on fine grids.
- Algebraic and two-equation models of turbulence.

Applications:

- Various internal heat transfer cases, including a branched duct geometry which models features found in coolant passages of turbine blades.
- Flow and heat transfer in turbine cascades, including heat transfer on blade tips.

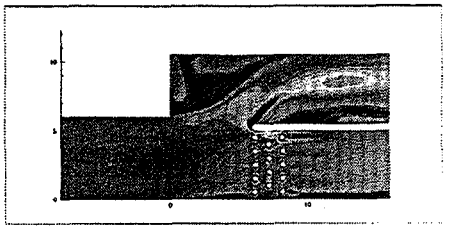

Ongoing and future research:

- Implement additional turbulence models.
- Parallel computing capability.
- Improved convergence acceleration schemes and preconditioning methods.
- Automatic solution adaptive refinement capability.

AERO-THERMO-STRUCTURAL OPTIMIZATION

Presented by Joe Gladden, NASA LeRC for George Dulikravich, Penn State University

Global Research Tasks

1) Optimization of blade hot surface pressure distribution
2) Optimization of blade hot surface shape, thermal boundary conditions and inlet temperature
3) Minimization of the number of coolant passages inside the blade
4) Optimization of thicknesses of blade walls and interior struts
5) Stress minimization in the blade material
6) Retrieval of cold and unloaded 3-D blade shape

Deliverables

The tangible deliverables resulting from various phases of the proposed effort will include computer codes with users' manuals, video-tapes of the 3-D color computer graphics, semi-annual reports and technical papers. Computer codes to be delivered are:

1. 3-D parametric blade outer geometry generator based on analytical surface patches and surface Bezier polynomials.
2. A constrained hybrid optimizer incorporating a genetic evolution algorithm, a gradient search algorithm, a Nelder-Mead sequential simplex with Rosen's projection, and our method for escaping from local minimas.
3. 3-D Blade outer surface shape inverse design based on Navier-Stokes equations and direct transpiration concept.
4. 3-D heat conduction FEM analysis code allowing for locally temperature-dependant heat conduction coefficients as well as thermally coated and non-coated surfaces.
5. 3-D heat conduction inverse boundary condition code for determining temperatures, heat fluxes and convective heat transfer coefficients on inaccessible surfaces.
6. 3-D elastic deformation analysis code for coated and non-coated blades.

Present Status

We have already developed and tested the following software:

1) Inverse design of single coolant passage shapes in 3-D coated & uncoated turbine blades,
2) Inverse determination of temperatures and heat fluxes on 3-D coolant passage walls,
3) 3-D finite element thermo-elasticity dynamic analysis of unsteady stresses and deformations,
4) A hybrid constrained optimizer incorporating gradient search, genetic and simulated annealing.

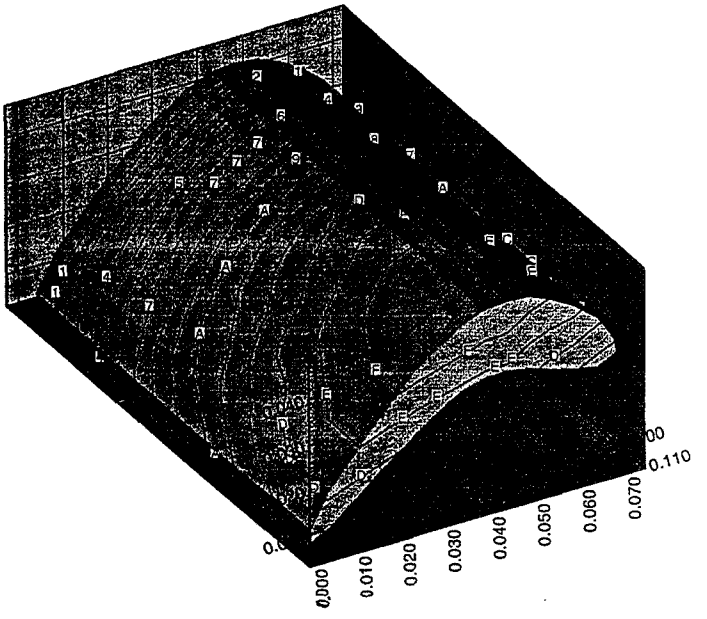

Axial displacements(u) in meters.

Session I

Internal Coolant Passage Presentations

ON THE USE OF STRUCTURED MULTI-BLOCK GRIDS FOR INTERNAL COOLANT FLOW CALCULATIONS

David L. Rigby
NYMA, Inc.
Brook Park, Ohio

A.A. Ameri
AYT Corporation
Brook Park, Ohio

and

E. Steinthorsson
NASA Lewis Research Center
Cleveland, Ohio

Outline

- Objective
- Requirements
- Approach
  - Multi-block Reynolds averaged Navier-Stokes
  - Method of Weakest Descent used to merge blocks
- Results
- Conclusions

Objective

- Production of more efficient and reliable gas turbines
- Reduced design time
- Advance technology used in coolant passage design
- Higher fidelity prediction in a reasonable time

Typical Cooled Turbine Blade

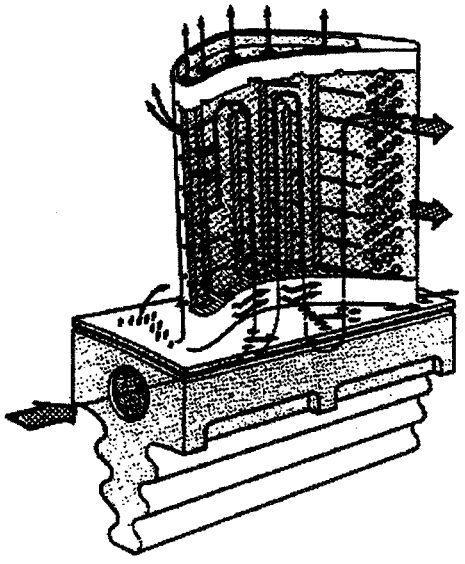

Requirements

- Grid generation
  - needs to be much more transparent to the user
- Turbulence Modeling
  - flow in the coolant passage is very three dimensional and highly turbulent
  - using distance to a wall as a reference is ambiguous, and tedious to implement
- Maximize numerical efficiency

Approach

Solver

- Reynolds Averaged Navier-Stokes
- Muiti-block approach currently being investigated
- Structured flow solver maximizes computational efficiency
- Wilcox k-ω turbulence model which does not require a reference to the distance from a wall

Approach

Grid Generation

- Multi-block grid generation currently able to handle complex geometries (GridPro)
- Block merging done using the recently developed Method of Weakest Descent

Method of Weakest Descent

- Algorithm to merge multi-block grid system to minimum number of blocks
- Increases numerical efficiency and reduces pre-post-processing load
- Can also improve load balancing for parallel computations

A Circle in a Box

12 blocks

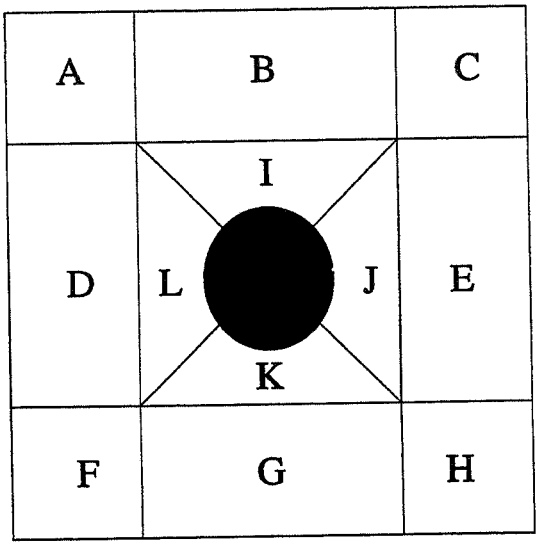

A Circle in a Box

Grade shown in circle

$G = N_{before} - N_{after}$

G = Grade

N = # of candidates

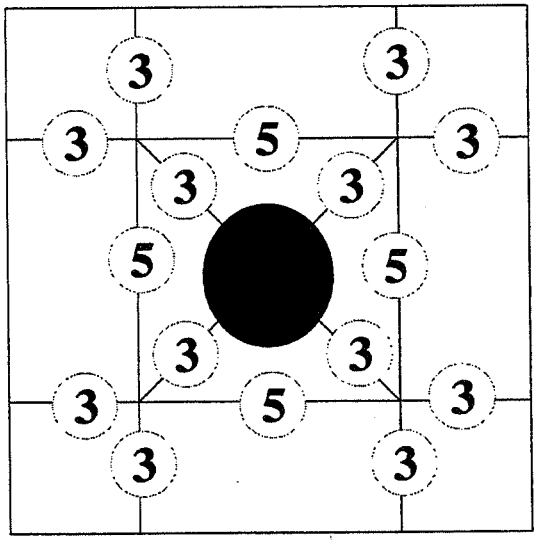

Stages for a twelve block case

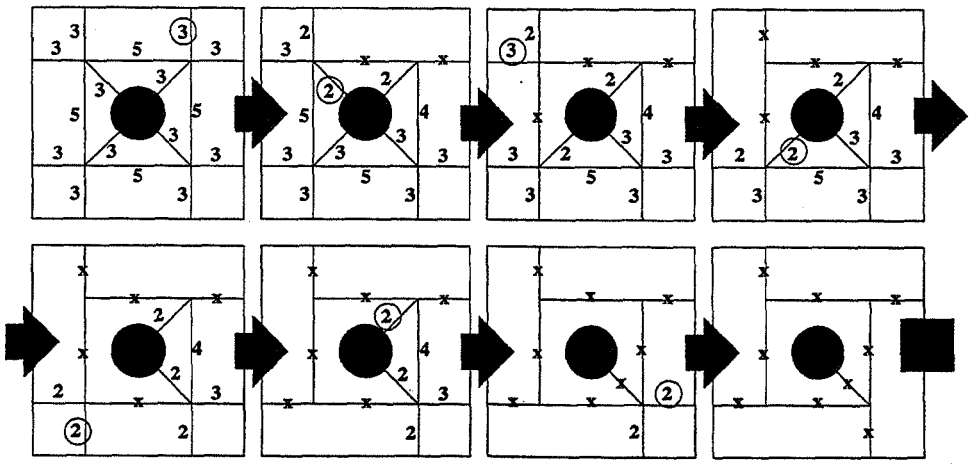

Grade shown near candidate. Invalid patches have x. Circle shows candidate which is about to be removed.

Branch Duct Topology, 283 blocks (thin lines), Minimum found was 27 blocks (thick lines)

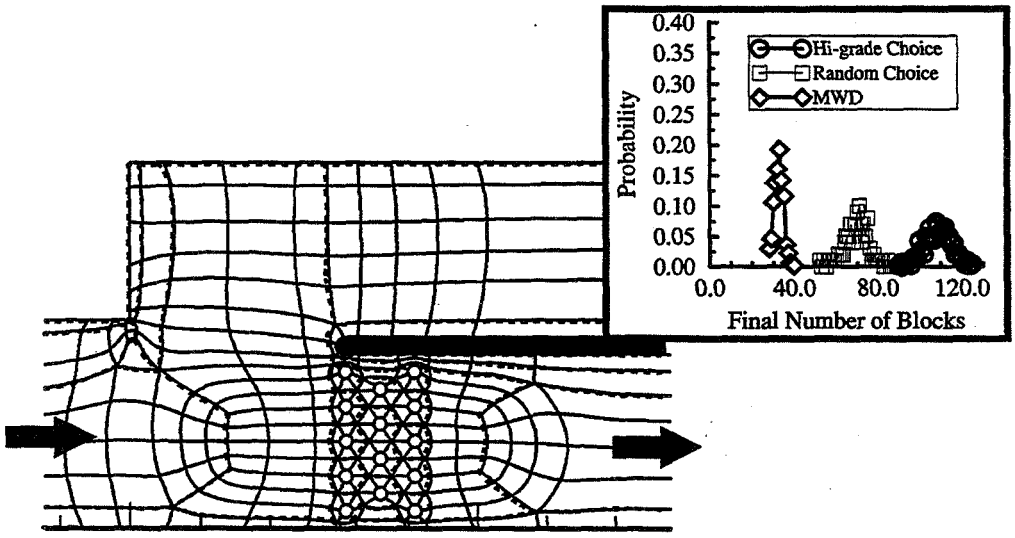

Film Cooling Hole topology, 51 blocks
Minimum number found was 12

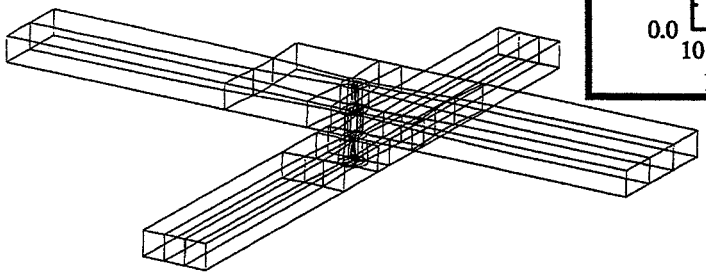

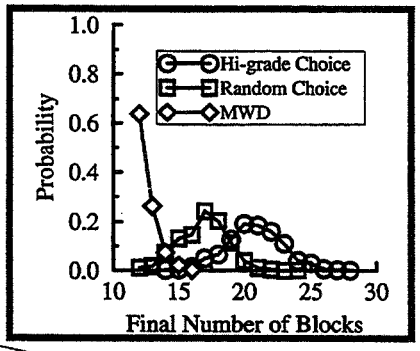

Ribbed channel with bleed holes, 283 blocks
Minimum number found was 22

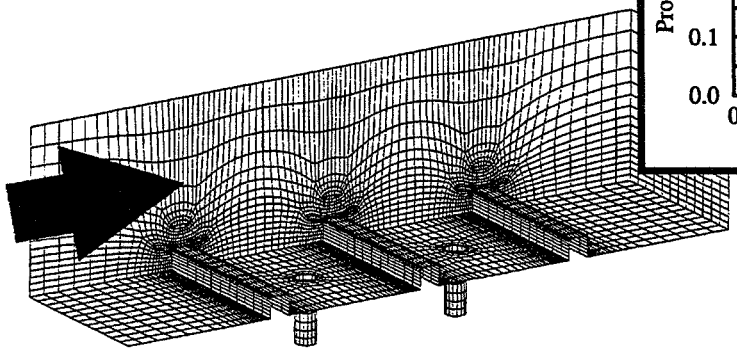

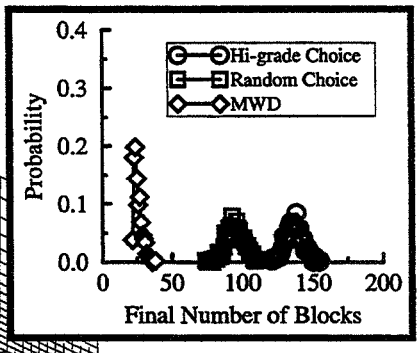

Schematic of 180° turn geometry

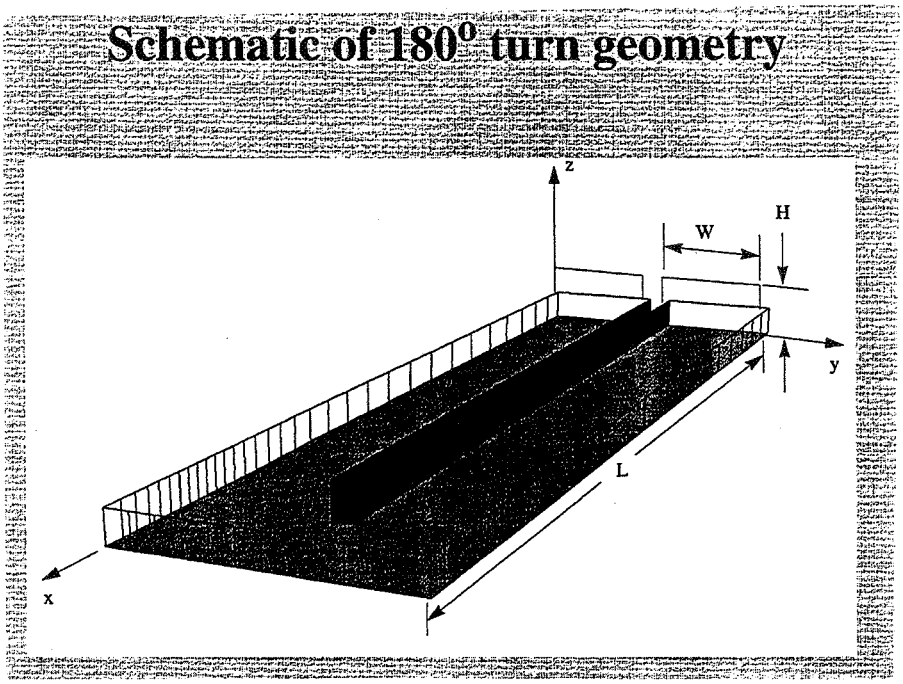

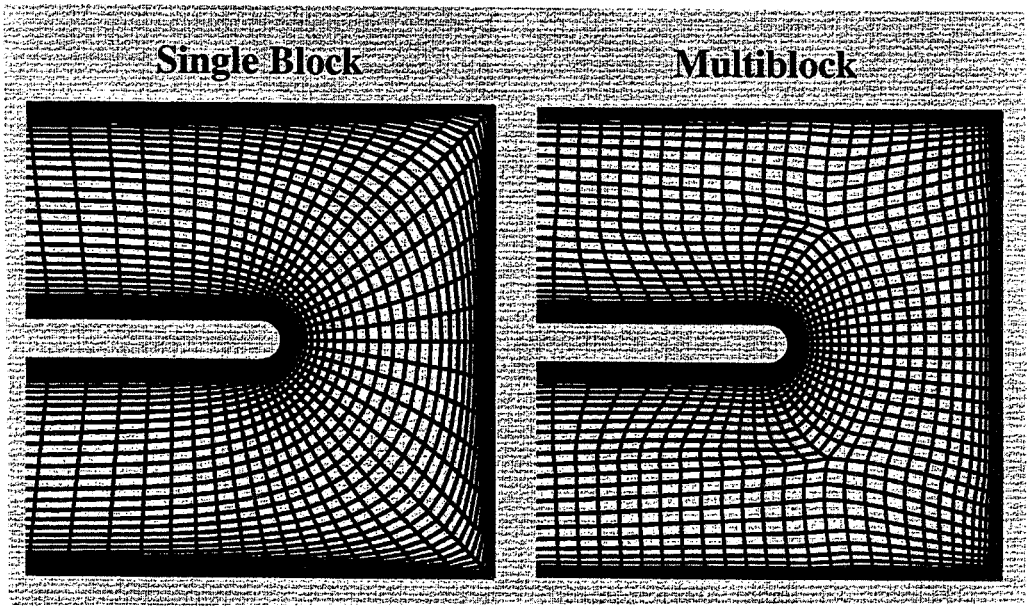

Surface Heat Transfer

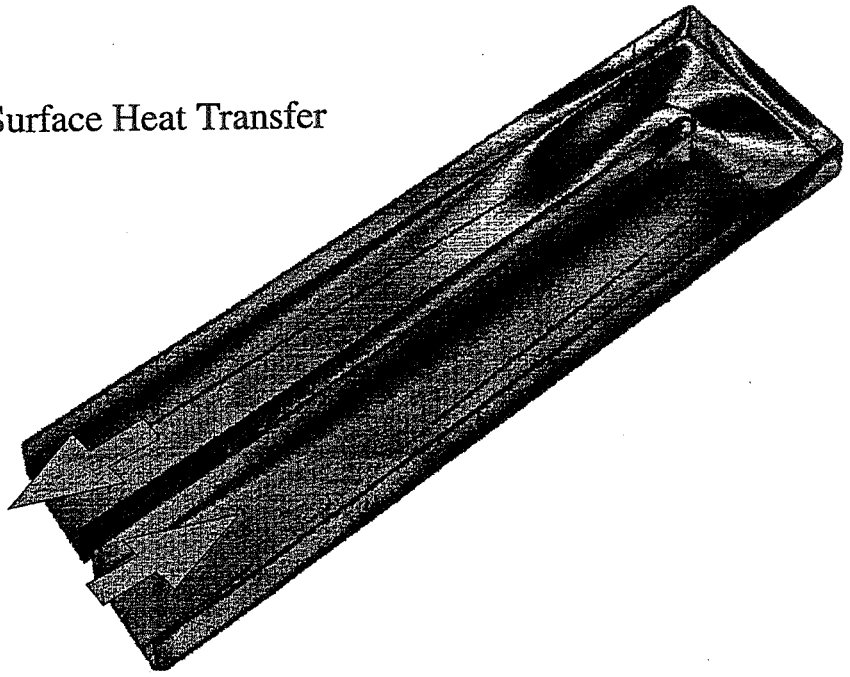

Channel with Ribs and Bleed Holes

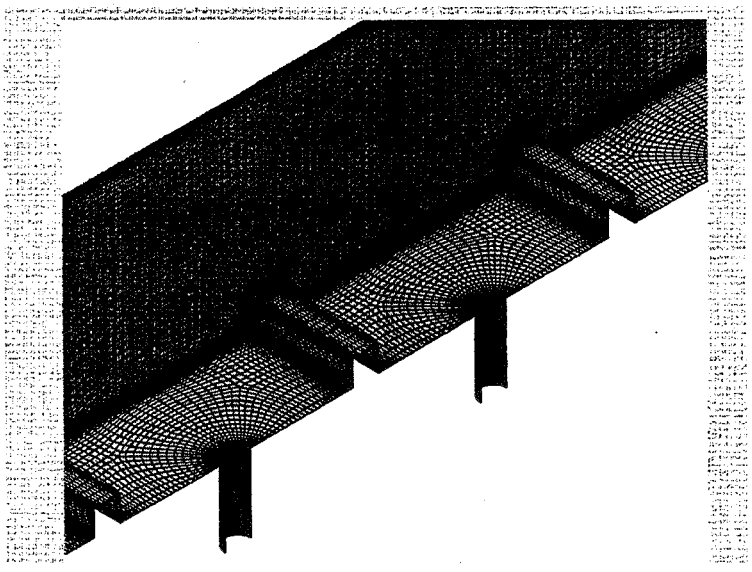

Grid in Symmetry Plane

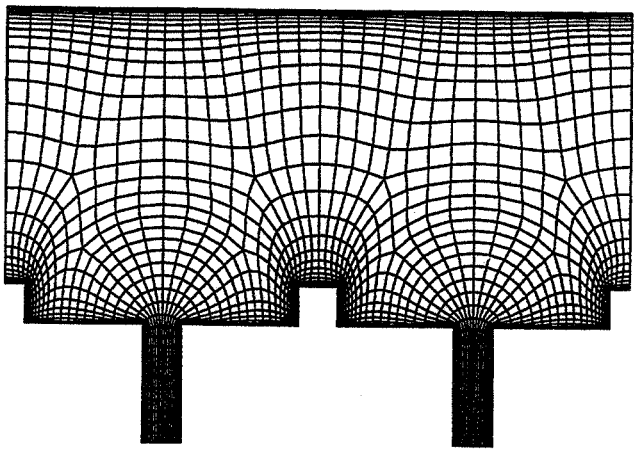

*Every other grid point

Surface Heat Transfer

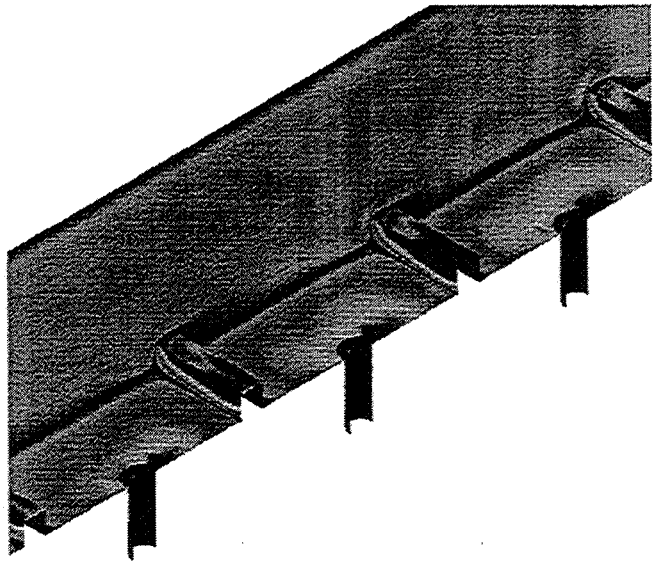

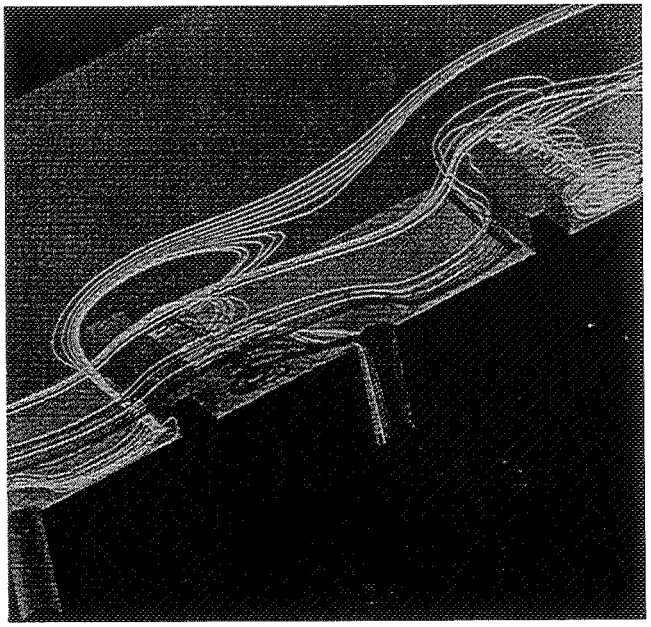

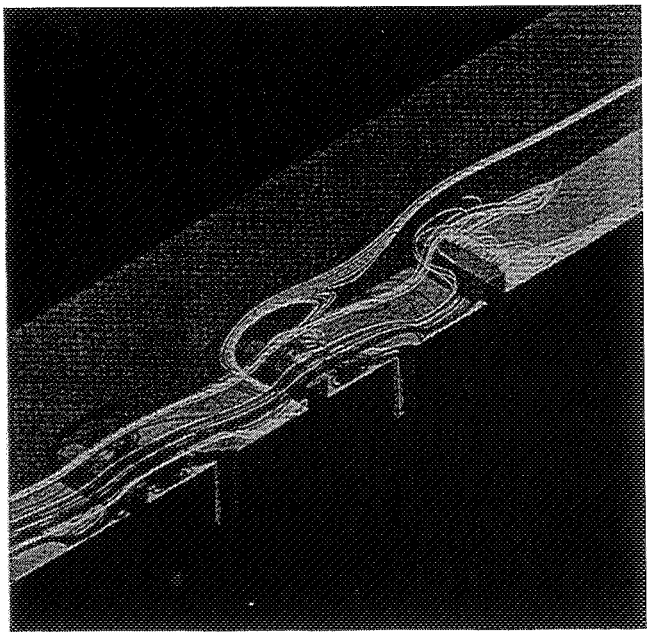

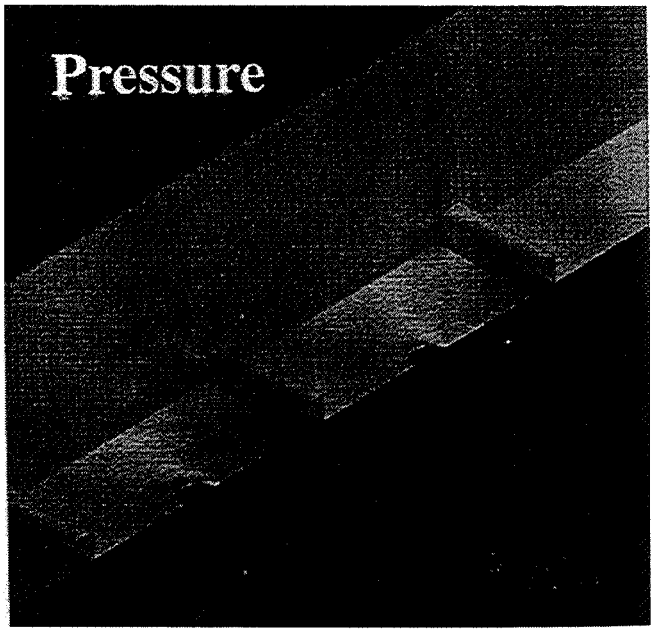

Spanwise Averaged Heat Transfer vs. X

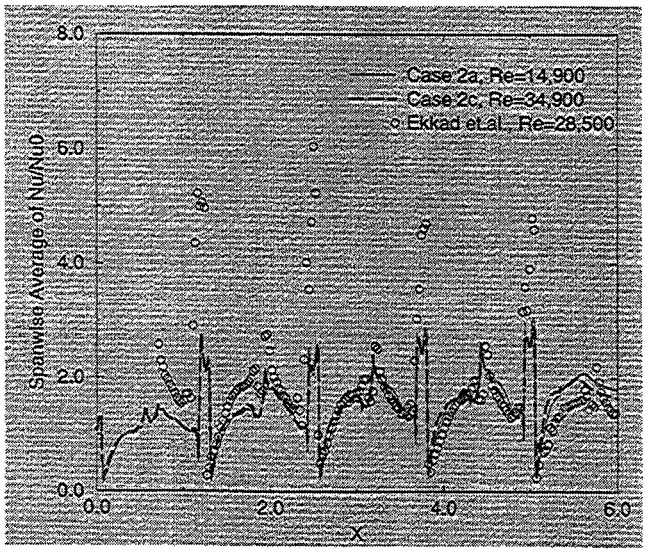

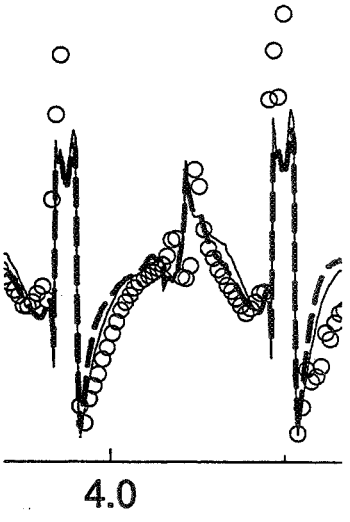

Conclusions

- Reasonable heat transfer prediction can be achieved in complex geometries
- Multi-block grid allows efficient placement of grid points, and efficient use of computer resources
- Wilcox k-ω turbulence model predicts heat transfer well, and has good numerical behavior

Future work

- Further development of grid generation process required
- Investigation of other turbulence models
- Pre- and post-processing still somewhat tedious

NUMERICAL SIMULATION OF TURBINE BLADE COOLING

Tom I-P.Shih, Mark A. Stephens, and Yu-Liang Lin
Carnegie Mellon University
Pittsburgh, Pennsylvania

Outline of Talk

- Objectives
- Approach
- Results
- Summary

Objectives

- Develop, adapt, and validate CFD codes for studying internal and film cooling of turbine blades.
- Apply CFD codes to study flow physics associated with internal and film cooling.
- Develop design strategies for more effective cooling.

Approach

Formulation

- compressible Navier-Stokes
- low Reynolds number k-ω
  (no wall functions!)

Algorithm

- flux-difference splitting with limiters
- diagonalized ADI with multigrid
- multiblock structured grids
  (patched perfectly, patched arbitraily, or overlapped)

Codes

- modified CFL3D
  (rotation, initial condition, boundary conditions, ...)
- RONNIE (patched grids)
  MAGGIE (overlapped grids)

Validation

Based on comparison with experimental data.

- For internal cooling:
  Chyu (non-rotating duct with ribs)
  Wagner, et al. (rotating smooth duct)
- For film cooling: data from Dave Bogard

Results

- Internal Cooling
- Leading-Edge Film Cooling

Internal Cooling

$D_h = 0.5"$
$R_m / D_h = (R_r + R_t) / 2 = 49$
$R_r / D_h = 41.85$
$R_t / D_h = 56.15$
$R_o / D_h = 1.44$
$R_i / D_h = 0.22$
$L / D_h = 14.3$
$p / e = 5$

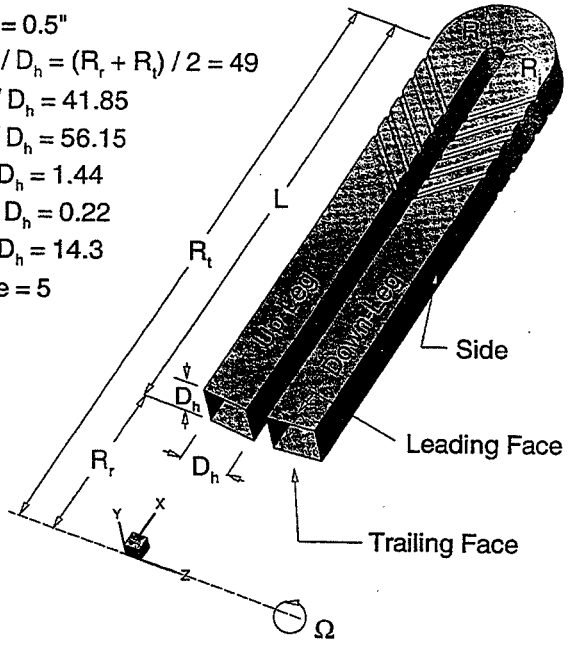

Grid System

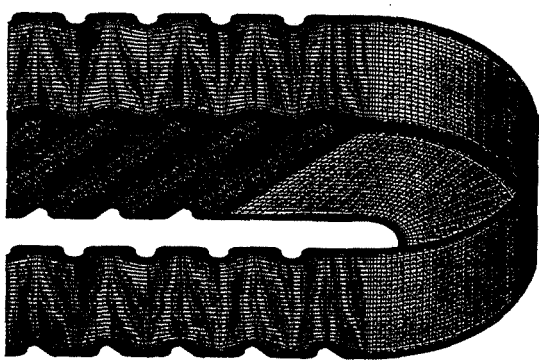

Rule-Based:

- For k-ω model, 5 points between $y^+ = 0$ and $y^+ = 5$.
- Constant grid spacings above the wall for the first 3 to 5 points.
- Grid lines should be aligned with the flow direction as much as possible.
- Cluster grid points to ensure that separation and reattachment points as well as other relevant flow physics are resolved accurately.
- Grid aspect ratio can be large in boundary layers where grid lines are nearly aligned with the flow, but should be near unity in regions with the flow recirculates.
- ...

RESULTS
Assess k-ω Model (and Code)

Comparison with experiments:

Computed

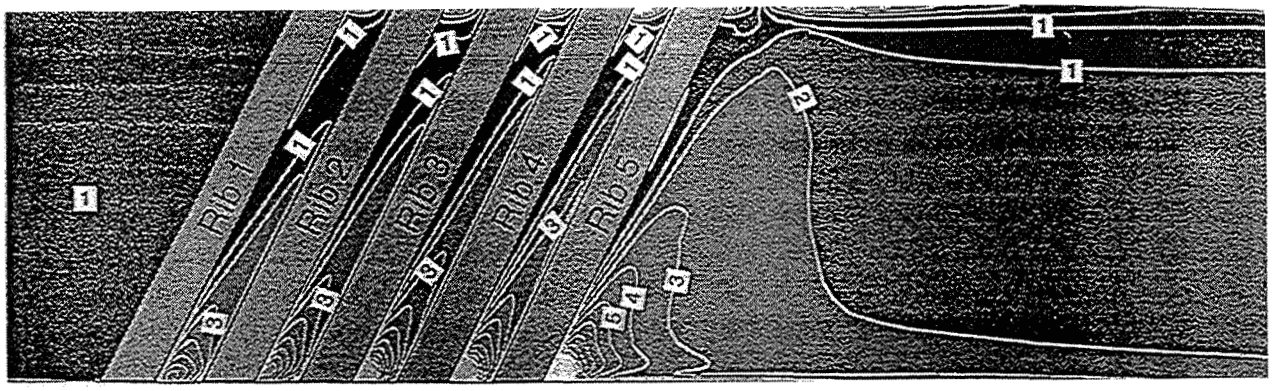

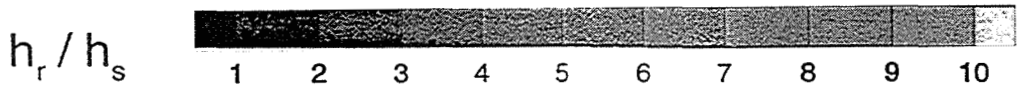

Measured

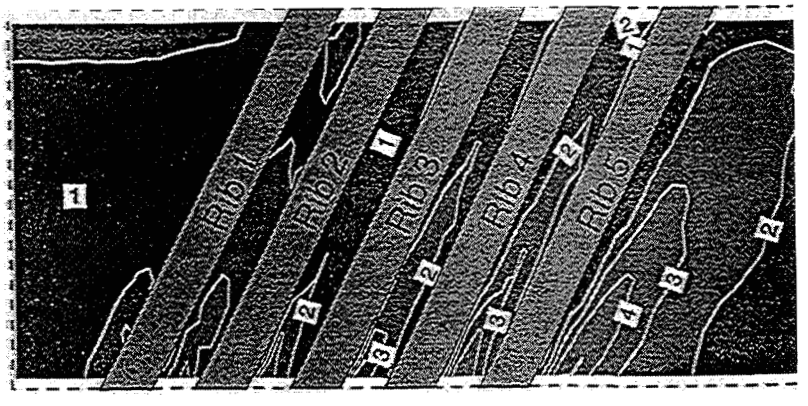

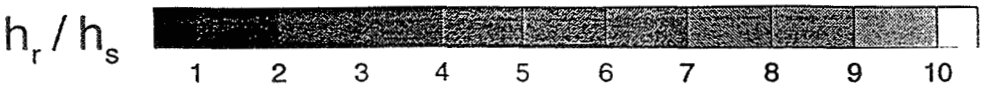

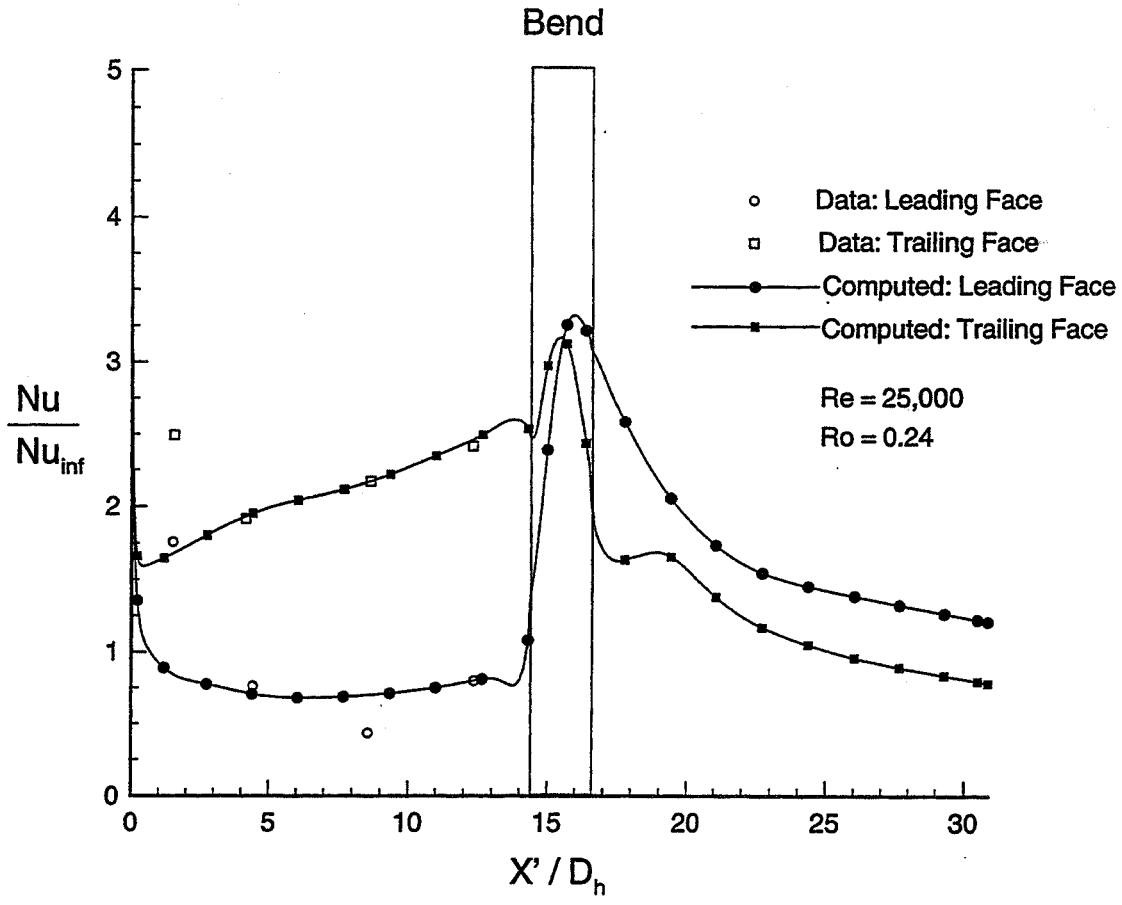
Bend
Nu / Nu_inf
X' / D_h
Data: Leading Face
Data: Trailing Face
Computed: Leading Face
Computed: Trailing Face
Re = 25,000
Ro = 0.24
0
1
2
3
4
5
0
5
10
15
20
25
30

1-D Model Predictions of p/p_{in} for
$Re = 25000$, $Ro = 0.24$, $T_{in} = 300.0$ K, $R_m/D_h = 49$

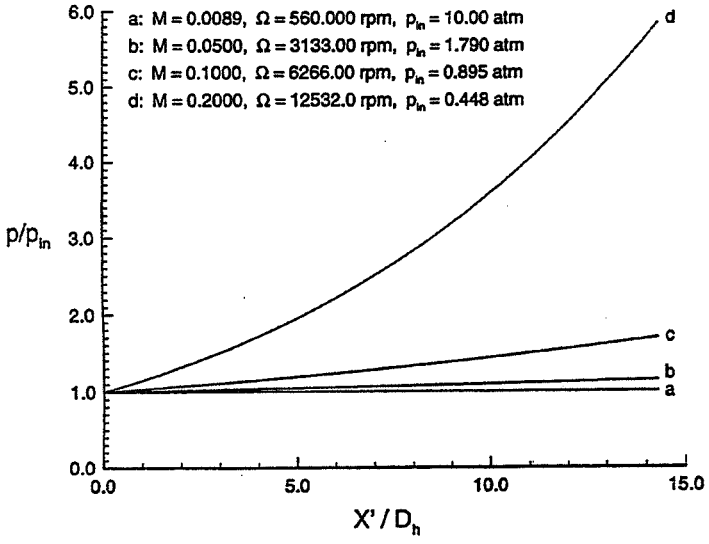

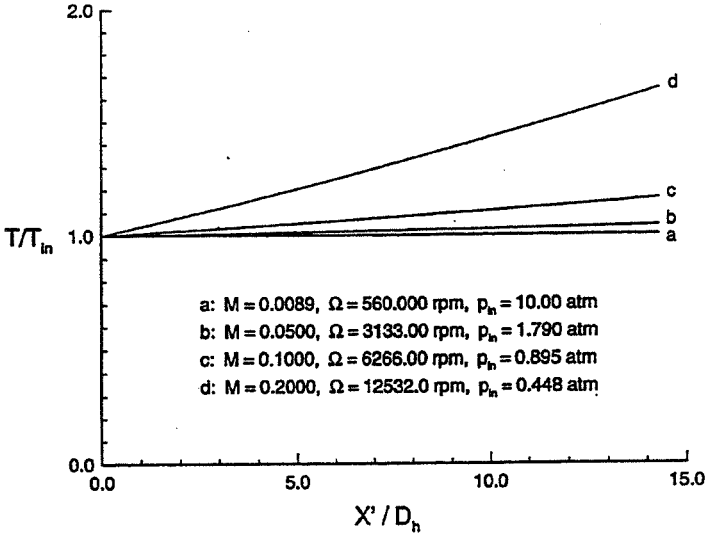

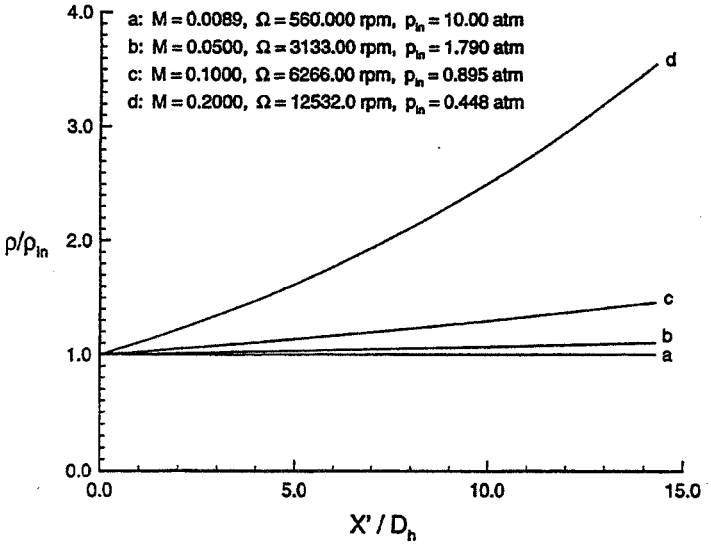

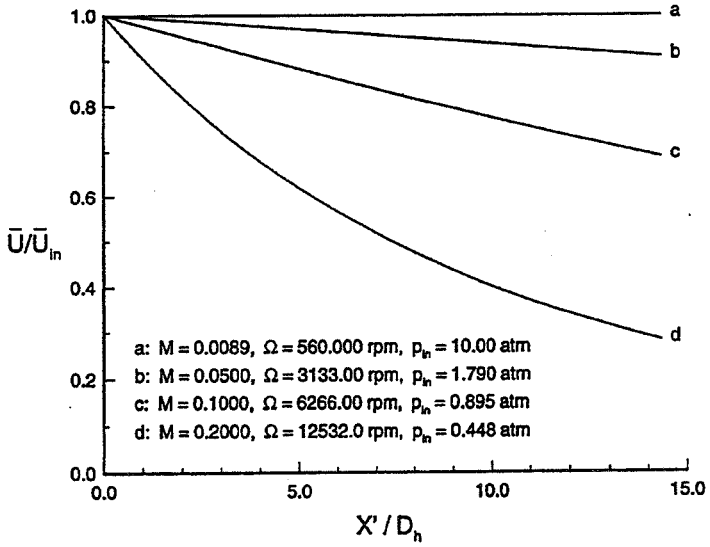

Ro = 0.0

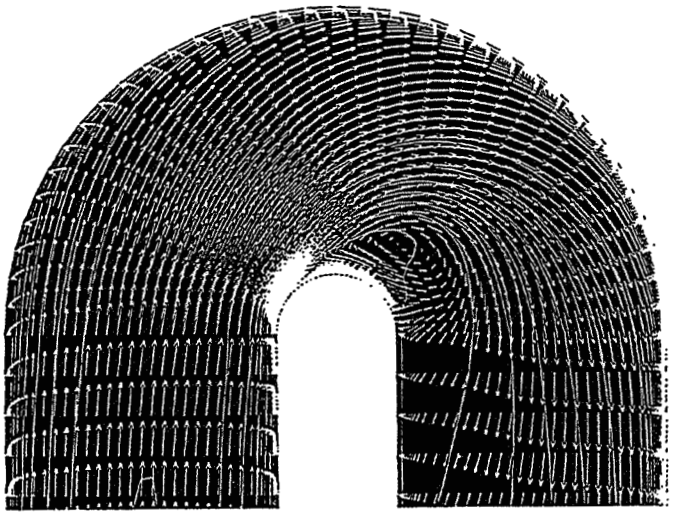

Ro = 0.24

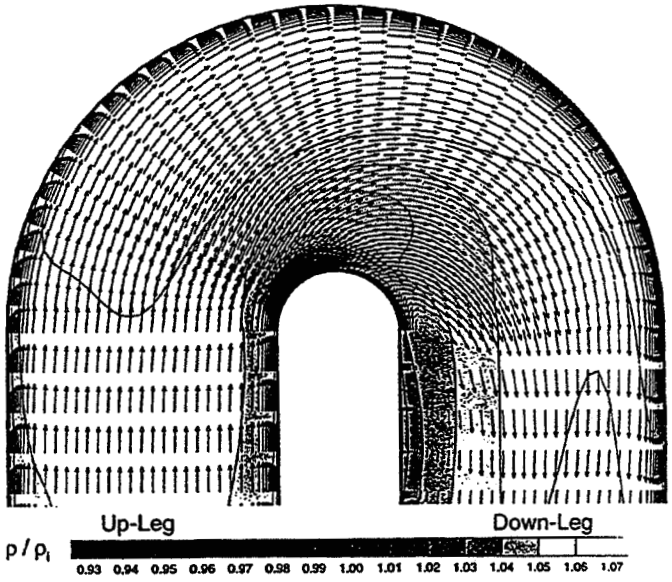

Ro = 0.48

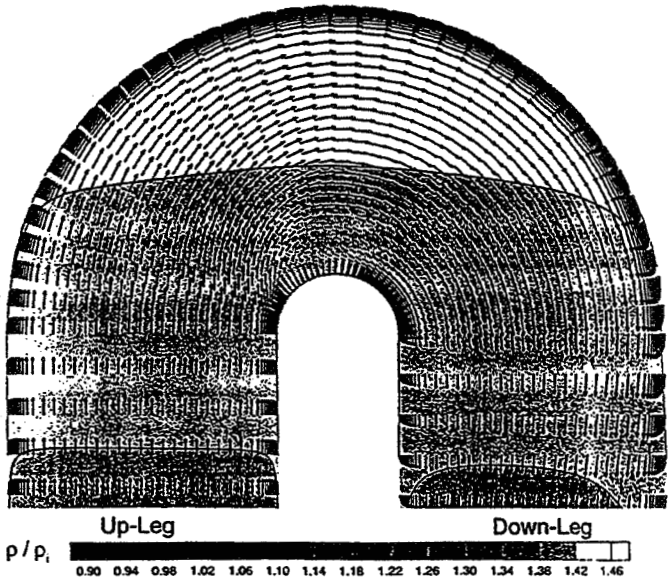

Velocity vectors and density contours in a plane midway between the leading and trailing faces around the bend for three rotation numbers (Ro = 0, 0.24, and 0.48). The Reynolds number for all three cases is 25,000.

Velocity vectors and density contours in a plane midway between the leading and trailing faces near the duct entrance for the "up-leg" and near duct exit for the "down-leg" for two rotation numbers. The Reynolds number for both cases is 25,000.

Ro = 0.24

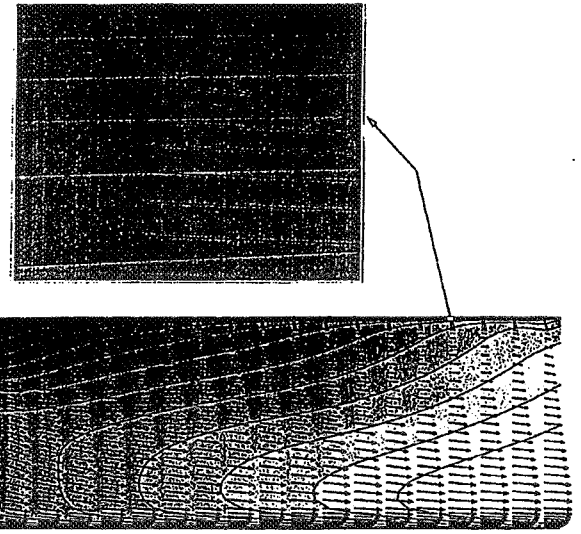

Up-Leg

Ro = 0.48

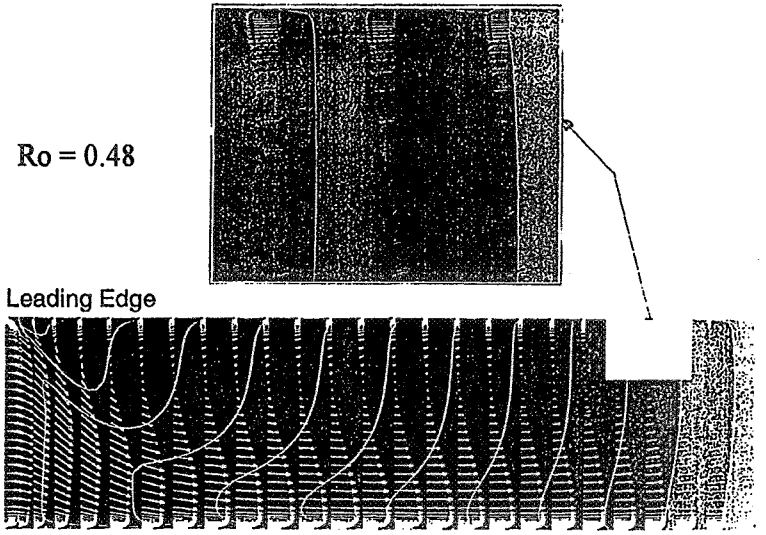

Up-Leg

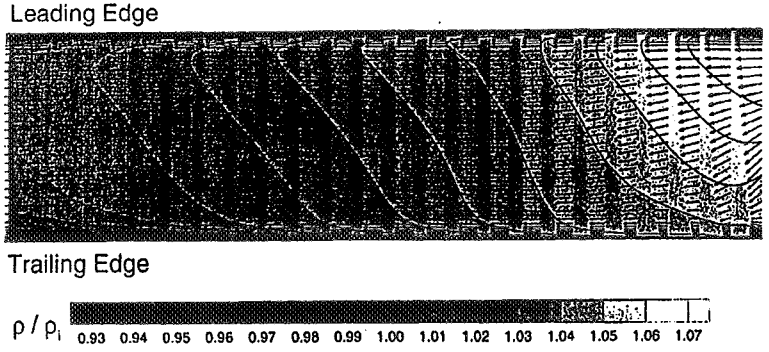

Down-Leg

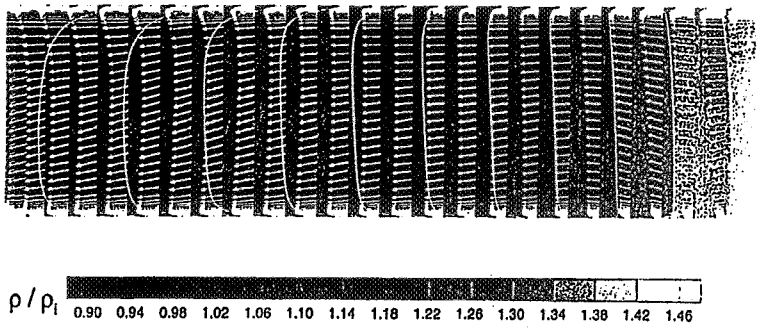

Down-Leg

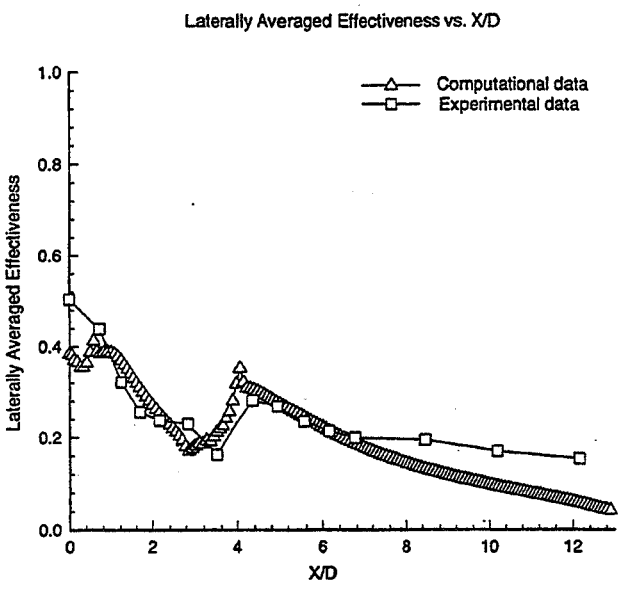
Laterally Averaged Effectiveness vs. X/D
Computational data
Experimental data
Laterally Averaged Effectiveness
X/D
0.0
0.2
0.4
0.6
0.8
1.0
0
2
4
6
8
10
12

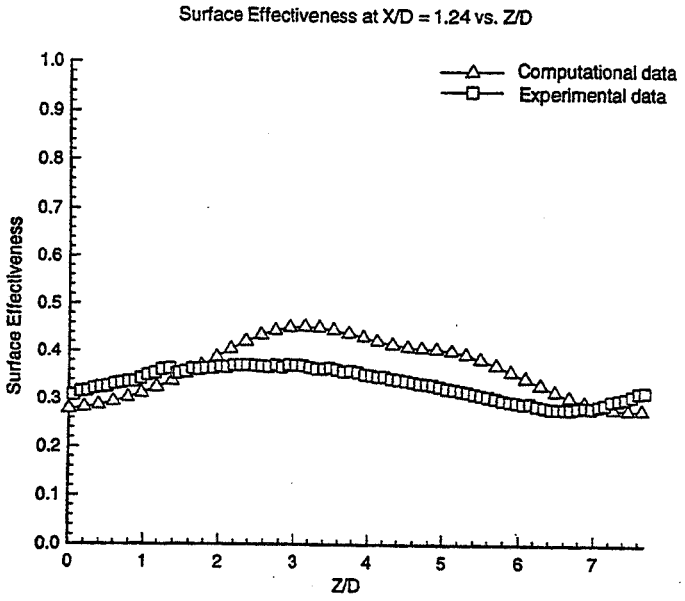
Surface Effectiveness at X/D = 1.24 vs. Z/D
Computational data
Experimental data
Surface Effectiveness
Z/D
0.0
0.1
0.2
0.3
0.4
0.5
0.6
0.7
0.8
0.9
1.0
0
1
2
3
4
5
6
7

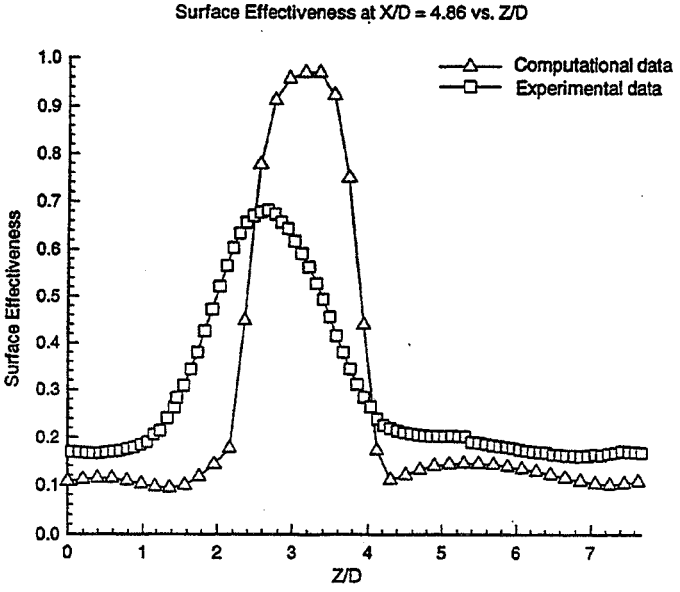
Surface Effectiveness at X/D = 4.86 vs. Z/D
Computational data
Experimental data
Surface Effectiveness
Z/D
0.0
0.1
0.2
0.3
0.4
0.5
0.6
0.7
0.8
0.9
1.0
0
1
2
3
4
5
6
7

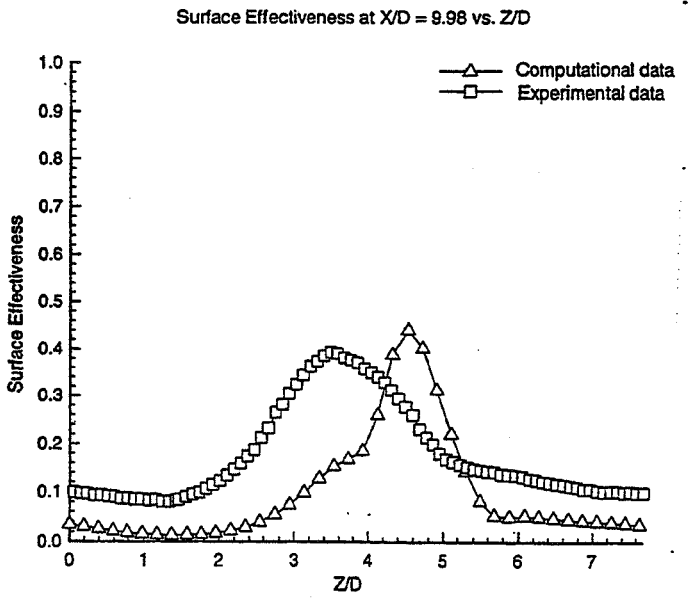
Surface Effectiveness at X/D = 9.98 vs. Z/D
Computational data
Experimental data
Surface Effectiveness
Z/D
0.0
0.1
0.2
0.3
0.4
0.5
0.6
0.7
0.8
0.9
1.0
0
1
2
3
4
5
6
7

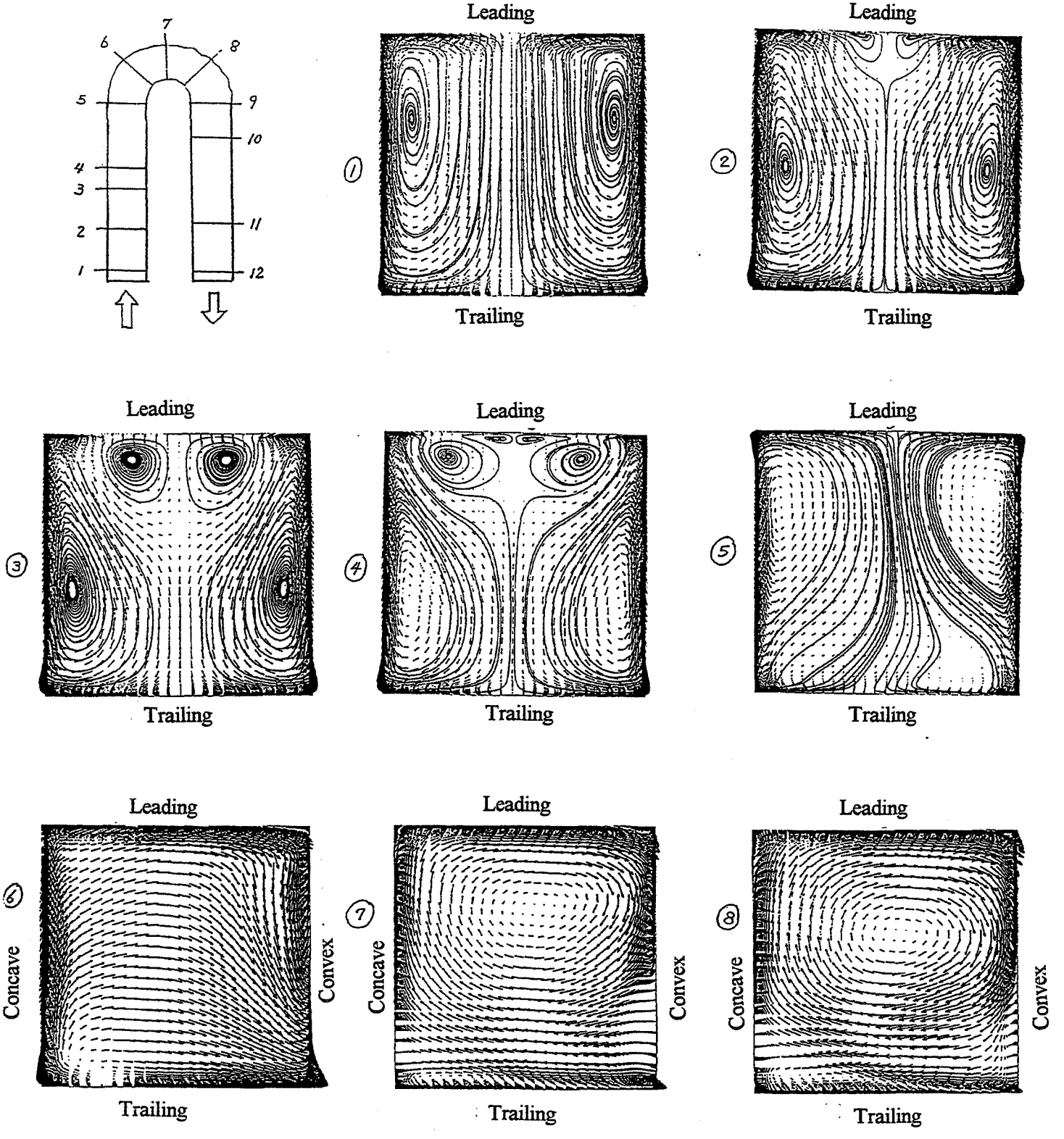

Velocity vectors in the cross stream plane at several streamwise locations along the U-duct. Stations 1, 2, 3, and 4 are respectively $1.45D_h$, $3.65D_h$, $5.15D_h$, and $7.4D_h$ from the duct entrance. Stations 10, 11, and 12 are respectively $3.45D_h$, $6.45D_h$, and $14.3D_h$ measured from the end of the bend (i.e., Station 9). Ro = 0.24, Re = 25,000.

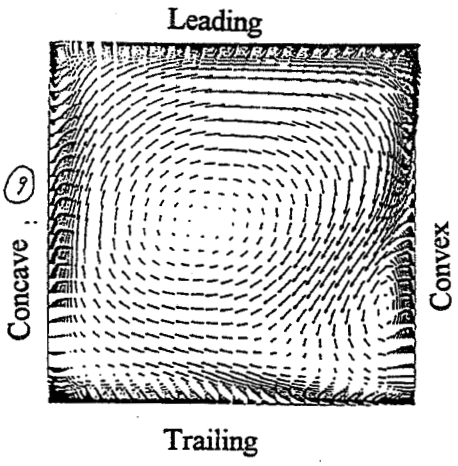

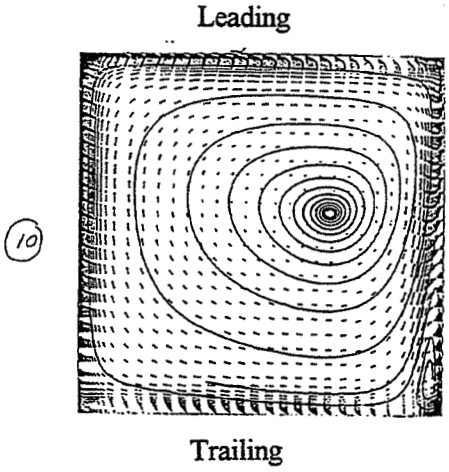

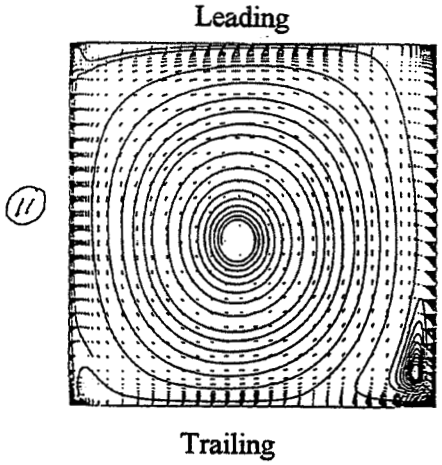

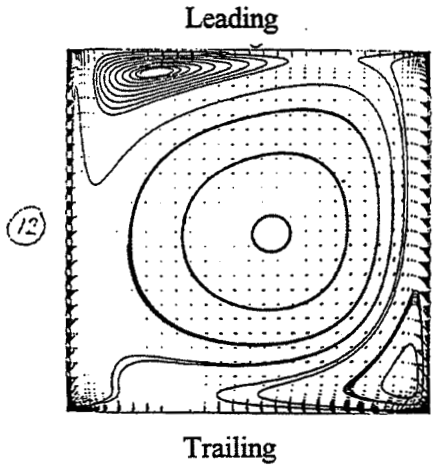

Continued.

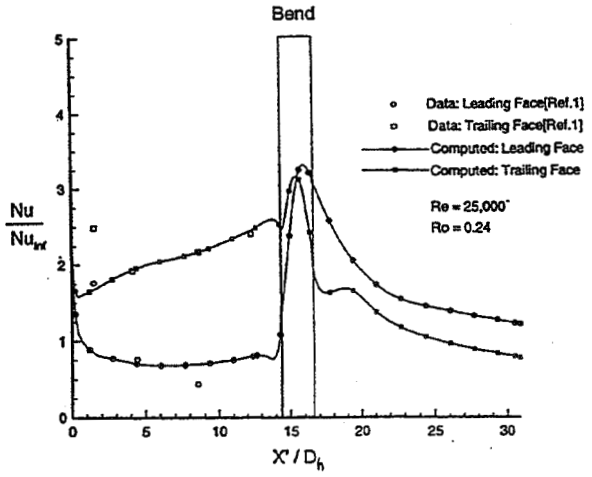

Computed and measured average Nusselt number along leading and trailing faces where $X' = x - R_r$ (see Fig. 1).

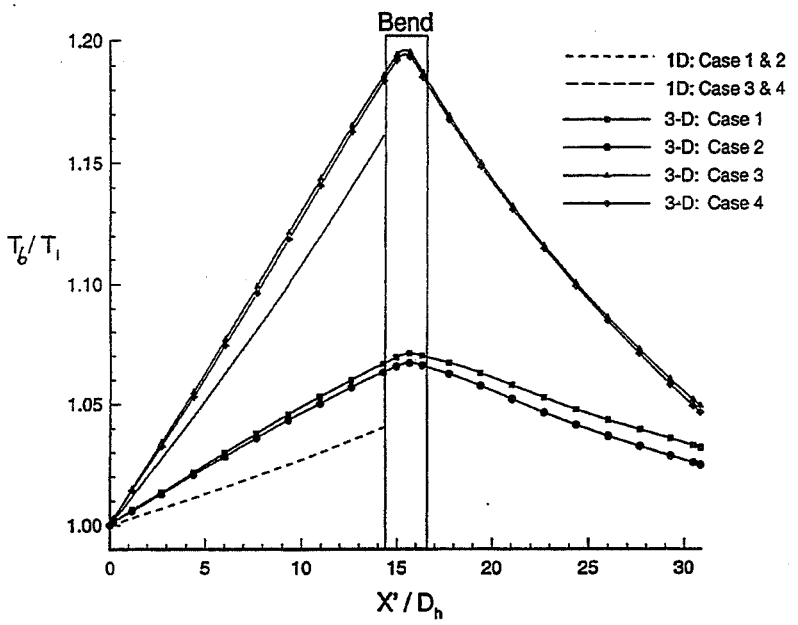
Bend
1D: Case 1 & 2
1D: Case 3 & 4
3-D: Case 1
3-D: Case 2
3-D: Case 3
3-D: Case 4
T_b / T_i
1.20
1.15
1.10
1.05
1.00
0
5
10
15
20
25
30
X' / D_h

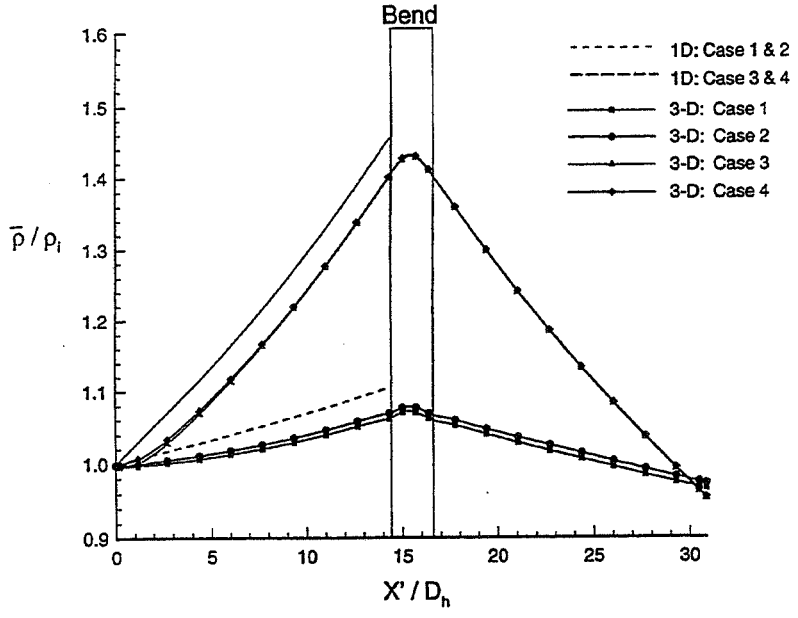
Bend
1D: Case 1 & 2
1D: Case 3 & 4
3-D: Case 1
3-D: Case 2
3-D: Case 3
3-D: Case 4
$\bar{\rho} / \rho_i$
1.6
1.5
1.4
1.3
1.2
1.1
1.0
0.9
0
5
10
15
20
25
30
X' / D_h

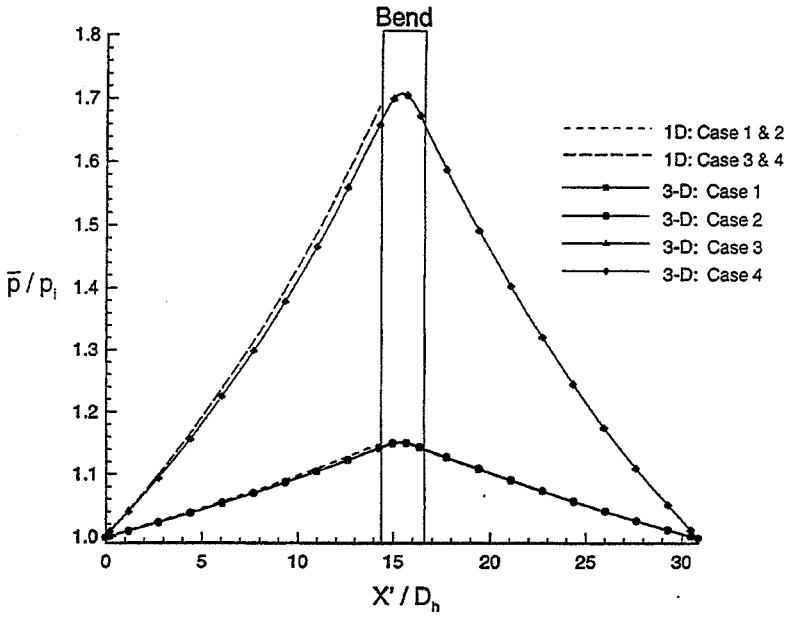
Bend
1.8
1.7
1.6
1.5
1.4
1.3
1.2
1.1
1.0
$\bar{p} / p_i$
0
5
10
15
20
25
30
X' / D_h
1D: Case 1 & 2
1D: Case 3 & 4
3-D: Case 1
3-D: Case 2
3-D: Case 3
3-D: Case 4

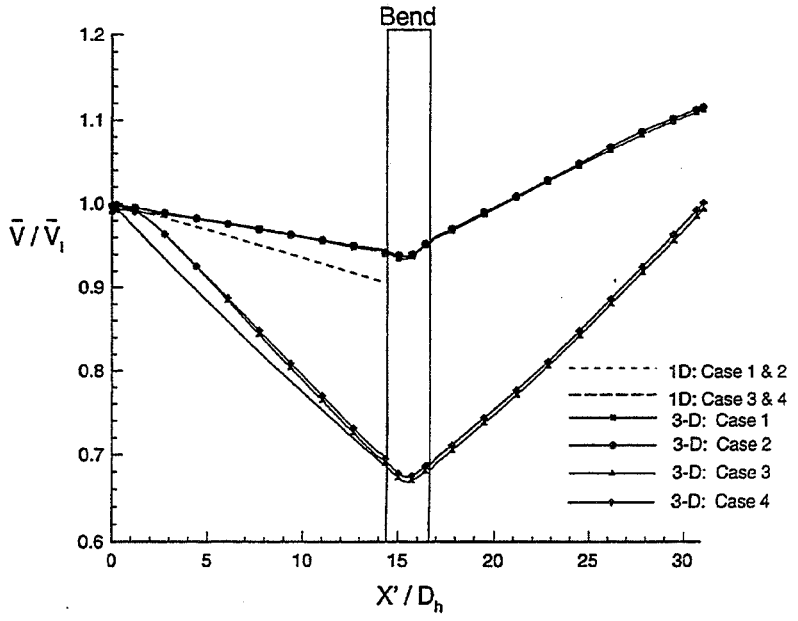
Bend
1.2
1.1
1.0
0.9
0.8
0.7
0.6
$\bar{V} / \bar{V}_i$
0
5
10
15
20
25
30
X' / D_h
1D: Case 1 & 2
1D: Case 3 & 4
3-D: Case 1
3-D: Case 2
3-D: Case 3
3-D: Case 4

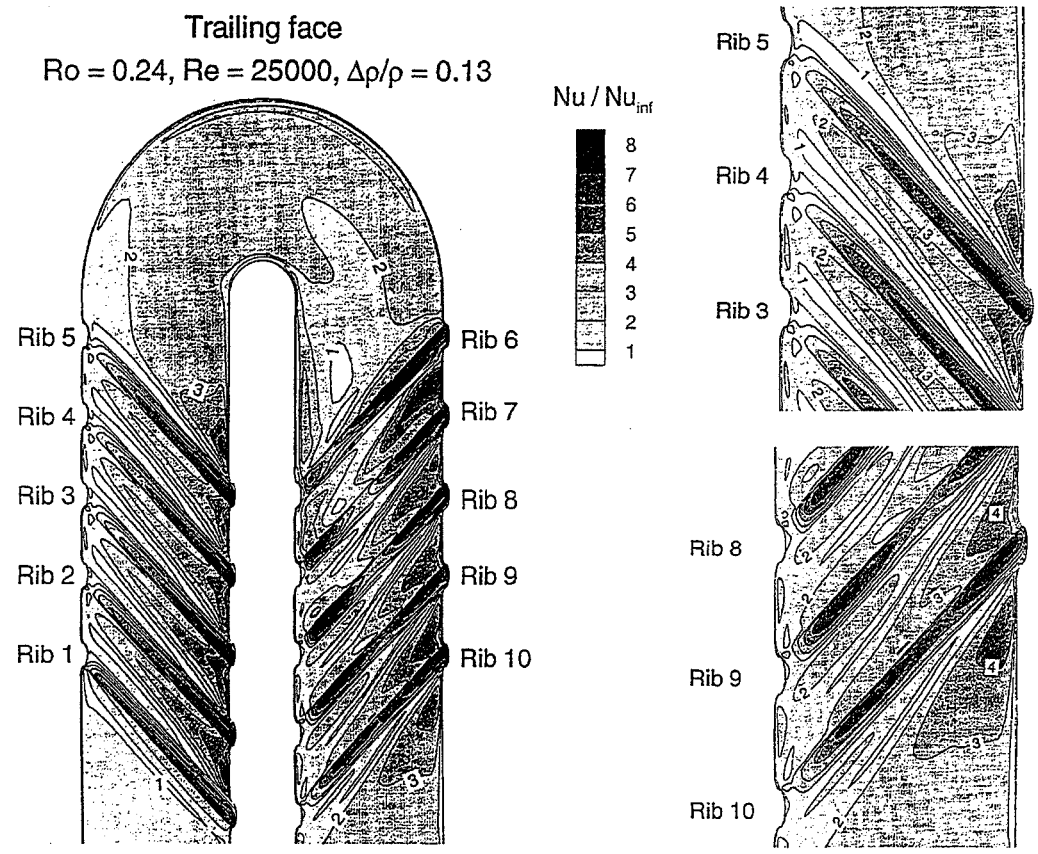
Trailing face
Ro = 0.24, Re = 25000, Δρ/ρ = 0.13
Nu / Nu_inf
8
7
6
5
4
3
2
1
Rib 5
Rib 4
Rib 3
Rib 2
Rib 1
Rib 6
Rib 7
Rib 8
Rib 9
Rib 10
Rib 5
Rib 4
Rib 3
Rib 8
Rib 9
Rib 10

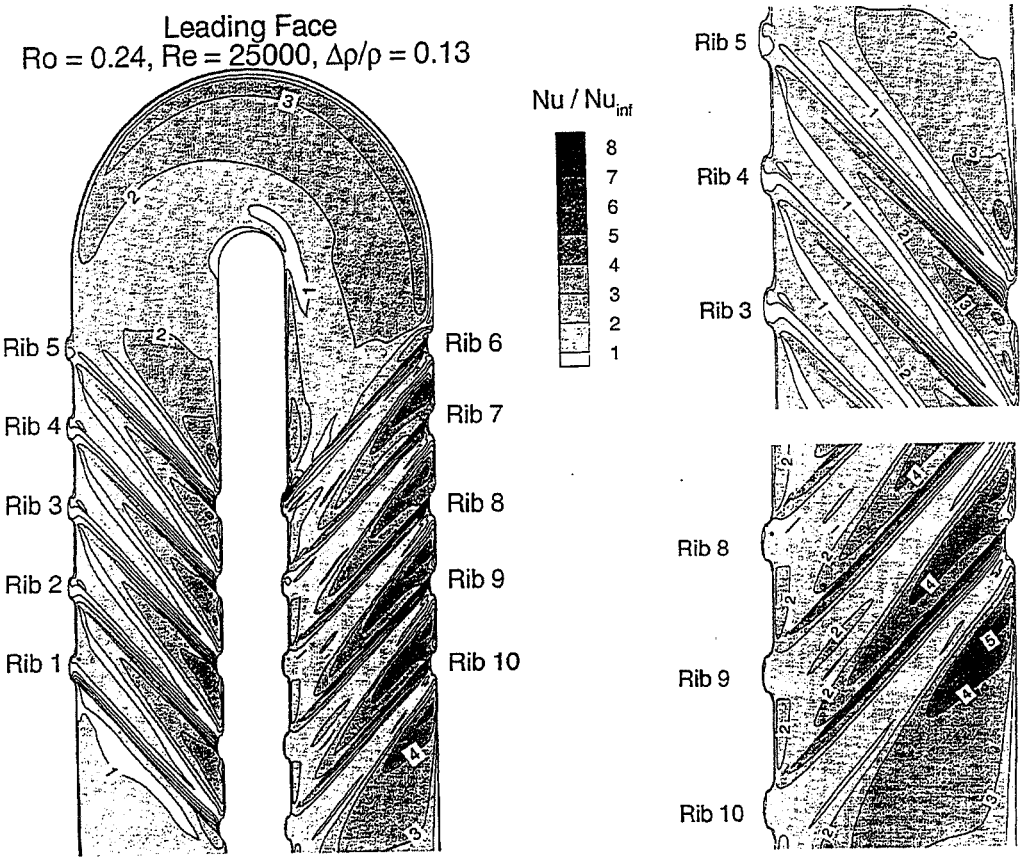
Leading Face
Ro = 0.24, Re = 25000, Δρ/ρ = 0.13
Nu / Nu_inf
8
7
6
5
4
3
2
1
Rib 5
Rib 4
Rib 3
Rib 2
Rib 1
Rib 6
Rib 7
Rib 8
Rib 9
Rib 10
Rib 5
Rib 4
Rib 3
Rib 8
Rib 9
Rib 10

Results

- Internal Cooling
- Leading-Edge Film Cooling

Film Cooling

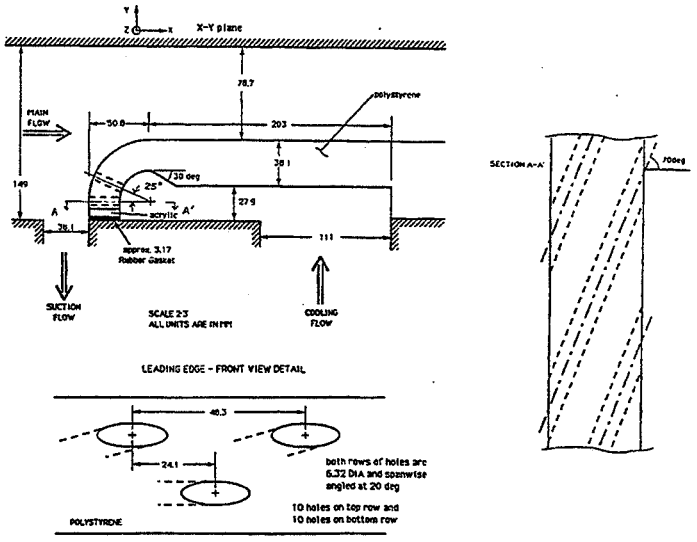

$U_\infty = 10$ m/s, $P_\infty = 1$ atm, $T_\infty = 27.5^\circ$C, $I_\infty = 0.5\%$

$\frac{\rho_c}{\rho_\infty} = 1.8$, $\frac{(\rho U)_c}{(\rho U)_\infty} = 2.0$, $\dot{m}_c = 14.5$ g/s

Summary

Internal Cooling:

- For smooth U-duct, specifying Re & Ro is inadequate. The actual rotational speed must be simulated.
- For U-duct with ribs, more study needed on the effects of rotational speed.
- Results showed secondary flows induced by Coriolis, centrifugal buoyancy, inclined ribs, and 180° bend, and how they interact and affect heat transfer.

Film Cooling:

- Need low-Reynolds no. models that can account for shear layers at the wall and at jet/freestream interaction region.
- Also need turbulence models to account for anisotropic spreading (lateral versus normal).
- ...

FLOW IN SERPENTINE COOLANT PASSAGE WITH TRIP STRIPS

David Tse
Scientific Research Associate, Inc.
Glastonbury, Connecticut

BACKGROUND AND INTRODUCTION

- **In advanced gas turbine engines increased temperatures, stage pressure ratios and rotor speeds are used to increase thrust/weight ratio and to reduce specific fuel consumption.**

- **Efficient internal cooling is essential to maintain structural integrity.**

- **Rotation gives rise to Coriolis and buoyancy forces which can significantly alter the local heat transfer in the coolant passage.**

- **A better understanding of interaction of Coriolis, buoyancy and trip induced secondary flows and the capability to predict heat transfer response to these effects is necessary for achieving efficient cooling.**

- **The complex coupling of Coriolis and buoyancy forces - many investigators to study the heat transfer characteristics of rotating cooling passage.**

- **Hajek, et al. (1991), Wagner, et al. (1991), Yang, et al. (1992), Mochizuki, et al. (1994) - experimental studies on heat transfer performance in rotating serpentine passages of square cross section with smooth walls.**

- **Significant increase in heat transfer at the turns and there were considerable differences between inward and outward flow in the straight passage.**

- **Velocity field - plays an important role in convective heat transfer. Velocity characteristics for flow in a passage smooth wall: Tse, et al. (1994) - NASA CR-4584, Tse and McGrath (1995), McGrath and Tse (1995). These results explain many of the heat transfer phenomena noted by previous investigators.**

BACKGROUND AND INTRODUCTION

- In practice, cooling passages contain trips, which create secondary flow to augment heat transfer.

- Taslim, et al. (1991a, 1991b), Wagner, et al. (1992), Prakash and Zerkle (1993), Johnson, et al. (1993, 1994) indicate that the secondary flow produced trips and trip orientations have large effects on heat transfer.

- This presentation deals with flow in a serpentine passage with ribbed walls.

- To explain the results of Johnson, et al. (1994)
  1. The large decrease in heat transfer in the inlet region, measured in models with smooth walls, does not occur in models with trips.
  2. The effects of density ratio and flow direction for models with trips are less than for models with smooth walls.

OBJECTIVE

- Benchmark quality velocity measurements were acquired by LDV at Re = 25,000 and Ro = 0.24 in a rotating serpentine passage having skewed trips.

- To assess the influence of Coriolis and trip induced secondary flows on the velocity characteristics.

- To explain the heat transfer phenomena observed in Johnson, et al. (1994) -ASME J. Turbomachinery, Vol 116.

- For validation of computational procedures.

- Results presented here are reported in detail: Tse and Steuber (1996) - NASA CR-xxxx (In preparation); Tse and Steuber (1996a); Steuber, et al. (1996).

APPROACH - 1: Experimental (SRA)

Velocity measurements were obtained with the aid of refractive-index-matching (RIM).

RIM - advantage

- Avoids defraction of laser beams at the solid liquid interface
- Allows measurements in complex geometries with multiple obstructions and curved internal surfaces
- Density and viscosity are close to those of water
- Can match Re and Ro of most turbomachinery applications

RIM - limitation

- RIM fluid is a liquid
- Cannot address buoyancy

APPROACH - 2: Computational (Gary Steuber of P&W)

- Flow and heat transfer characteristics were examined using periodic full-developed "conveyor-belt" boundary conditions.

- Boundary conditions at the exit of the computational domain were used to create the inlet conditions.

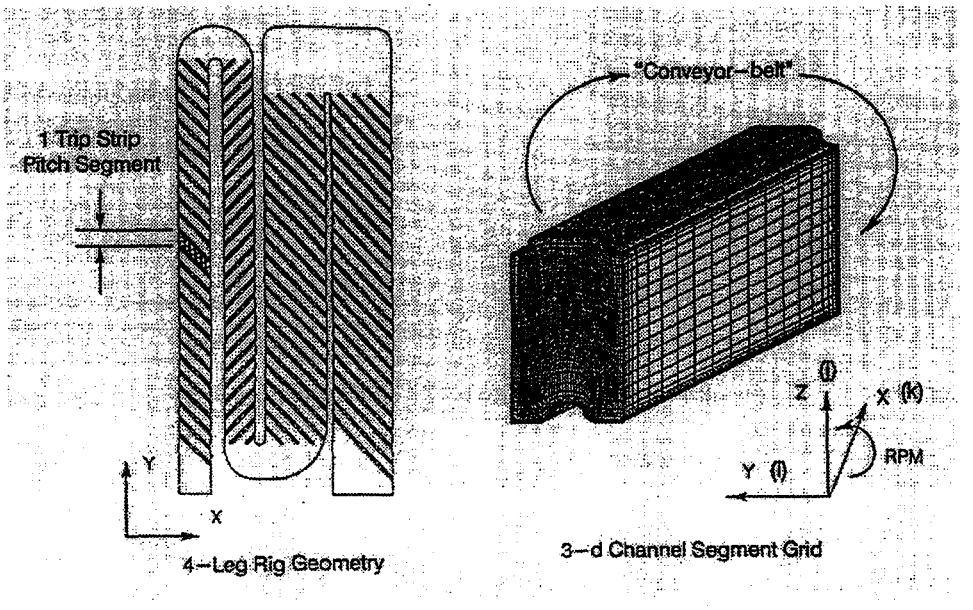

SRA Rig View from outside of model "looking in"

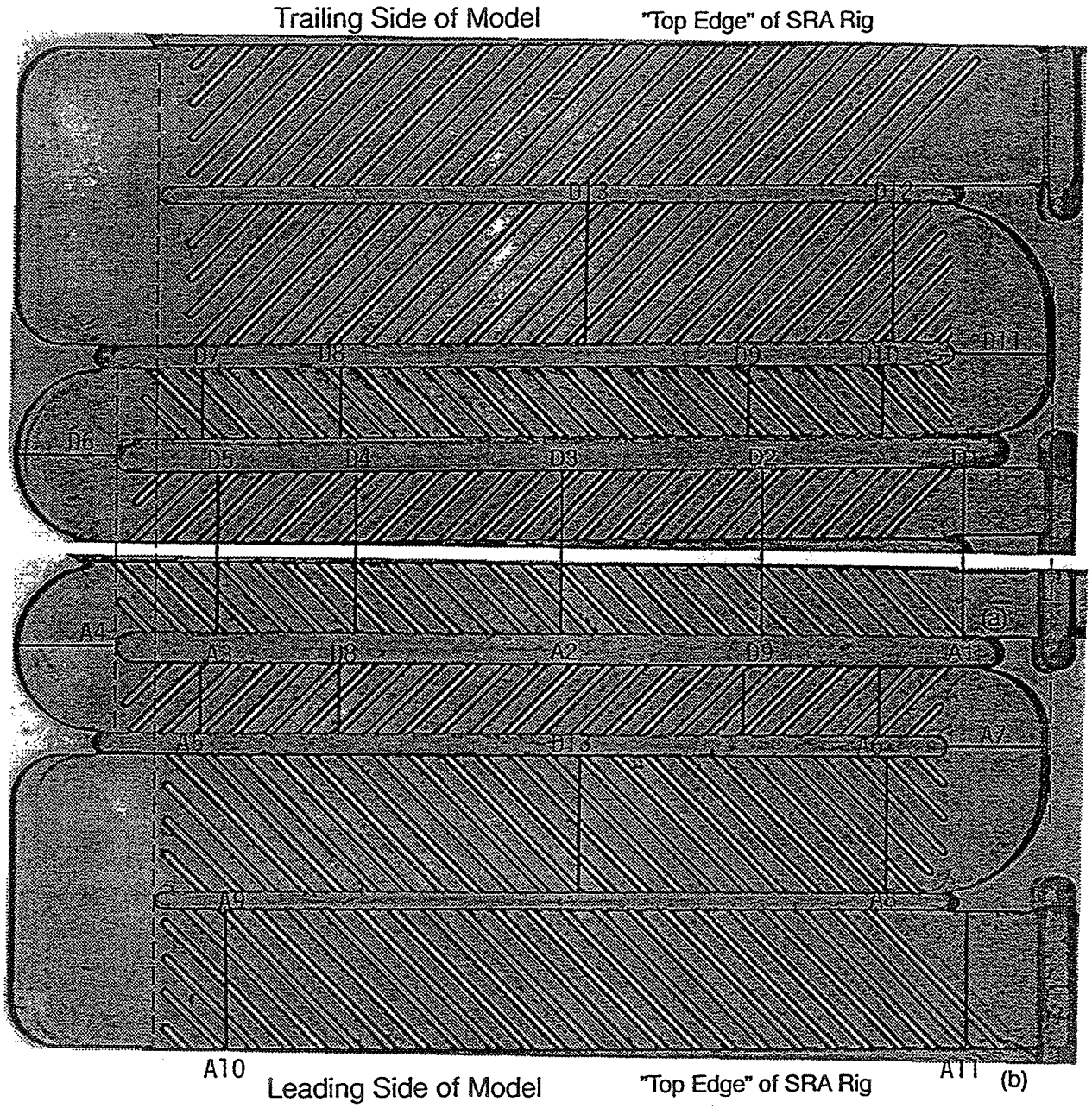

Measuring Locations of Passage 1.

RESULTS (SUMMARY & COMPARISON WITH SMOOTH WALL)

Three components of velocity - Re = 25,000 and Ro = 0.24

- **First passage (radially outward flow passage)**

Ribbed wall	Smooth wall
Entrance effect - 1.0 D	Entrance effect - 6.5 D
Coriolis & trip secondary flow	Coriolis effect

- **First turn (Ribbed wall & Smooth wall)**
  Effect of the turn - Swirl

- **Second passage(radially inward flow passage)**

Ribbed wall	Smooth wall
Effect of the turn - 1.0 D	Effect of the turn- 4.0 D
Coriolis & trip secondary flow	Coriolis effect

- **Second turn (Ribbed wall)**
  Effect of the turn - Swirl (weaker than the first turn)

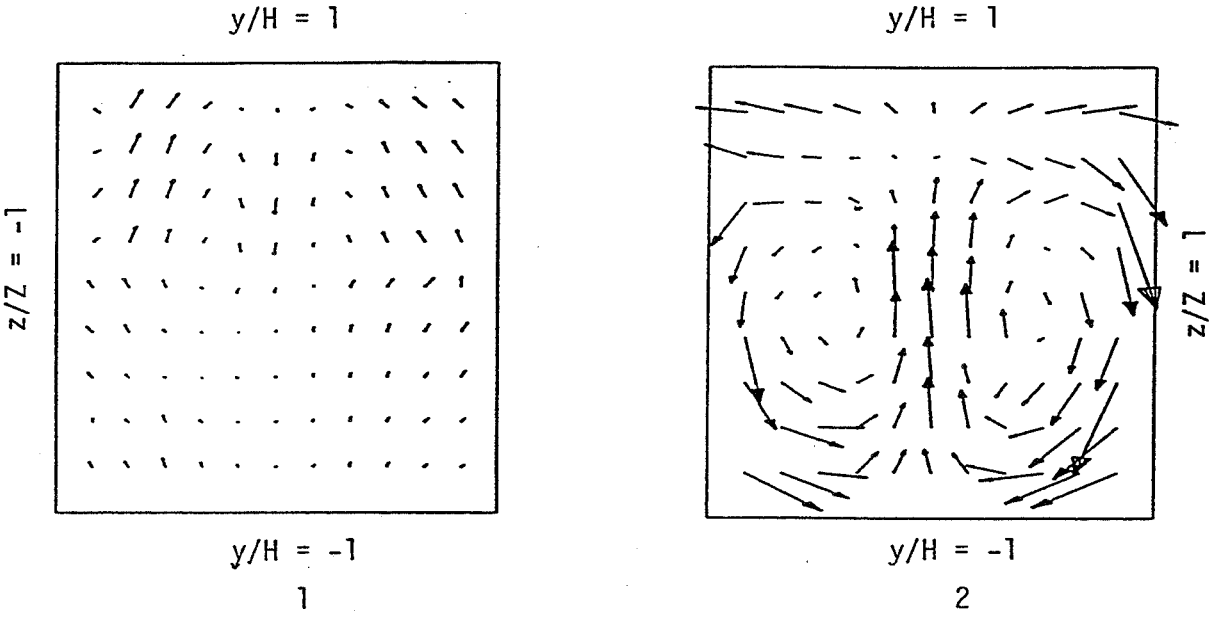

Velocity vectors in the first passage.

1 x/D = 1 2 x/D = 7

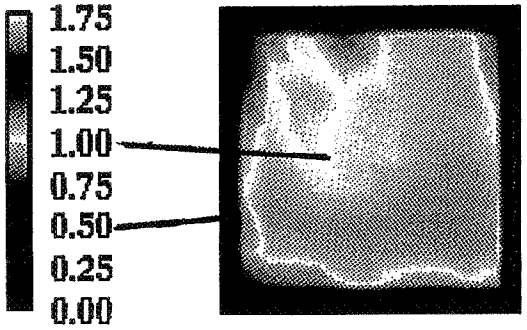

x/D = 1

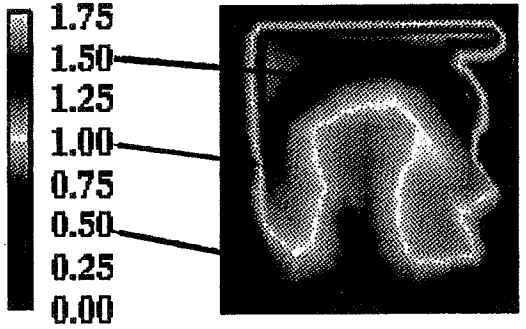

x/D = 7

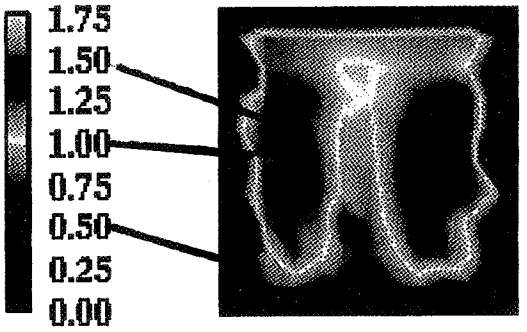

1D upstream of T1

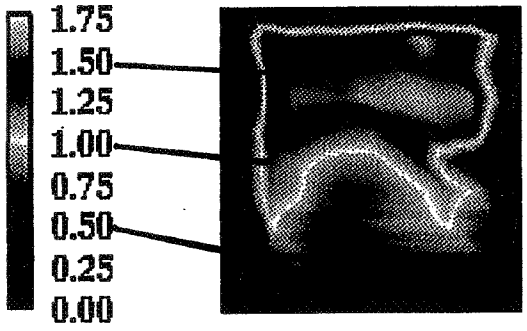

1D downstream of T1

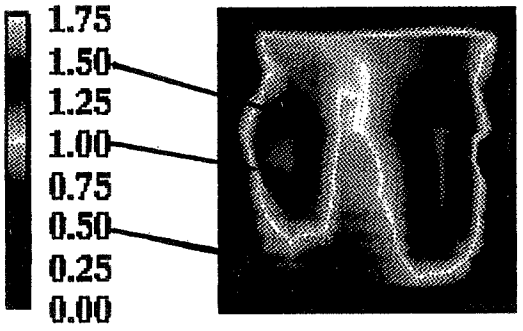

1D upstream of T2

Streamwise velocity contour

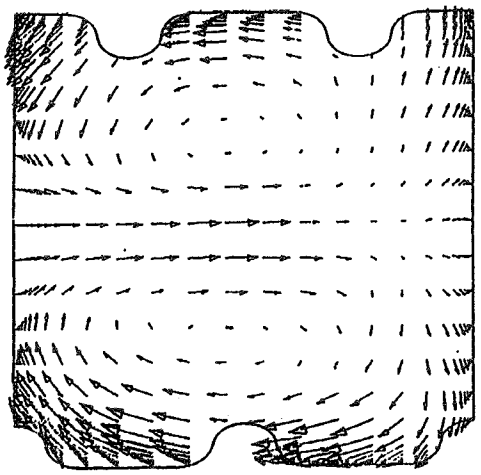

(SRA Data) Velocity Vector Field

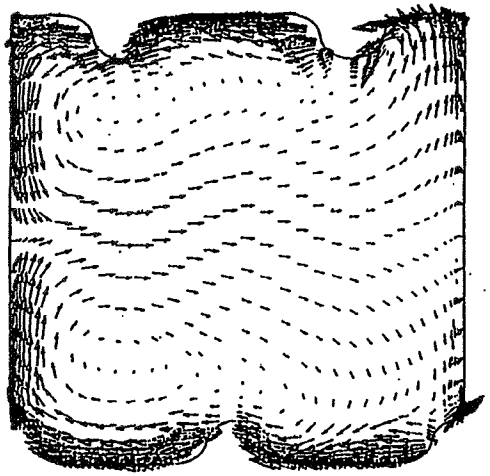

(CFD) Vectors – Incomp Flow

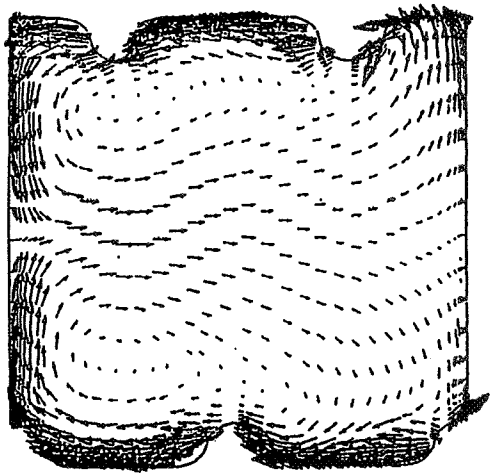

(CFD) Vectors – Comp Flow

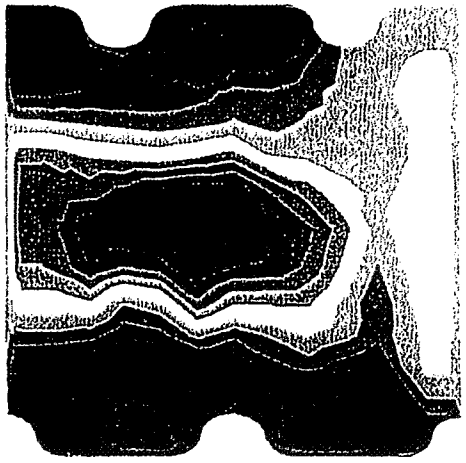

(SRA Data) U–Velocity Component

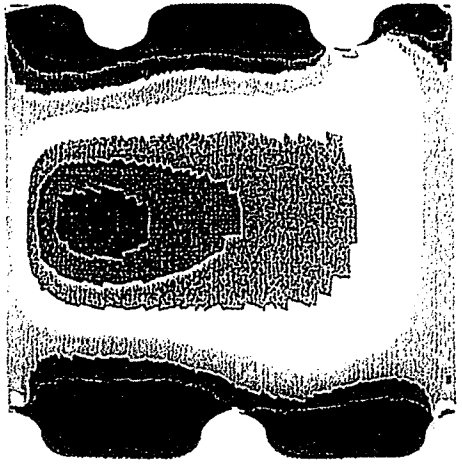

(CFD) U–Velocity – Incomp Flow

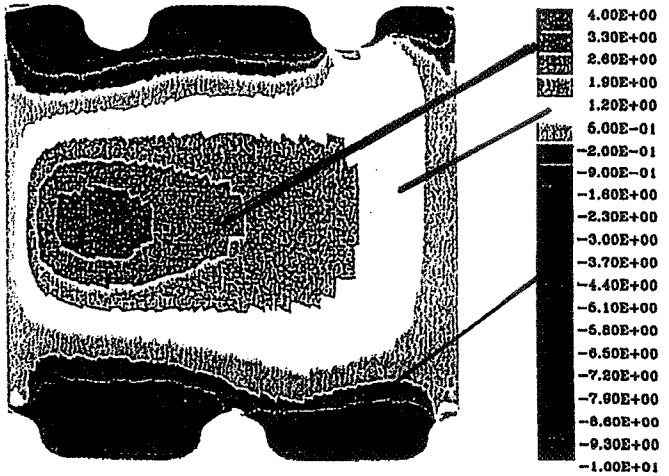

(CFD) U–Velocity – Comp Flow

(ft/sec)

m/s = ft/sec / 3.281

Velocity Vector Field and U–Component Velocity Contours – Stationary Channel Location A2

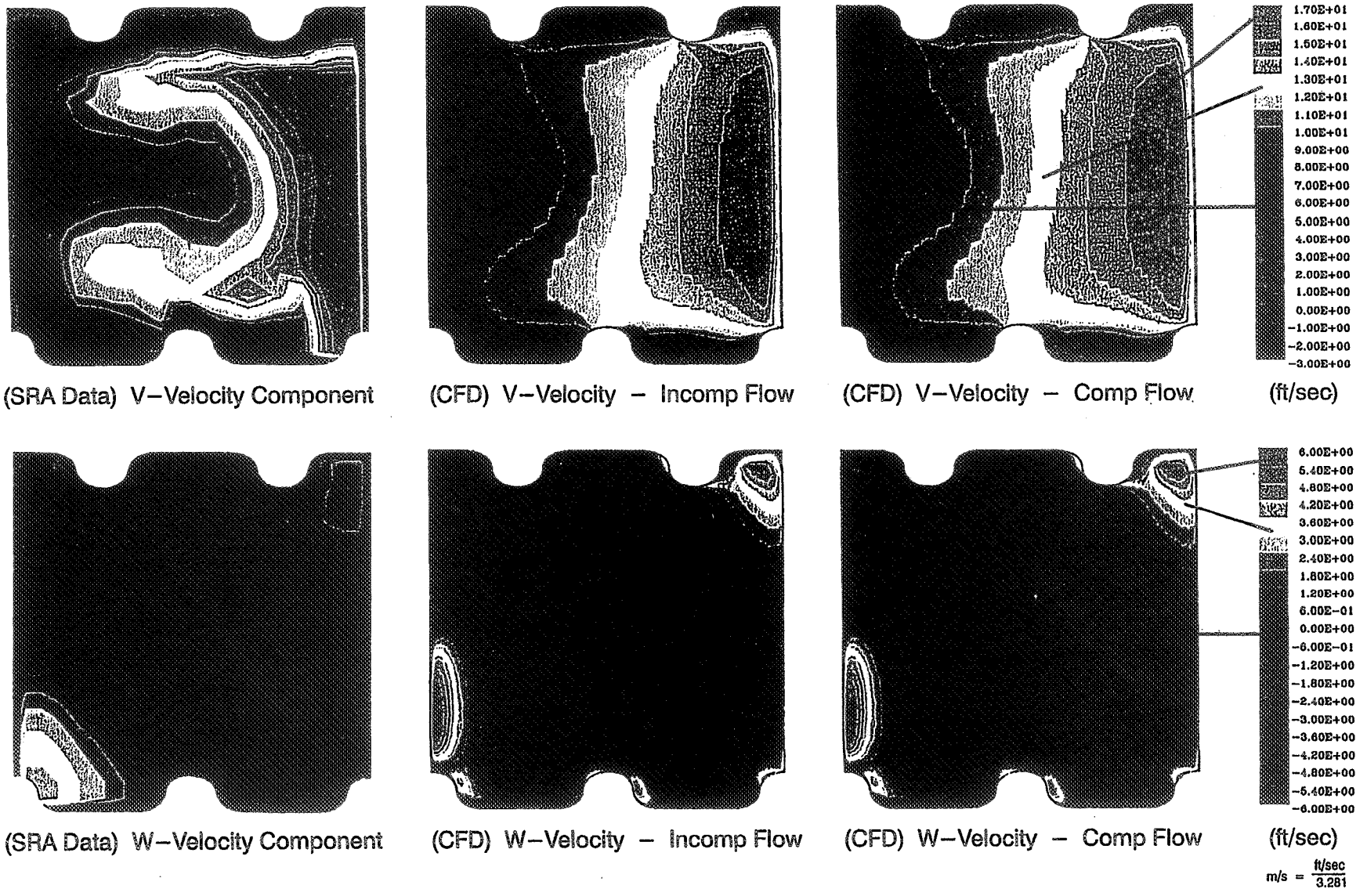

V-Component and W-Component Velocity Contours - Stationary Channel Location A2

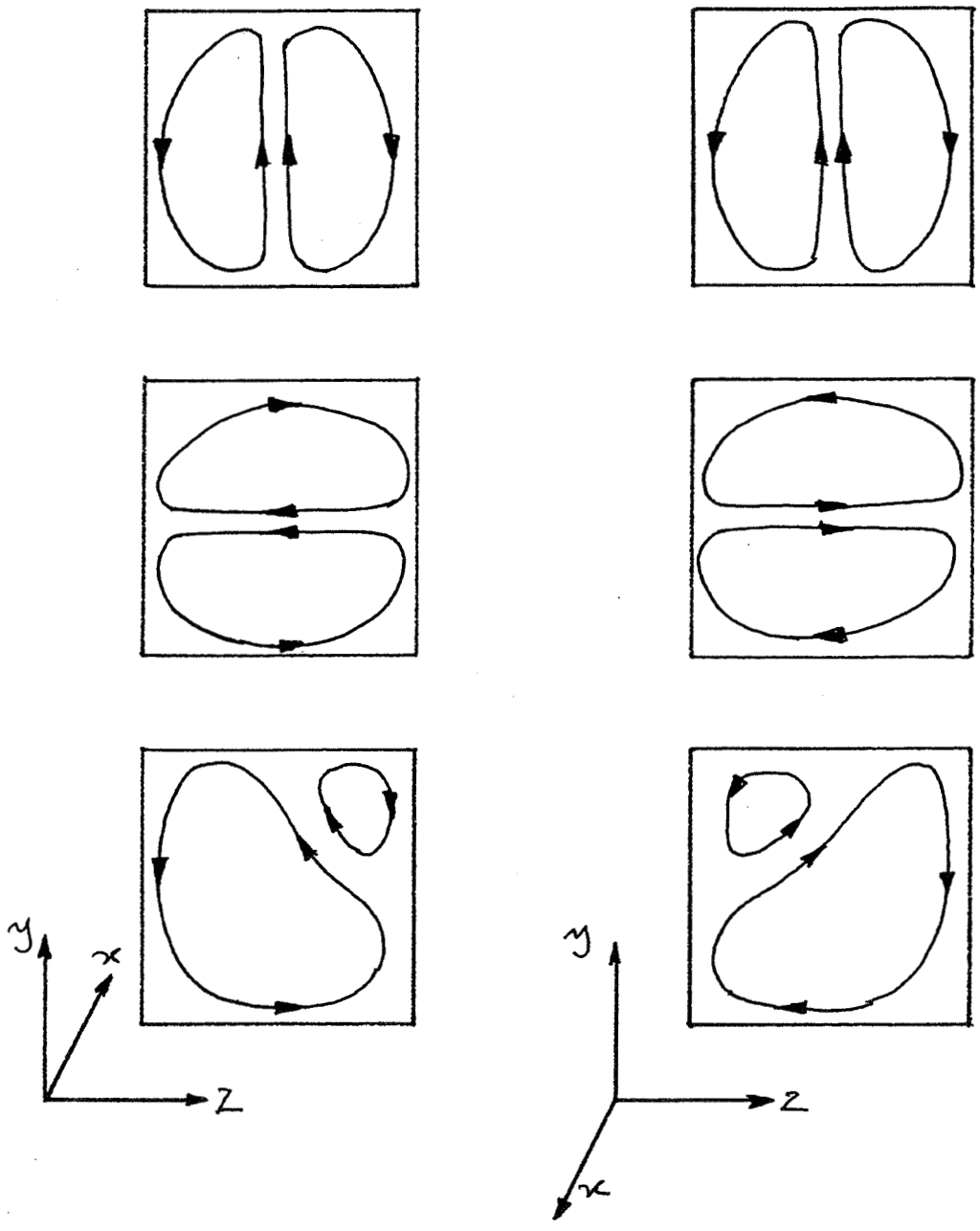
y
x
z
y
z
x

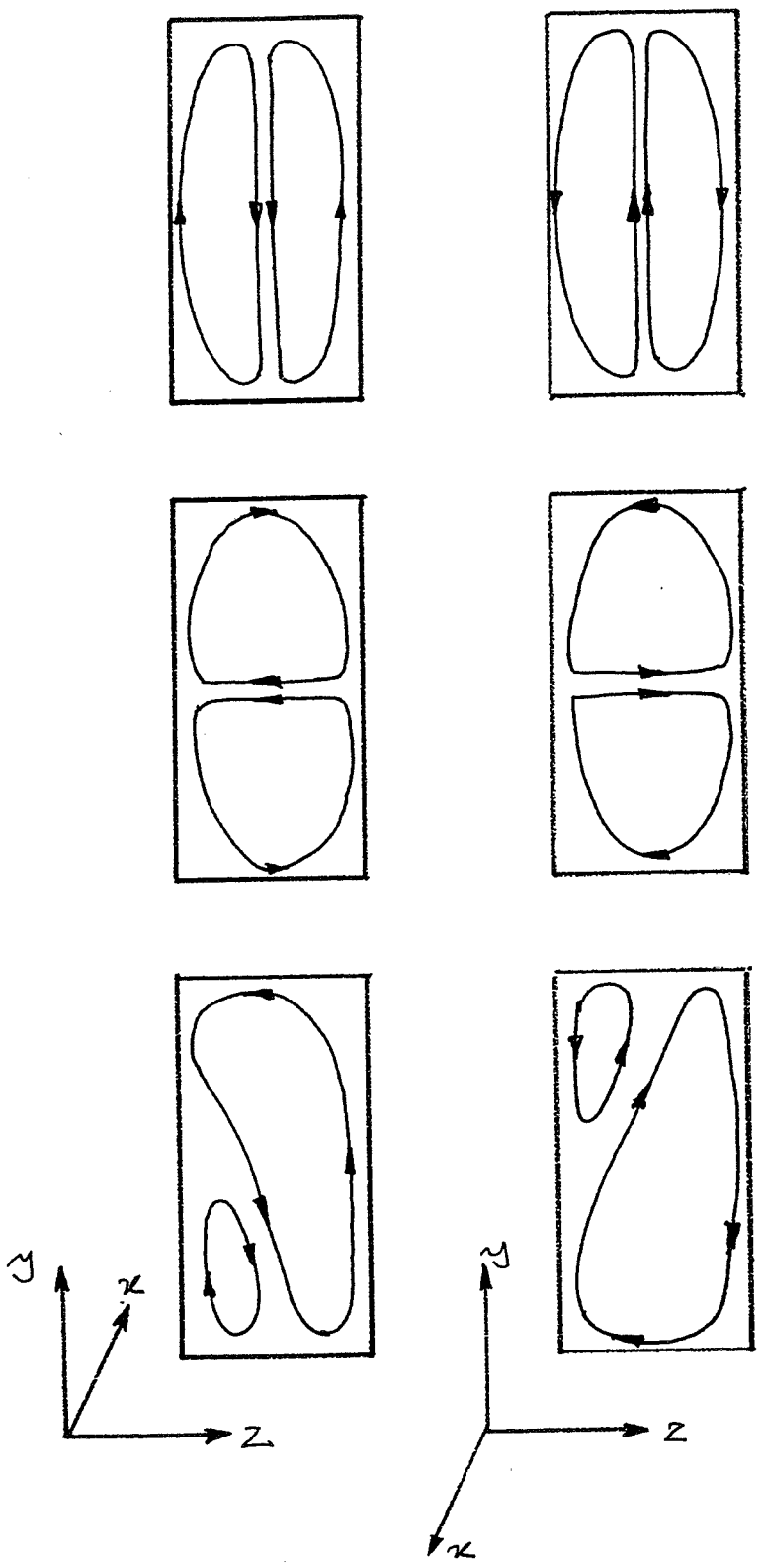
y
x
z
z
x

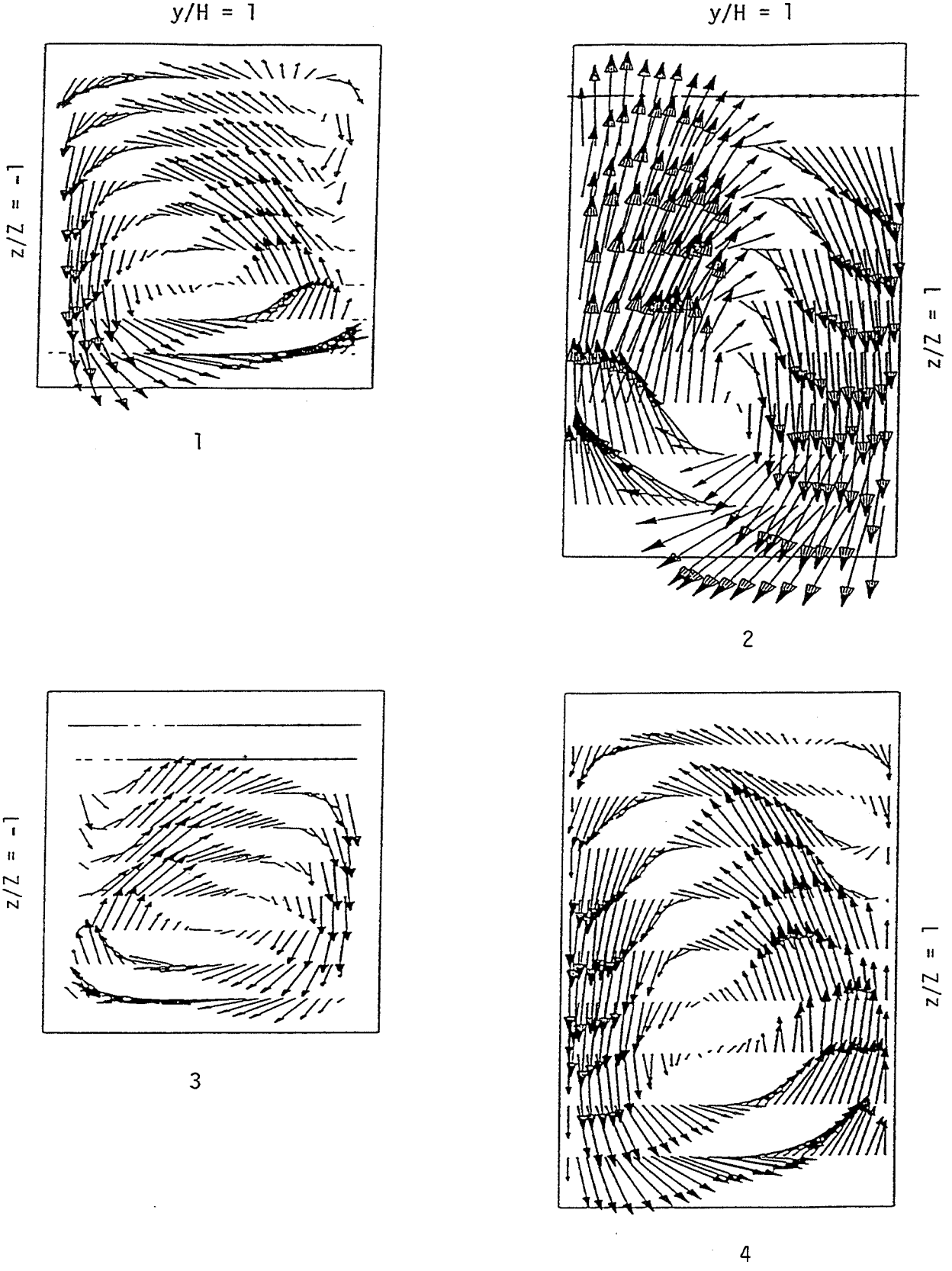

Velocity vectors

1 x/D = 7
2 lst turn, T1
3 1D downstream of T1
4 2nd turn, T2

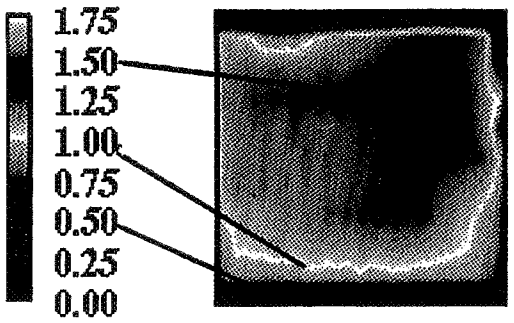

x/D = 1

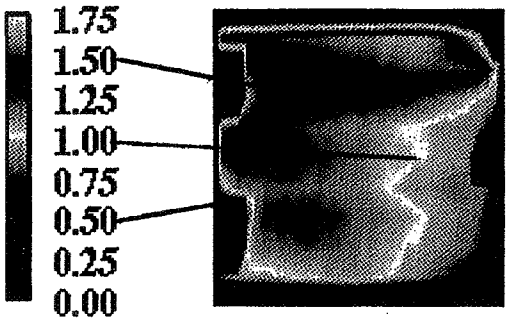

x/D = 4

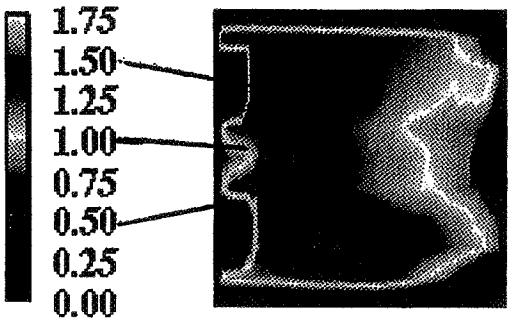

x/D = 7

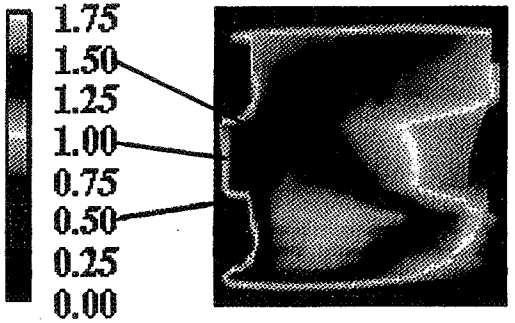

x/D = 10

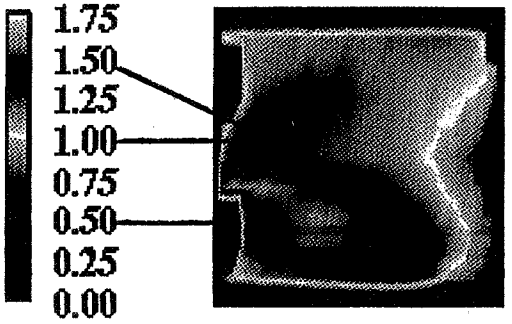

x/D = 12

Streamwise velocity contours

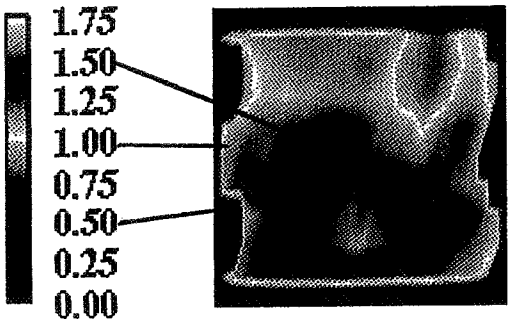

1D downstream of T1

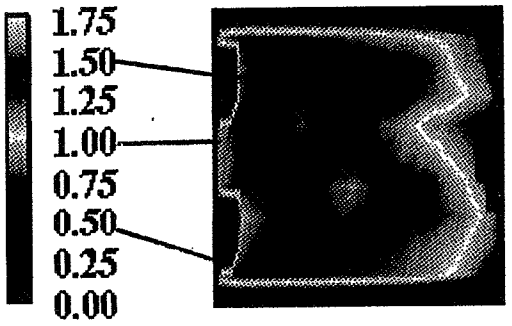

3D downstream of T1

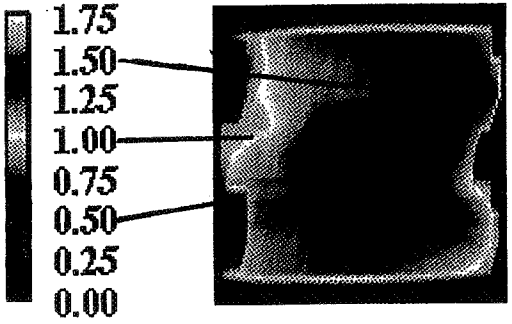

9D downstream of T1

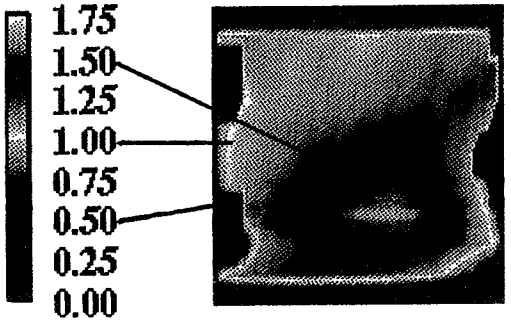

11D downstream of T1

Streamwise velocity contours

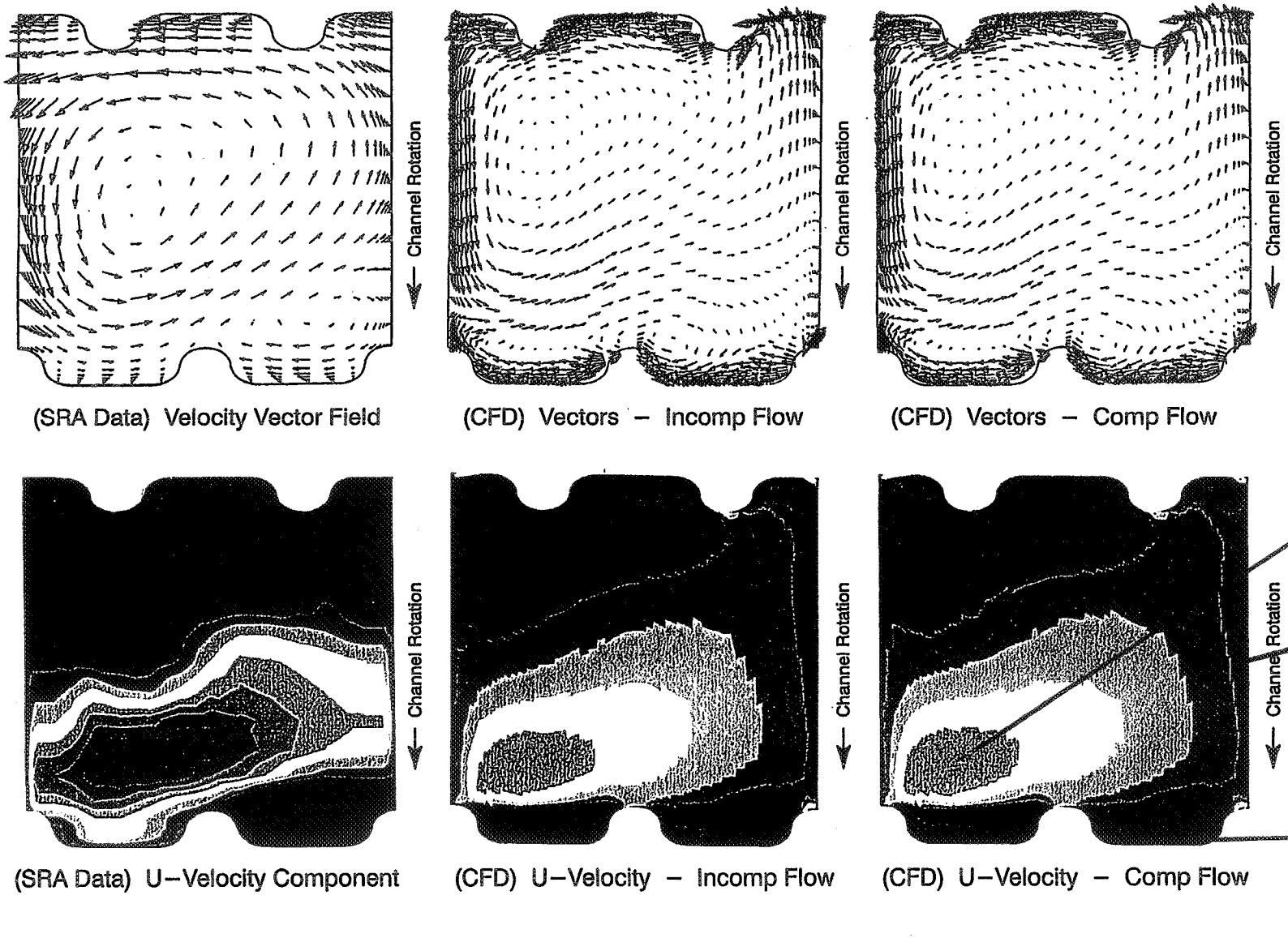

Velocity Vector Field and U–Component Velocity Contours – Rotating Channel Location D3

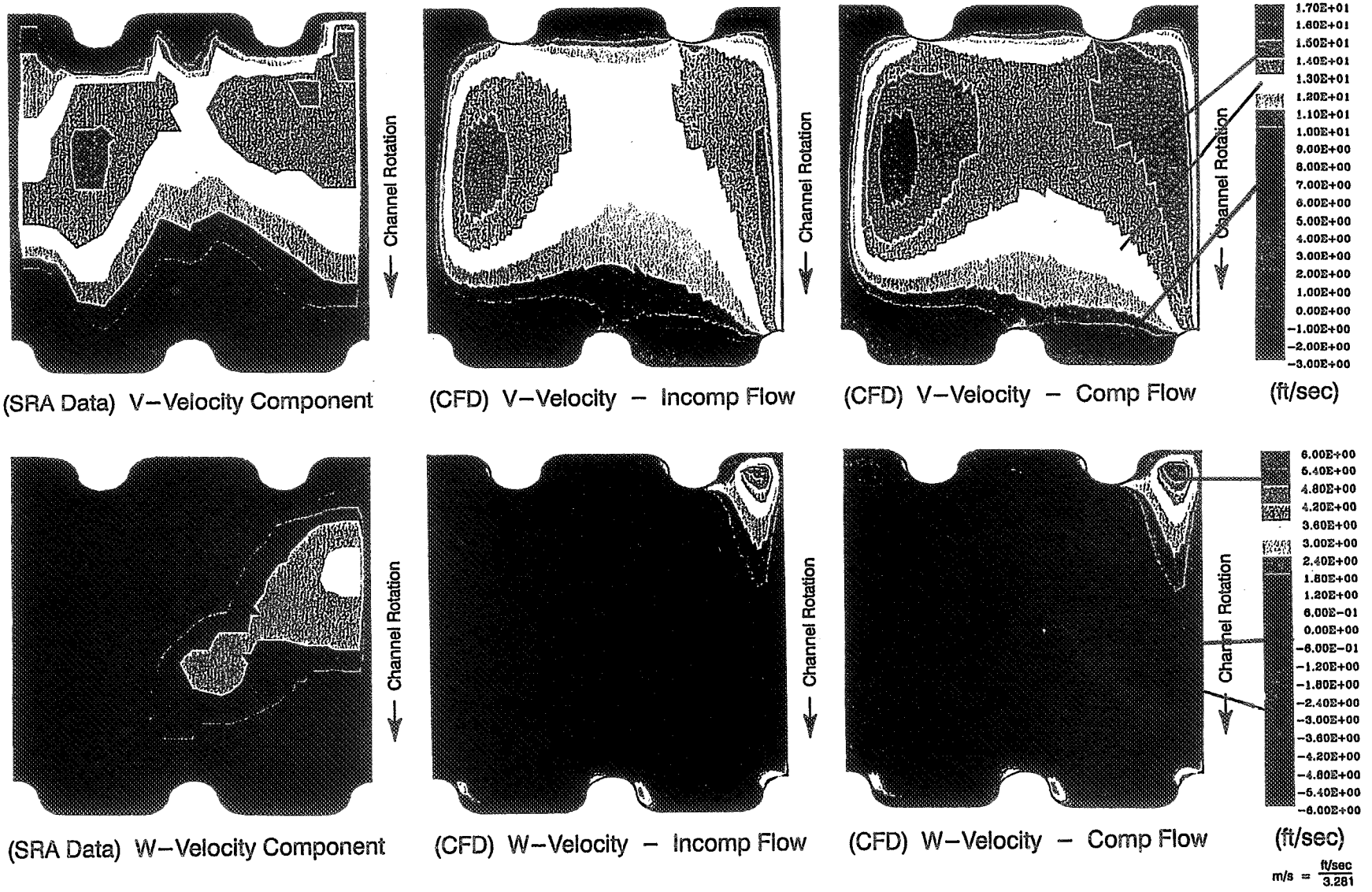

V-Component and W-Component Velocity Contours - Rotating Channel Location D3

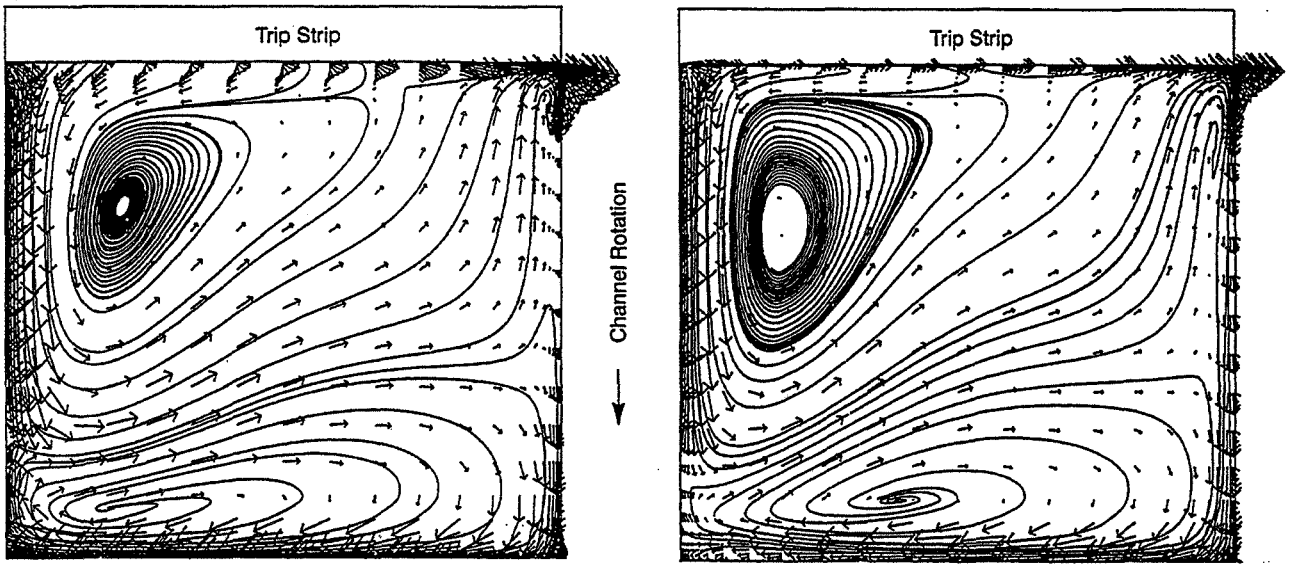

(a) Compressible Flow Channel Simulation
Rotating Channel (at i–Plane = 760)

(b) Compressible Flow "Conveyor–belt" Simulation
Rotating Channel Segment

Comparison of Secondary Flow Velocity Vector Fields—Channel vs "Conveyor-Belt" Simulation

CONCLUSIONS - 1: Stationary measurements (Re = 25,000 and Ro = 0.0)

- **Skewed trips generate strong secondary flows. Outward flow and trips skewed at -45° lead to a two-vortex structure with upward velocity of 0.6 U_b in the center and a downward velocity of -0.95 U_b at 0.09 D from the wall. When both trip orientation and flow direction are reversed, i.e., inward flow and trips skewed at +45°, the vortices circulate in the same direction. When either trip orientation or flow direction alone is reversed, the vortices circulate in the opposite direction.**

- **The streamwise development of primary flow is considerable, as a consequence of the strong secondary flow. Skewed trips transform a plug flow to two regions of high velocity, velocity exceeding 1.50 U_b close to the side walls within 12 D of entrance.**

CONCLUSIONS - 2: Rotating measurements (Re = 25,000 and Ro = 0.24)

- **With clockwise rotation, outward flow and trips skewed at -45° generate counter-clockwise swirl and a corner recirculation zone at the upper corner of the leading side. Inward flow and trips skewed at +45° generate clockwise swirl and a corner recirculation zone at the upper corner of the trailing side. Outward flow and trips skewed at +45° generates clockwise swirl and a corner recirculation zone at the lower corner of the trailing side.**

- **With trips skewed at +45°, the secondary flows remain qualitatively unaltered as the cross-flow proceeds from the first passage to the turn. The flow characteristics at these locations differ when trips are skewed at -45°. Changes in the flow structure are expected to augment heat transfer, in agreement with the heat transfer measurements of Johnson, et al. (1994). Trips skewed at -45° in the outward flow passage and trips skewed at +45° in the inward flow passage maximize heat transfer.**

CONCLUSIONS - 3: Computational (Re = 25,000 and Ro = 0.24)

- **The overall agreement between the SRA velocity data and the P&W CFD calculations is very good.**

- **The agreement between the "conveyor-belt" segment and the full skewed trip strip channel simulation is excellent.**

- **Flow, temperature and pressure fields in a ribbed-wall passage can be modeled by the assumption of a periodic repeating pattern in the streamwise direction.**

- **The use of "conveyor-belt" segment reduces the computational domain from ~1,700,000 grid points to ~100,000 grid points (less than 6% of the requirement for full channel simulation).**

MILESTONES

Experimental

- **RIM and laser velocimetry can produce highly detailed maps of flow field in a serpentine coolant passage.**

- **RIM requires an isothermal flow field and can not include buoyancy forces. However, it does quantify the effect of the interacting Coriolis and trip driven secondary flows and provides one more piece to the puzzle.**

Computational

- **Flow, temperature and pressure fields in a ribbed-wall passage can be modeled by the assumption of a periodic repeating pattern in the streamwise direction.**

- **The use of "conveyor-belt" segment reduces the computational domain from ~1,700,000 grid points to ~100,000 grid points (less than 6% of the requirement for full channel simulation).**

FUTURE WORK

- **SRA velocity data show that the flow in the first passage is characterized by a swirling vortex and a corner recirculation zone but the P&W CFD calculations show a third recirculation bubble in the inter-rib region.**

- **The largest difference between the experimental data and the numerical simulation is in the inter-rib region. The differences could be in part due to the sparse nature of the data set near the wall. The resolution of the existing LDV system in the inter-rib region is inadequate.**

- **Improved resolution can be achieved by microscopic imaging and PIV. PIV utilizes a laser sheet and resolves the diffraction problem associated with the crossing of two laser beams.**

- **Microscopic imaging and PIV has the potential to investigate air flow and address experimentally the effect of buoyancy.**

ASSESSMENT OF HEAT TRANSFER COEFFICIENTS IN TURNS OF TURBINE BLADE COOLANT PASSAGES

Joel Wagner
United Technologies Research Center
East Hartford, Connecticut

Objective

- **Experimentally measure, assess, and analyze the heat transfer within the internal cooling configuration of a serpentine coolant passage for comparison with CFD and numerical heat transfer prediction codes.**

Approach

- **Conduct experiments using rotating models employing previously developed measurement techniques, including a transient heat transfer technique and liquid crystals to determine the heat transfer distribution throughout the model coolant passage.**

Status

- Design and Fabrication
- H(0.5) Model Tests
- Analysis and Final Report

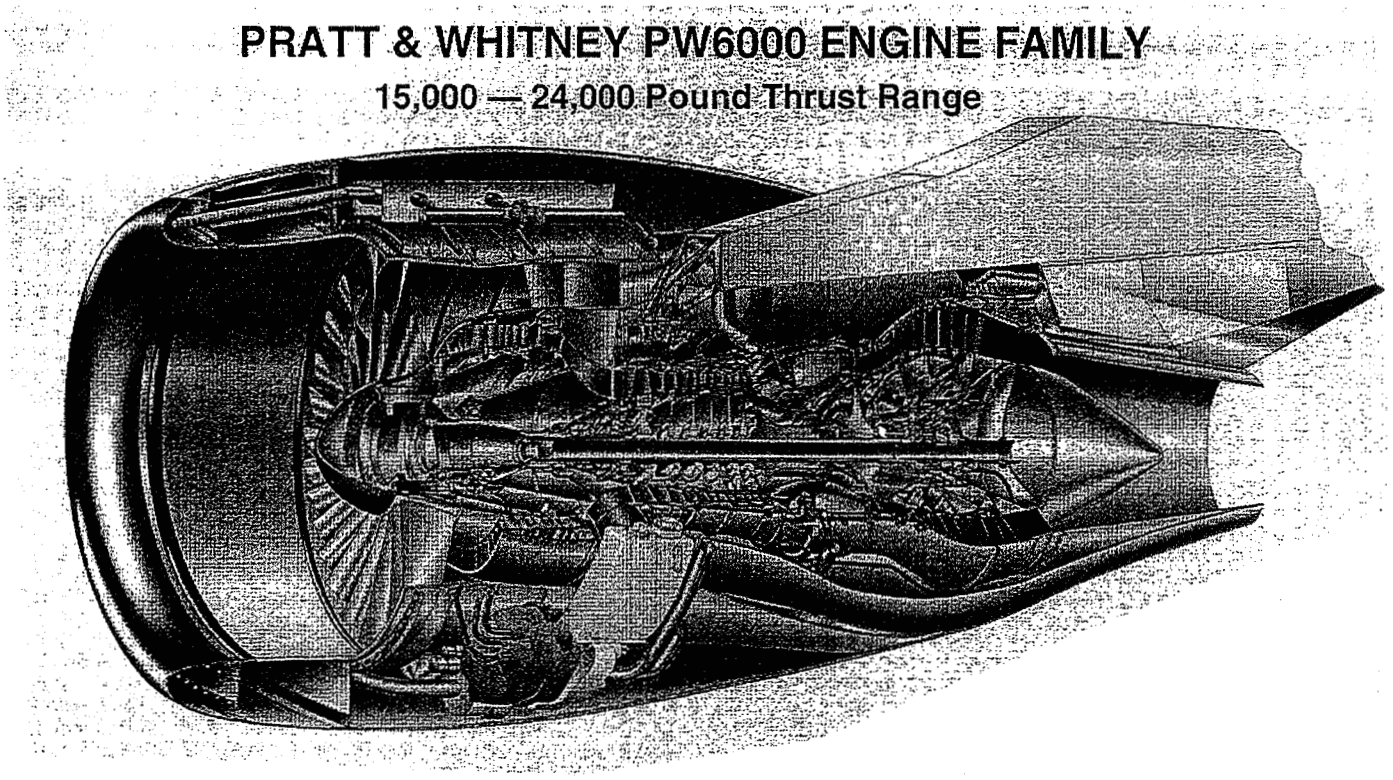

UTRC Rotating Heat Transfer Facility

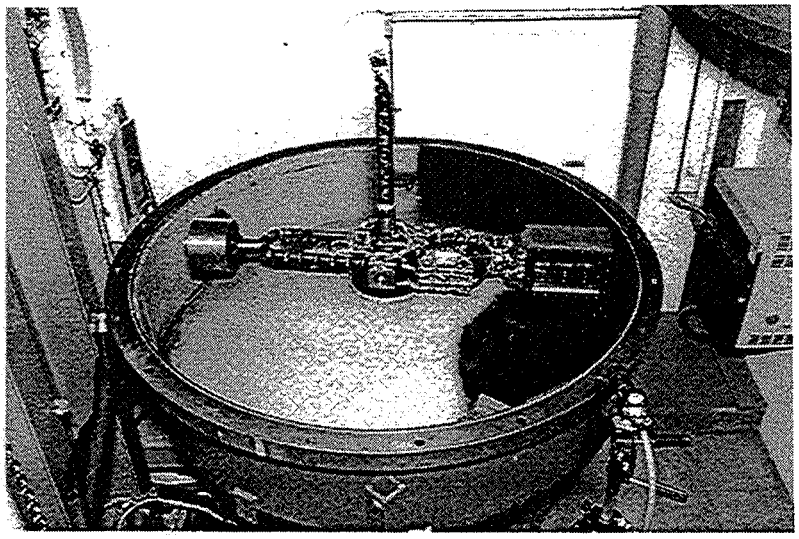

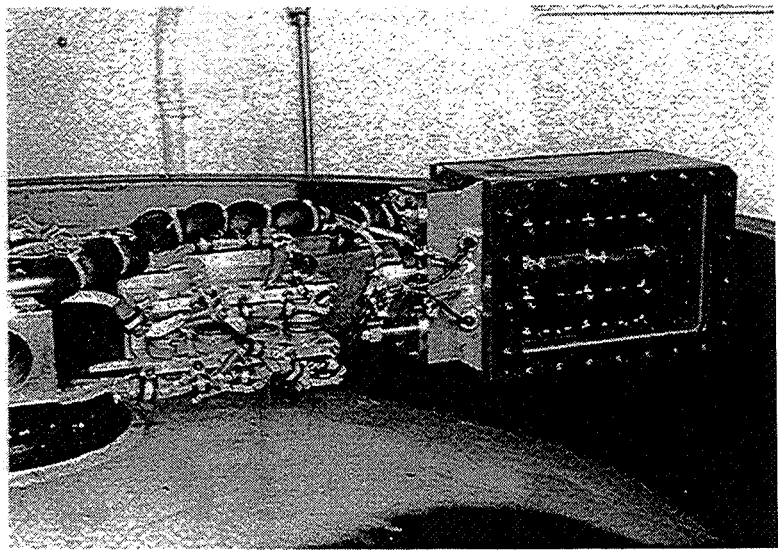

Photograph of NASA HOST Model

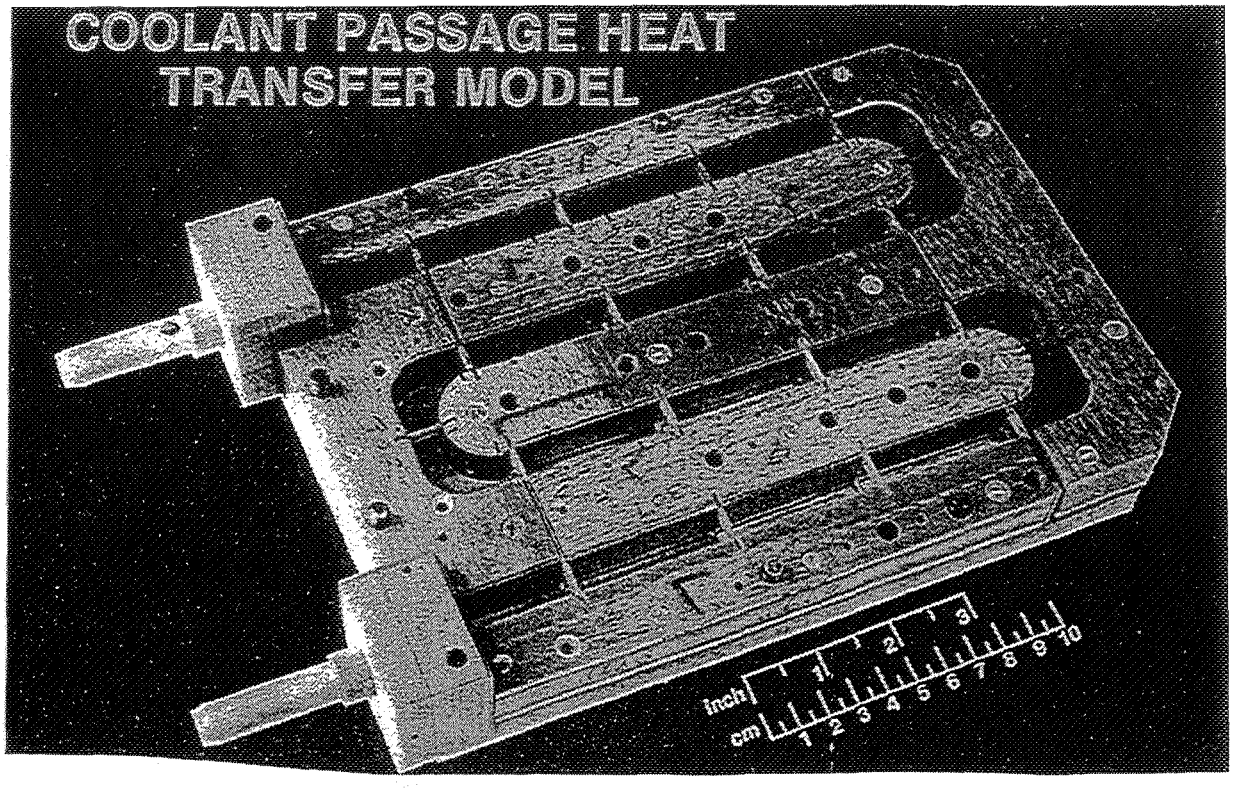

Heat Transfer Ratio - NASA HOST - 1st Passage - Middle

Symbol	○	◇	⬠	△	▷	□	◿	▽
Rotation No.	0.00	0.006	0.05	0.12	0.18	0.25	0.35	0.50

Re = 25,000 α = 0 $\bar{R}/d$ = 49

Skewed Trips - open symbols
Smooth Wall - solid symbols

HP - High Pressure
LP - Low Pressure

Symbol Flag	ΔT_{in} °C (°F)
	22.4 (40)
	44.4 (80)
	66.7 (120)
	88.9 (160)

Heat Transfer Ratio, Nu/Nu_∞

Leading Surface

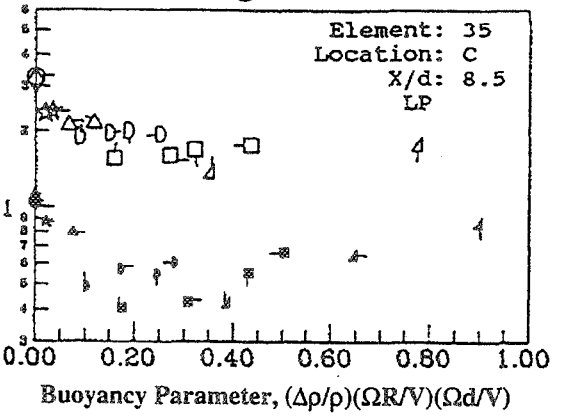

Buoyancy Parameter, $(\Delta\rho/\rho)(\Omega R/V)(\Omega d/V)$

Trailing Surface

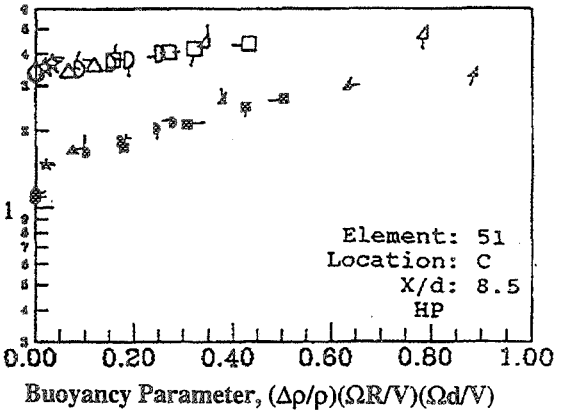

Buoyancy Parameter, $(\Delta\rho/\rho)(\Omega R/V)(\Omega d/V)$

Heat Transfer Ratio - NASA HOST - 1st Turn - In

Symbol	○	◇	☆	△	▷	□	◿	▽
Rotation No.	0.00	0.006	0.05	0.12	0.18	0.25	0.35	0.50

Re = 25,000 α = 0 $\bar{R}/d$ = 49

Skewed Trips - open symbols
Smooth Wall - solid symbols

Symbol Flag	ΔT_{in} °C (°F)
	22.4 (40)
	44.4 (80)
	66.7 (120)
	88.9 (160)

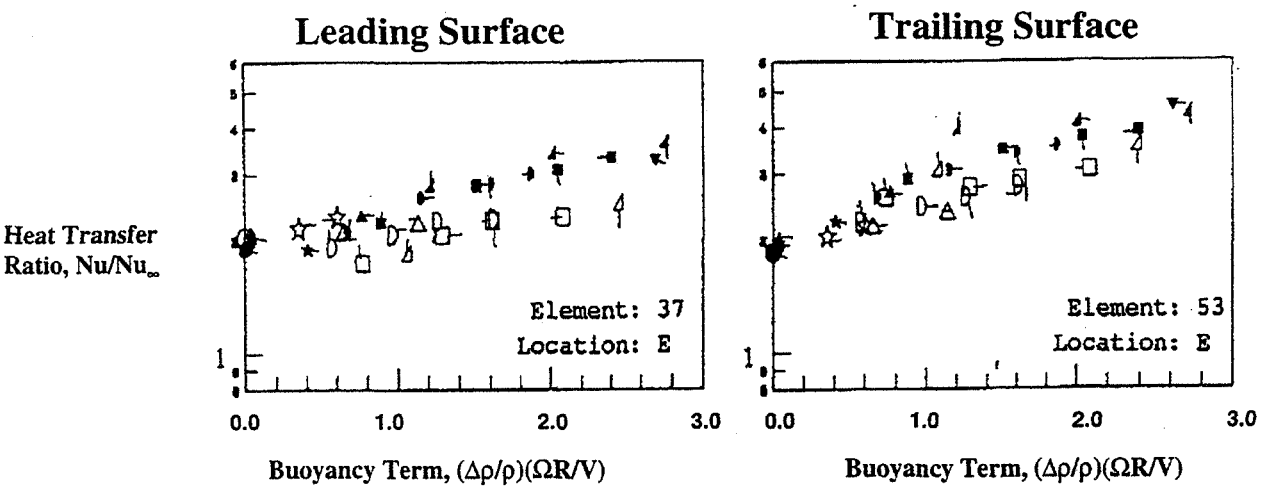

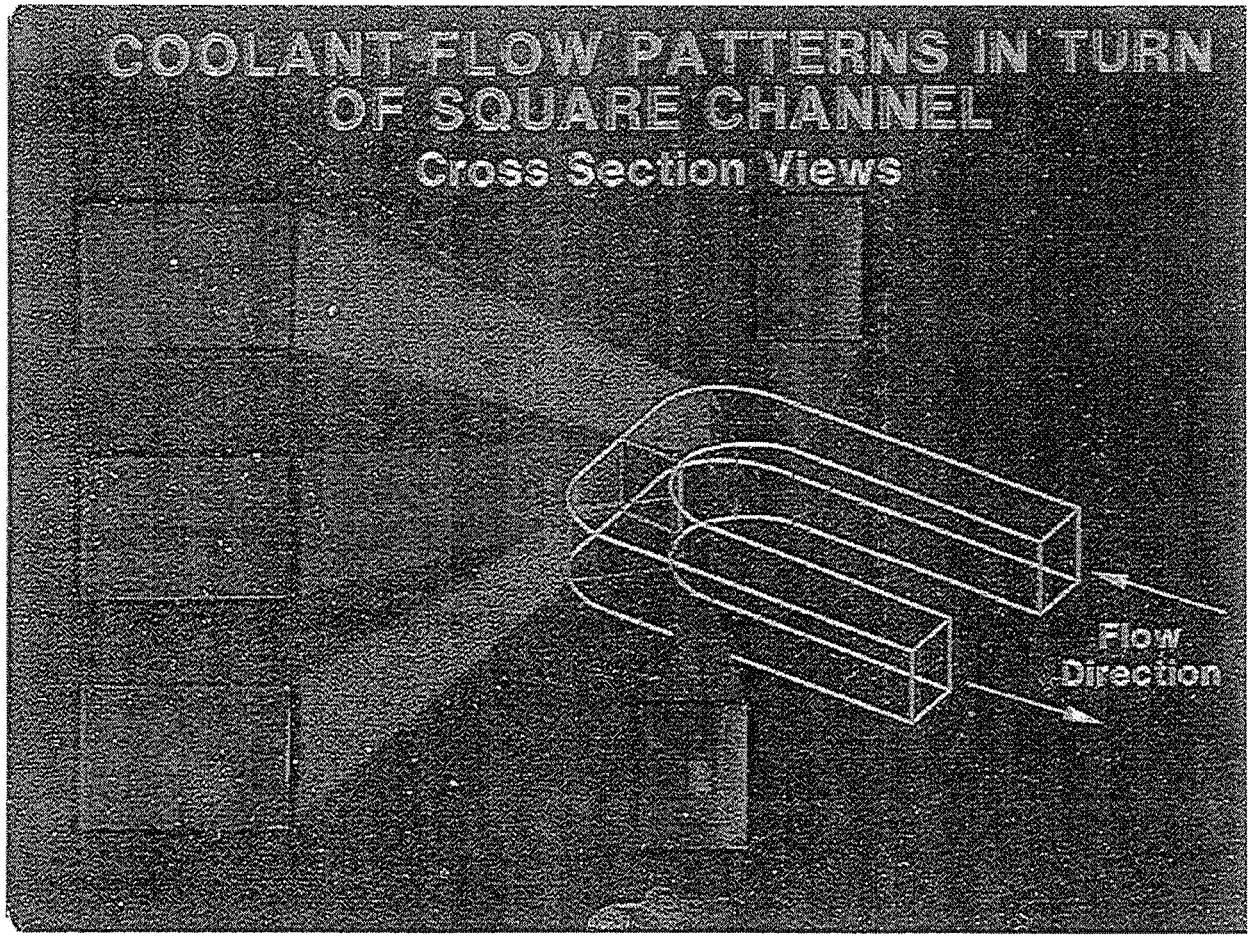
COOLANT FLOW PATTERNS IN TURN OF SQUARE CHANNEL
Cross Section Views
Flow Direction

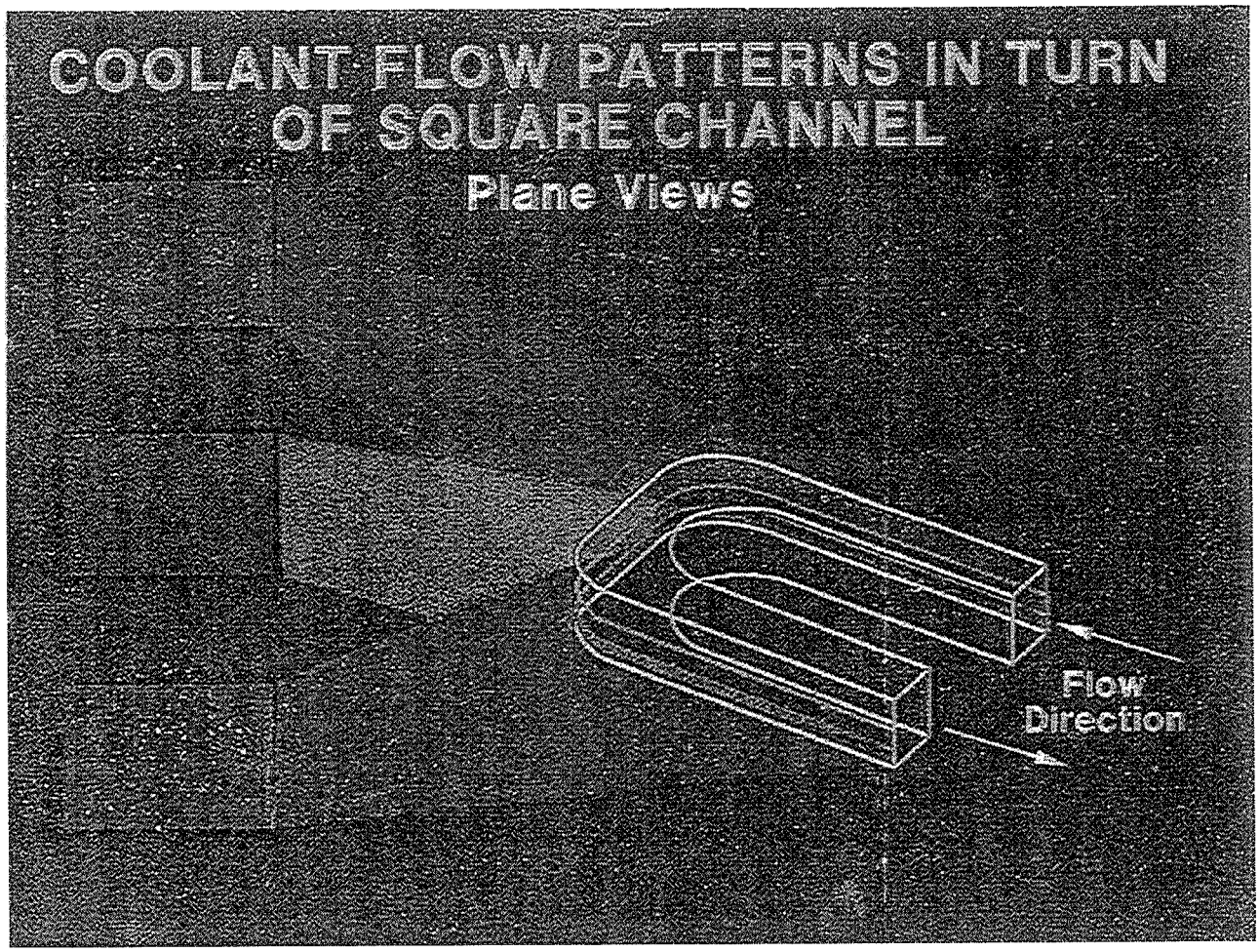
COOLANT FLOW PATTERNS IN TURN OF SQUARE CHANNEL
Plane Views
Flow Direction

Low Cost Models Employed to Simulate Advanced Turbine Blade Cooling

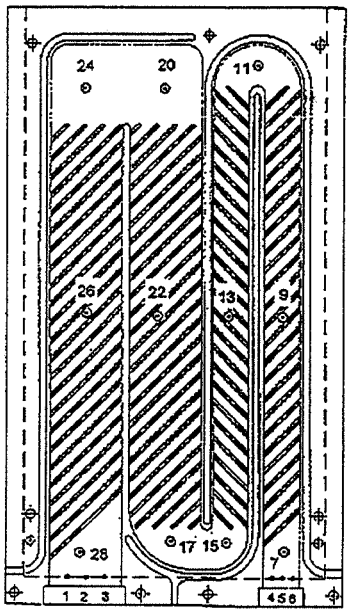

NASA/UTRC Model

Thermocouple Layout

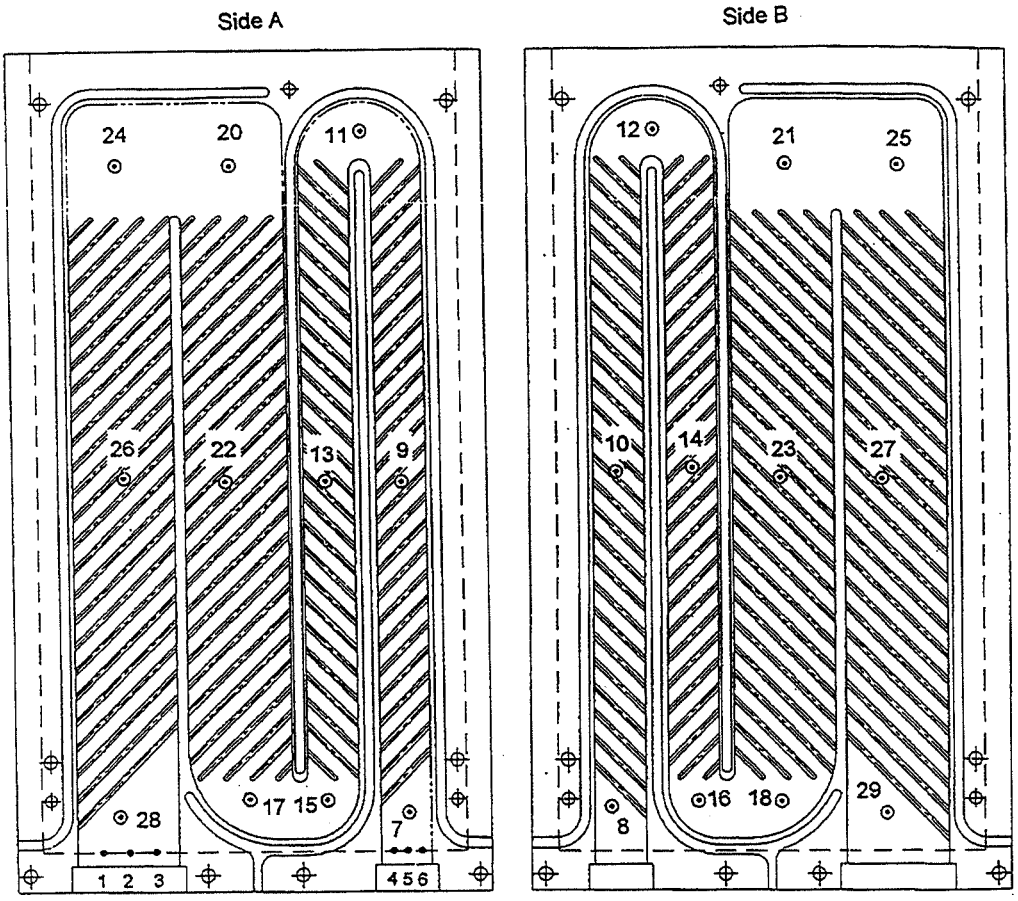

Photograph of Model

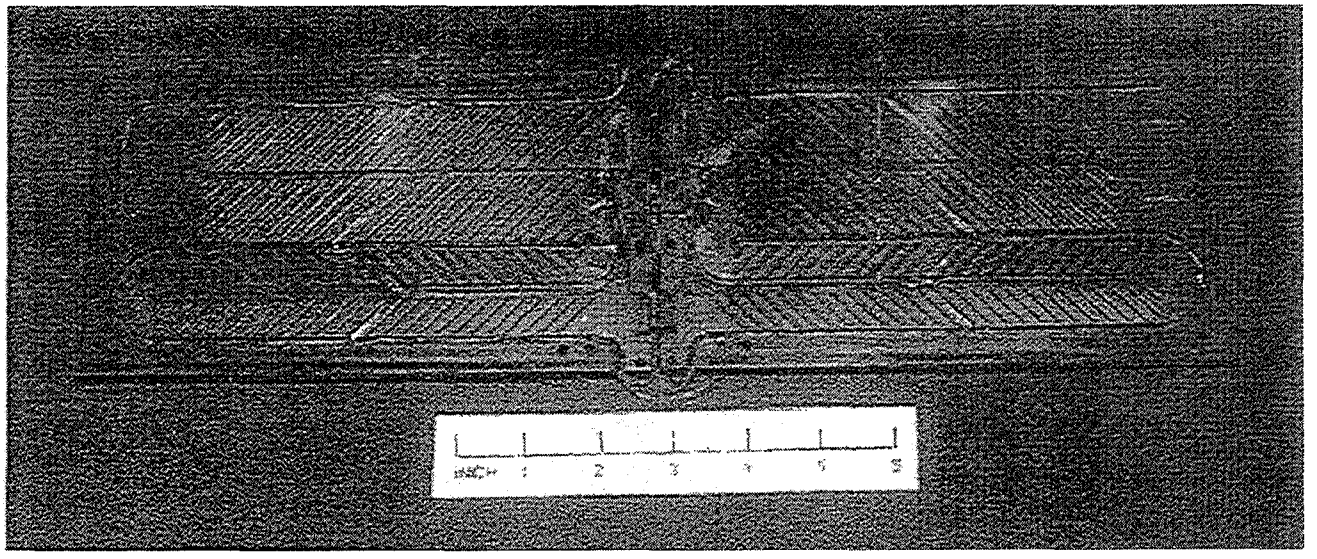

Test Matrix

	Test No.				Basic Dimensional Parameters							Secondary Dimensionless Parameters					
	UTRC Run.Pt		Series #									1st Passage Width= 0.5000			4th Passage Width= 1.0000		
	FD1	FD4	FD1	FD4	Ω rpm	m-dot lb/sec	Pr psia	T bulk (F)	T initial (F)	α deg	δρ/ρ	Re-D	Ro-h	Gr/Re^2	Re-D	Ro-h	Gr/Re^2
*	25.02	19.05	301	401	0	0.0062	147.0	10	160	0	0.15	12000	0.000	0.0000	8000	0.000	0.0000
	26.01	19.06		402	0	0.0132	147.0	10	180	0	0.15	25000	0.000	0.0000	16667	0.000	0.0000
*	25.01	19.03	303	403	0	0.0264	147.0	10	180	0	0.15	50000	0.000	0.0000	33333	0.000	0.0000
	27.01											25000	0.240				
		21.06		404	87	0.0063	117.6	50	135	0	0.07	12000	0.060	0.0129	8000	0.120	0.0516
*	24.04	21.05	305	405	139	0.0063	147.0	50	135	0	0.07	12000	0.120	0.0516	8000	0.240	0.2064
		21.04		406	146	0.0132	147.0	50	140	0	0.07	25000	0.060	0.0129	16667	0.120	0.0516
		21.03		407	293	0.0132	147.0	50	140	0	0.07	25000	0.120	0.0516	16667	0.240	0.2064
		21.02		408	293	0.0264	147.0	50	140	0	0.07	50000	0.060	0.0129	33333	0.120	0.0516
*	24.03	21.01	309	409	585	0.0264	147.0	50	140	0	0.07	50000	0.120	0.0516	33333	0.240	0.2064
		20.05		410	85	0.0062	117.6	10	160	0	0.15	12000	0.060	0.0276	8000	0.120	0.1106
*	24.02	20.04	311	411	136	0.0062	147.0	10	160	0	0.15	12000	0.120	0.1106	8000	0.240	0.4424
		20.01		412	146	0.0132	147.0	10	180	0	0.15	25000	0.060	0.0276	16667	0.120	0.1106
		20.03		413	292	0.0132	147.0	10	180	0	0.15	25000	0.120	0.1106	16667	0.240	0.4424
		20.06		414	292	0.0264	147.0	10	180	0	0.15	50000	0.060	0.0276	33333	0.120	0.1106
*	24.01	20.08	315	415	585	0.0264	147.0	10	180	0	0.15	50000	0.120	0.1106	33333	0.240	0.4424
	23.04	22.06	316	416	139	0.0063	147.0	50	135	45	0.07	12000	0.120	0.0516	8000	0.240	0.2064
	23.02	22.03	317	417	136	0.0062	147.0	10	160	45	0.15	12000	0.120	0.1106	8000	0.240	0.4424
	23.03	22.05	318	418	585	0.0264	147.0	50	140	45	0.07	50000	0.120	0.0516	33333	0.240	0.2064
	23.01	22.04	319	419	585	0.0264	147.0	10	180	45	0.15	50000	0.120	0.1106	33333	0.240	0.4424

Note: FD1 - Flow Inlet in 0.5 in. wide passage
FD4 - Flow Inlet in 1.0 in. wide passage
* - Tests for alternate turn geometires

Temperature

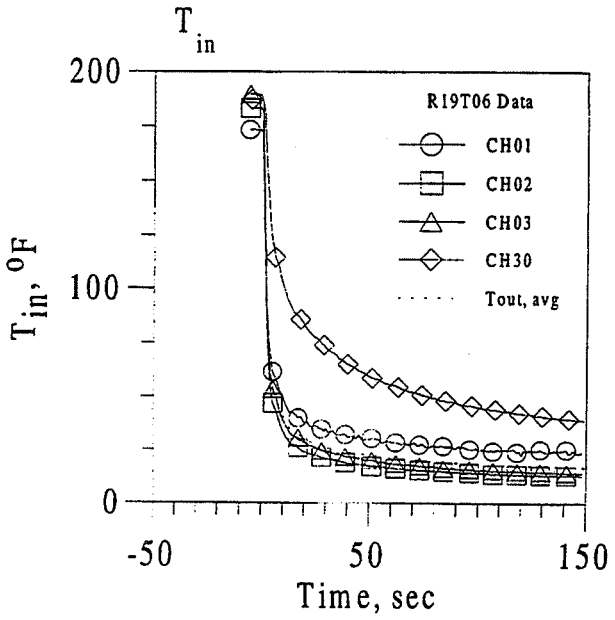

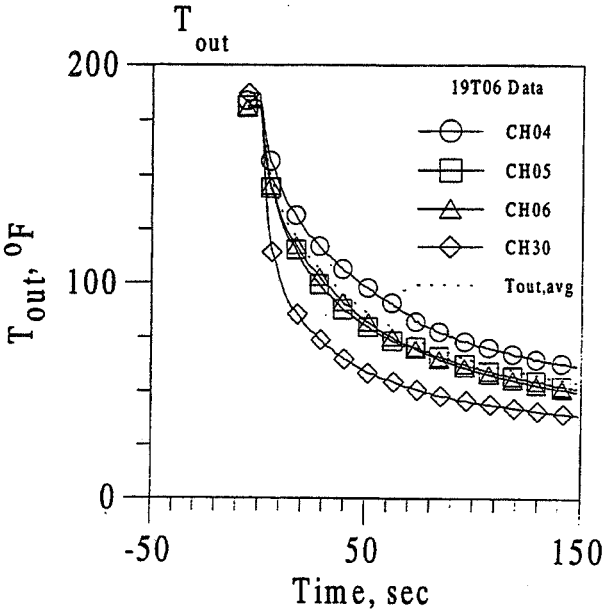

Temperature

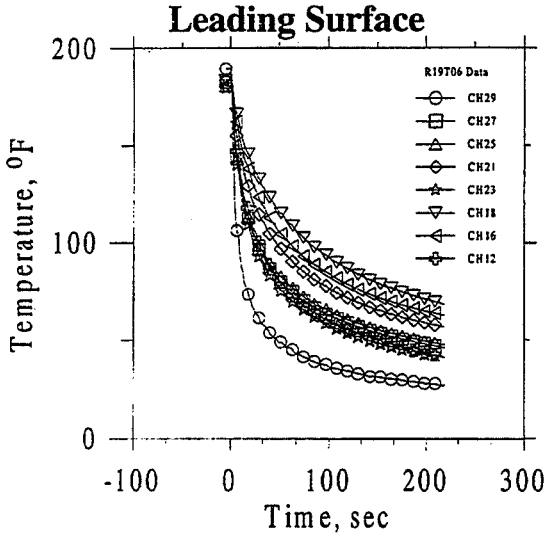

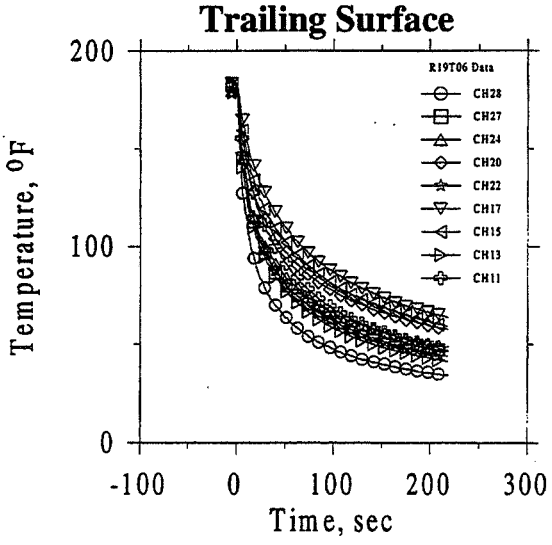

Heat Flux

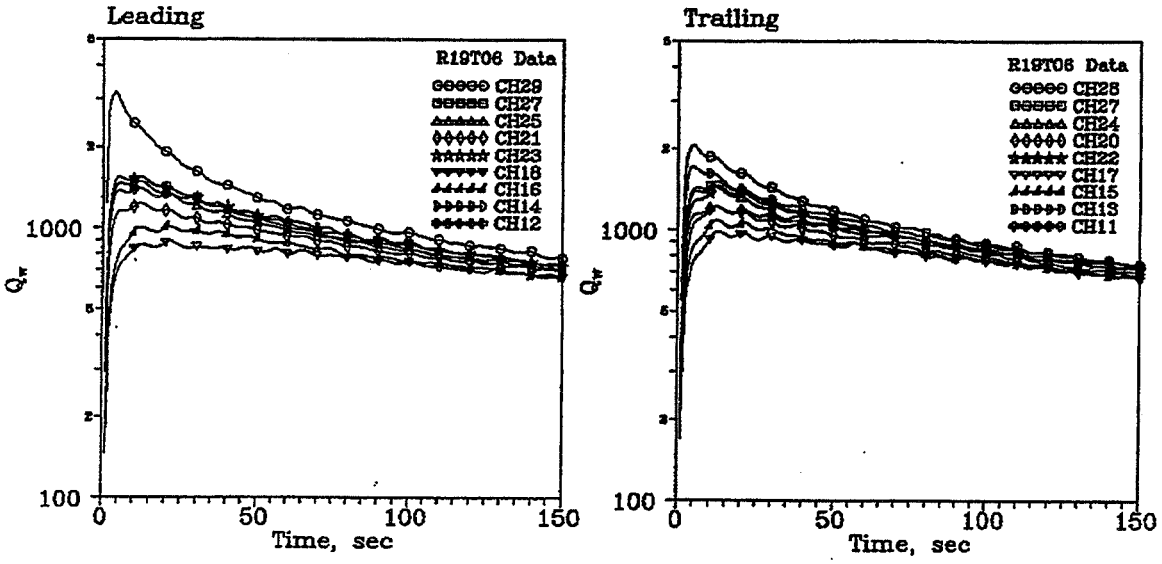

Heat Transfer Ratio - 1st Passage - Middle

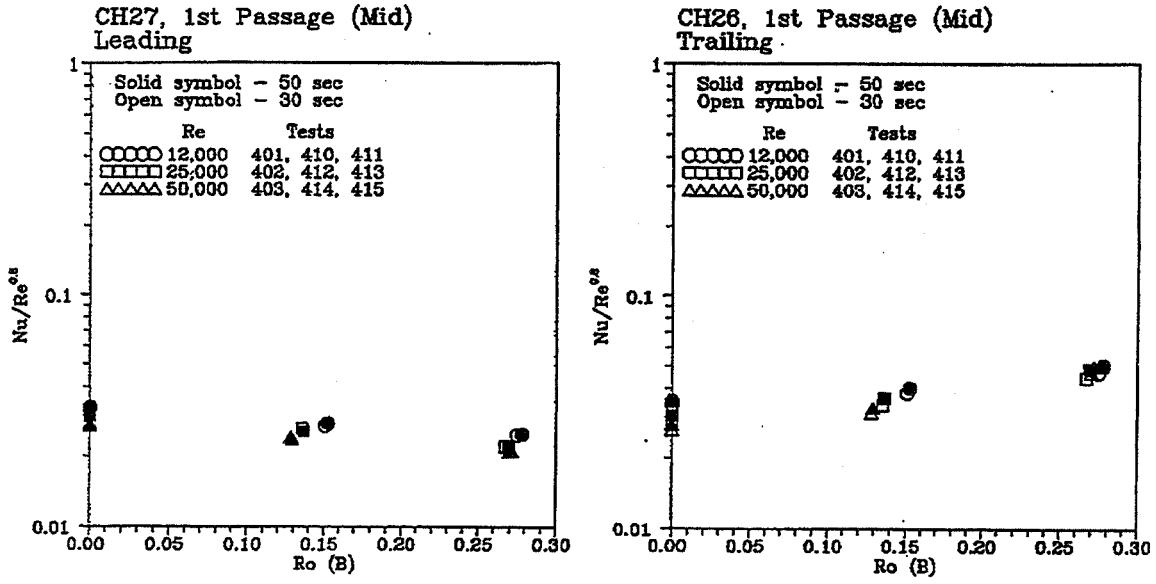

Heat Transfer Ratio - 1st Turn - In

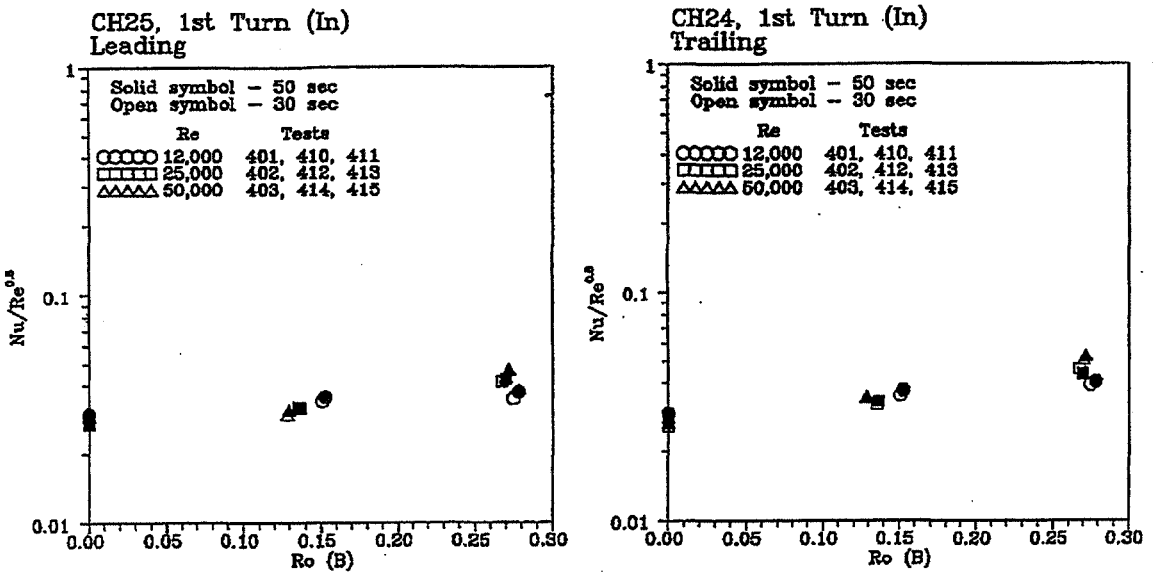

Results

- **Thermocouple results show significant increases in heat transfer in the tip and root turn regions. Liquid crystal results show variation in heat transfer distribution in turns due to flow and thermal conditions.**

Heat Transfer Distribution

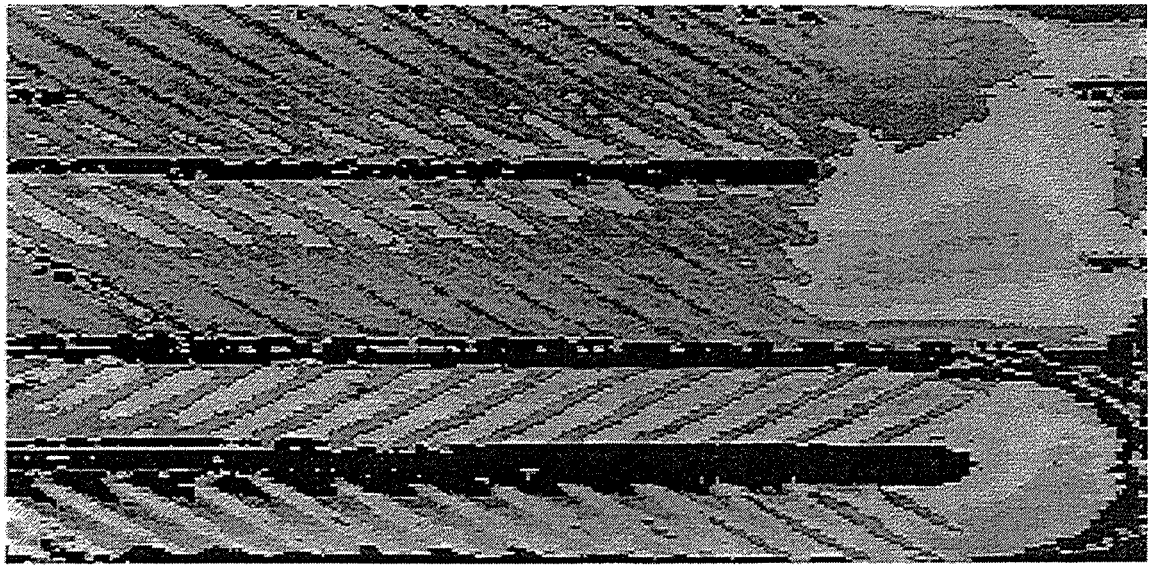

EXPERIMENTAL MULTIPASS HEAT TRANSFER WITH TRIPS AND BLEED

Douglas Thurman and Philip Poinsatte
NASA Lewis Research Center
Cleveland, Ohio

Testing is currently in progress to acquire simple geometry surface heat transfer data for internal channels with trips and bleed holes which can be used in the development and validation of models. The transient liquid crystal technique is used on a simple multipass model with rectangular channels and normal ribs. Normal bleed holes are located on the floor of the model in the first channel. Each hole is attached to a flow meter, allowing various bleed flow rates to simulate external pressures on the blade.

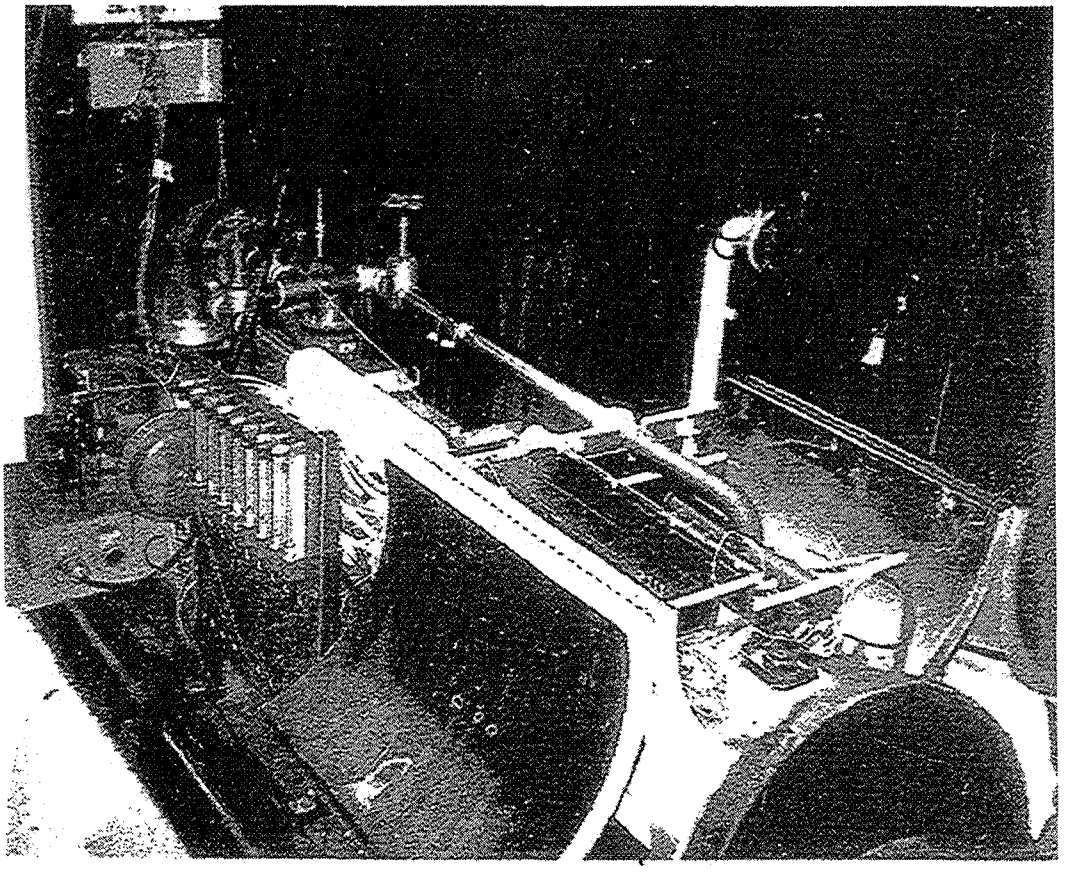

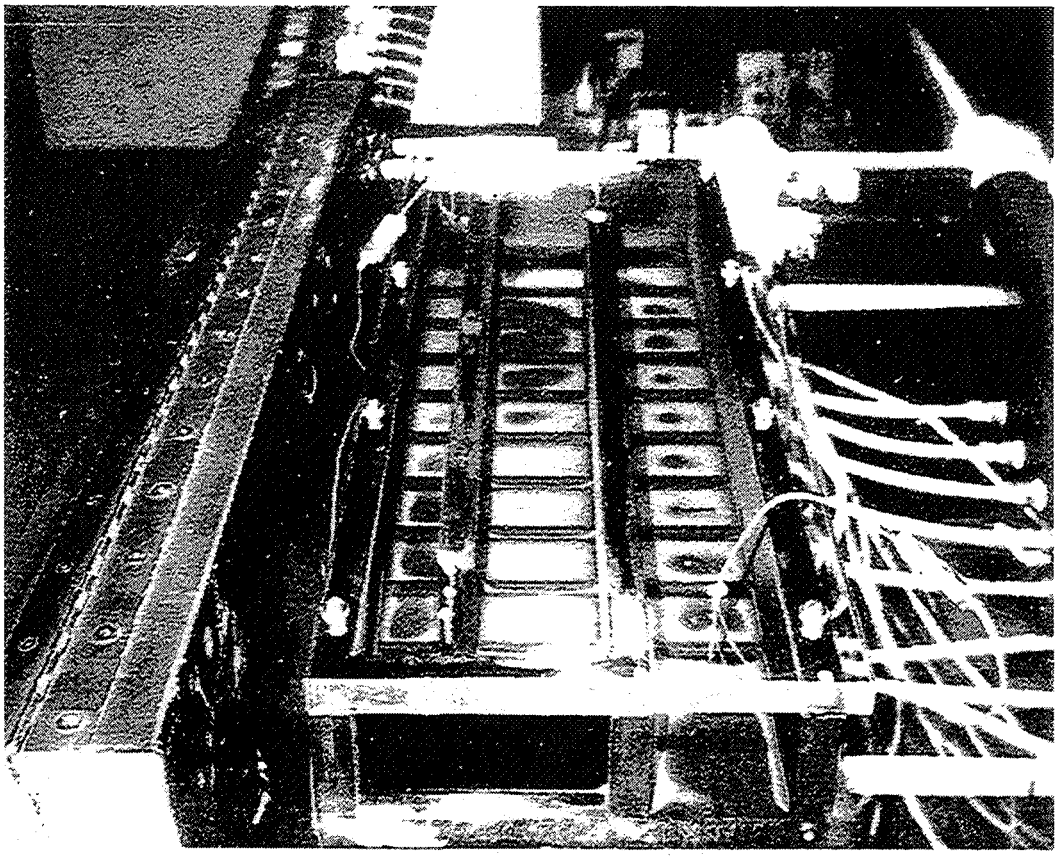

No Ribs

Re_{inlet} = 42,000

Nu/Nu_{ref}	= 2.8, 4.7
	= 1.8, 2.8
	= 1.6, 2.4
	= 1.4, 2.0
	= 1.1, 1.6
	= 1.0, 1.4
	= .9, 1.2

45° Ribs

Re_{inlet} = 42,000

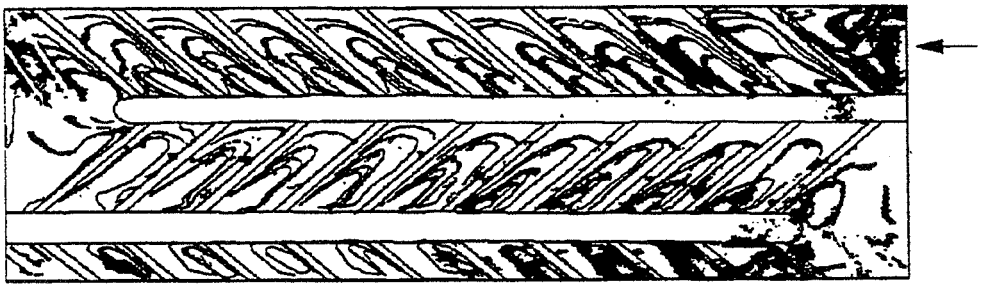

Nu/Nu_{ref}	= 14, –
	= 9.4, 59
	= 6.8, 21
	= 3.1, 5.7
	= 1.9, 3.4

90° Ribs
Low Re_{inlet} = 43,000

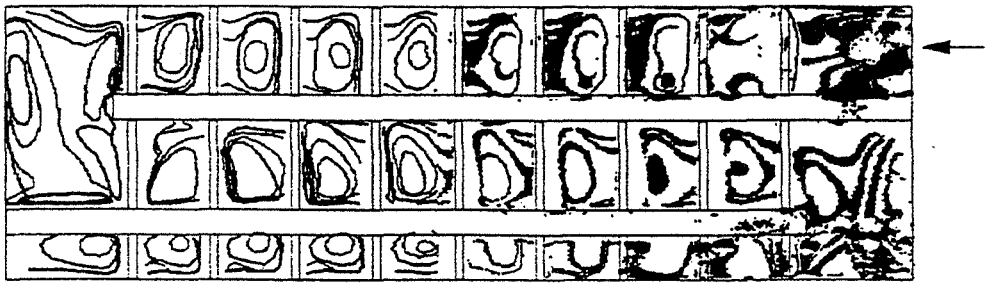

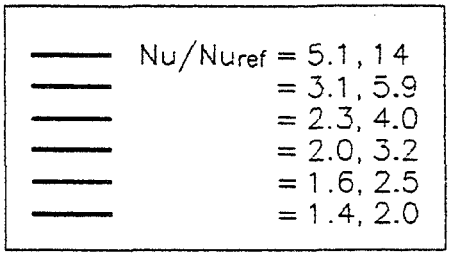

Uniform Bleed
Re_D = 28,600

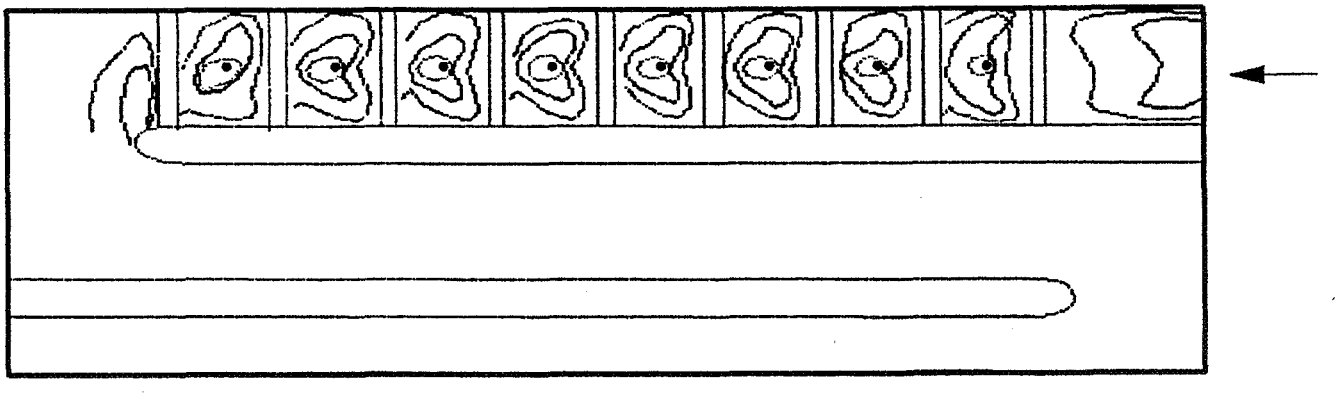

Increasing Bleed
$Re_D = 28,400$

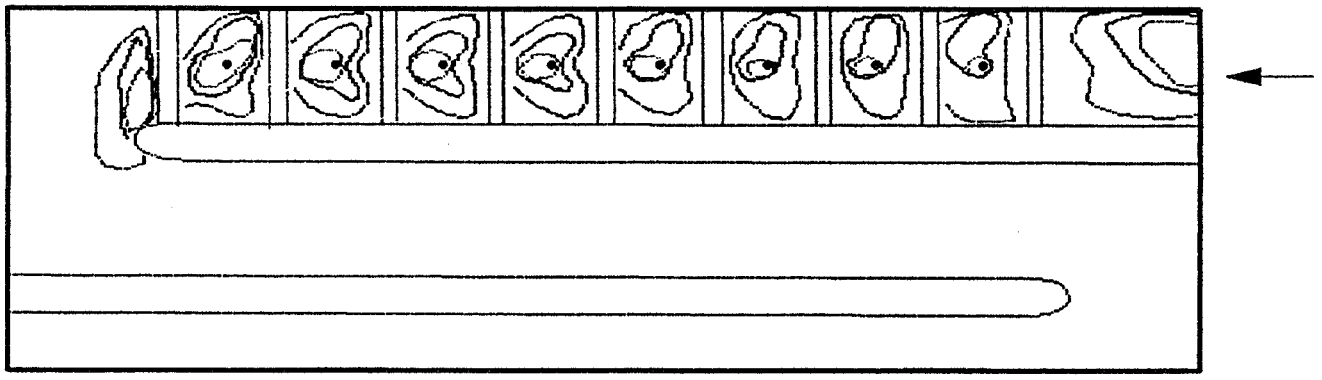

Decreasing Bleed
$Re_D = 28,400$

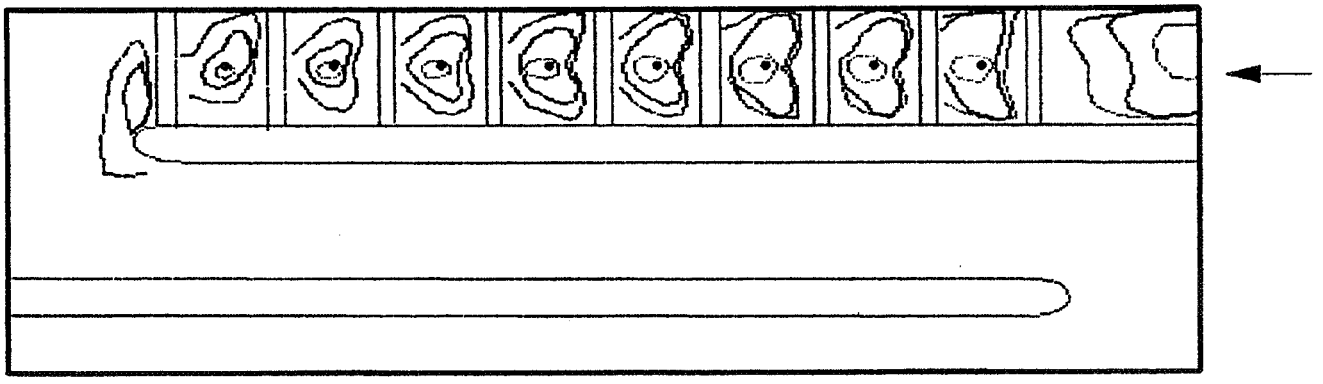

AIRSTREAM TEMPERATURE MEASUREMENTS THROUGH A 3-LEG/2-TURN REAL GEOMETRY MODEL

Temperature fluctuated somewhat (especially in the first leg) but "generally" the temperature rise through the model could be modeled linearly with a few anomalies (especially in turns) which are being examined.

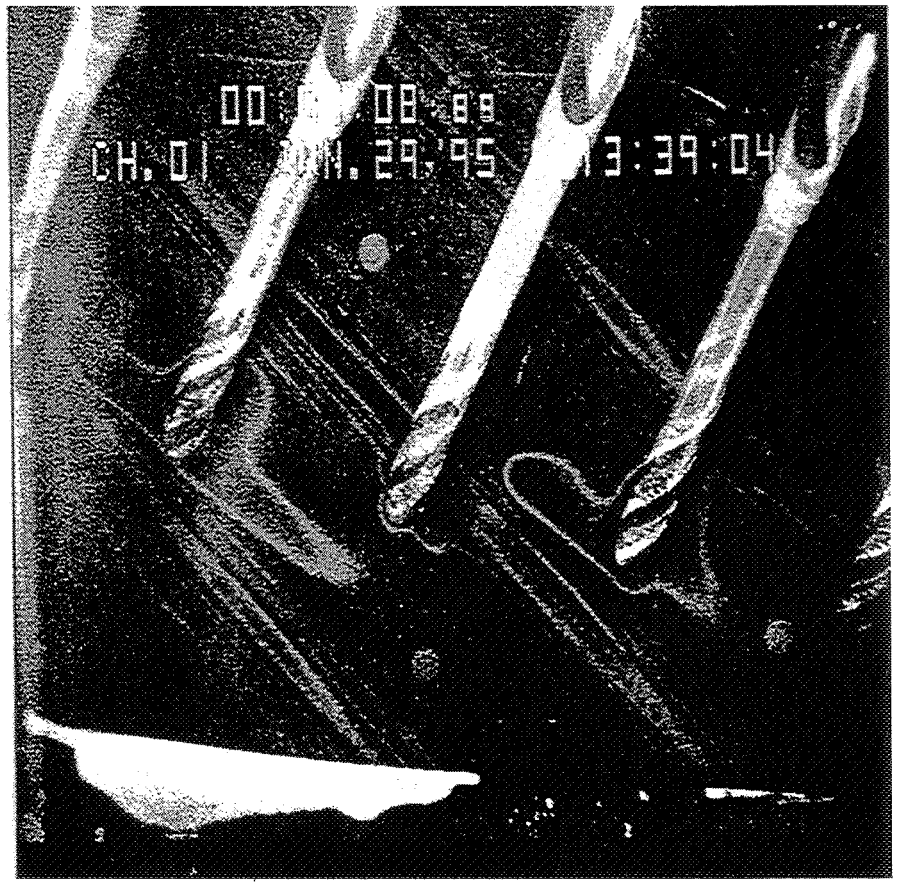

HEAT TRANSFER LOCAL DISTRIBUTIONS IN ROTATING MULTIPASS CHANNELS WITH BLEED

S.C. Lau, C.W. Park, R.T. Kukreja, and M. Kandis
Texas A&M University
College Station, Texas

OBJECTIVES:

The main objective is to make available detailed local experimental data with rotating multipass channel models:

- to enable better understanding of the effects of rotation, sharp turns, channel geometry, and rib turbulators on the heat transfer distributions in cooling serpentine passages in modern gas turbine blades; and
- to help improve the design of these cooling passages.

HEAT TRANSFER IN SERPENTINE PASSAGES IN TURBINE BLADES:

- Flow Parameters — Reynolds number, Rotation number, and buoyancy parameter relate viscous, inertia, Coriolis, and buoyancy forces in the flow.
- Thermal Parameters — Heat transfer distribution also depends on Prandtl number and thermal boundary conditions.
- Geometric Parameters: entrance geometry, passage cross section, variation of cross section along the main flow direction, wall orientation with respect to rotation axis, turn configuration, and inward or outward main flow direction.
- Turbulator Parameters: rib cross sectional shape, size, and pitch; rib angle and orientation with respect to main flow direction; and rib configurations on opposite walls.

SELECTION OF PRIOR PUBLICATIONS:

Turbulent flow in unheated channels:

Johnston et al. (1972), Wagner and Velkoff (1972), Rothe and Johnston (1979), and Tse and McGrath (1995)

Turbulent heat transfer in straight channels:

Mori et al. (1971), Morris and Ayhan (1979), Clifford et al. (1984), Harasgama and Morris (1988), Soong et al. (1991), Taslim et al. (1991a, 1991b), El-Husayni et al. (1994), Hwang and Kuo (1994), and Kuo and Hwang (1996)

SELECTION OF PRIOR PUBLICATIONS:

Turbulent heat transfer in multipass channels:

Hajek et al. (1991), Wagner et al. (1991a, 1991b, and 1992), Johnson et al. (1993, 1994), Yang et al. (1992), Mochizuki et al. (1994), Han and Zhang (1992), Han et al. (1993), Parsons et al. (1994), Zhang et al. (1995)

Numerical Studies:

Prakash and Zerkle (1992), Dutta et al. (1994a), Bo et al. (1995), Tse and Steuber (1996), and Shih et al. (1996)

APPROACH:

Naphthalene sublimation experiments are conducted to obtain the local mass transfer distributions in rotating multipass channels. By applying the heat/mass transfer analogy, the distributions of the normalized Nusselt number may be determined from the measured distributions of the normalized Sherwood number.

NAPHTHALENE SUBLIMATION TECHNIQUE: (Goldstein and Cho, 1995)

- Same governing equations for heat and mass transfer — negligible viscous dissipation and compression work in energy equation; no coupling between temperature and concentration fields; negligible property variation; same Pr_t and Sc_t (Simpson and Field, 1972).
- Boundary condition — naphthalene surface is analogous to isothermal surface.

NAPHTHALENE SUBLIMATION TECHNIQUE: (Goldstein and Cho, 1995)

- Negligible disturbance of velocity field by sublimation — small change of surface shape and low normal velocity at naphthalene surface.
- Negligible surface temperature change due to latent heat of sublimation.
- Heat/mass analogy: $Nu/Sh = (Pr/Sc)^n$. If $Nu_{ref} \propto Pr^n$ and $Sh_{ref} \propto Sc^n$,

$$Nu/Nu_{ref} = Sh/Sh_{ref}.$$

FACILITY/RESULTS:

- The experimental facility consists of a rotation test rig, an open air flow loop, and mass transfer measurement equipment, in an air-conditioned laboratory. Typical results include the local distributions of Nu/Nu_{fd} or Sh/Sh_{fd} on the leading and trailing walls of a test channel and the distributions of the spanwise or regionally averaged Nu/Nu_{fd} or Sh/Sh_{fd} along the main flow direction on the leading and trailing walls.

MILESTONES:

Results have been obtained for rotating two-pass square channels with smooth walls and with 90° and 60° ribs of various sizes on the leading and trailing walls. Reynolds number ranged from 5,500 to 14,500, and rotation number was varied up to 0.24. Attention was focused on the sole effect of rotational Coriolis forces under zero buoyancy and isothermal wall conditions, and its coupling with the effects of turn-induced and rib-induced secondary flows.

RESULTS:

- *Re* and *Ro* effects for a smooth channel and a channel with 90° ribs
- blockage effect of 90° ribs on leading wall on trailing wall heat transfer
- blockage effect of 90° ribs on trailing wall on leading wall heat transfer
- rib angle effect with 90° and 60° ribs
- rotation-turn coupling effect and rotation-rib coupling effect on local heat transfer

RESEARCH PLAN:

Experiments will be conducted with two-pass channels and three-pass channels to study the effects of coolant extraction through bleed holes, channel geometry, and channel orientation (with respect to the rotation axis) on the local heat transfer distributions on the leading and trailing walls of the channels.

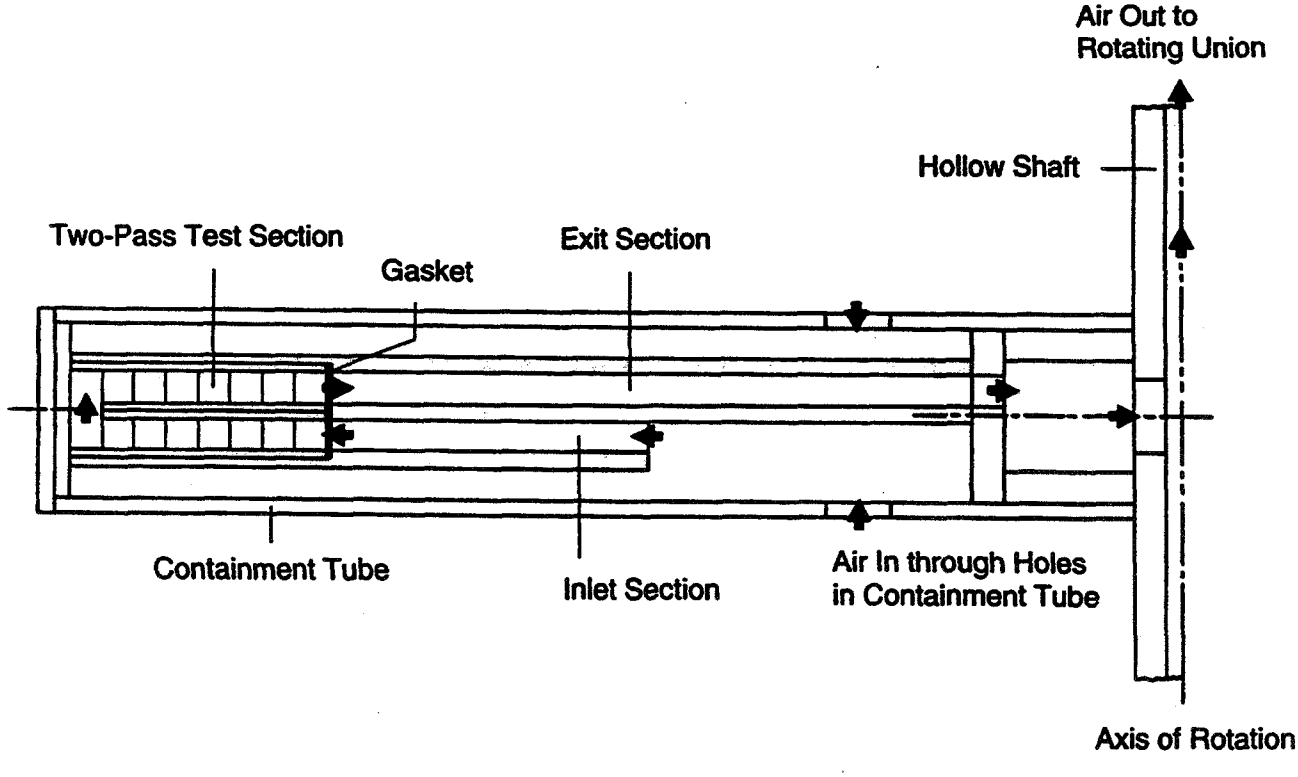

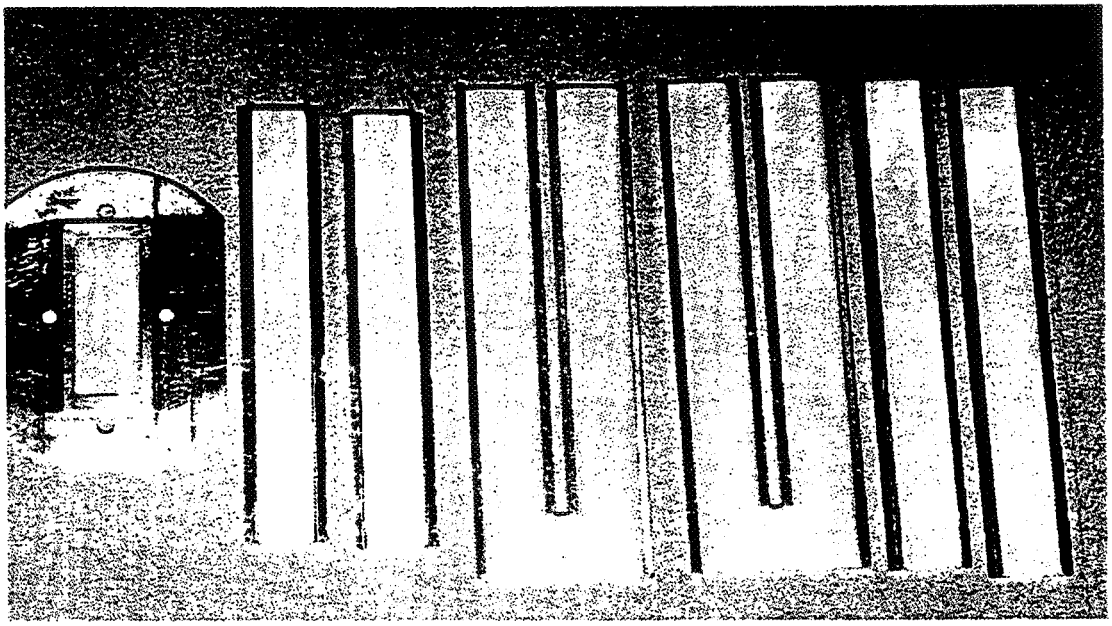

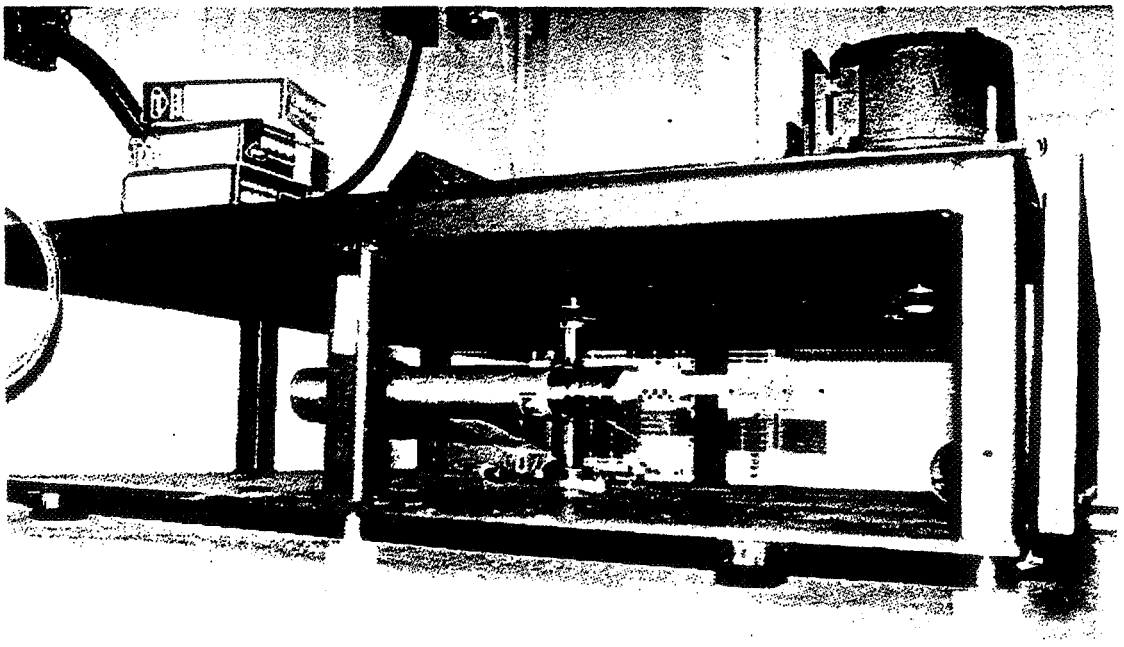

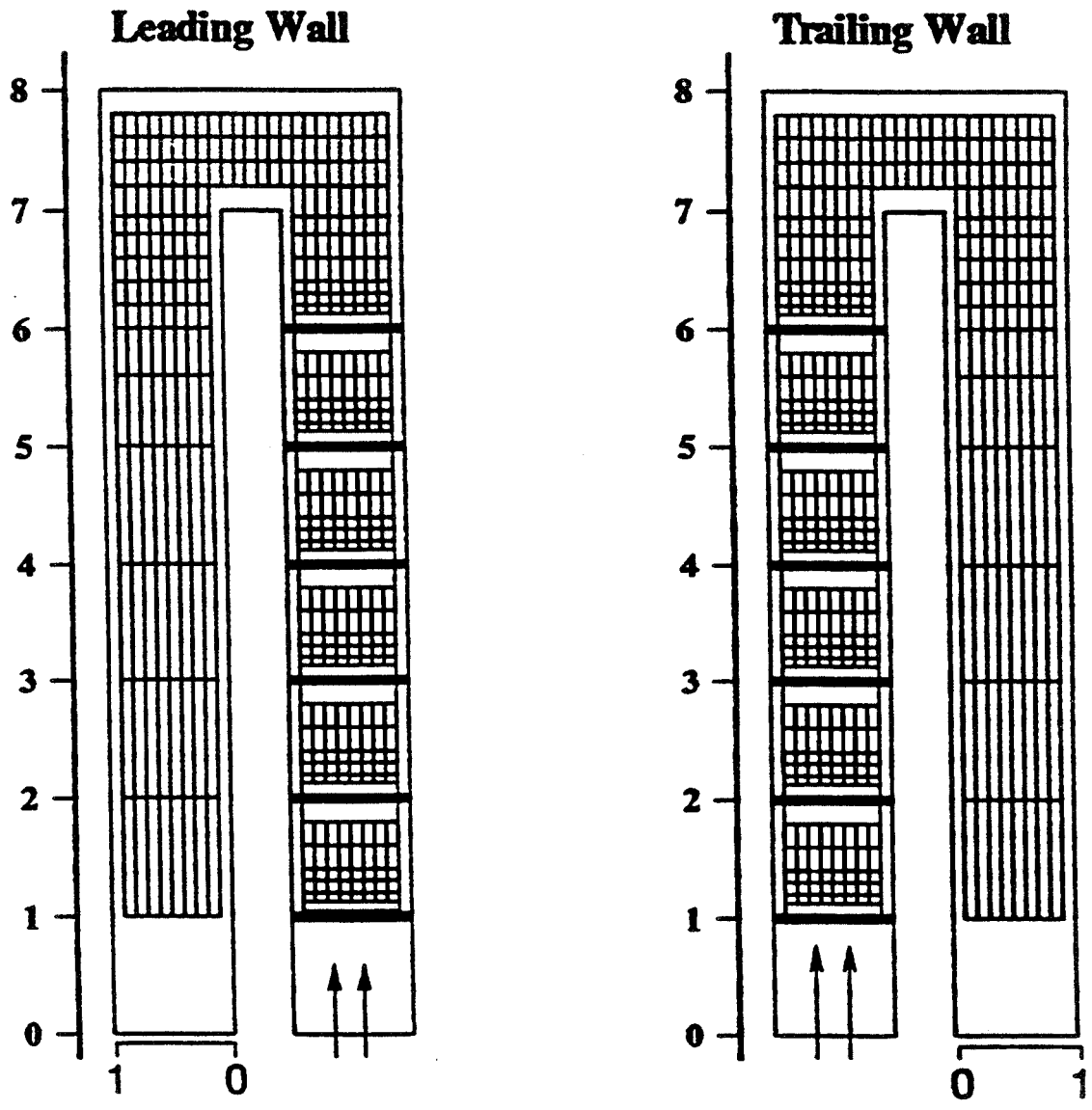

Typical grid for local mass transfer measurements (ribbed channel)

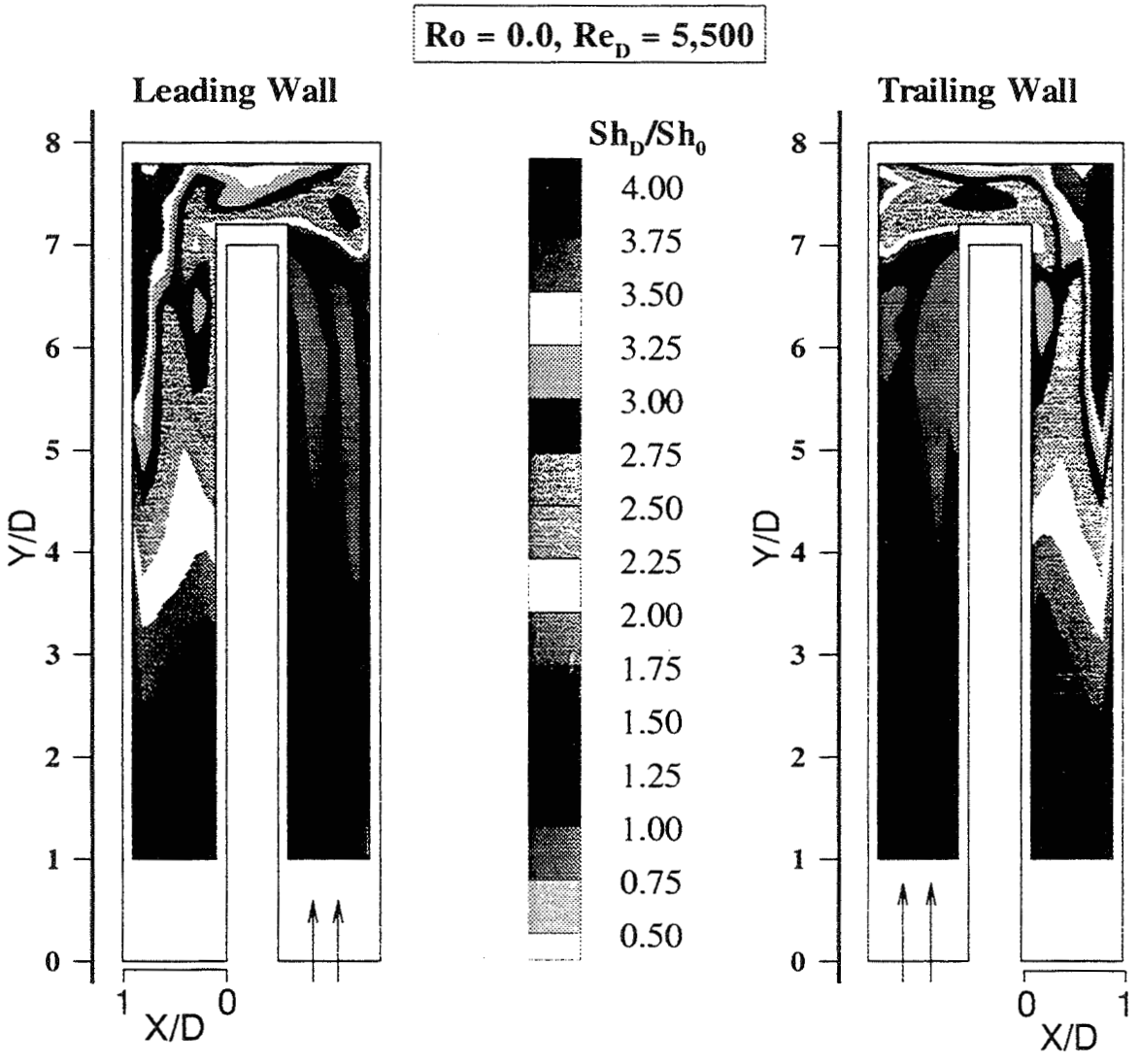

Local mass transfer distributions in a smooth channel; Re = 5,500, Ro = 0.0

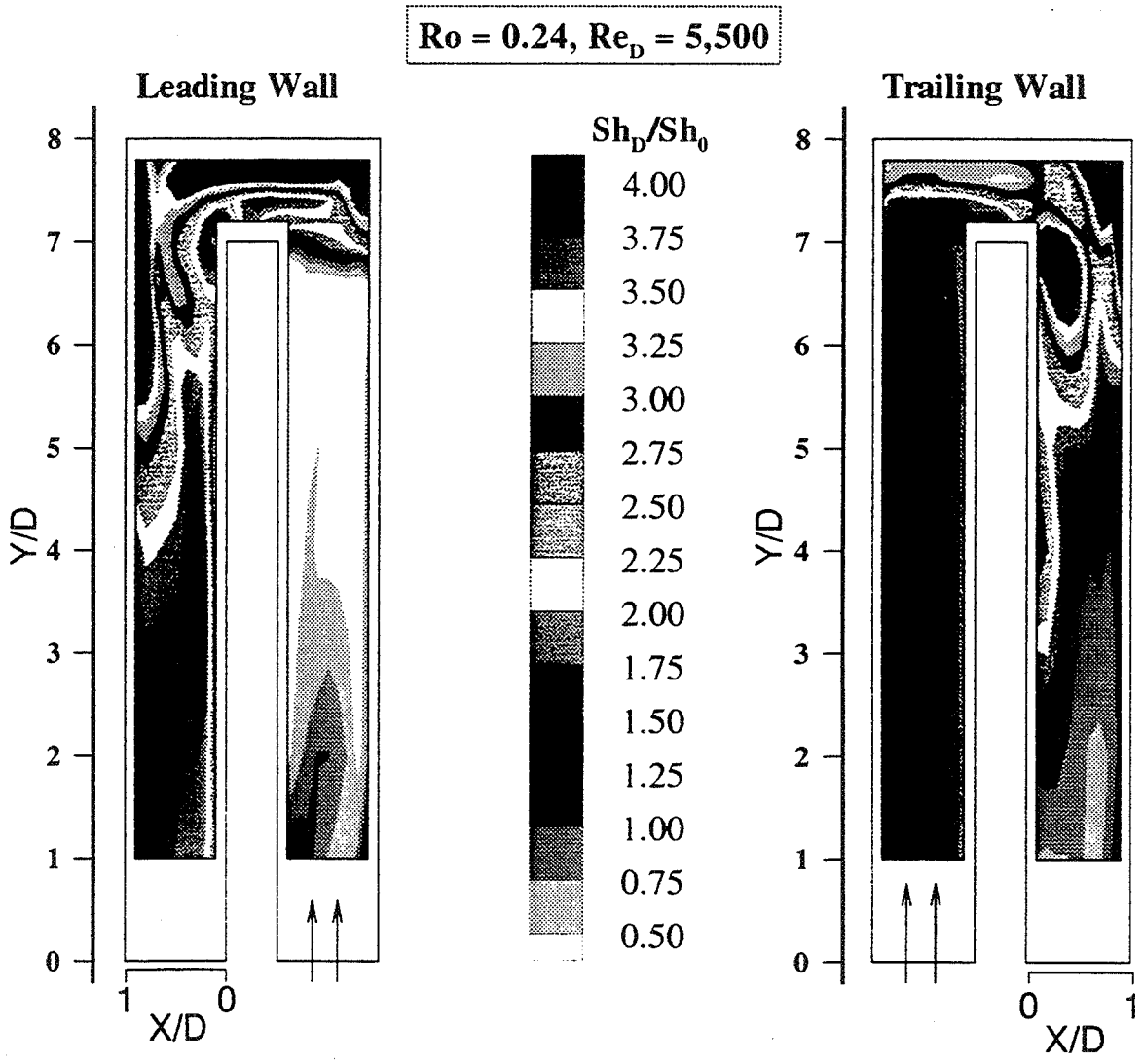

Local mass transfer distributions in a smooth channel; Re = 5,500, Ro = 0.24

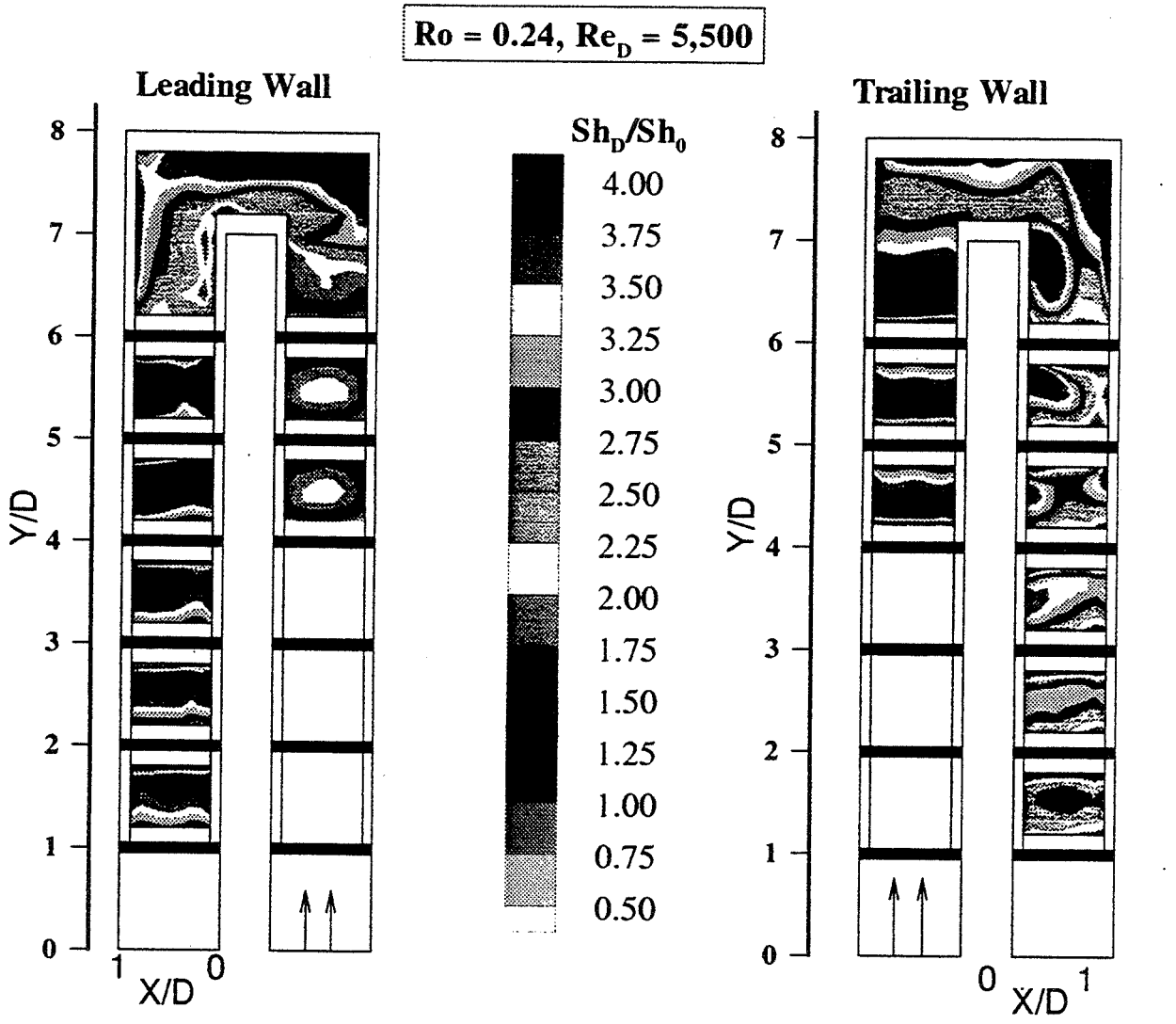

Local mass transfer distributions in a 90° ribbed channel with ribs on all principal walls; Re = 5,500, Ro = 0.24, D/e = p/e = 10

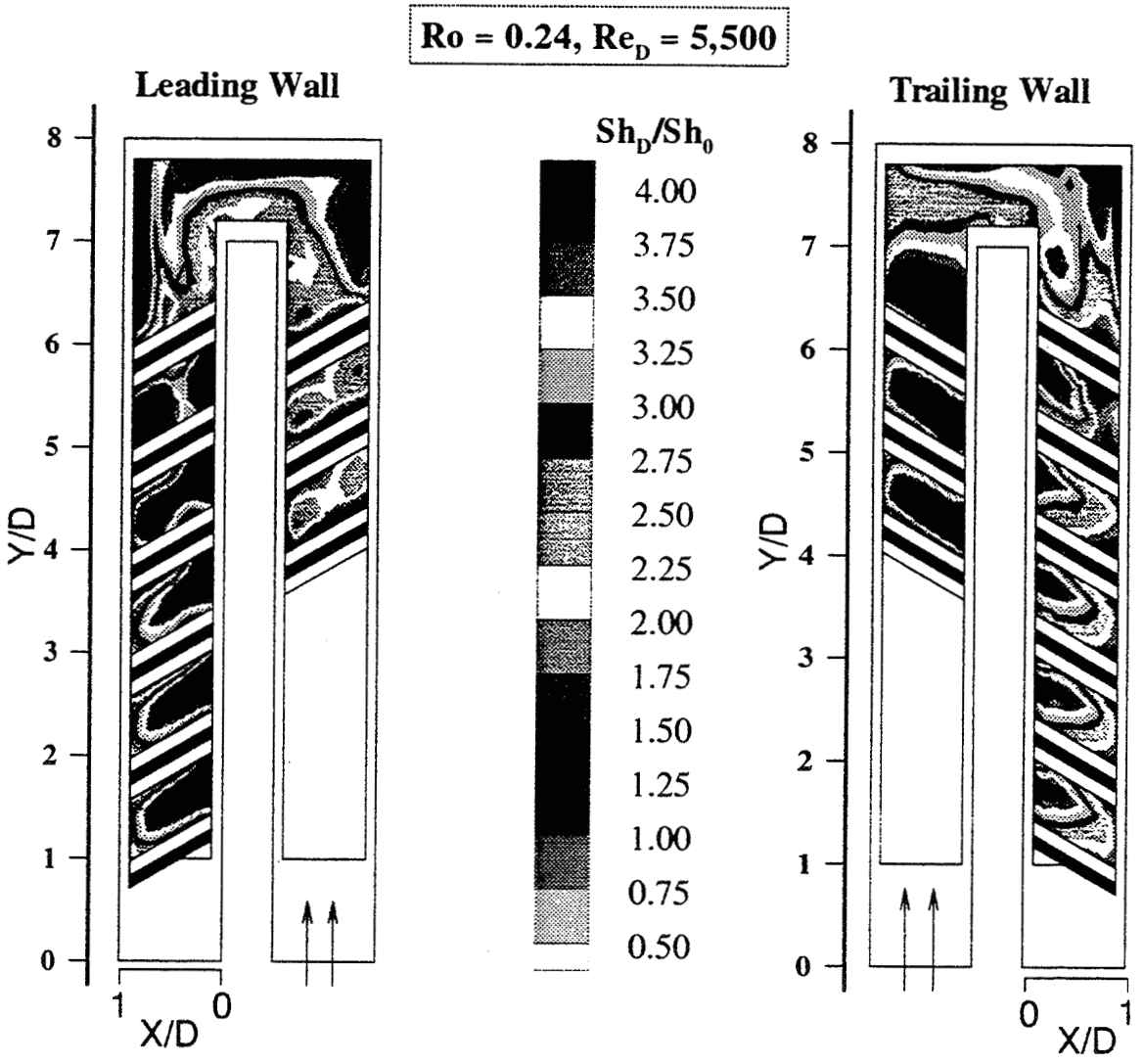

Local mass transfer distributions in a 60° ribbed channel with ribs on all principal walls; Re = 5,500, Ro = 0.24, D/e = p/e = 10

GROUP DISCUSSION - DECEMBER 12, 1996

SESSION I. INTERNAL COOLANT PASSAGE PRESENTATIONS

Kestutis C. Civinskas - Facilitator Phil Ligrani - Scribe

Clarifications and questions.

Status of work.

Assessment of what needs to be done.

Rob Norton

How many grid points - full internal cooling geometry? How many points?

Dave Rigby [Answer]

Millions.
600,000 for results shown today.
Depends on turns. 2.4 million to do a 180° turn.
Inside & outside blade, 5 million.
Hopefully with models, you will not have to grid every feature.
Structured grid takes many manhours to generate grid.
How about unstructured methodology to get a grid?
Why have fast solvers when so much time goes into grid generation?
[Answer]
Grid line generation, structured, unstructured - long way to go.
Unstructured, resolve viscous layers - not automatic.

Joe Gladden

Need impact in the '98-'99 timeframe.
Why structured direction?
Unstructured takes longer.
Multi-block question - does it take long?

Joel Wagner

Unstructured - where do we need to go. Number of grid points drop a lot for adaptive unstructured meshes.

Tom Shih

Grid generation - not just geometry, but also physics.

Boris Glezer

How to model?
Two processes:
    Academic - detailed flow predictions.
    Industry - reasonable/short term.
More years needed to get details.
Rotation is a different story - need simplified correlations.
Rotation is first priority for industry.

Bob Simoneau

What level of spatial resolution (for heat transfer) is important?
People doing research, what is really needed to know is: what are best estimates of what is needed?
Kinds of resolution and locations of detail needed.
More CFD, unstructured direction.

Bob Bergholtz

Simoneau's point is important.
Probabilistic design systems - what is required precision for a particular type of computation.
Given natural uncertainty: Wagner picture of a turbine blade with $\pm$ values is helpful.
Example: combustor profile is an important issue regardless of grid points.
Need balance precision.

Boris Glezer

What level of resolution?
Spacing?
Internal channel different from outside structure?
Third order of interest - very discrete grid - predicted results.

Yong Kim

Did Rigby look at any particular turbulence models other than k-omega?

Dave Rigby

Not really. We did try the Baldwin-Lomax model on the branched duct and the results were pretty good.

Ali Ameri

Choose particular model for generality.

Joel Wagner

CFD used to calculate losses.
Takes large number of iterations to get loss.
Need times 10 normal grids to get losses and maybe even more to get heat transfer.

Dave Rigby

If you want heat transfer, it takes longer to get global flow features.

Joel Wagner

Accuracy required, Simoneau.
50°F means a factor of 2 in live.
Need surface temperatures to 5 to 10° F of actual for temperatures of 2000-3000° F.

Bob Simoneau

Spatial resolution also important.
How locally universal is flow physics.
Measured very little of local gas temperatures.
All were referenced to some inlet conditions.
If you have total temperature distribution, how right is local heat transfer distribution.
Computationally, there might be some help.

Joel Wagner

For heat transfer coefficients, we struggled a long time because of using the bulk mean temperature.
Likewise, for laminar and turbulent calculations over an airfoil to predict transition, how do you get momentum thickness on a 3-D airfoil flow? What is the driving potential? We struggled with that.
For transient tests its even more pronounced.

Kaz Civinskas

Are there questions for other speakers ?
Metal temperatures, hot.
Do we need 10 times the number of grid points or we will miss some physical phenomena?

Boris Glezer

Figure with rotation?

Joel Wagner

Yes, P&W blade; inside passage - correlations for rotating effects.

Ming-King Chyu

Why physics - fewer points. Why is temperature lower?

Joel Wagner

Passages have low pressure and high pressure sides that are not related to the external pressures.
Heat transfer is up on the high pressure side of an internal passage which might be on either side of the blade.
One spot / a drop / different flow directions.
A flow divider wall is there.

Jim VanFossen

Liquid crystal measurements - what is best reference temperature for a gas?
What does engine designer need?

Joel Wagner

Use local coolant flow, bulk mixed flow mean for current internal coolant flow design systems.
Aerodynamic and internal cooling calculations are not separate anymore.
Current design systems use the local bulk mean temperature.
Copper model, hot.

Rob Norton

Cannot scale Nusselt number to inflow conditions, you must use local temperatures.

Ming-King Chyu

Local bulk mean temperature, ways to correct now, papers in next IGTI Congress - there are ways to correct for this nonlinear change.
Experiment - more convenient to use inlet temperature.

Steven Hippensteele

Thurman and Poinsatte measured data recently in a large scale model having 3 pass internal cooling flow with ribs. They recorded temperatures as function of time and location throughout the transient liquid crystal test. The temperatures looked almost linear with location for many cases.

J. C. Han

Transient large crystals - two parts. Thermocouples in my experiment in different locations.
High Reynolds numbers - 50,000/60,000: almost no change of temperature with time.

Dave Rigby

Spanwise integration of bulk temperature showed very linear results.
Much numerical data - post processing of numerical data.
Experimentally, depending on where global energy addition, can be linear.
Curved portions different.
Isothermal surface conditions.

Bob Bergholtz

What temperature to use in blade design?
What is dovetail condition - designer, look at various changes in engine, seal conditions, etc.
Either. Design blade or reduce uncertainty in blade life.
Thermal and mechanical interactions are driver to these computations.
Look more at engine in reducing design uncertainty - interesting computationally.

Rob Norton

No such thing as a perfect engine.
Must design for good and bad engines.

Ron Bunker

Need to reduce design uncertainty, and increase accuracy in prediction methods.
Turbine designs - designs pushing to other limits, i.e. no film cooling at all.
Accuracy on CFD predictions will be tighter.
Still need a lot more detail. Goal of coolant flow management is to take out as much coolant as possible.
Experimental basis - need tighter knowledge of uncertainty.

Satish Ramadhyani

High thermal stresses in the vicinity of the holes.
Large uncertainties in approach flow.
Need resolution in the computations for flow details.

Rob Norton

80% of the cost of the engine (or components) is decided in the first 20% of design cycle.
Feed data into correlations which designer needs for estimates.

Bob Simoneau

Bleed hole question on internal channels: just one more variable in a complicated problem.
What bleed conditions to test should come from industry.
Numerical people - where to put their energies to address this?
Delighted to see questions about how can these people direct research so that results are obtained quickly.

Sumanta Acharya

Must define a fine mesh, not coarse grids, to get fine flow details.

Bob Bergholtz

Promote - not a plea for in-precision. Detailed accuracy is needed.
Computation - do simulation, low order internal passage configuration. Then compute blade flow - prescribed flow characteristics of flow and coolant: lower order resolution of internal flow passage.
Very interesting to see; help to reduce uncertainties.

David Rigby

From simulation, several calculations. Changes give reliable trends.
If you don't do high resolution calculation - not same result as low resolution calculation.

Bob Bergholtz

Careful to put precision emphasis correctly.

Tom Shih

Geometries - internal cooling not that complicated.
Solver/structured and unstructured meshes.

Rob Norton

Not interested if unstructured; less accurate if we have good test data.

Erlendur Steinthorssen

Grid structure, grid points are a concern.
Need more resolution with an unstructured grid.
Detailed simulation/more viable for structured grid.
[To Dave Rigby] Pitch-to-height ratio covered but not correct value. Then vary all cases over a weekend.

Dave Rigby

Grids done overnight/topology is established if doing grids of holes.

Rob Norton

Working on CAD systems to change geometry is separate from grid generation.
Unstructured meshes in short term.

Erlendur Steinthorssen

Grid generation and block structures done simultaneously.
Adaptive refinement can also be done in structured grids.
Proved in a workshop some time ago.
Structured grid codes better able to calculate some flow features.

Rob Norton

Better ways to estimate errors needed - rather than just depend on gradients.

Erlendur Steinthorssen

Reference temperatures and internal flows are important - need more than pieces of information.

Yong Kim

[To David Tse] Conclusion: is heat transfer better with -45° and +45° ribs?

David Tse

Combination of rib angle and rotation.
Ribs are important. Are positive in one channel and negative in another channel.
Detailed explanation of relations between heat transfer and flow patterns.

Kaz Civinskas

Comments.

Adjourn.

Session II

Film Cooling Presentations

FILM COOLING LATERAL DIFFUSION AND HOLE ENTRY EFFECTS

Terry Simon
University of Minnesota
Minneapolis, Minnesota

PRESENTATION OUTLINE:

- INTRODUCTION:
- OBJECTIVES:
- EXPERIMENTAL FACILITY & INSTRUMENTATION:
- MEASUREMENTS:
  - Anisotropy of Turbulent Transport
  - Velocity and Temperature Fields to Document:
    - Velocity Ratio Effects
    - Free-Stream Turbulence Effects
    - Hole Delivery Length Effects
    - Effects of Delivery Plenum Geometry
- CONCLUSIONS:

OBJECTIVES:

Support film cooling modeling and design by describing the effects on film cooling performance of

(1) anisotropic eddy transport, and
(2) the geometry of the plenum from which the film cooling flow enters the holes.

In the process, we documented the effects of:

(1) Freestream Turbulence
(2) Hole L/D
(3) Blowing Ratio

- Will lead to more accurate computation with design models,
- Will aid in the assessment of film cooling data in the literature, and
- Will assist in the selection of supply plenum geometric features.

Also, lends a glimpse into the physics of this complex flow.

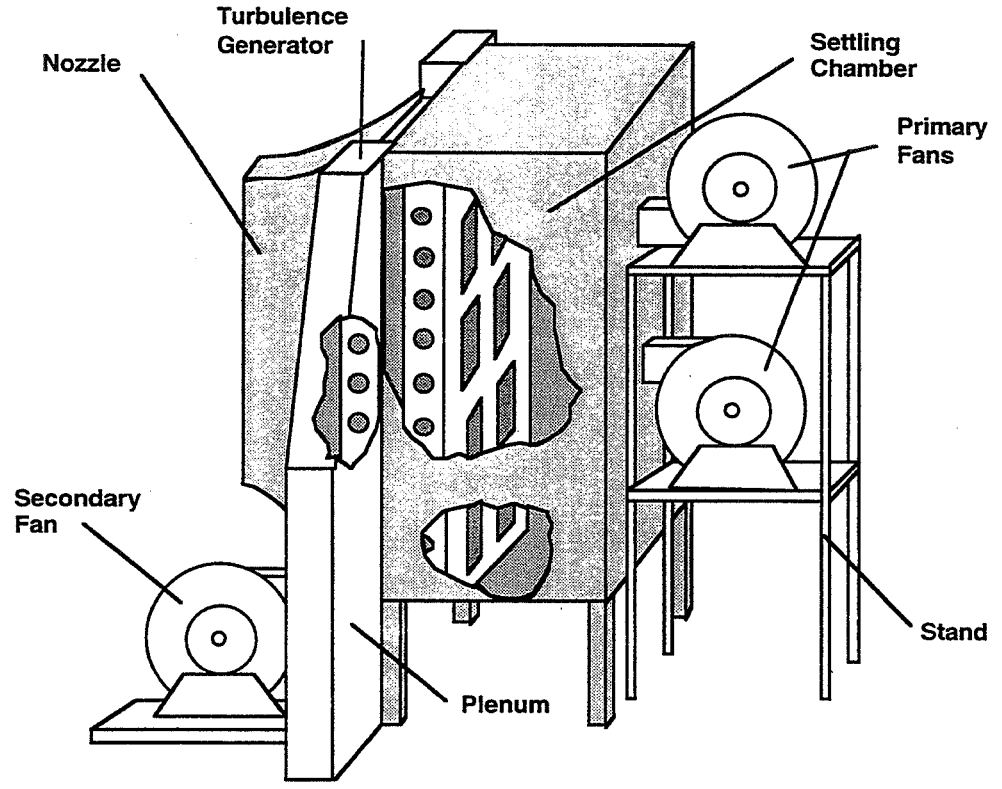

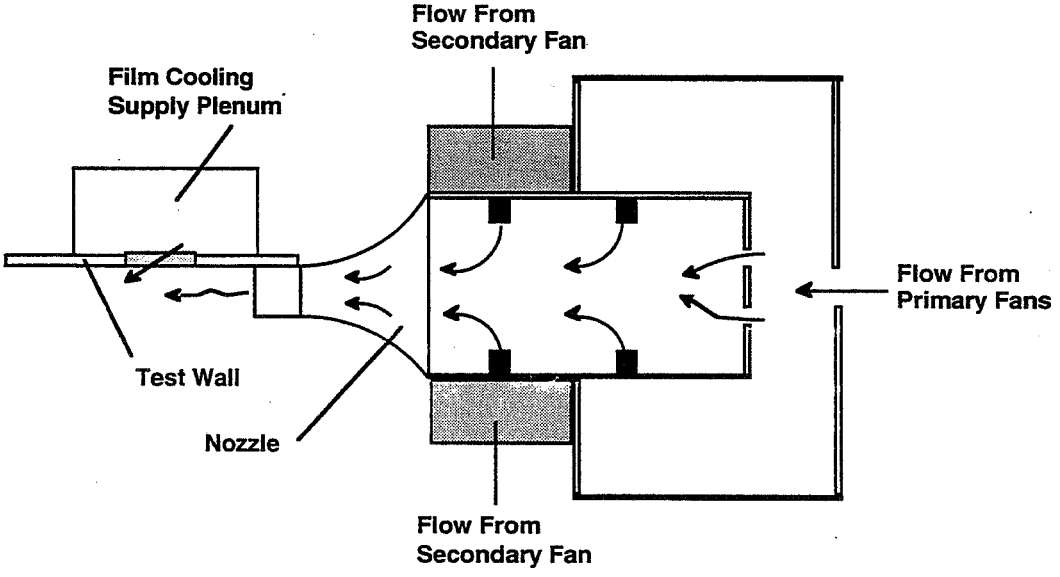

High Turbulence Facility

Film Cooling Test Facility

Freestream Facilities:

- High FSTI: 12% at 10.8 m/s
- Low FSTI: 0.5% at 10.8 m/s

Film Cooling Configuration

- One Row of 11 holes
- 35° Streamwise Injection
- L/D=7.0 and 2.3
- Hole Diameter = 1.9 cm

Coolant/Freestream Parameters and Ratios

- Velocity Ratio = 1.0 (0.5)
- Hole Reynolds Number= 13,000 (6,500)
- Density Ratio = 1.0

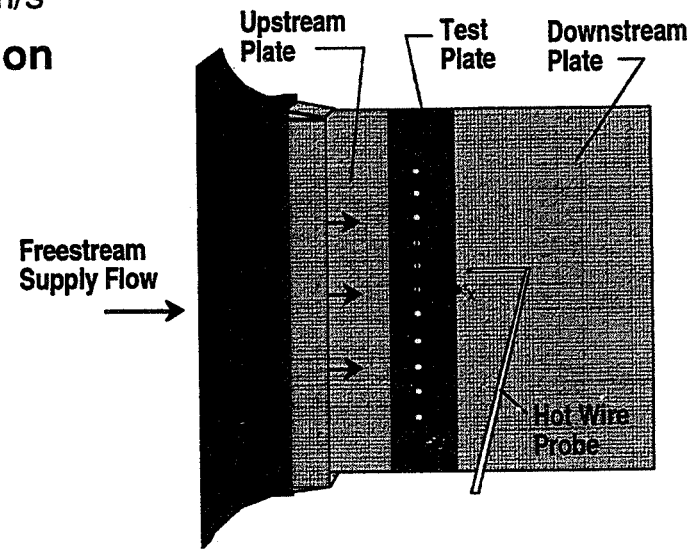

Film Cooling Geometries

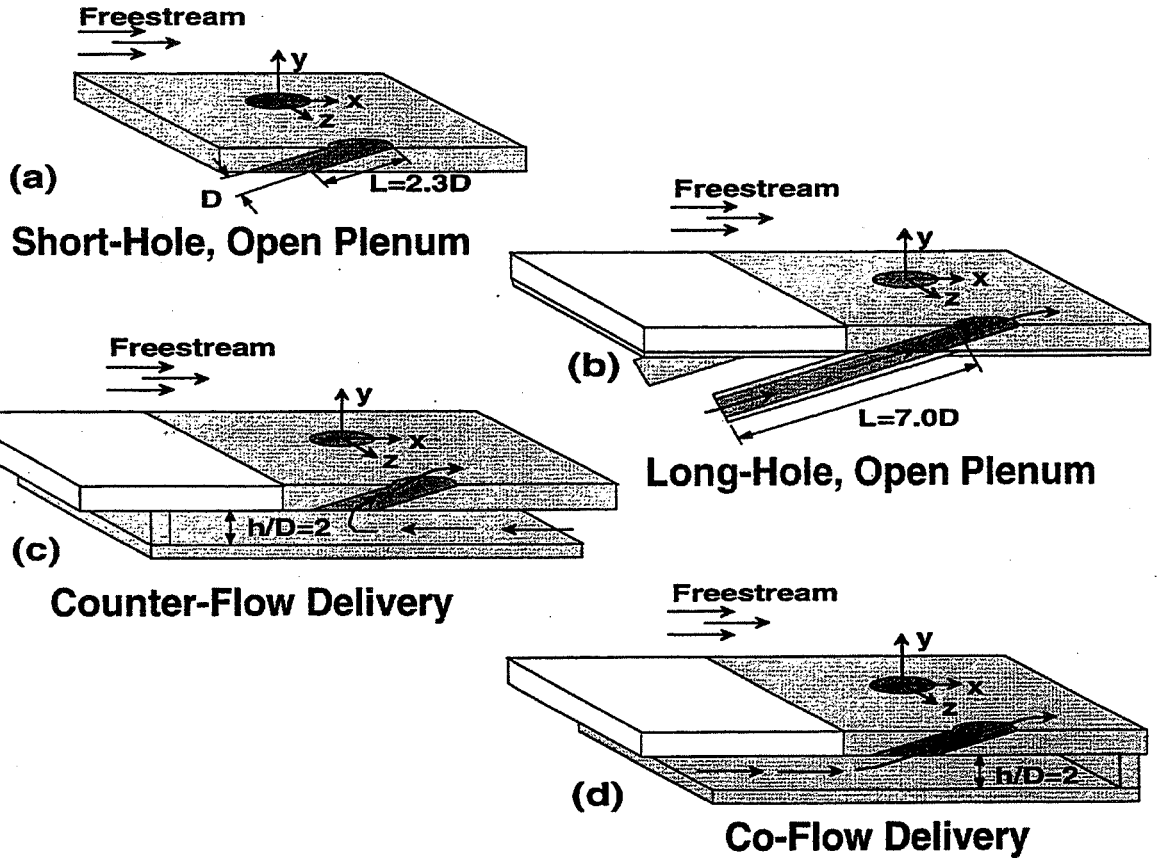

Velocity distribution at x/D=5.0, z=zo

(H=12% FSTI, L=0.5% FSTI)

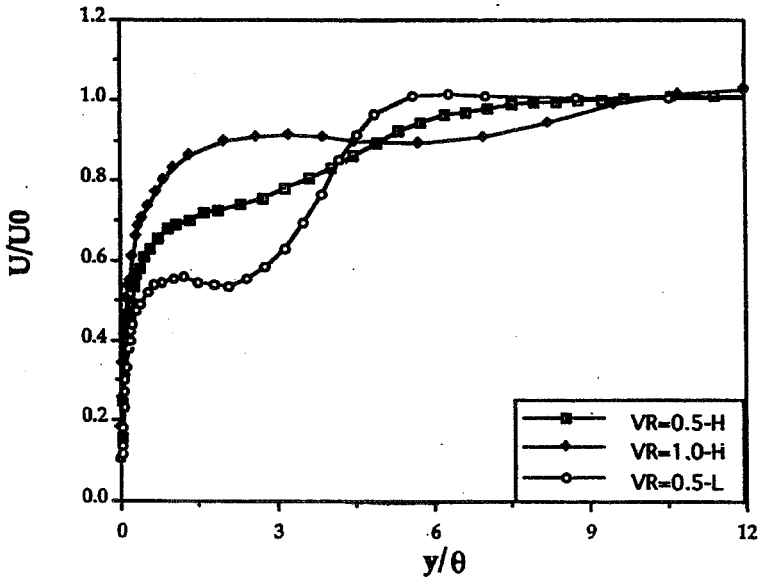

COMPUTATION

Film cooling --- Streamwise injection

Isotropic turbulence model

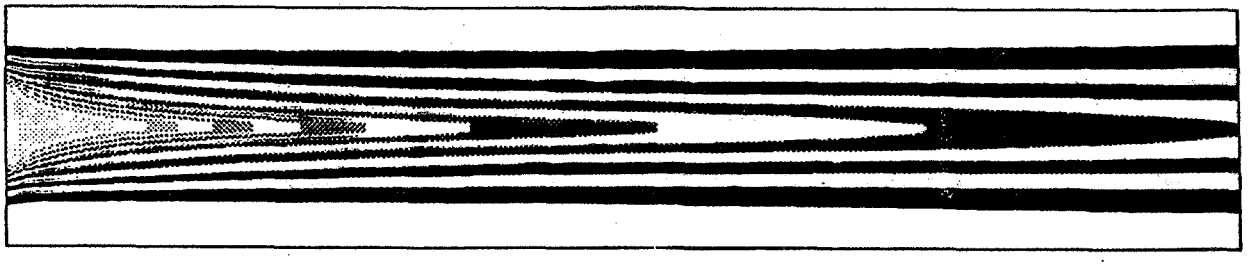

Anisotropic turbulence model

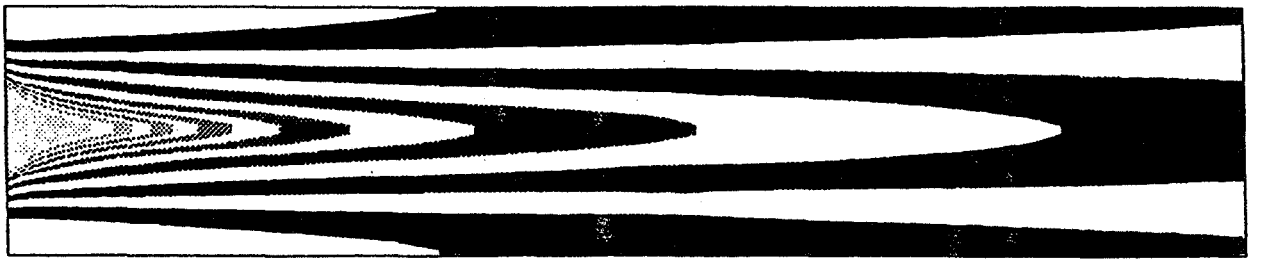

Fig. 11 Cooling effectiveness distributions predicted by the isotropic and anisotropic turbulence models
(from Sathyamurthy and Patankar, 1992)

COMPUTATION

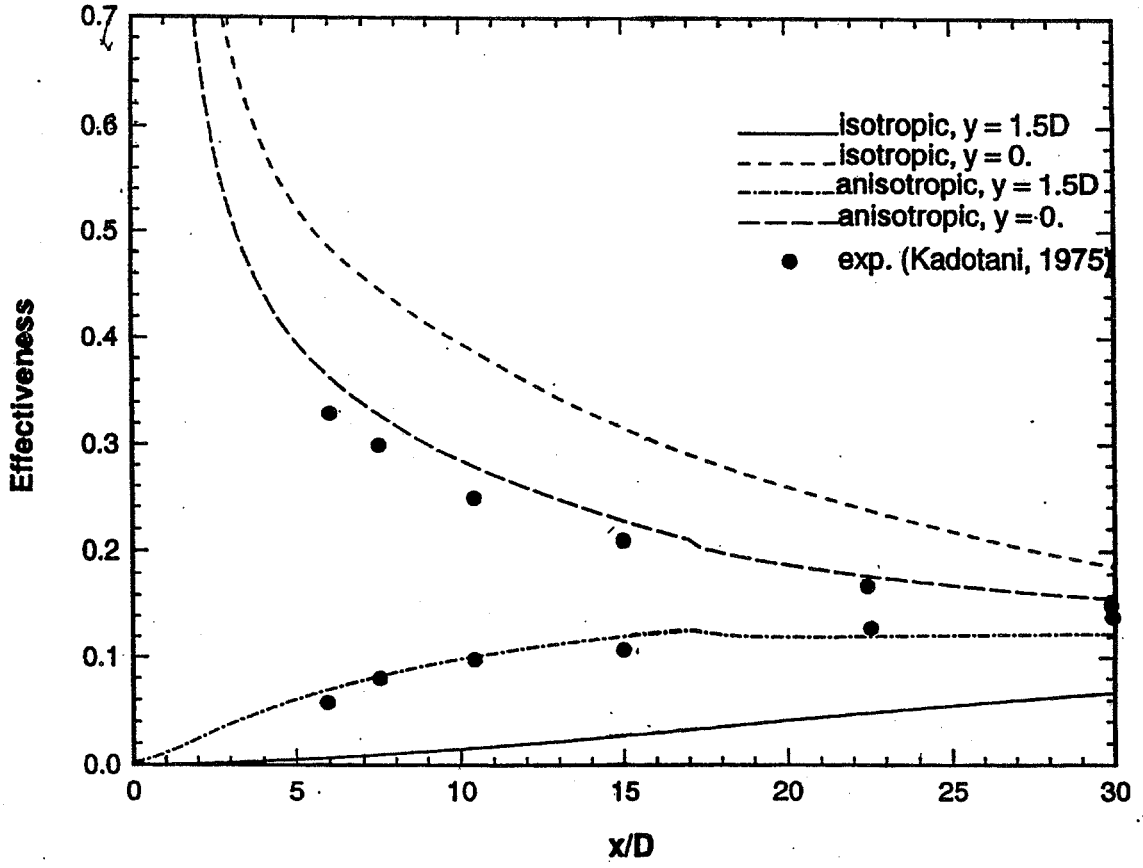

Comparison of measured and predicted values of film-cooling effectiveness
(from Sathyamurthy and Patankar, 1992)

M=0.5

Velocity Distribution at VR=0.5, x/D=5, FSTI=12% for three z-planes

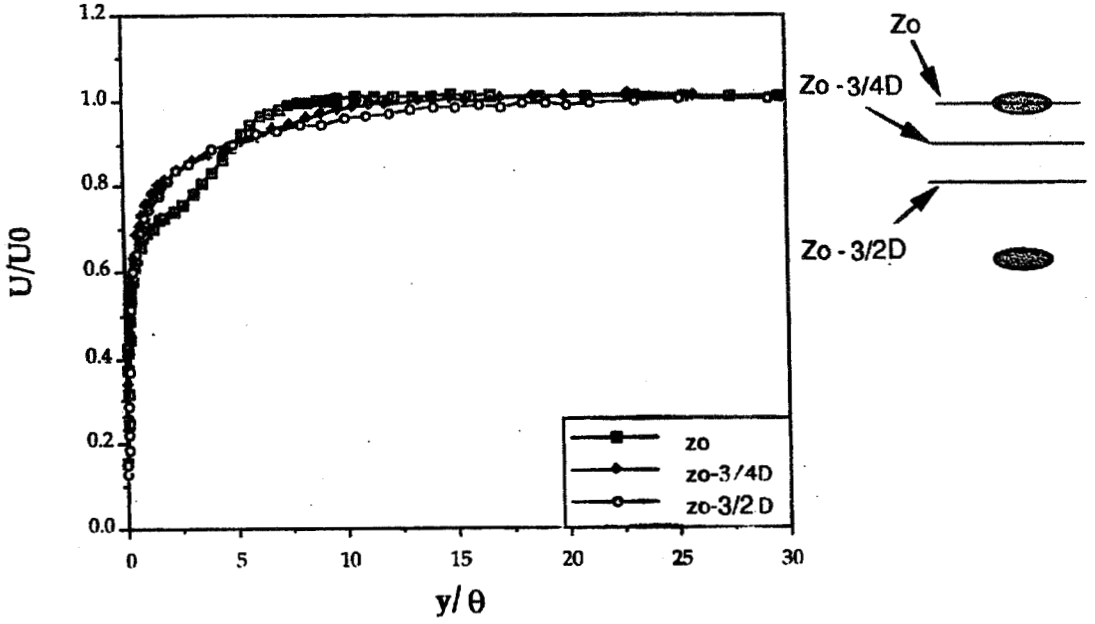

Boundary layer velocity right behind holes is strongly affected by film cooling flow.

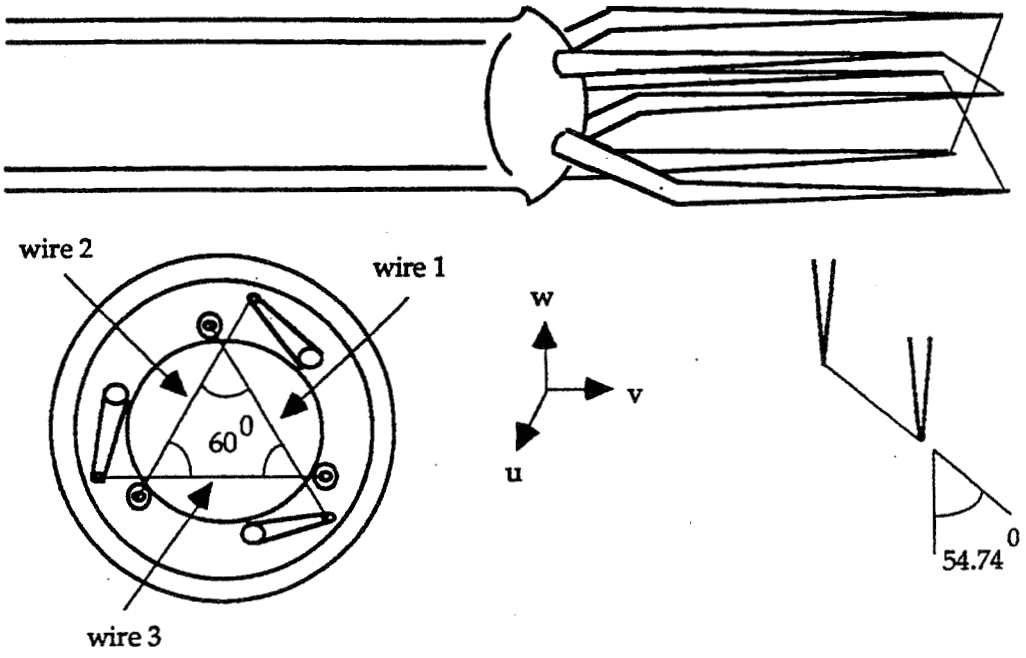

Triple hot-wire probe

Turbulent diffusion of momentum:

y-transport: $\varepsilon_{M,y} = \dfrac{-\overline{u'v'}}{\dfrac{\partial \bar{u}}{\partial y}}$ normal to the wall

z-transport $\varepsilon_{M,z} = \dfrac{-\overline{u'w'}}{\dfrac{\partial \bar{u}}{\partial z}}$ lateral direction

anisotropy $\dfrac{\varepsilon_{M,z}}{\varepsilon_{M,y}} - 1$

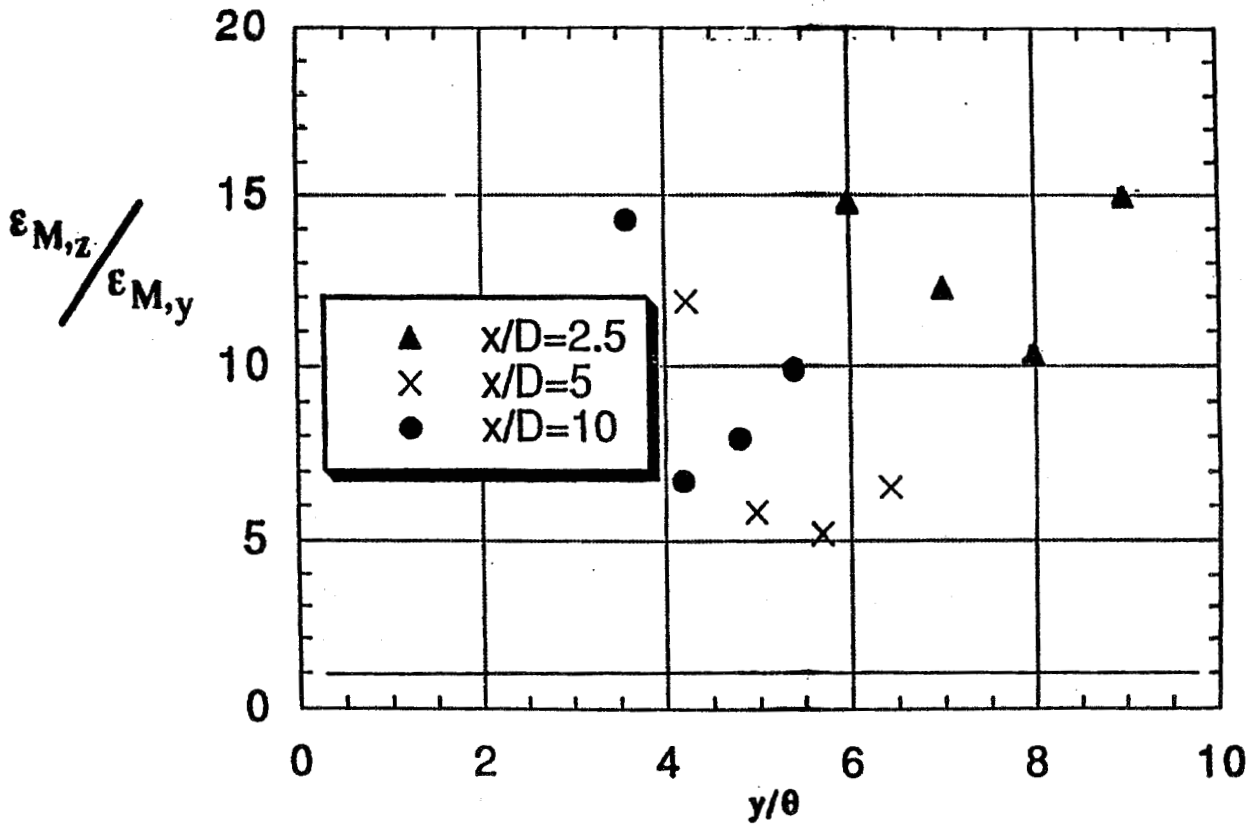

$\varepsilon m,z = -\overline{u'w'} / (dU/dz)$,

$\varepsilon m,y = -\overline{u'v'} / (dU/dy)$

Eddy diffusivity ratio at different turbulence intensity

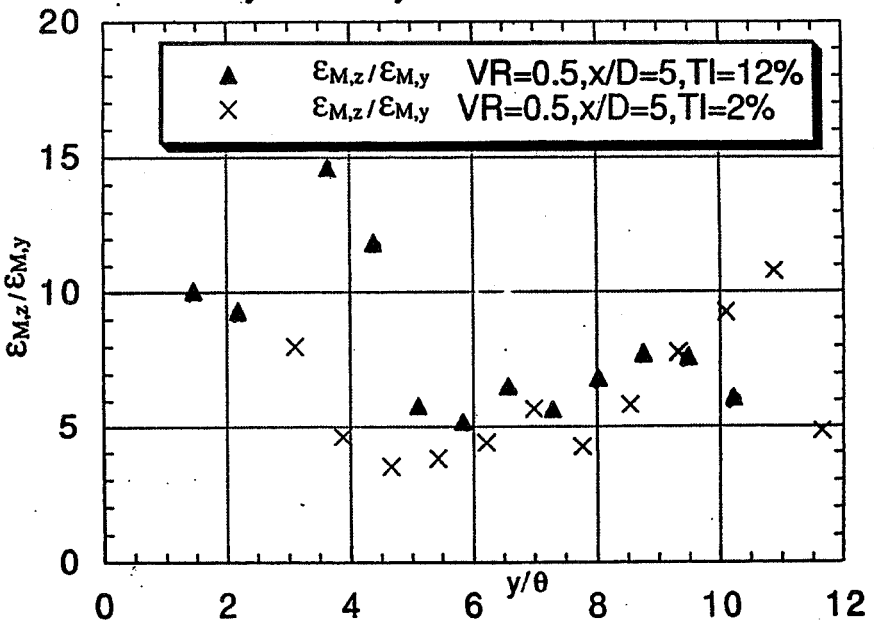

COMPUTATION WITH STRONG ANISOTROPY

$$\varepsilon_{M,z}/\varepsilon_{M,y} = 1 + \left(C\left[1 - y/\delta\right]\right)$$

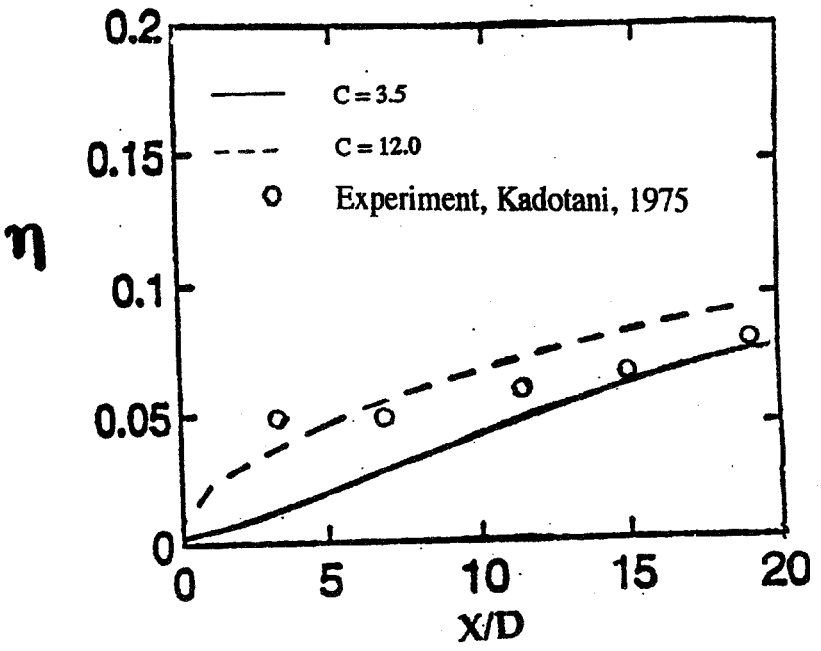

CONCLUSIONS THUS FAR:

- The eddy diffusivity ratio, $\varepsilon_{M,z}/\varepsilon_{M,y}$, is in the range 4-15. It begins high and asymptotically decays, reaching about 4 by x/D=5.0. Anisotropy is not significantly dependent on freestream turbulence or blowing ratio.

- Computational evidence suggests that use of these measured anisotropy values improves predictions of effectiveness values between the holes.

- With low VR, the film cooling flow acts like a blockage to the main flow. The blockage effect is greatly reduced after 10 hole diameters (but the vorticity imparted on the flow persists).

Measurements

- Hole-Exit Profile Measurements
  - Document Differences in Effective Velocities and Turbulence Due to Hole-Length
- Flowfield Measurements
  - Document Distributions of "Streamwise" Velocities and Local Turbulence Levels at x/D=2.5 and 5.0
  - Compare Distributions for Different Cases to Quantify Effect

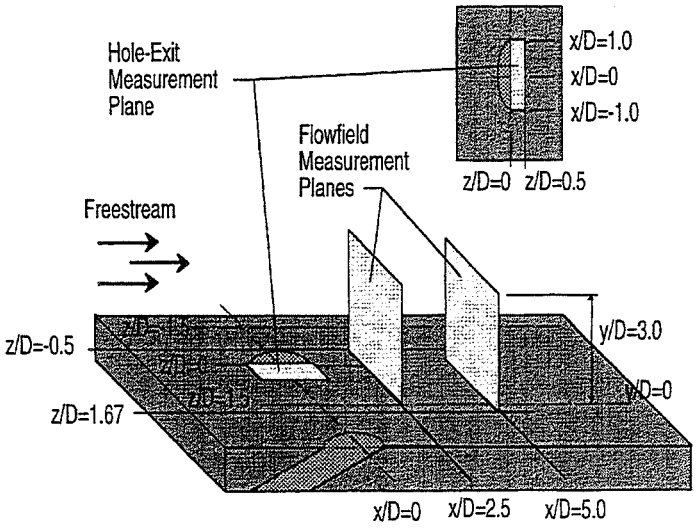

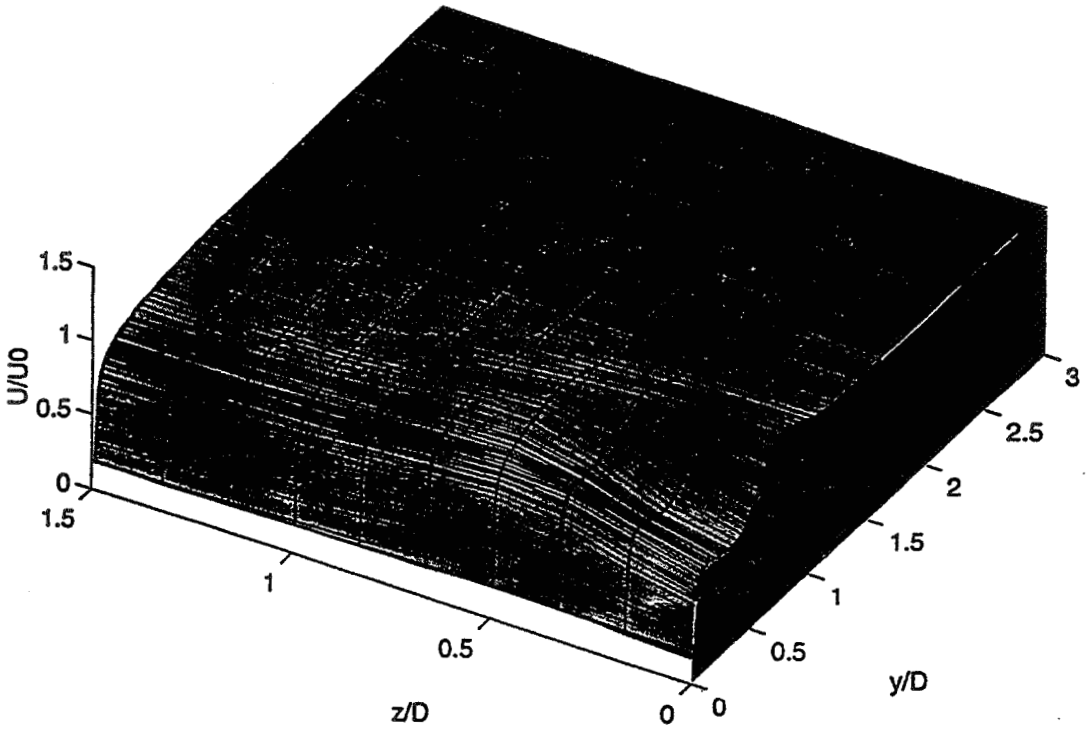

Mean Velocity
Long L/D, VR=1.0, x/D=2.5, FSTI=12%

Flowfield Measurements

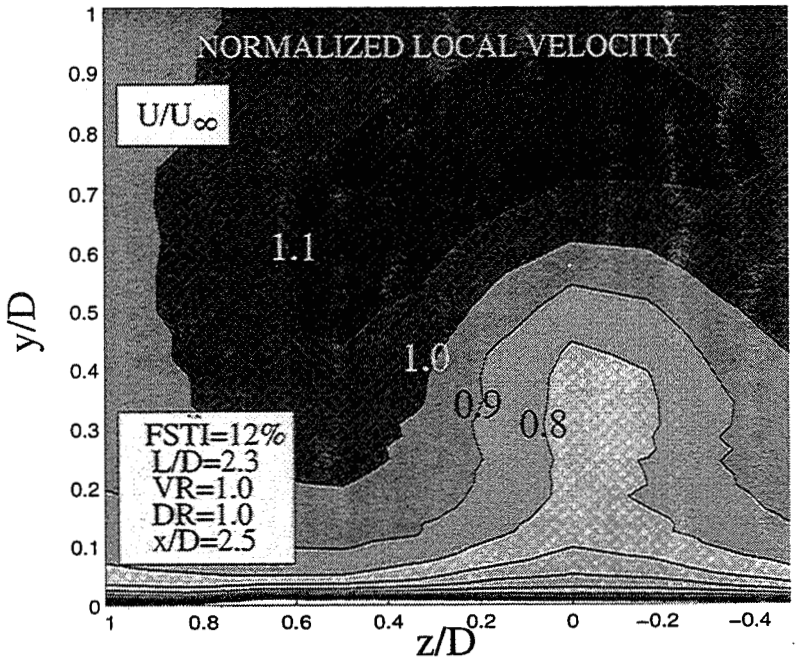

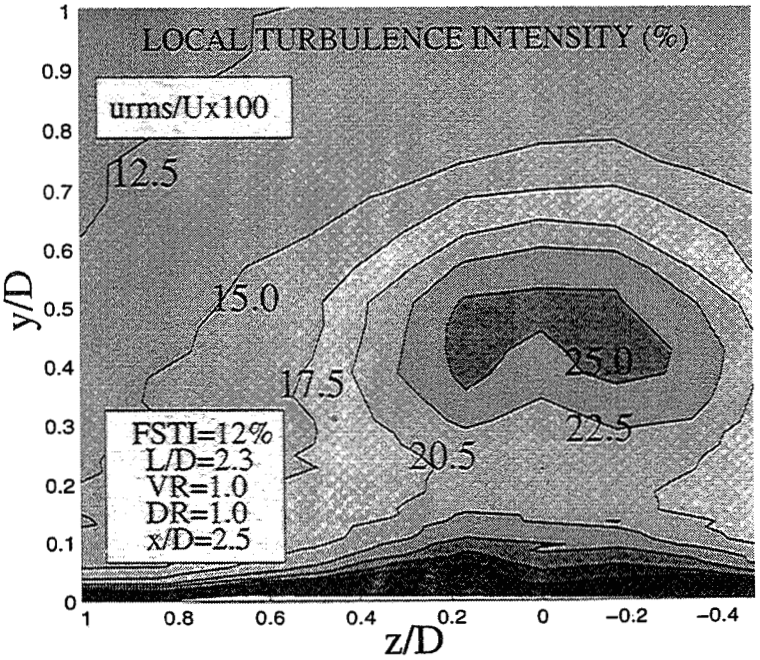

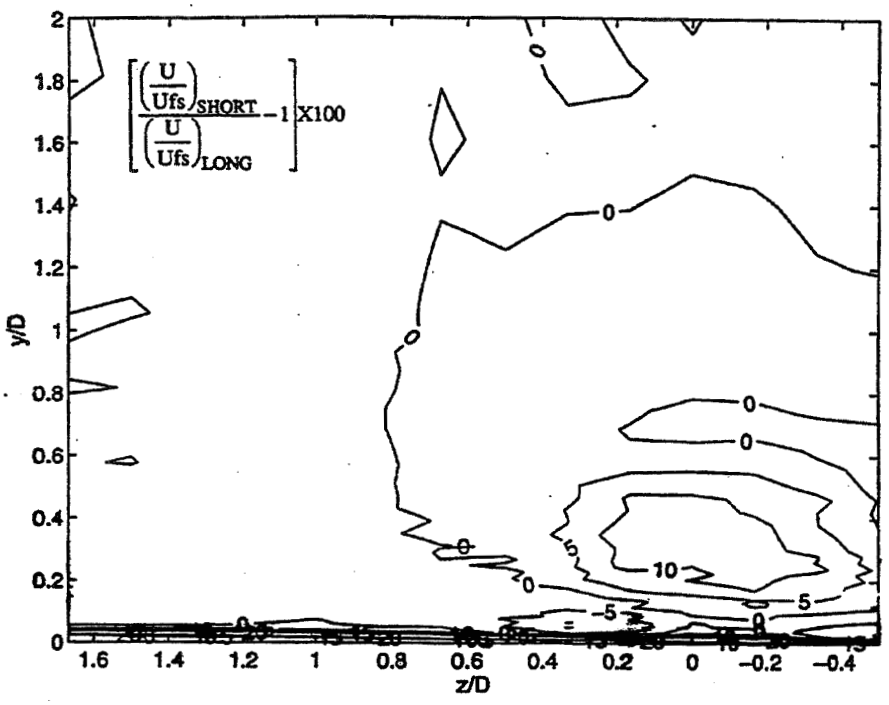

% Difference in Normalized Mean Velocity
Long vs. Short L/D
(VR=1.0, x/D=2.5, FSTI=12%)

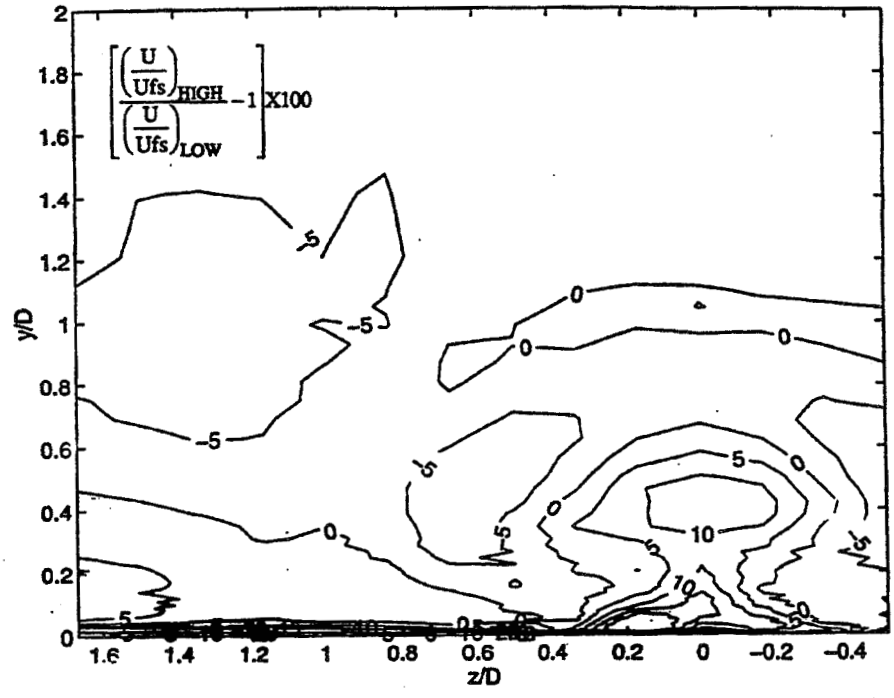

% Difference in Normalized Mean Velocity
High vs. Low FSTI
(VR=1.0, x/D=2.5, Short L/D)

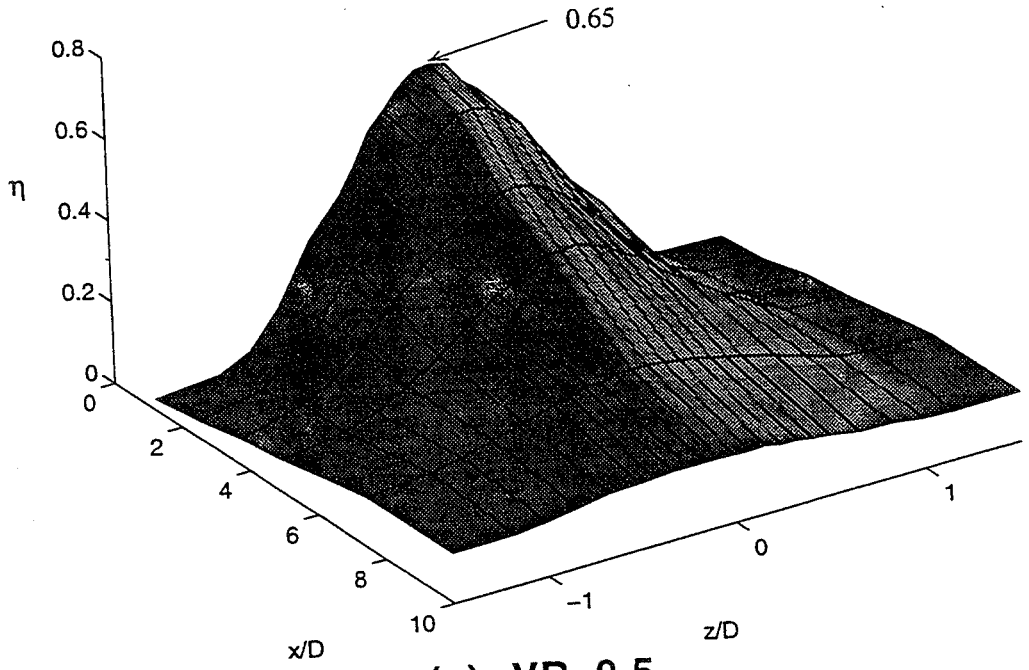

(a) VR=0.5

Adiabatic Effectiveness for Short-Hole Injection at Two VelocityRatios. FSTI = 12%

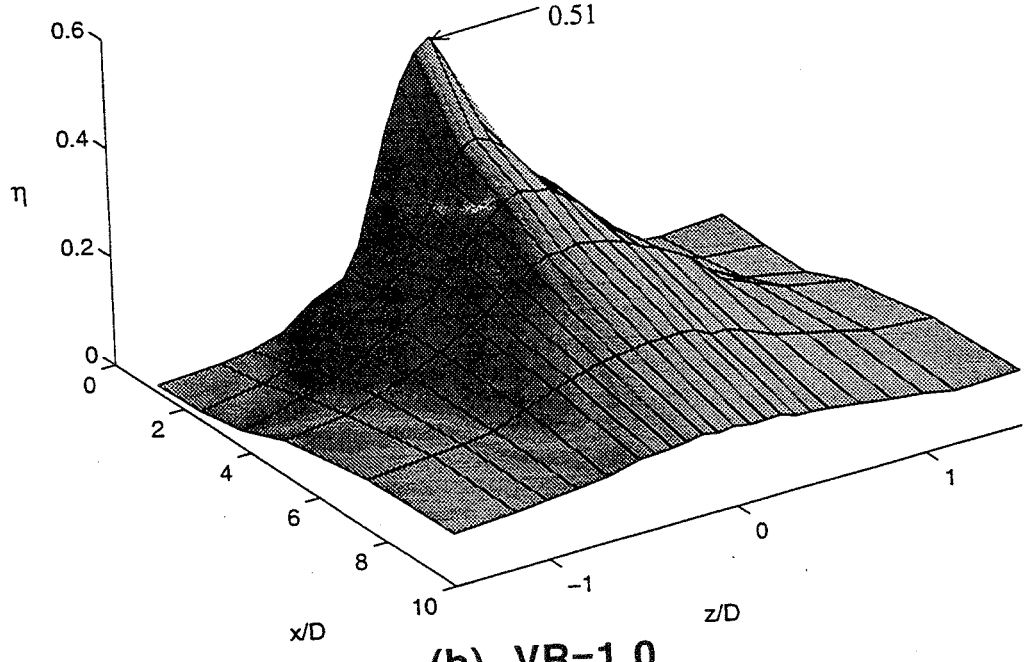

(b) VR=1.0

Results and Discussion:

Effect of L/D

- **Adiabatic Effectiveness**

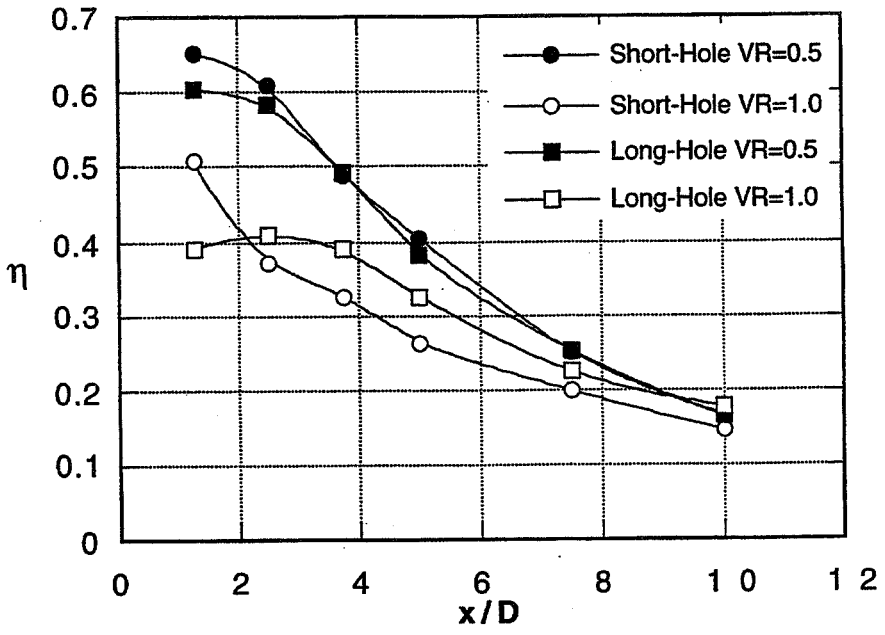

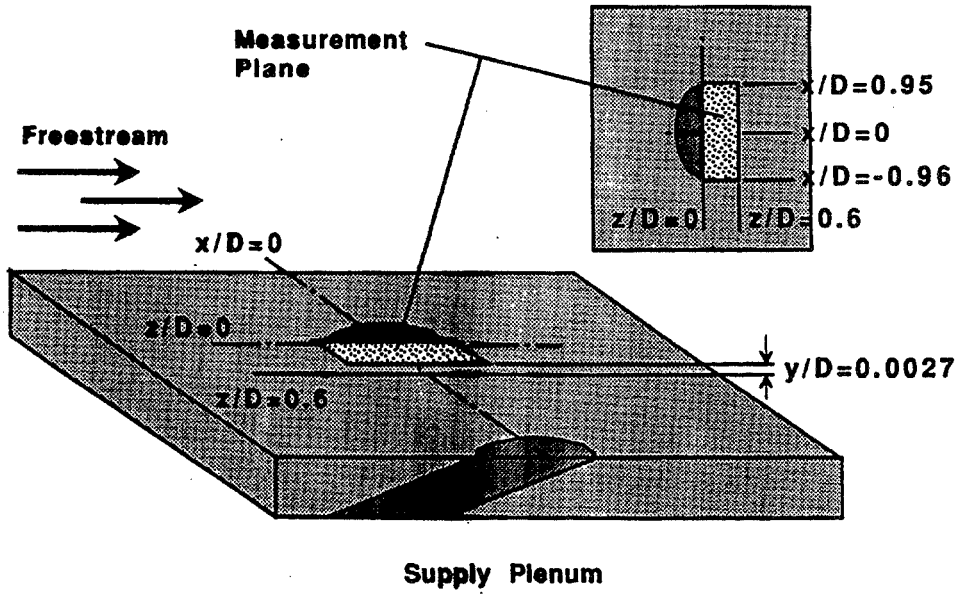

Hole Profile Measurements

Hole-Exit Measurements

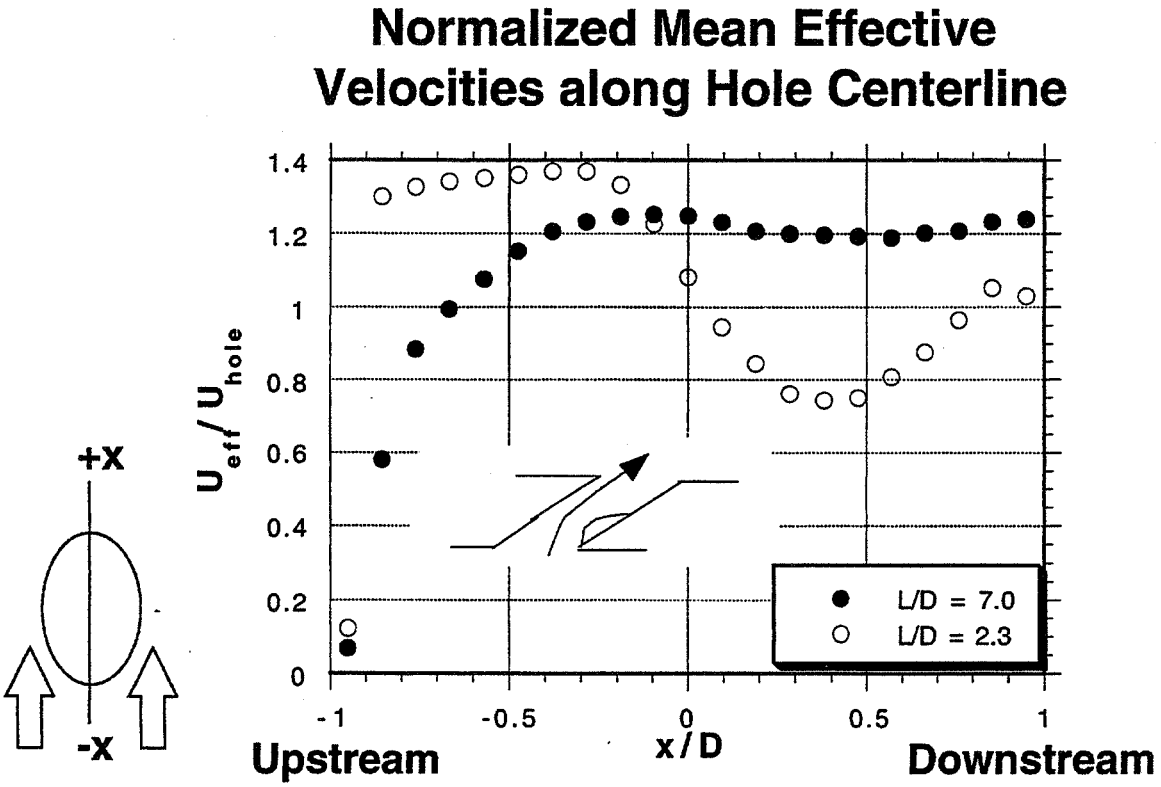

CONCLUSIONS THUS FAR:

- Short hole injection results in "jetting" characterized by further penetration of the film cooling flow into the mainstream. It has a profound effect on the mixing zone between the two flows.

- The flow between holes is more strongly influenced with short hole injection than with long holes. This effect diminishes with elevated FSTI.

Hole Centerline Velocity Profiles
FSTI=12%, y/D=0.0027

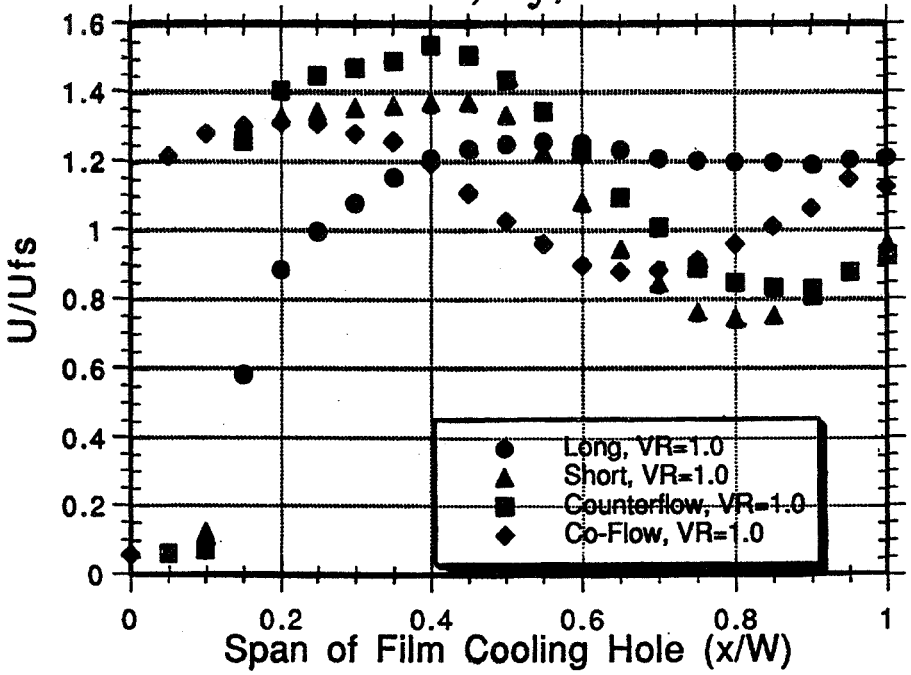

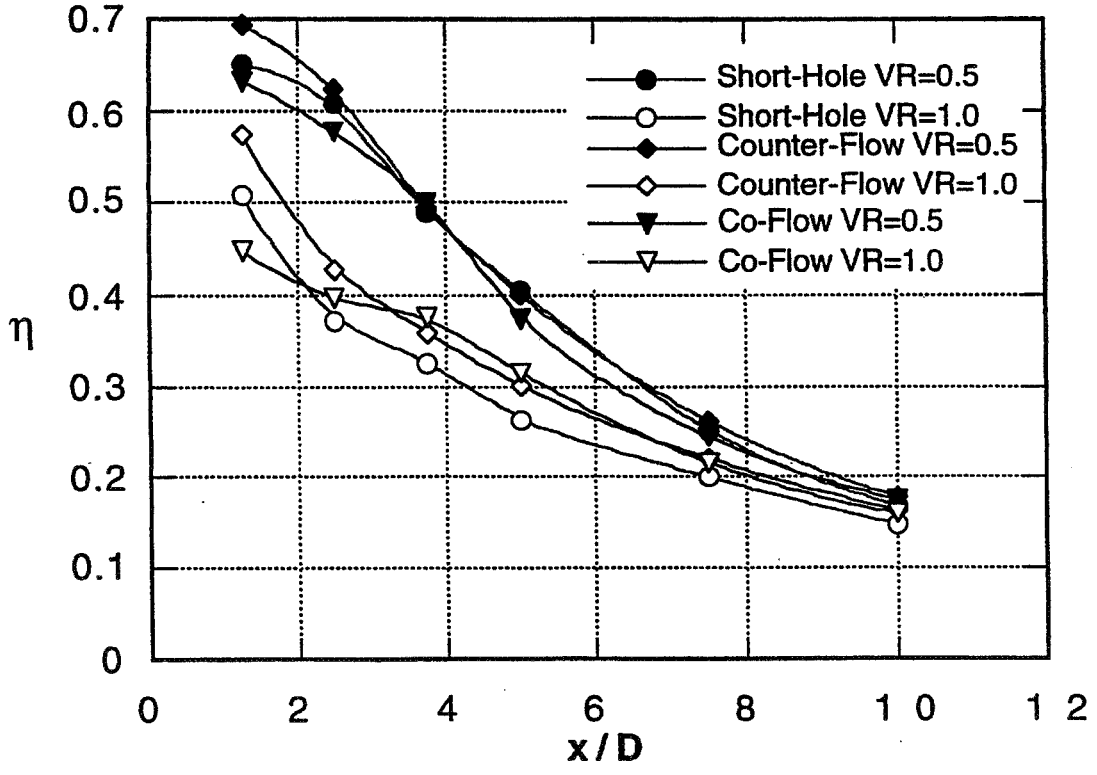

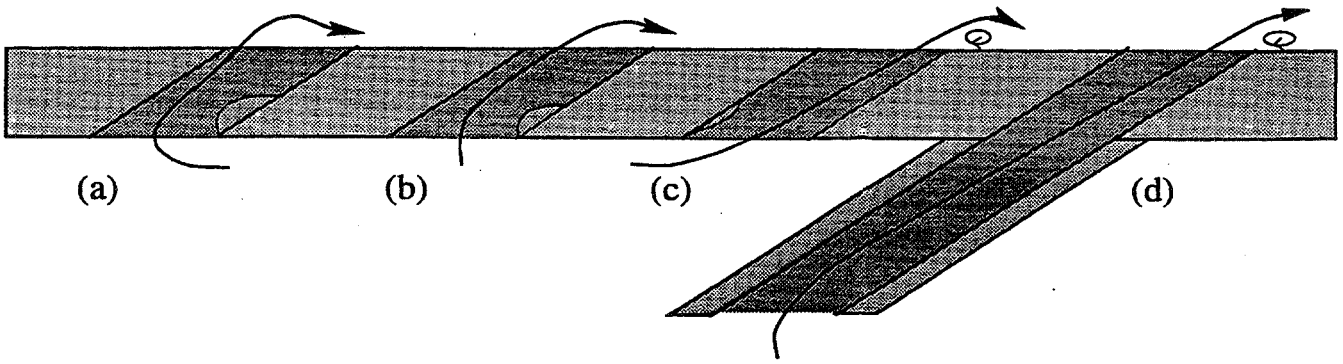

Flow Streamlines for the Various Injection Geometries:
(a). Short hole injection with an open plenum.
(b). Short hole injection with counter-flow approach.
(c). Short hole injection with co-flow approach.
(d). Long hole injection.

CONCLUSIONS FROM THIS PHASE:

- The plenum geometry has a significant effect when the plenum height is two diameters or smaller. Sensitivity to the way in which the flow is delivered to the holes rises with VR.

- Computational evidence is consistent with the experimental findings.

- The plenum geometry is of secondary importance relative to the hole length.

NUMERICAL SIMULATION OF A FILM COOLING JET IN CROSSFLOW

Sumanta Acharya
Louisiana State University
Baton Rouge, Louisiana

Background

- The hydrodynamics of a film-cooling jet in crossflow is rather complex. Near field is dominated by coherent vortical structures.These include: Jet-shear layer vortices,Counter-rotating vortex pair,Horse-shoe vortices and Wake vortices. Need to accurately predict these dynamical structures.

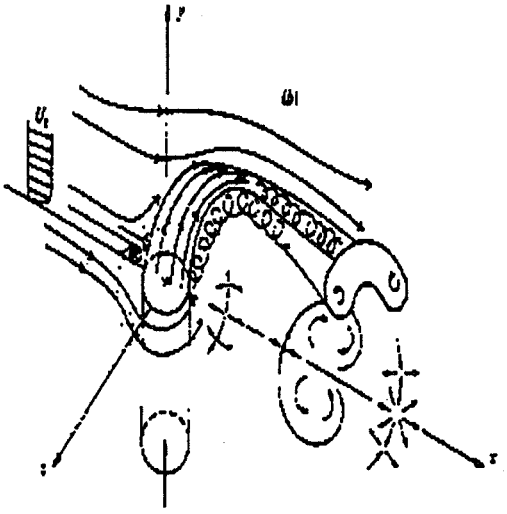

From Andreopoulos (1985)

- In jet and mixing-layer flows, the near-field dynamical structures control the mixing and entrainment behavior.
- The dynamics of these structures can not be predicted by time-averaged predictive procedures.

Film Cooling Jet: Measurements

- Measurements of Ajersch et al. (1995)
- Square coolant holes(12.5 mmm); Jet Velocity=5.5 m/s; Blowing ratio-0.5,1,1.5;Ninety-degree simple injection; Evidence of dynamical effects.

From Ajersch et al (1995)

- Reynolds-averaged predictions do not compare well with measurements

Film Cooling: Measurements

- UTRC data; Circular film cooling hole(22.73 mm dia); Free stream velocity=15.25m/s; Blowing ratio=0.5,1, 2; Simple injection at 35 degrees.
- Reynolds-Averaged predictions over-predict jet penetration due to inaccurate representation of large scale effects.

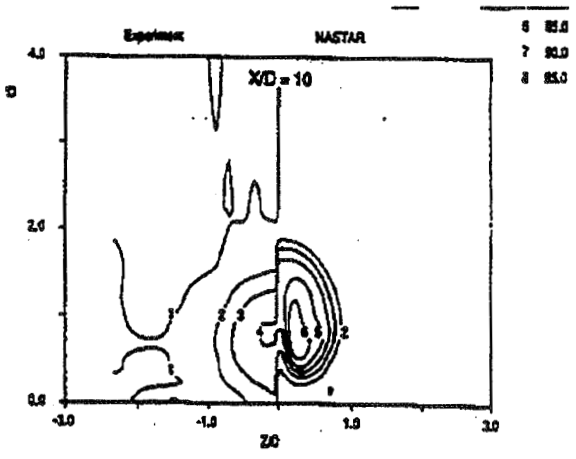

Film Cooling Effectiveness

- Due to overprediction of jet penetration, film cooling effectiveness is poorly predicted.

- Due to overprediction of jet penetration, film cooling effectiveness is poorly predicted.

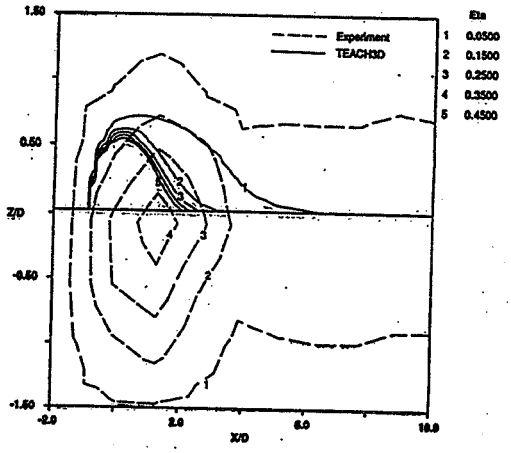

FROM UTRC DATA AND REPORT

Goal of This Study

- To accurately predict the near-field large scale structures, and to model the smaller-scales. Goal is to correctly predict the jet penetration so that calculations of film cooling effectiveness are meaningful.
- Toward this goal, Direct Numerical Simulation (DNS) and Large Eddy Simulation (LES) will be undertaken. Comparison with RANS predictions will guide the evaluation and improvement of turbulence models

RESEARCH PLAN

- Ajersch et al
  - DNS
  - LES
  - RANS
- Improved understanding and predictive capability
- Completed DNS code
- Ongoing DNS simulations and LES simulations
- UTRC Data
  - LES
  - RANS
- Ongoing RANS simulations
- LES simulations to follow

DNS Code Development

- INS-3D
  - Pseudocompressibility with pseudo-time iterations
  - Fifth-order accurate approximation for the convective terms
  - Fourth order accurate approximations for the diffusion terms
  - Second order accurate temporal discretization
  - Body fitted coordinates
  - Fourth-order approximation for all metrics
- INS-Poisson(LES)
  - Fractional step approach
  - Third-order, upwind biased scheme for the convection terms
  - Second order central scheme for the diffusion terms
  - Second-order accurate pressure Poisson Equation
  - Samgorinsky's scheme for subgrid scale stresses

RANS CODE & TURBULENCE MODELS

- Control-Volume formulation to solve time-averaged equations
- Second-order accurate schemes; QUICK for convection, CDS for diffusion
- Pressure and pressure-correction schemes as in SIMPLER
- Line-by-line Gauss -Seidel Relaxation
- Standard k-ε model; Non-linear k- ε model; Functionalized k- ε model

INS-3D-DNS

- Governing Equations:

$$\frac{\partial \hat{u}}{\partial t} = -\frac{\partial(\hat{e}-\hat{e}_v)}{\partial \xi} - \frac{\partial(\hat{f}-\hat{f}_v)}{\partial \eta} - \frac{\partial(\hat{g}-\hat{g}_v)}{\partial \zeta} \equiv -\hat{r}$$

$$\frac{\partial p}{\partial \tau} = -\beta\left[\frac{\partial(U/J)}{\partial \xi} + \frac{\partial(V/J)}{\partial \eta} + \frac{\partial(W/J)}{\partial \zeta}\right]$$

- Discretised Equation has the form:

$$\left[I_{tr} + \left(\frac{\partial \hat{R}}{\partial \hat{D}}\right)^{n+1,m}\right](\hat{D}^{n+1,m+1} - \hat{D}^{n+1,m}) = -\hat{R}^{n+1,m} - \frac{I_m}{\Delta t}\begin{pmatrix}1.5\hat{D}^{n+1,m} - 2\hat{D}^{n} \\ +0.5\hat{D}^{n-1}\end{pmatrix}$$

- Used fifth order upwind-biased discretization for convection; fourth order CDS for diffusion; Gauss-Seidal Line Relaxation SCheme or GMRES solver

INS-Poisson-LES

- Fractional step Approach

$$\frac{\rho^{n+1}V^* - \rho^n V^n}{\Delta t} = C(V) + D(V)$$

$$\nabla.\left(\frac{\nabla p^{n+1}}{\rho^{n+1}}\right) = \nabla.V^*$$

$$\frac{\rho^{n+1}V^{n+1} - \rho^n V^*}{\Delta t} = -\nabla p$$

- Temporal accuracy increased by using either an Adams-Bashforth scheme, or by a second loop-through the steps.

LES: Subgrid Models

- Filtered equations of motion

$$\frac{\partial \overline{u}_i}{\partial t}+\frac{\partial}{\partial x_j}(\overline{u}_i\overline{u}_j)=-\frac{1}{\rho}\frac{\partial \overline{p}}{\partial x_i}+\frac{\partial}{\partial x_j}(\tau_{ij})+\nu\frac{\partial^2}{\partial x_i \partial x_j}(\overline{u}_i)$$

- Subgrid scale stresses: $\tau_{ij}=u_iu_j-\overline{u}_i\overline{u}_j$
- Smagorinsky's model: Eddy viscosity
- Dynamic subgrid scale model: test filter

RANS: Turbulence Models

- Standard k-ε model
- Non-linear k- ε model of Speziale
- Functionalized model of Dutta and Acharya
- Other models: RNG, RS, Durbin

Preliminary Flow Results

- Ajersch et al's test case

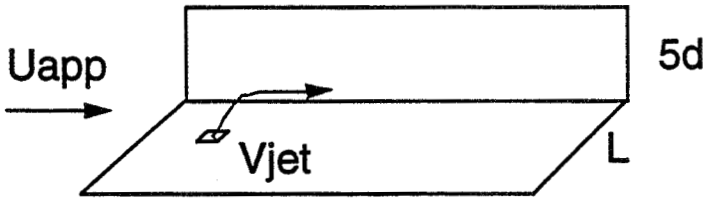

Uapp=2.75 m/s; Vjet=5.5 m/s; d=12.7mm; L=4d

- Results obtained on a 140x40x40 non-uniform mesh; 80 points in the hole region; Resolves large scale features; No subgrid stress models

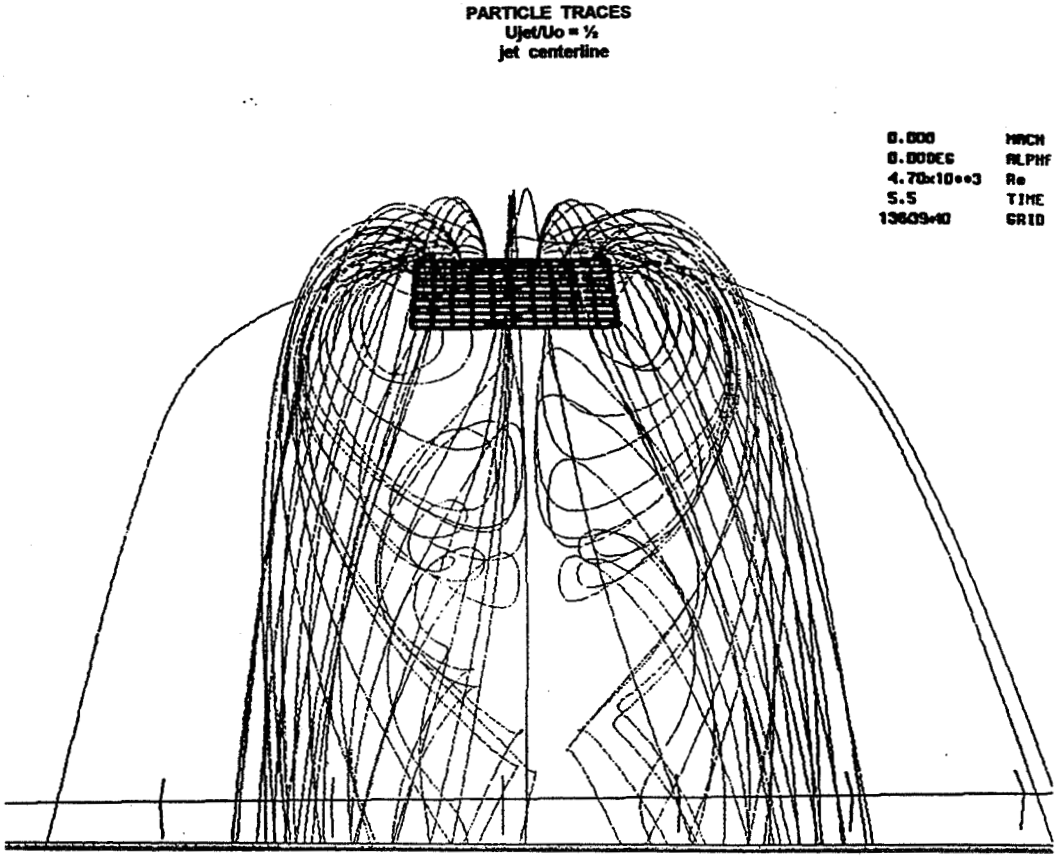

PARTICLE TRACES
Ujet/Uo = 1/2
jet centerline

0.000 MACH
0.000EG ALPHF
4.70x10**3 Re
5.5 TIME
13639x40 GRID

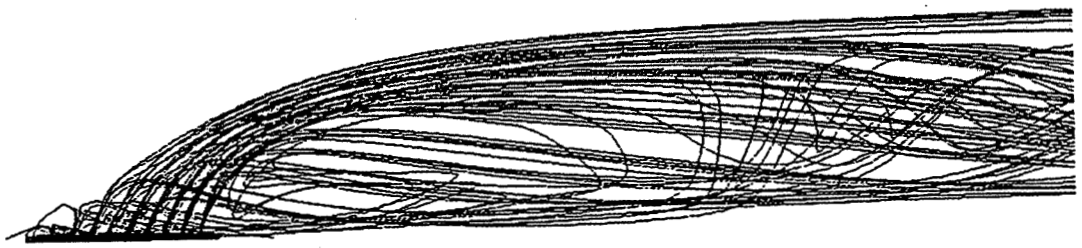

PARTICLE TRACES
Ujet/Uo = 1/2
jet centerline

0.000 MACH
0.000EG ALPHF
4.70x10**3 Re
5.5 TIME
13639x40 GRID

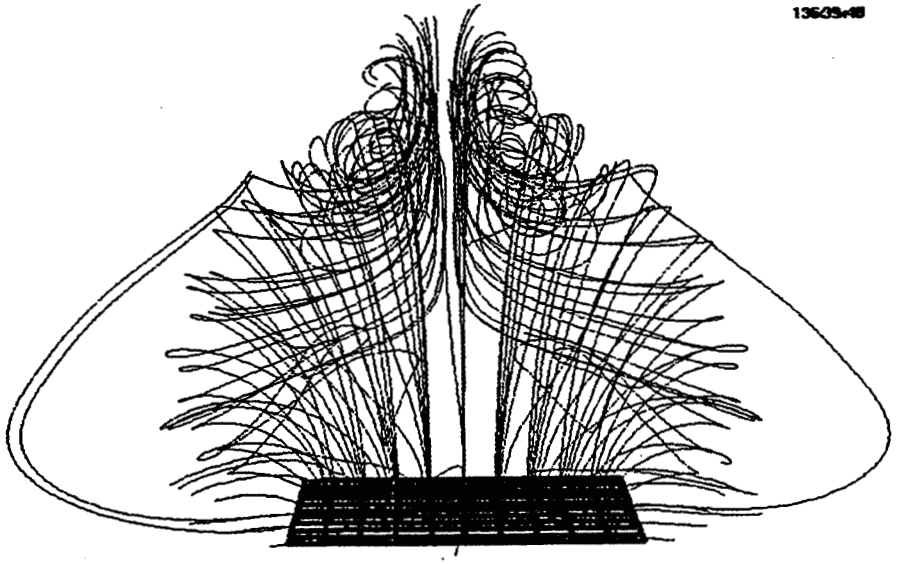

PARTICLE TRACES
Ujet/Uo = 1/2
y/D = .672

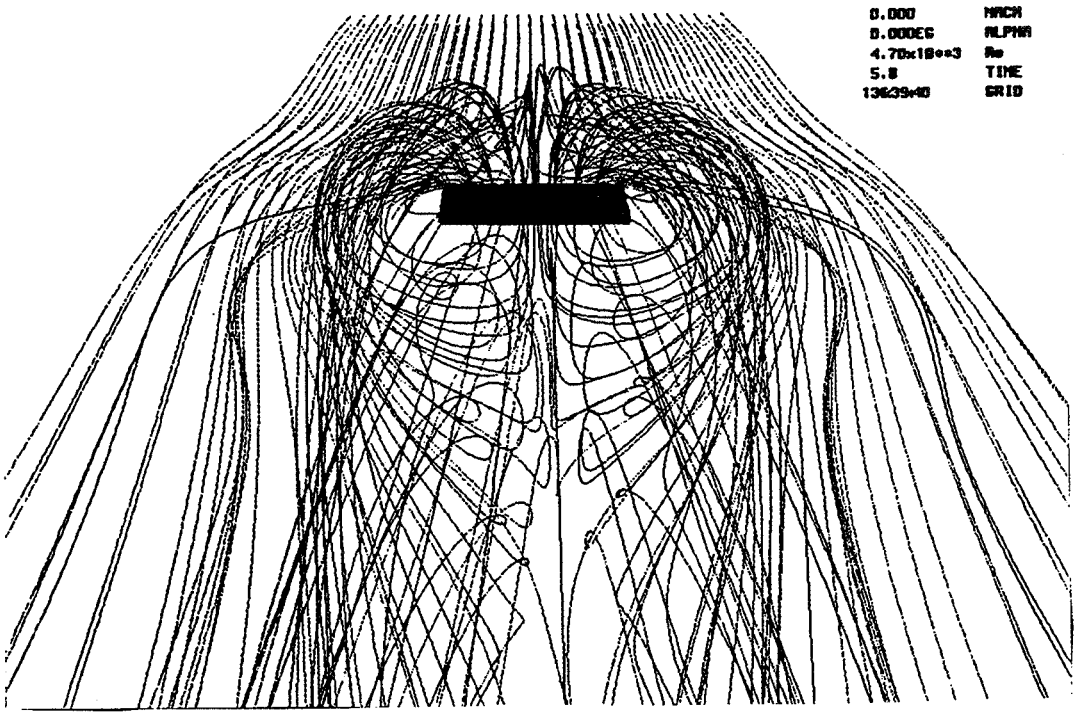

U VELOCITY
Ujet/Uo = 1/2
jet centerline

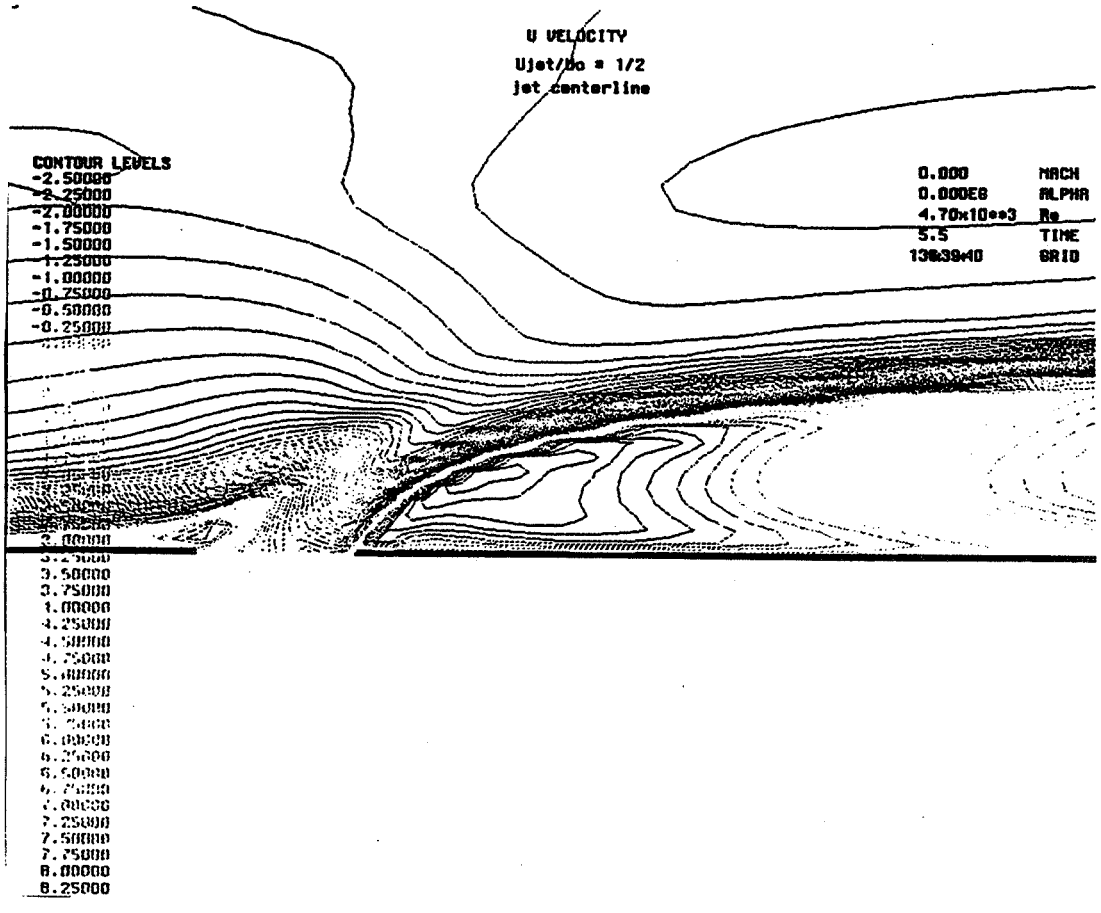

X-COMPONENT OF VORTICITY

Ujet/Uo = 1/2

1.011 D downstream from center of jet

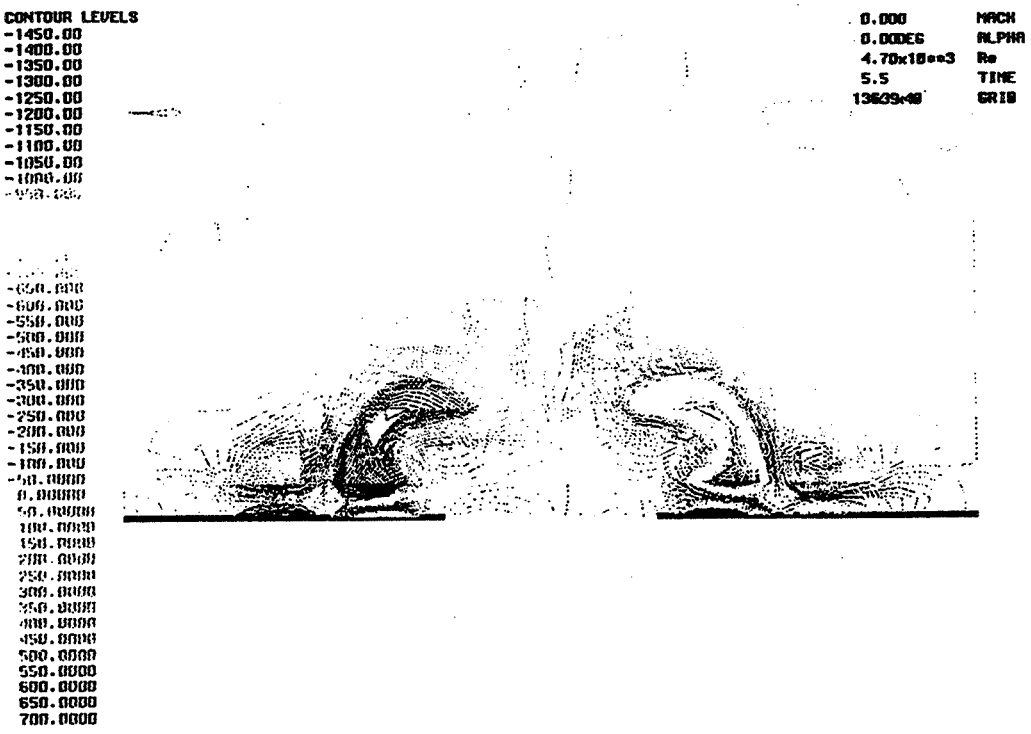

X-COMPONENT OF VORTICITY

Ujet/Uo = 1/2

2.985 D downstream from center of jet

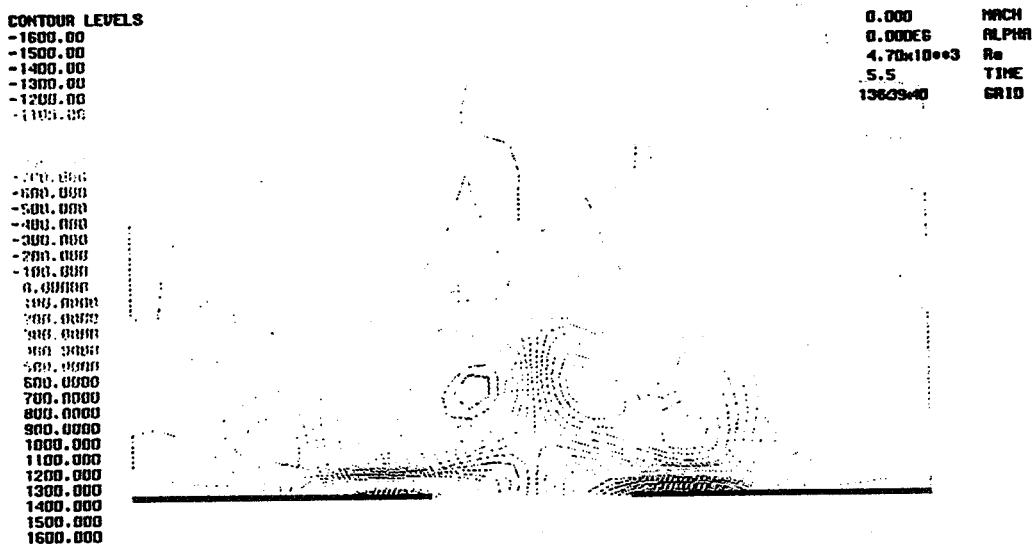

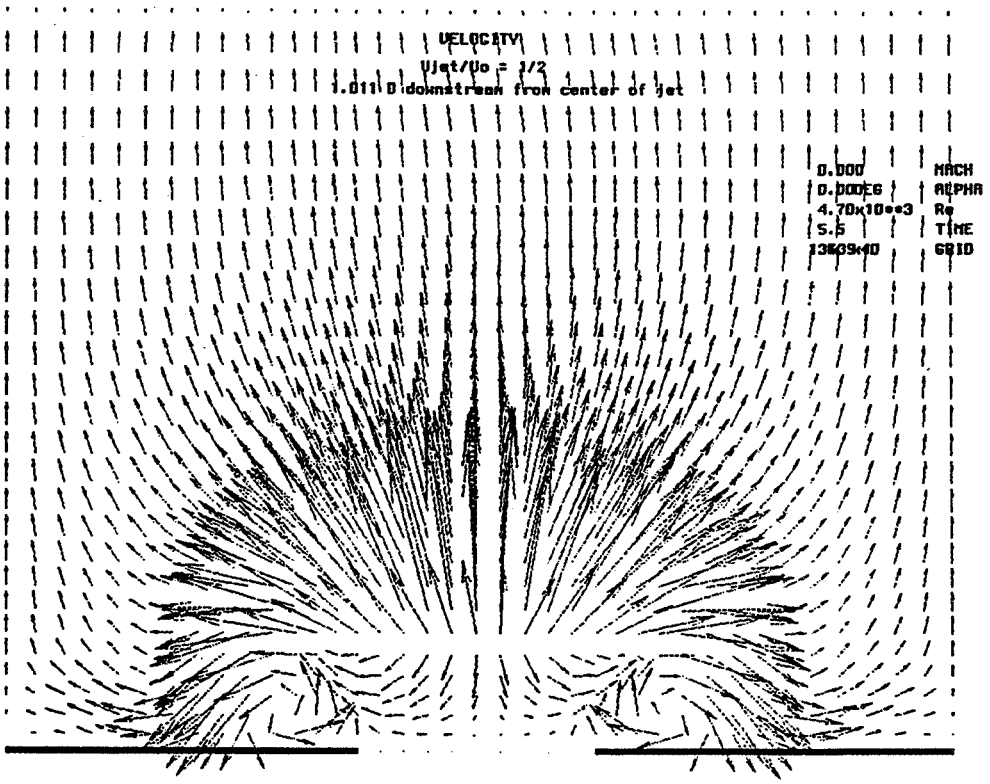
VELOCITY
Vjet/Vo = 1/2
1.011 D downstream from center of jet
0.000
0.000EG
4.70x10e3
5.5
13639x40
MACH
ALPHA
Re
TIME
GRID

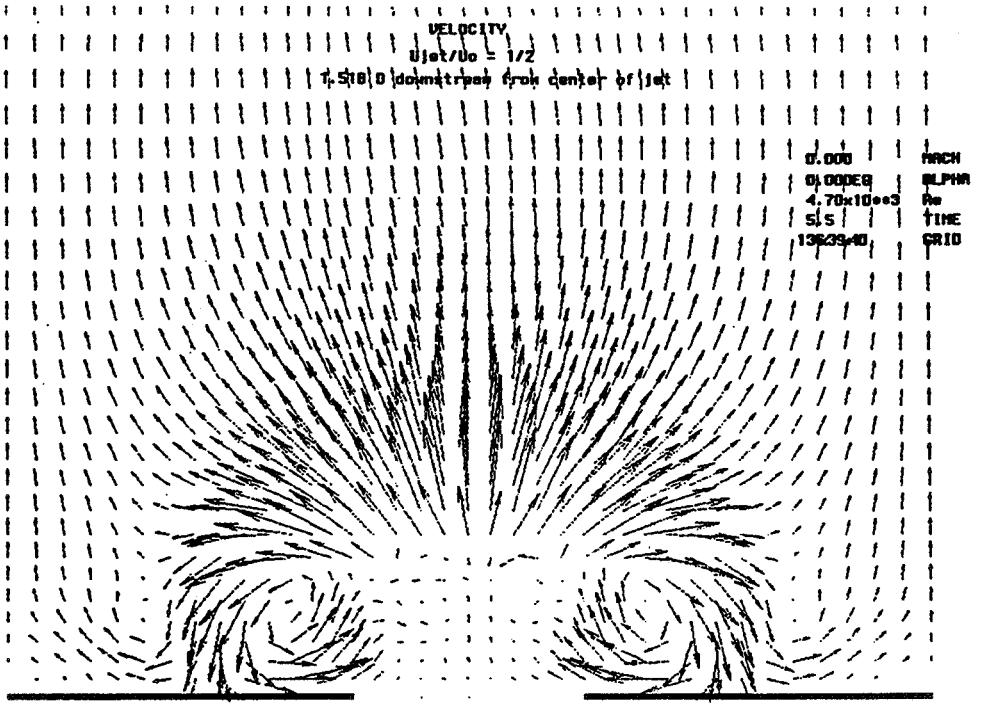
VELOCITY
Vjet/Vo = 1/2
1.518 D downstream from center of jet
0.000
0.000EG
4.70x10e3
5.5
13639x40
MACH
ALPHA
Re
TIME
GRID

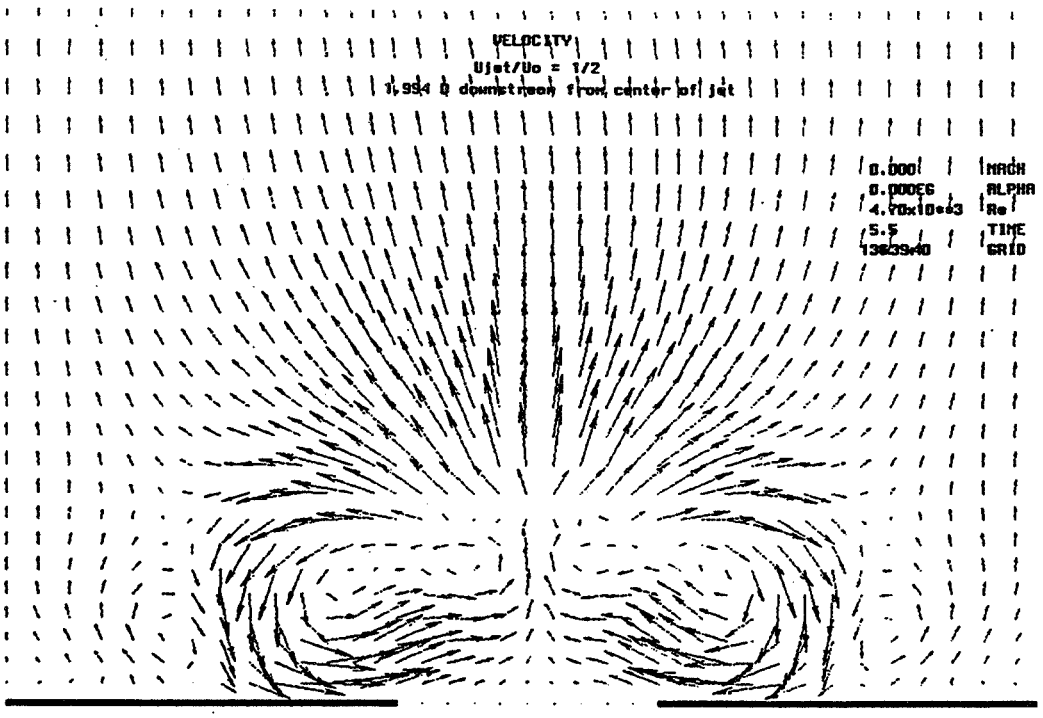
VELOCITY
Ujet/Uo = 1/2
1.994 D downstream from center of jet
0.000
MACH
0.000E6
ALPHA
4.78x10e+3
Re
5.5
TIME
13639x40
GRID

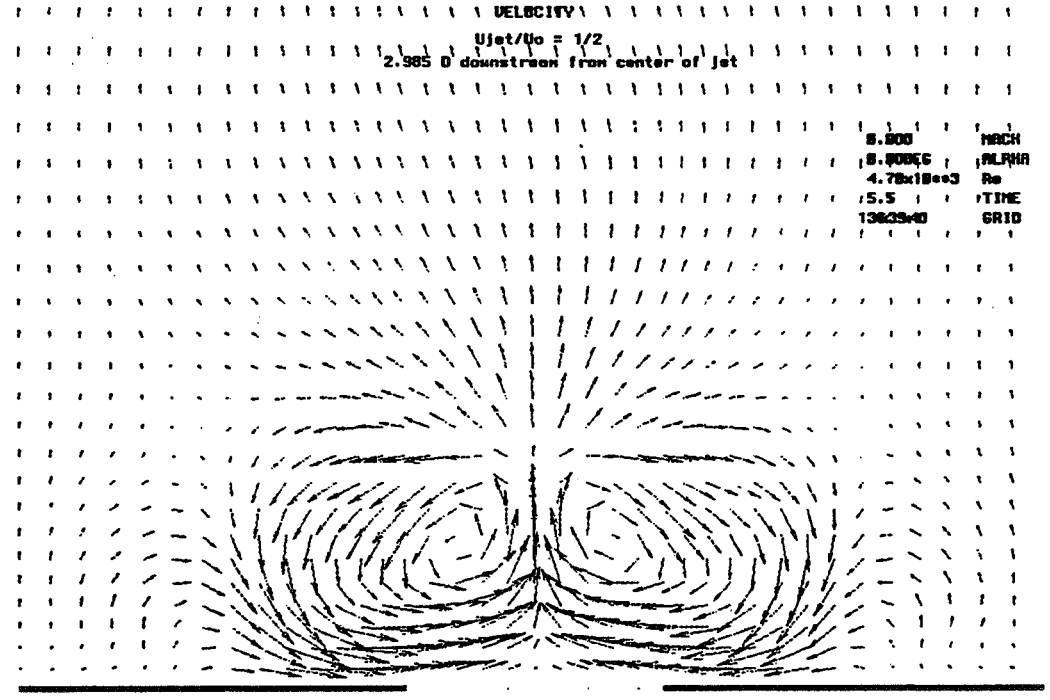
VELOCITY
Ujet/Uo = 1/2
2.985 D downstream from center of jet
0.000
MACH
0.000E6
ALPHA
4.78x10e+3
Re
5.5
TIME
13639x40
GRID

ONGOING WORK

- DNS on a finer grid for Ajersch's data
- LES with Smagorinsky's model
- RANS with improved models

HEAT TRANSFER IN FILM-COOLED TURBINE BLADES

Vijay Garg
AYT Corporation
NASA Lewis Research Center
Cleveland, Ohio

MOTIVATION

- **TENDENCY TO USE HIGHER TURBINE INLET TEMPERATURE**
  - **TO INCREASE SPECIFIC POWER OUTPUT & THERMAL EFFICIENCY**

- **NEED THEREFORE TO COOL THE BLADES AND SIDE WALLS**
  - **TO ENSURE REASONABLE LIFETIME OF MACHINE**

OBJECTIVE

- **TO DEVELOP TOOLS & MODELS TO ACCURATELY PREDICT HOT GAS SIDE HEAT TRANSFER TO A FILM-COOLED TURBINE BLADE**

- **TO MINIMIZE THE INJECTED MASS FLOW FOR A GIVEN COOLING EFFICIENCY**

- **TO DECREASE AERODYNAMIC LOSSES INDUCED BY THE JET-SECONDARY FLOW INTERACTION**

FORMULATION

- 3–D COMPRESSIBLE NAVIER–STOKES EQUATIONS
- BALDWIN–LOMAX TURBULENCE MODEL WITH MAYLE'S TRANSITION CRITERION; ALSO TWO–EQUATION MODELS (k–ε, q–ω, k–ω); ($y+ < 1$ near wall)
- BODY–FITTED COORDINATE SYSTEM; C–GRID USED
- APPROPRIATE BOUNDARY CONDITIONS SPECIFIED
- FOREST'S MODEL FOR LEADING EDGE HEAT TRANSFER AUGMENTATION DUE TO FREE–STREAM TURBULENCE
- CRAWFORD'S MODEL FOR EDDY VISCOSITY AUGMENTATION DUE TO FILM COOLING

FILM COOLING CONSIDERATIONS

- EXIT AREA OF EACH HOLE DISTRIBUTED OVER SEVERAL CONTROL VOLUMES
- ABILITY TO ANALYZE DIFFERENT HOLE SHAPES
- DIFFERENT VELOCITY AND TEMPERATURE PROFILES SPECIFIED AT THE HOLE EXIT
- SPECIFIED HEAT FLUX OR VARIABLE TEMPERATURE ON THE BLADE SURFACE

NUMERICAL SOLUTION

- TRAF3D CODE (by Andrea Arnone) MODIFIED
- CELL-CENTERED FINITE VOLUME APPROACH
- FOUR-STAGE RUNGE-KUTTA TIME STEPPING SCHEME
- 3-D EIGENVALUE SCALING OF ARTIFICIAL DISSIPATION
- VARIABLE COEFFICIENT IMPLICIT RESIDUAL SMOOTHING
- FULL APPROXIMATION STORAGE MULTI-GRID METHOD
- EFFECT OF COOLANT VELOCITY AND TEMPERATURE DISTRIBUTION AT THE HOLE EXIT ON THE HEAT TRANSFER COEFFICIENT ON VARIOUS TURBINE BLADES
- COMPARISON WITH EXPERIMENTAL DATA FOR ALL BLADES

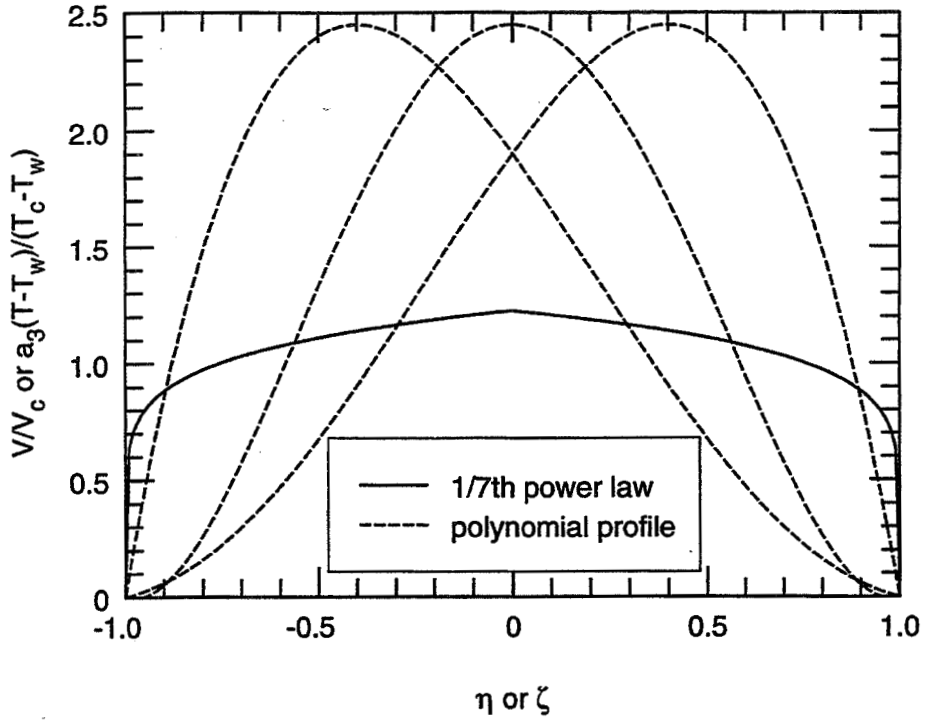

Different velocity and temperature profiles at the hole exit

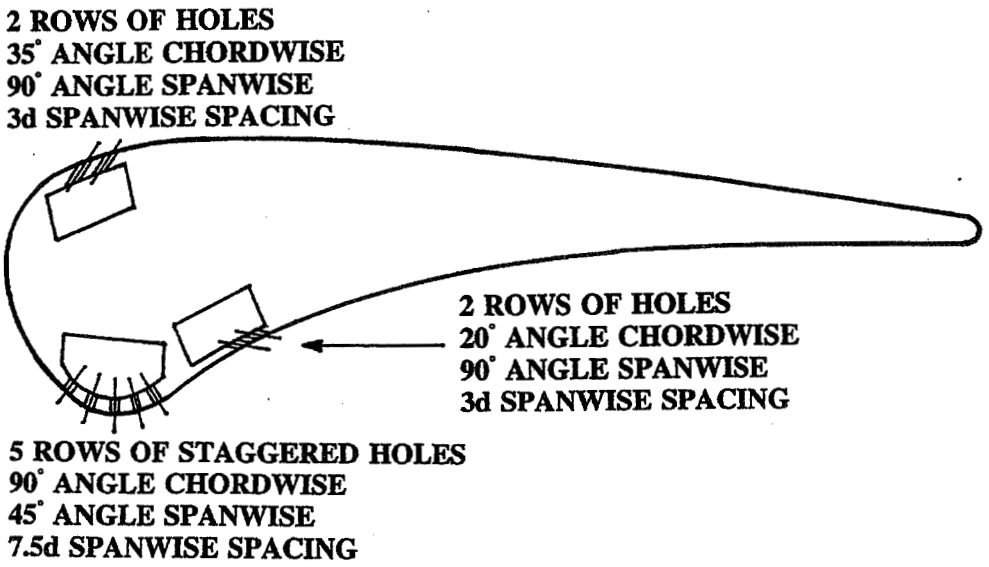

C3X vane and cooling hole details

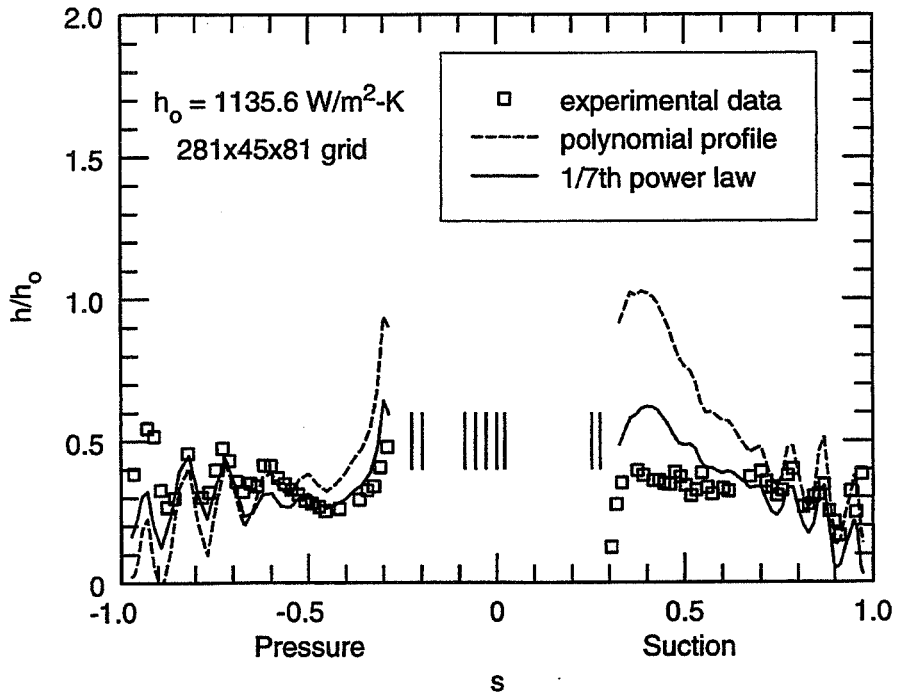

Effect of Velocity & temperature profiles at the hole exit (C3X vane: B–L turbulence model; case 44155)

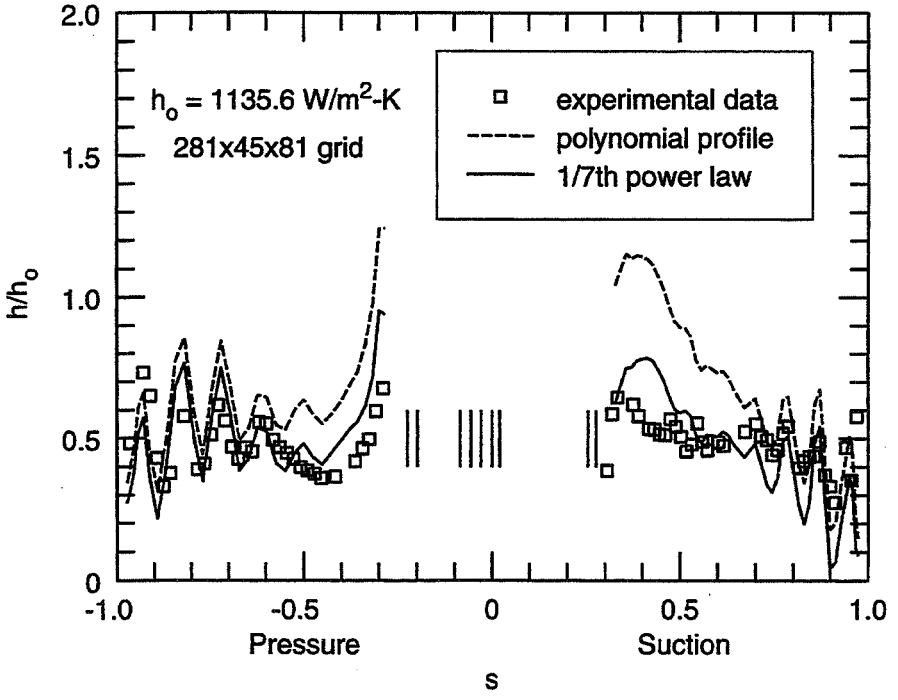

Effect of Velocity & temperature profiles at the hole exit (C3X vane: B–L turbulence model; case 44355)

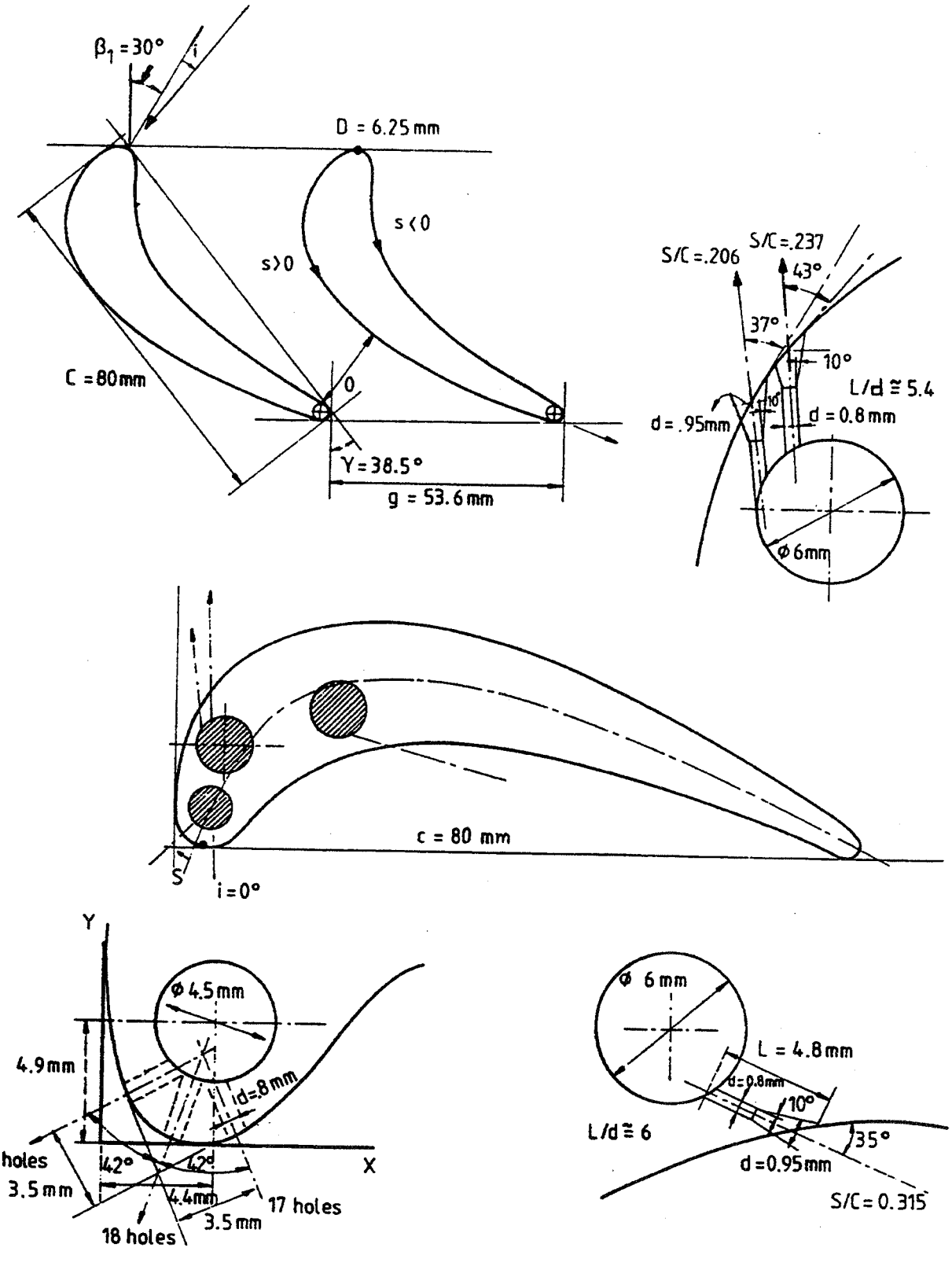

VKI rotor and cooling hole details

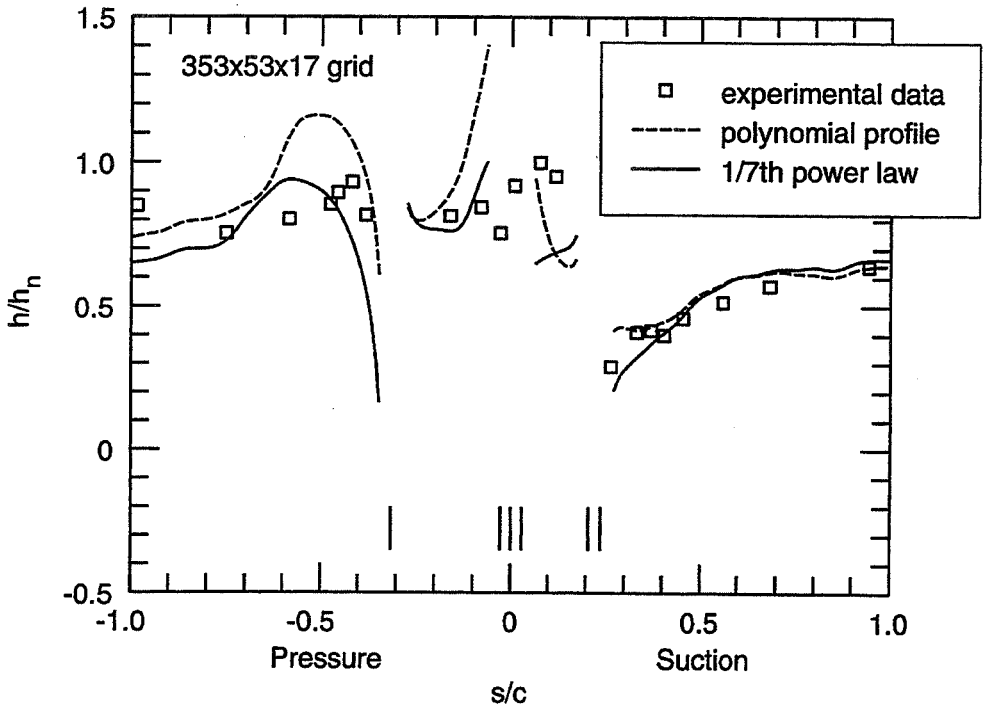

Effect of Velocity & temperature profiles at the hole exit (VKI rotor: B–L turbulence model; 2.07% coolant)

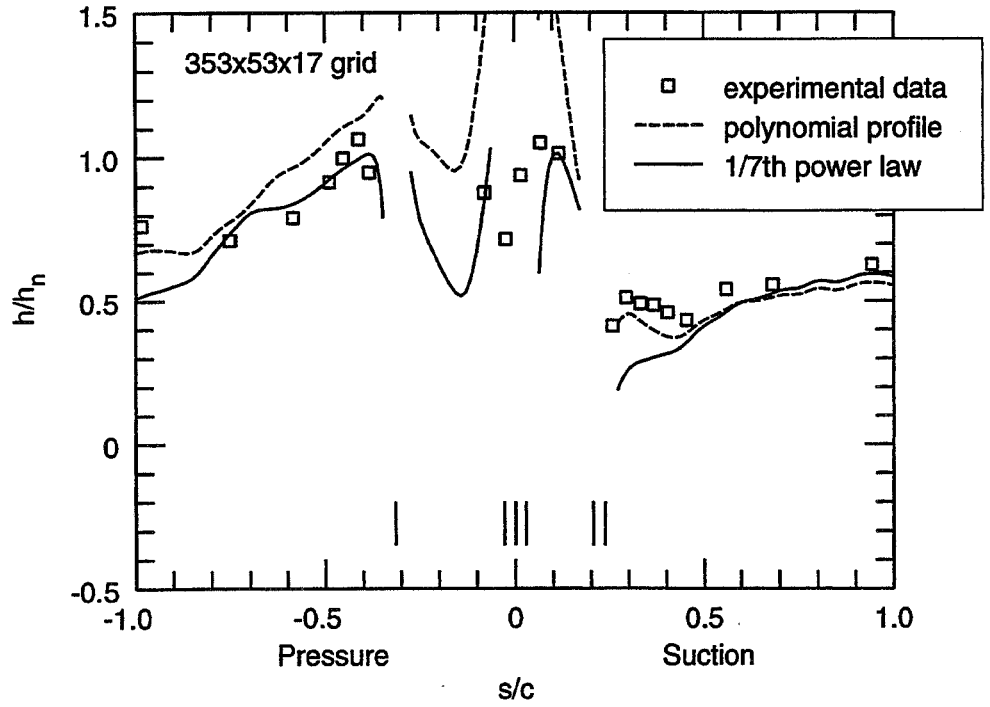

Effect of Velocity & temperature profiles at the hole exit (VKI rotor: B–L turbulence model; 3.09% coolant)

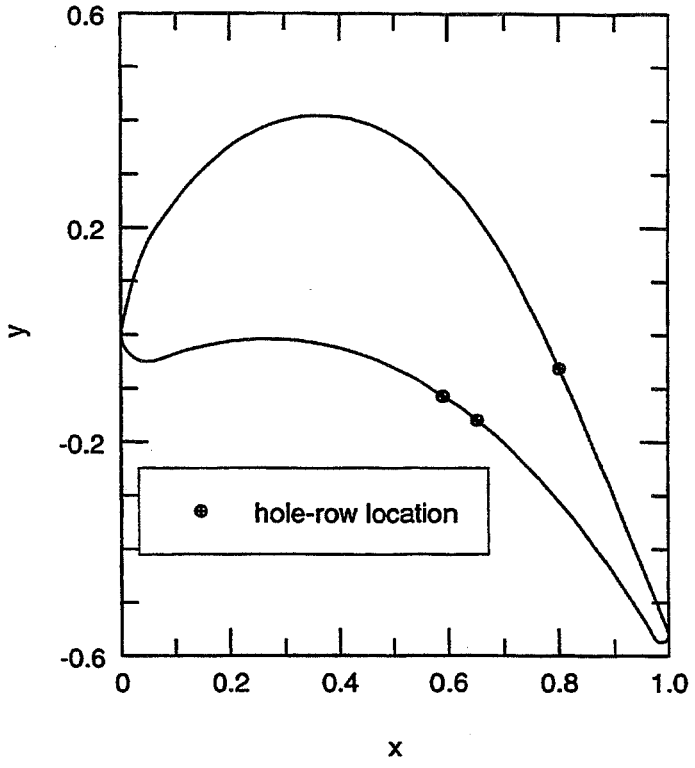

ACE rotor (non–rotating) with film–cooling hole locations

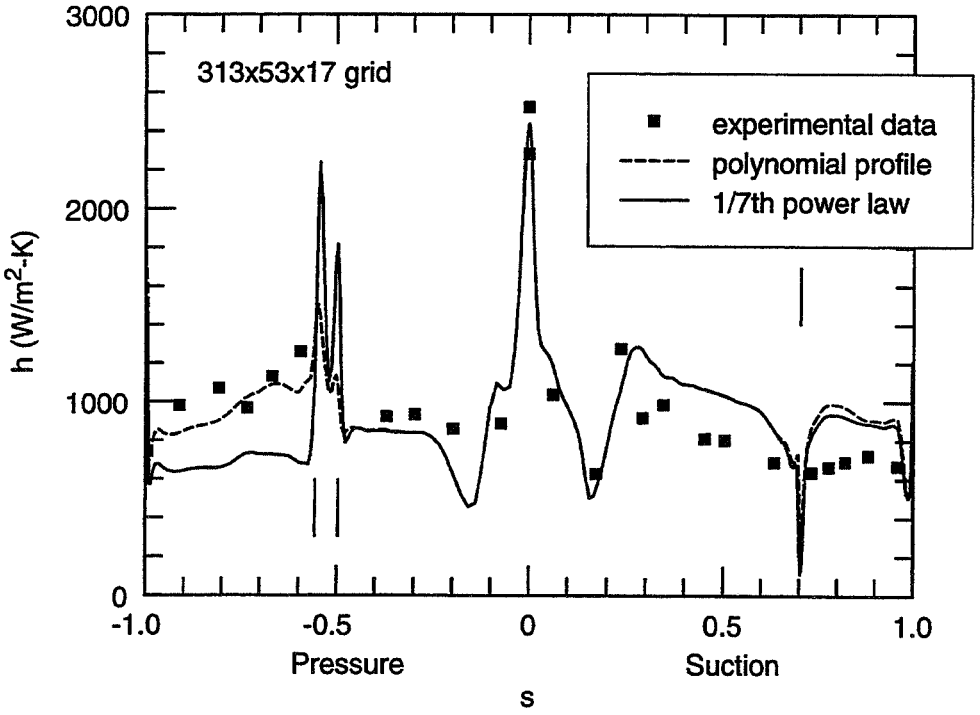

Effect of Velocity & temperature profiles at the hole exit (ACE rotor: B–L turbulence model; case 6109)

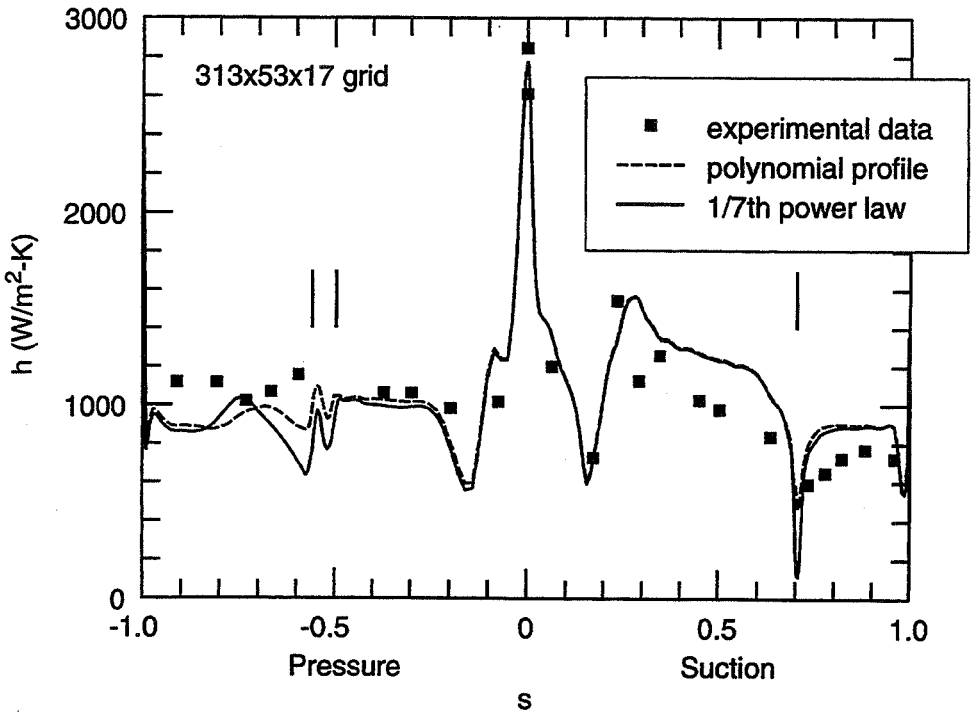

Effect of Velocity & temperature profiles at the hole exit (ACE rotor: B–L turbulence model; case 6115)

- **EFFECT OF BLADE ROTATION**

- **EFFECT OF DIRECTION OF COOLANT INJECTION FROM THE SHOWER-HEAD HOLES**

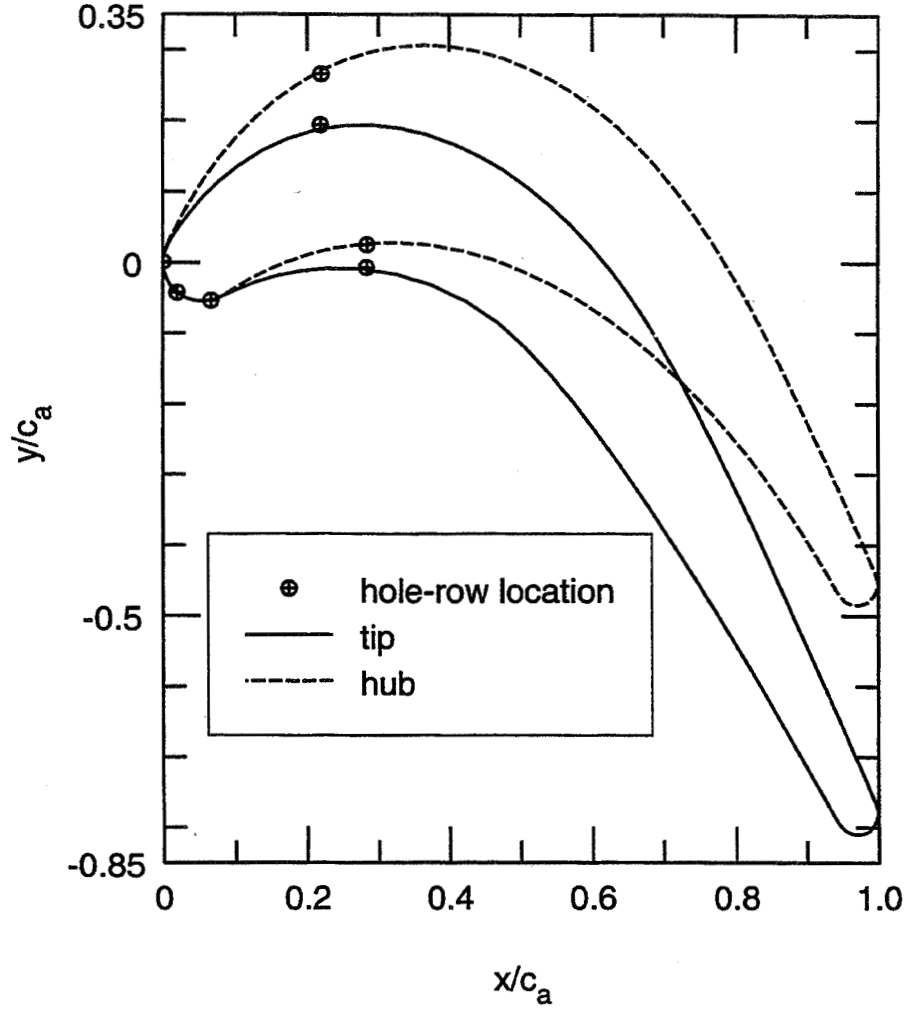

UTRC rotor geometry and hole–row locations at hub & tip

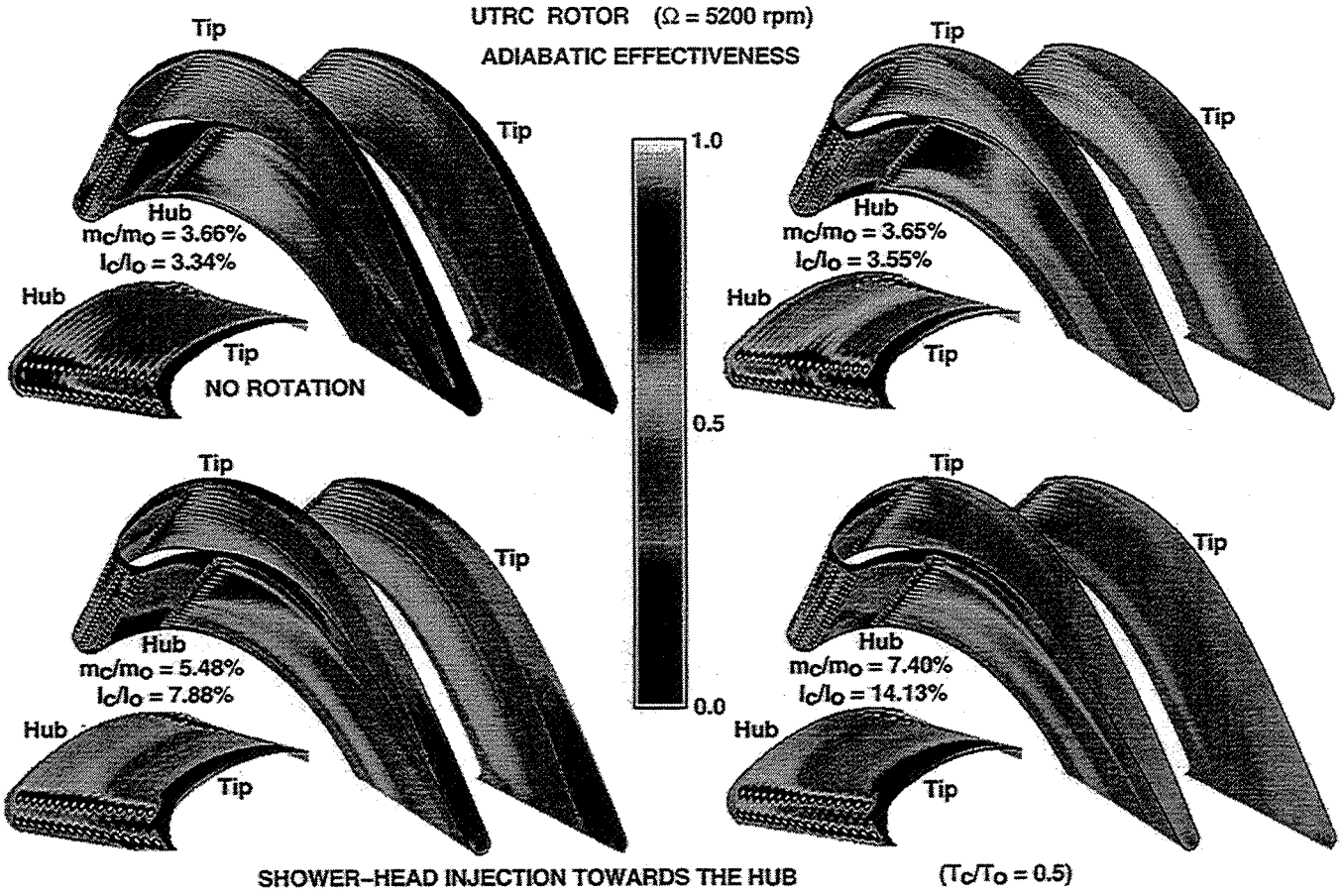
UTRC ROTOR (Ω = 5200 rpm)
ADIABATIC EFFECTIVENESS
Tip
Tip
Hub
mc/mo = 3.66%
lc/lo = 3.34%
Hub
Tip
NO ROTATION
1.0
0.5
0.0
Tip
Tip
Hub
mc/mo = 3.65%
lc/lo = 3.55%
Hub
Tip
Tip
Tip
Hub
mc/mo = 5.48%
lc/lo = 7.88%
Hub
Tip
Tip
Tip
Hub
mc/mo = 7.40%
lc/lo = 14.13%
Hub
Tip
SHOWER-HEAD INJECTION TOWARDS THE HUB
(Tc/To = 0.5)

Demonstration of Advanced Film Cooling Model to a Turbine Blade Thermal Design Problem (Adjusting Coolant Injection Angles to Maximize Cooling Effectiveness)

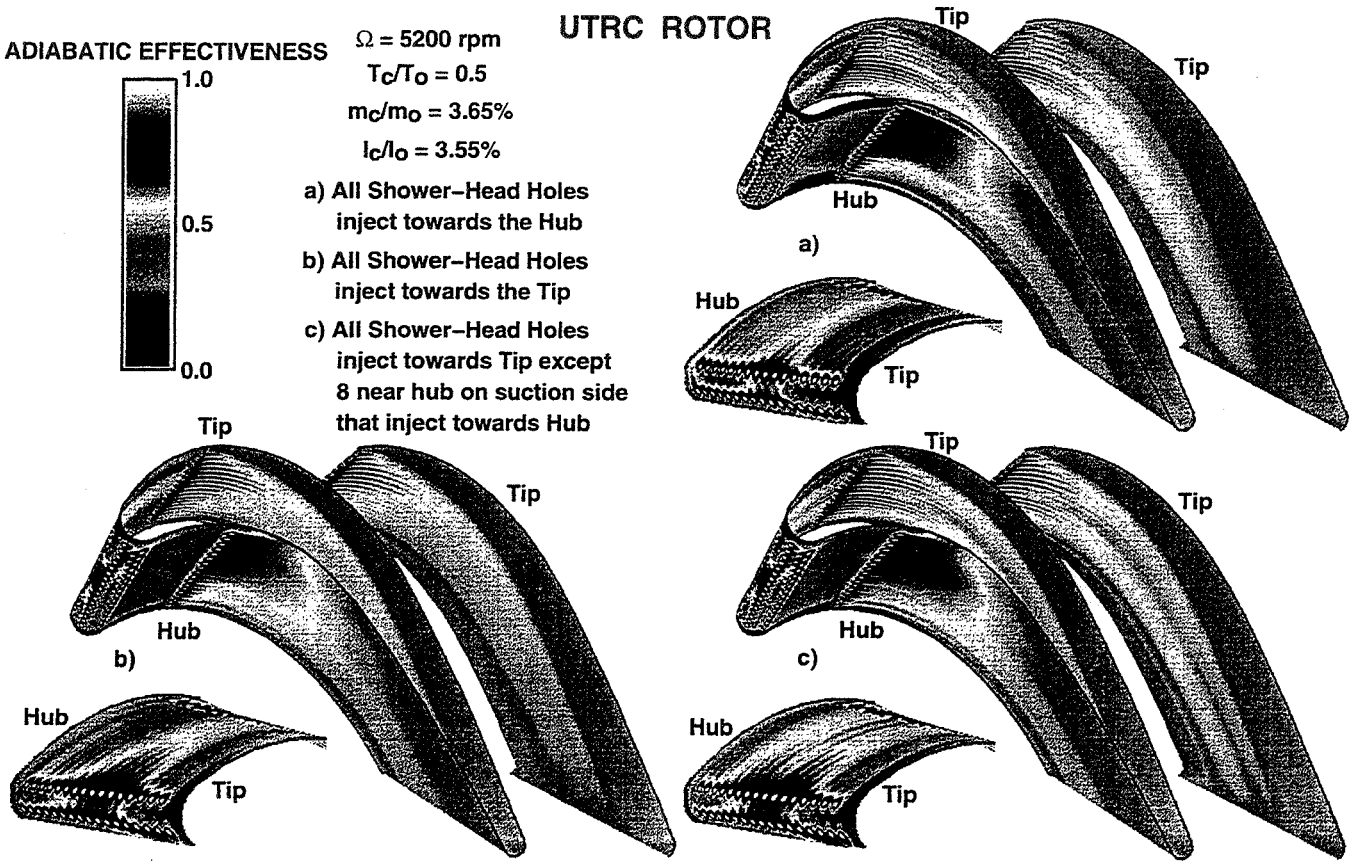

- **EFFECT OF TURBULENCE MODELING:**

  Baldwin–Lomax model
  Coakley's q–ω model
  Chien's k–ε model
  Wilcox's k–ω model

- **COMPARISON WITH EXPERIMENTAL DATA FOR ALL BLADES**

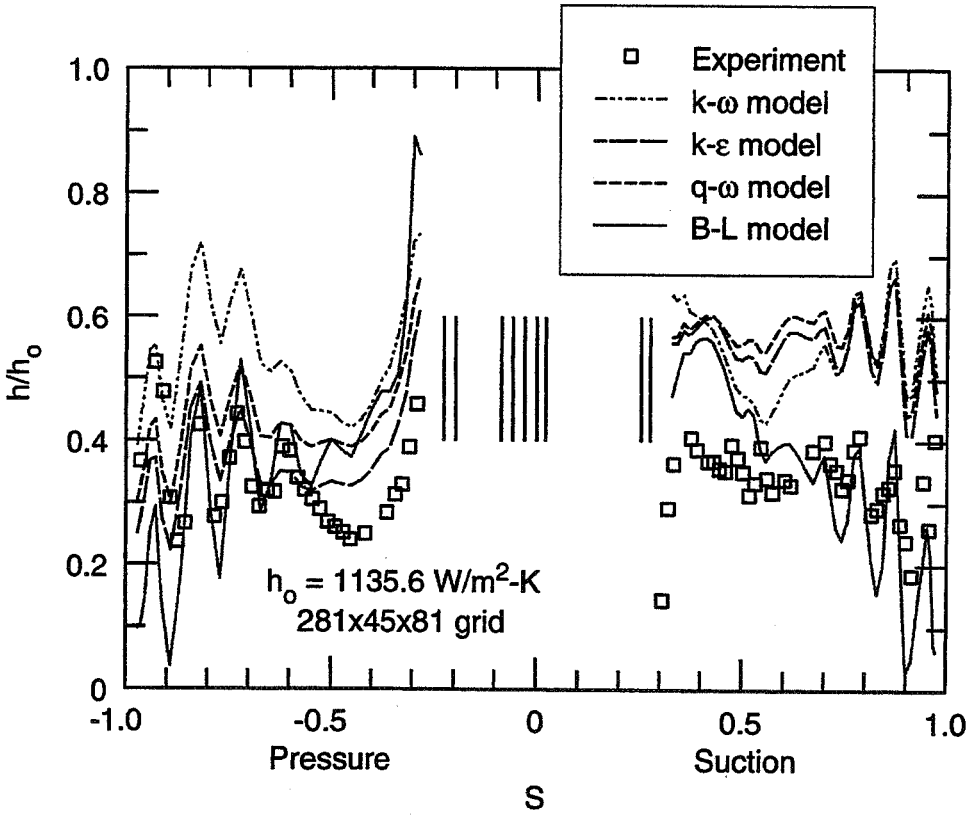

Various Turbulence Models: C3X vane near mid–span (case 44135)

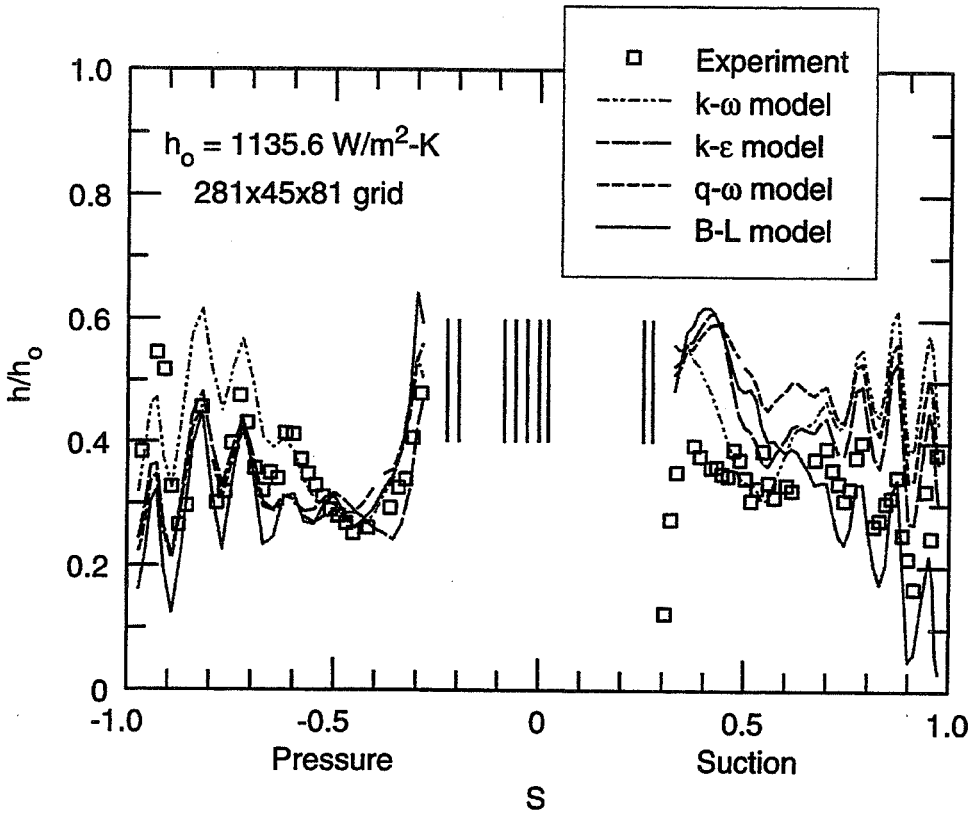

Various Turbulence Models: C3X vane near mid-span (case 44155)

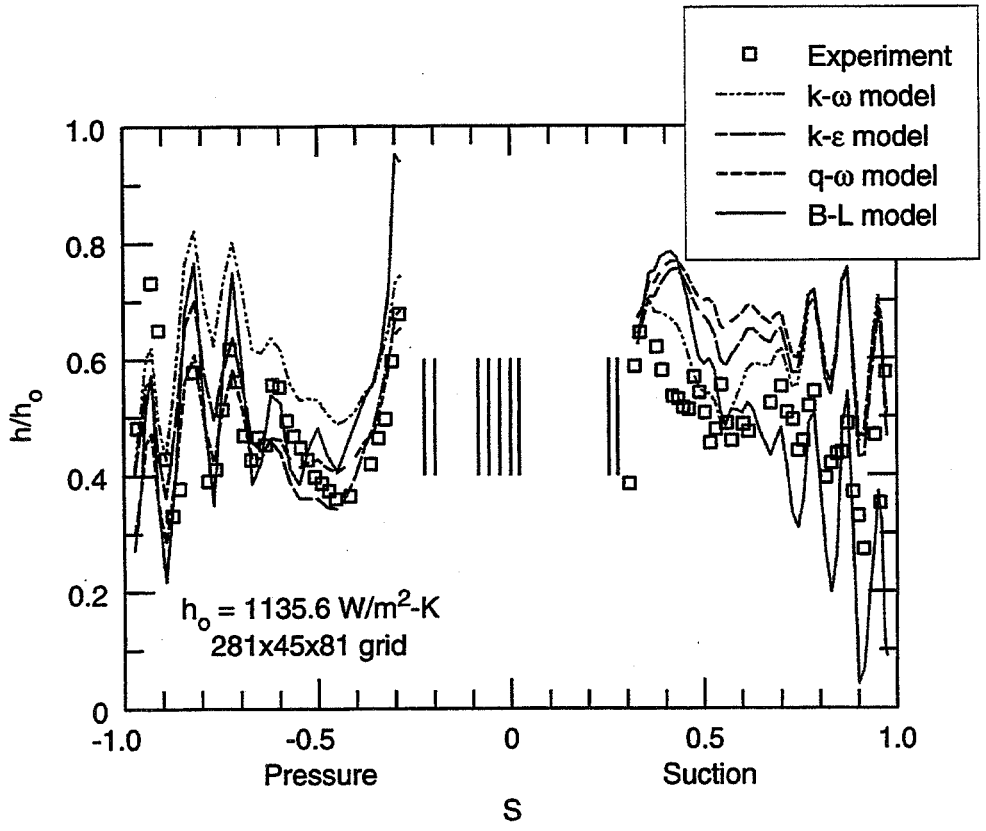

Various Turbulence Models: C3X vane near mid-span (case 44355)

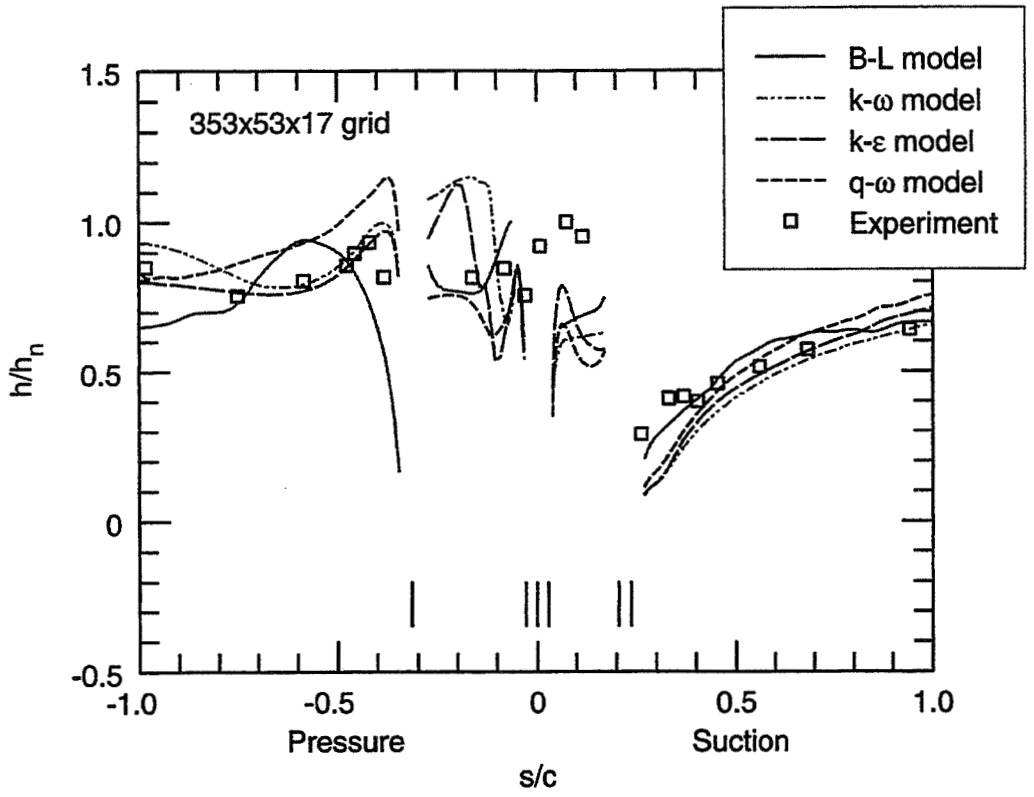

Various turbulence models: vki rotor (coolant = 2.07%)

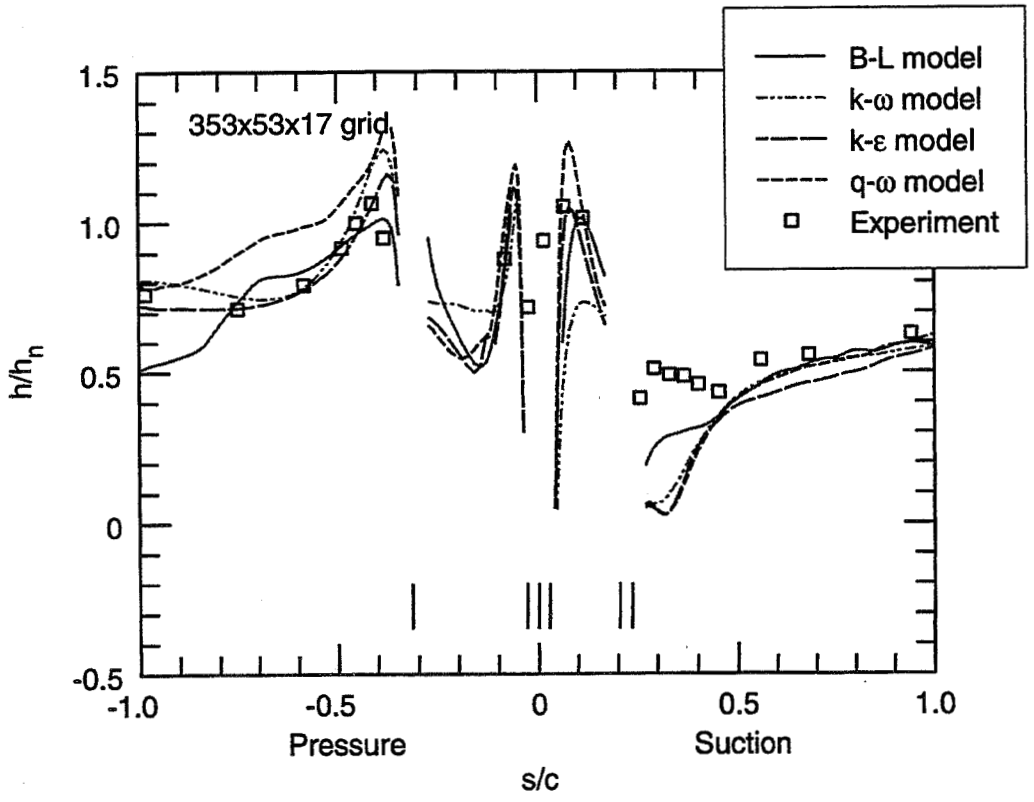

Various turbulence models: vki rotor (coolant = 3.09%)

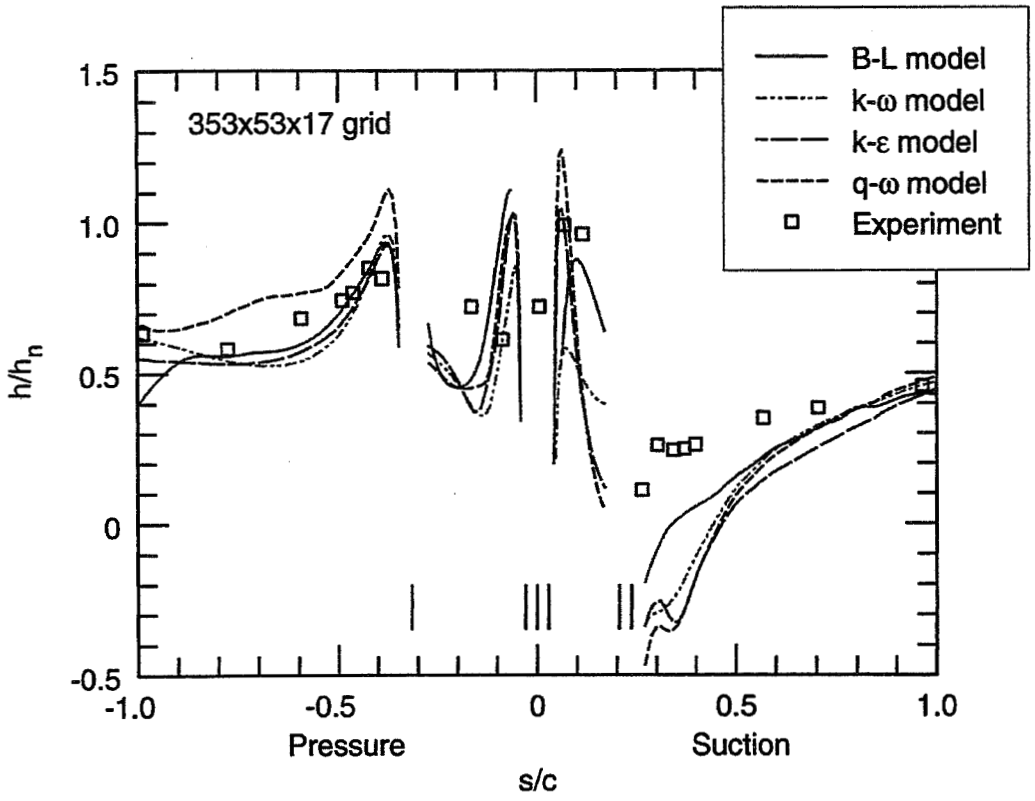

Various turbulence models: vki rotor (coolant = 3.32%)

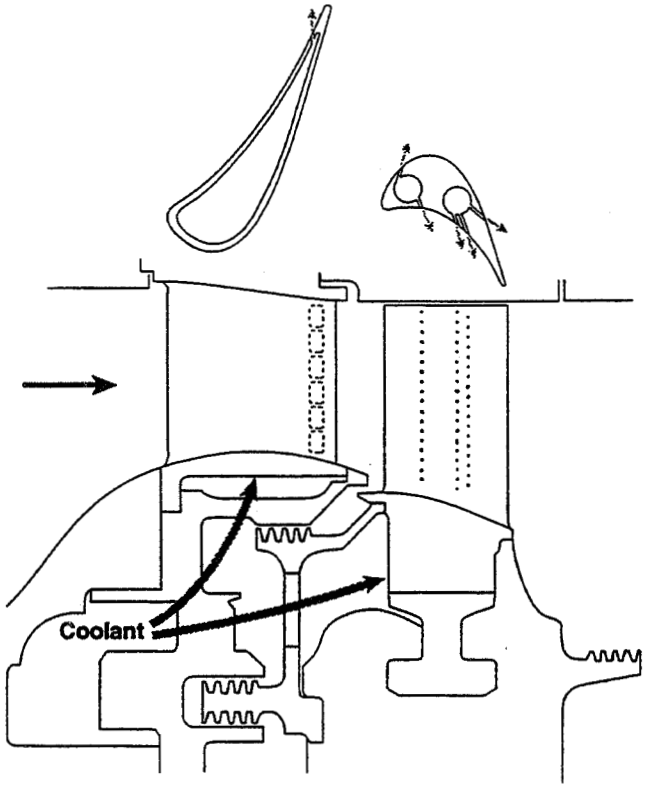

ACE turbine geometry and cooling arrangement

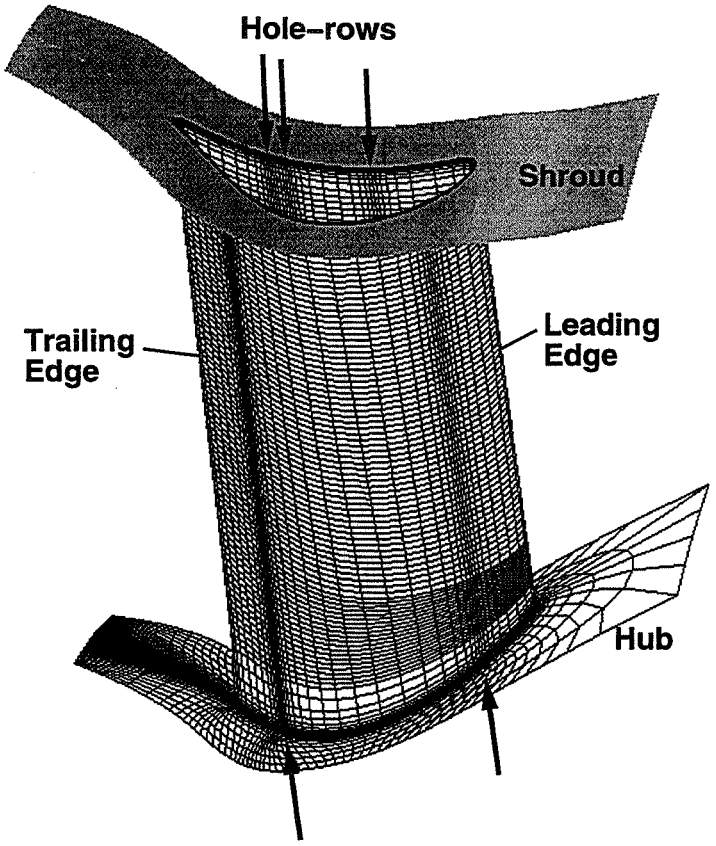

Grid on the blade surface, and C–grid on the hub. Suction surface is in the front. Alternate grid lines shown.

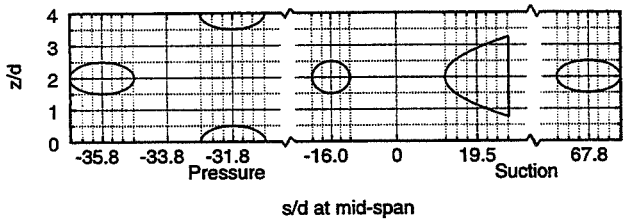

Shape of film cooling holes at exit on the ACE rotor surface

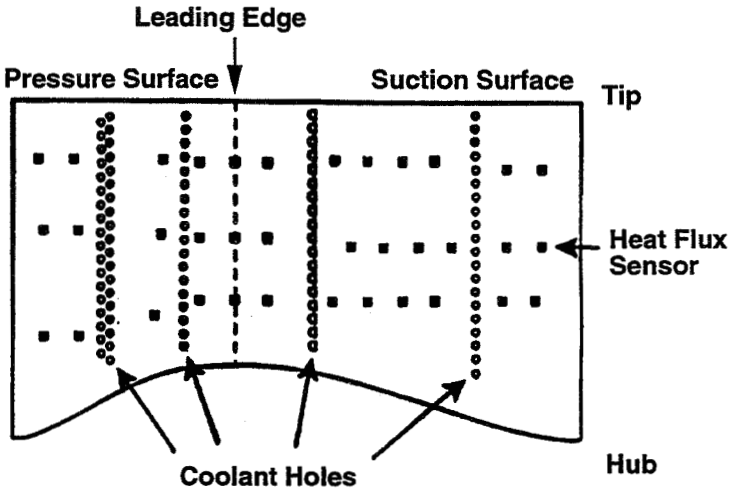

Heat flux gauges and cooling hole locations on the projected blade surface with each of the three chordwise rows of gauges on a separate blade

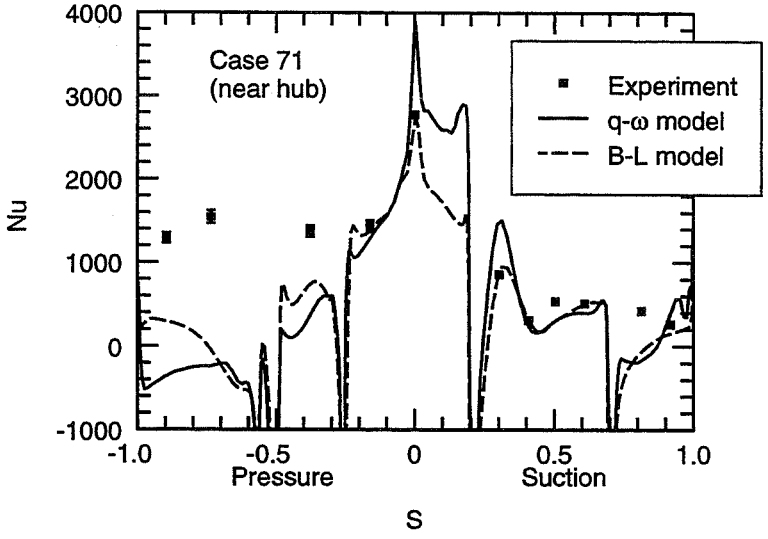

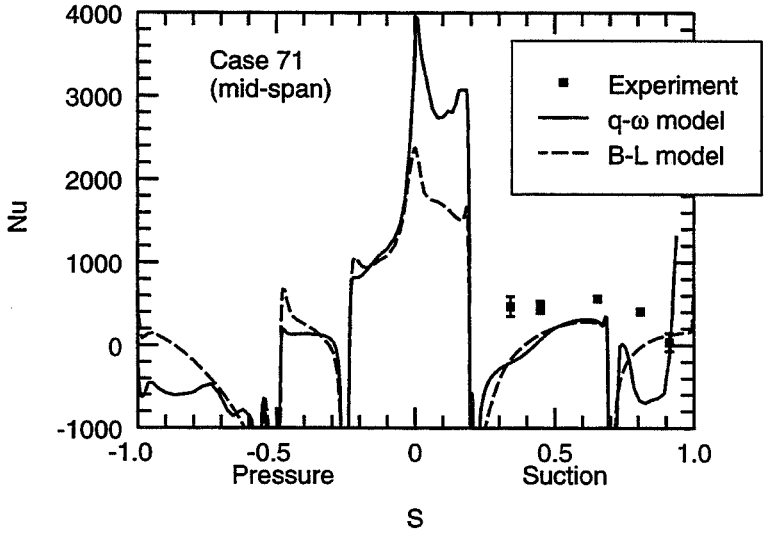

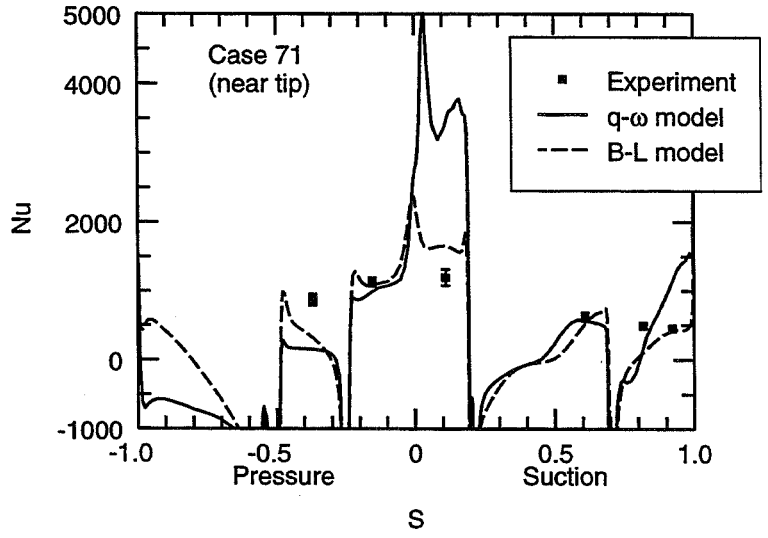

Nusselt Number on the Blade Surface for Cooled Case 71

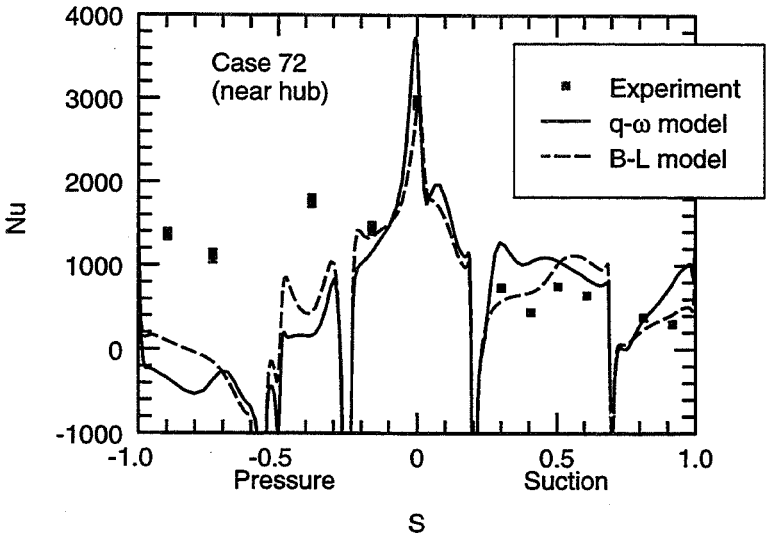

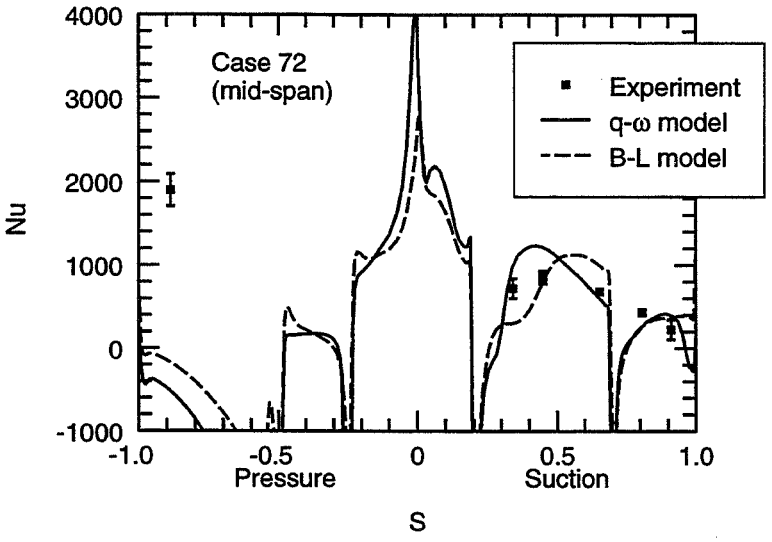

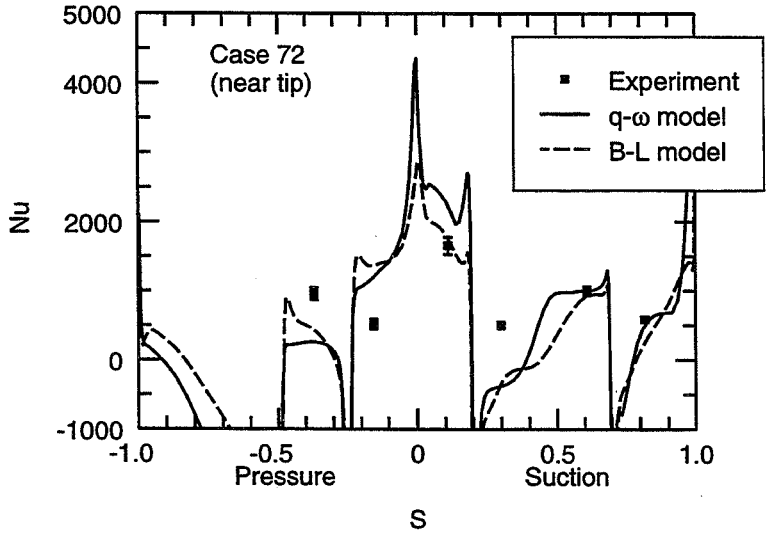

Nusselt Number on the Blade Surface for Cooled Case 72

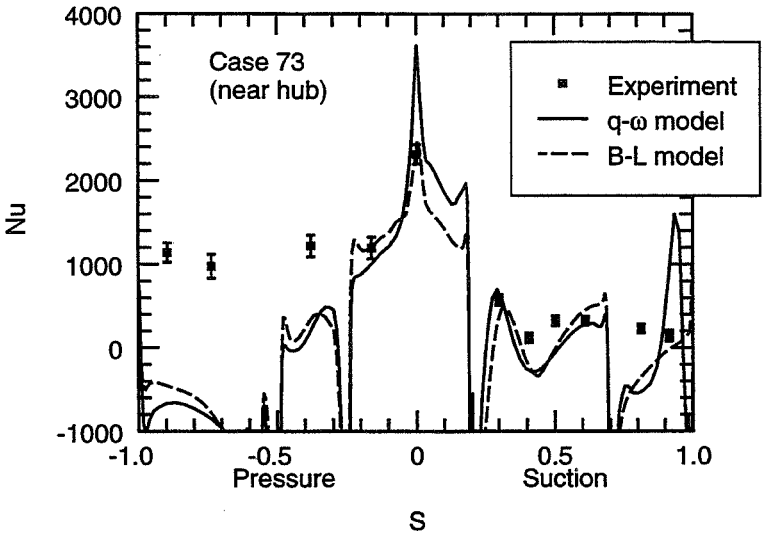

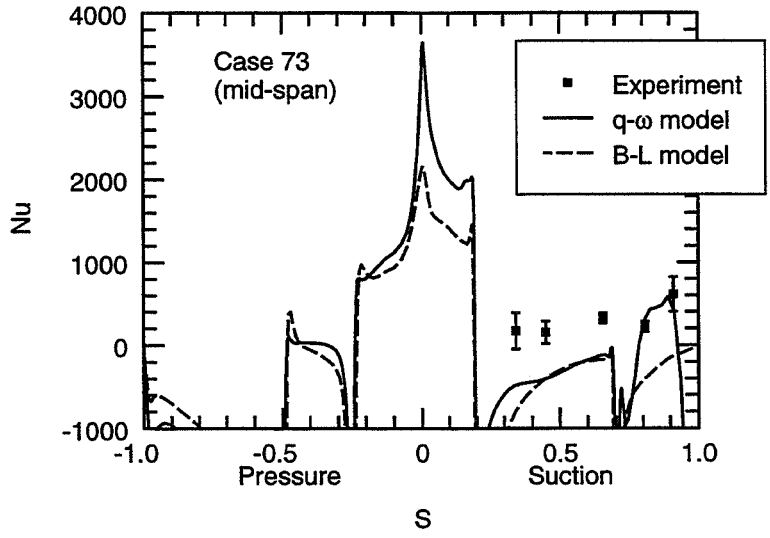

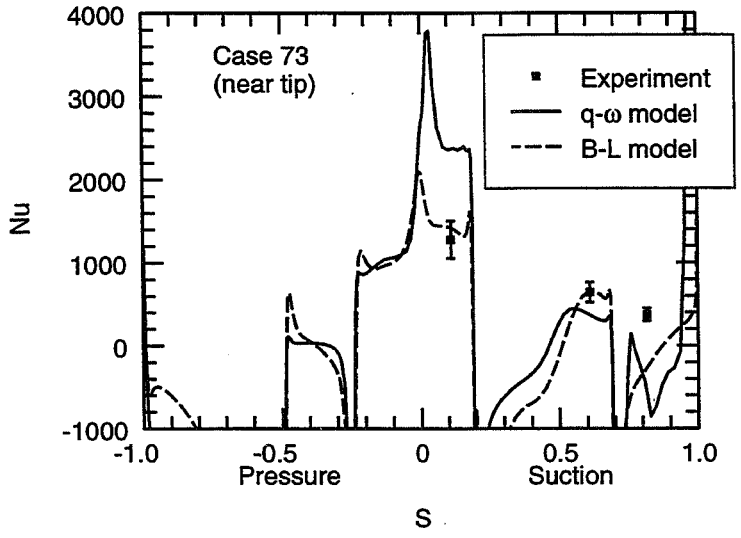

Nusselt Number on the Blade Surface for Cooled Case 73

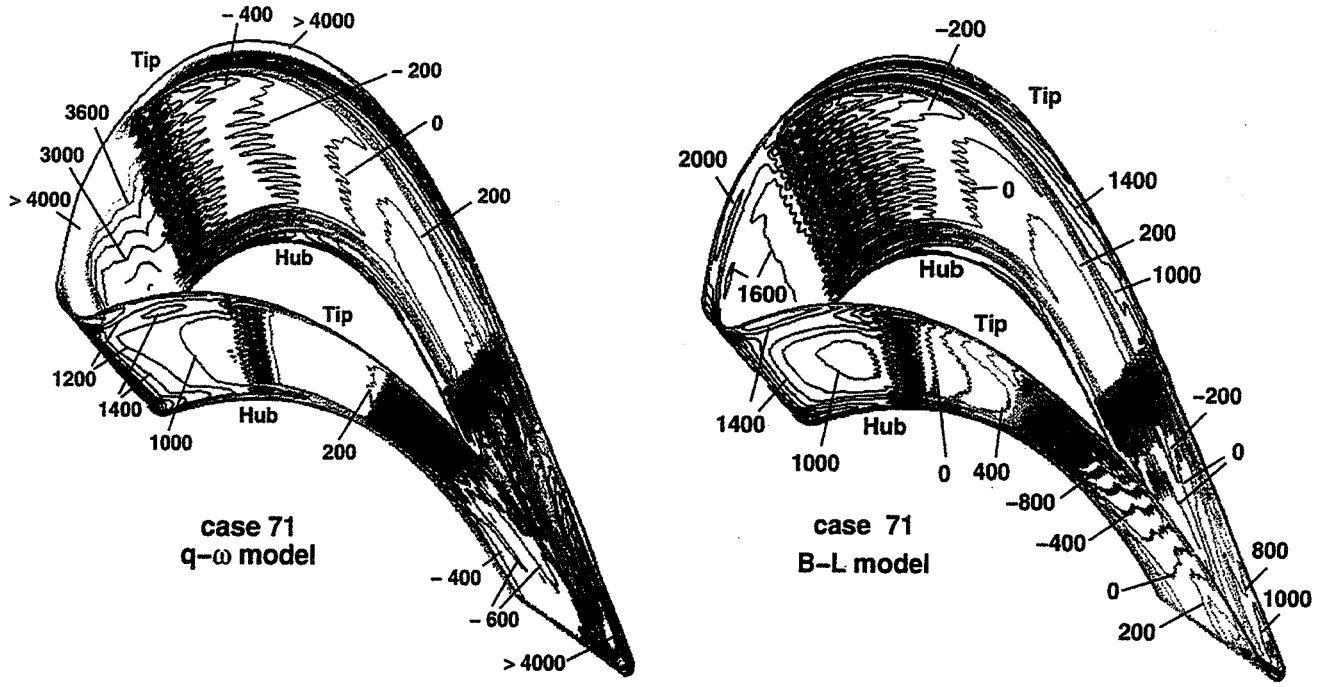

Nusselt number contours on the ACE rotor for two turbulence models

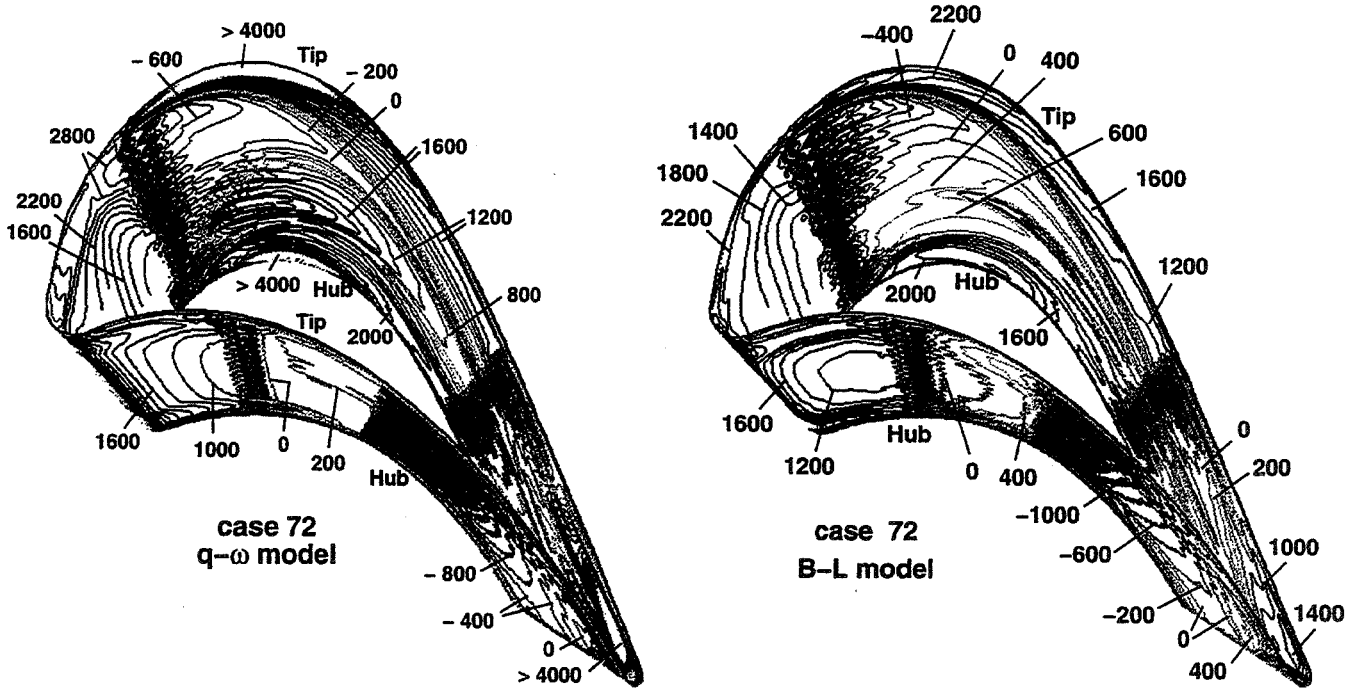

Nusselt number contours on the ACE rotor for two turbulence models

ALSO STUDIED

- EFFECT OF SPANWISE PITCH OF SHOWER-HEAD HOLES
- EFFECT OF COOLANT TO MAINSTREAM MASS FLOW RATIO
- EFFECT OF COOLANT TO MAINSTREAM TEMPERATURE RATIO

CONCLUSIONS

- A LARGE CHANGE IN HEAT TRANSFER COEFFICIENT AT THE BLADE SURFACE CAUSED BY DIFFERENT VELOCITY AND TEMPERATURE PROFILES AT THE HOLE EXIT
- DIFFERENT EFFECTS OBSERVED ON THE PRESSURE AND SUCTION SURFACE DEPENDING UPON THE BLADE & HOLE SHAPE (CONICAL OR CYLINDRICAL) AND HOLE LOCATION
- BLADE ROTATION AND DIRECTION OF INJECTION HAS A SIGNIFICANT EFFECT ON THE FILM COOLING EFFECTIVENESS
- BALDWIN-LOMAX TURBULENCE MODEL SEEMS TO BE AS GOOD AS ANY TWO-EQUATION MODEL, AND IS 40-50% LESS EXPENSIVE

FUTURE DIRECTIONS

- DETAILS OF IN-HOLE AND NEAR-HOLE PHYSICS REQUIRED UNDER CONDITIONS RELEVANT TO THE GAS TURBINE (DENSITY RATIO; CURVATURE EFFECTS; HIGH Tu; etc.)

- EXPERIMENTAL DATA ON ROTATING FILM-COOLED BLADES REQUIRED

- INCORPORATE HOLE-EXIT PROFILES BASED ON RECENT EXPERIMENTAL DATA

- USE A MULTI-BLOCK CODE TO DEVELOP HOLE-EXIT PROFILES ON A ROTATING BLADE

- INCORPORATE SIMPLIFIED FILM-COOLING MODEL TO SPEED-UP THE CODE

THE EFFECT OF TABS ON A JET IN A CROSS-FLOW

Khairul Zaman and Judith Foss Van Zante
NASA Lewis Research Center
Cleveland, Ohio

Objective:

A tab placed on the leeward side of the nozzle was expected to increase jet penetration into the cross-flow. An experiment at UTRC showed insignificant effect. The primary objective of the present study was to confirm and explain the ineffectiveness.

Approach:

- Experiments in a low speed wind tunnel.
- Conduct hot-wire measurements for mean velocity and streamwise vorticity fields.

Results:

- Ineffectiveness of tab, when placed on leeward side, is confirmed.
- Static pressure distribution around the nozzle provides an explanation for the ineffectiveness.
- Tab placed on the windward side of the nozzle is found to reduce the jet penetration.

Milestones:

- 5/97 Experiments to optimize tab geomery for maximum reduction in jet penetration.
- 5/98 Active control for increasing jet penetration and mixing.

SCHEMATIC OF 'DELTA-TAB' FITTED TO CIRCULAR NOZZLE

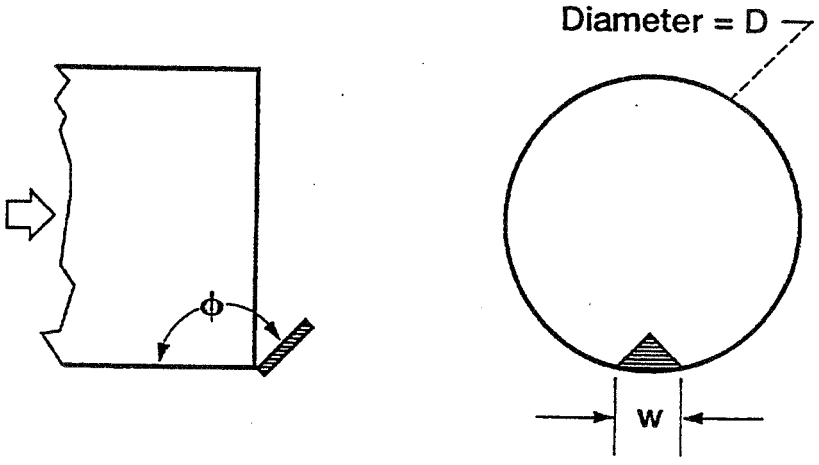

Fric & Roshko JFM 1994

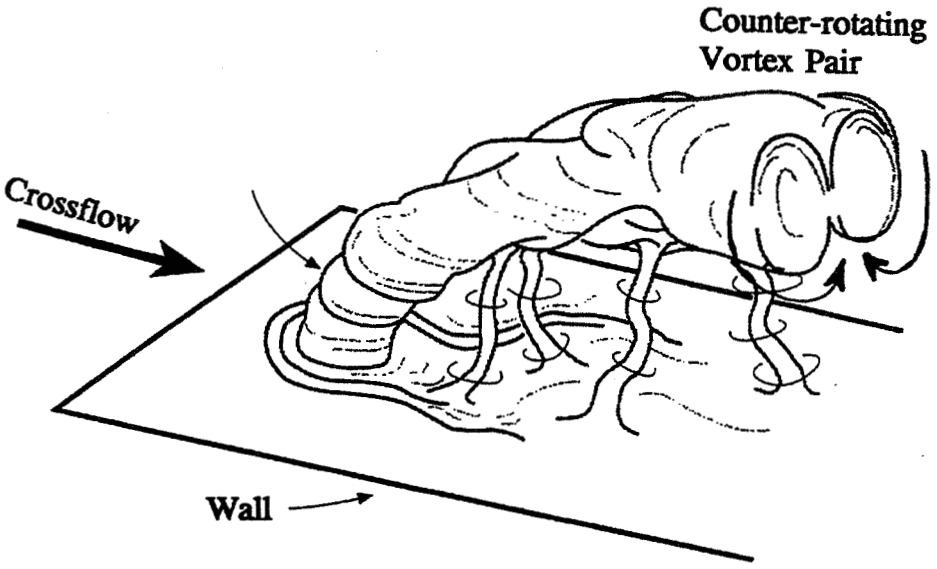

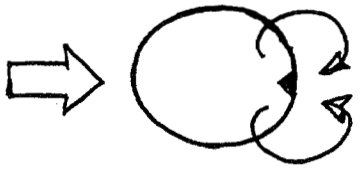

A Tab on the downstream edge may be expected to reinforce the Counter-rotating Vortex Pair

Liscinsky, True & Holdeman AIAA 95-2998
(Experiment at UTRC)

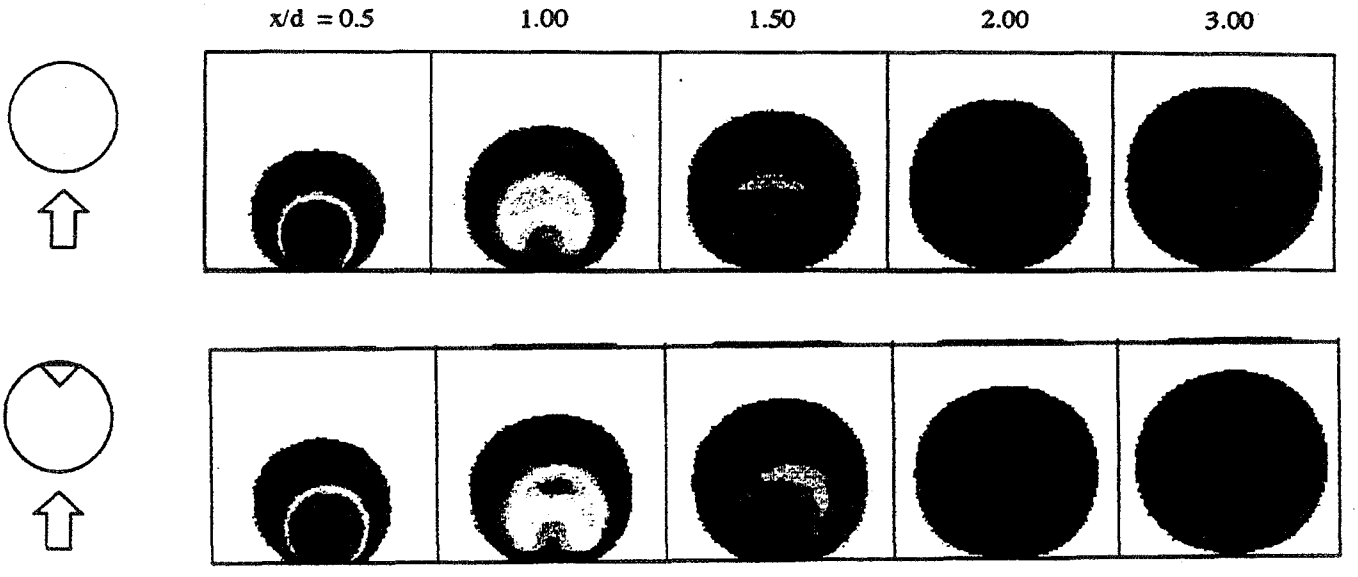

WIND TUNNEL TEST SECTION

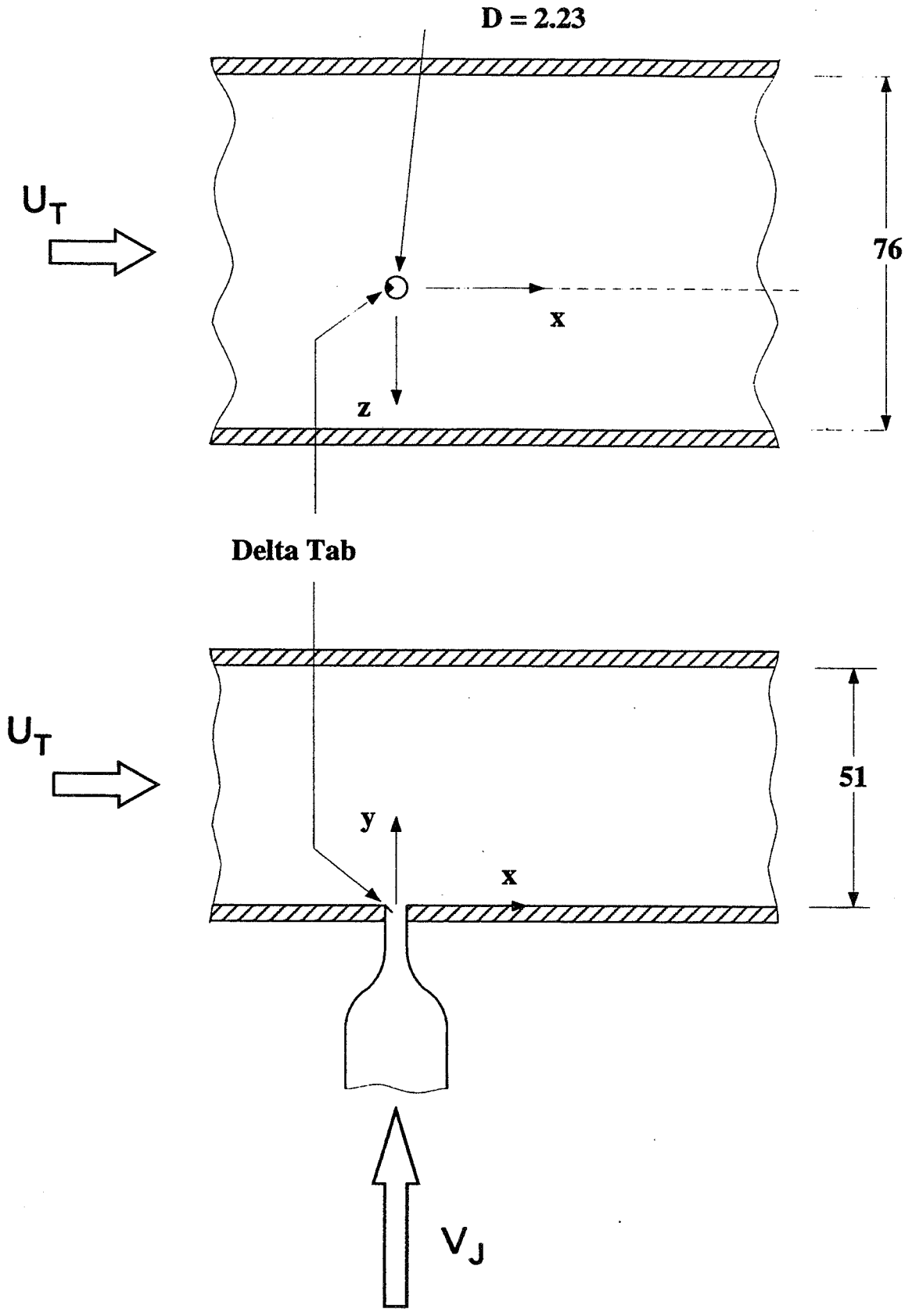

MEAN VELOCITY DISTRIBUTIONS AT x/D=4, J=21 FOR VARIOUS TAB CASES

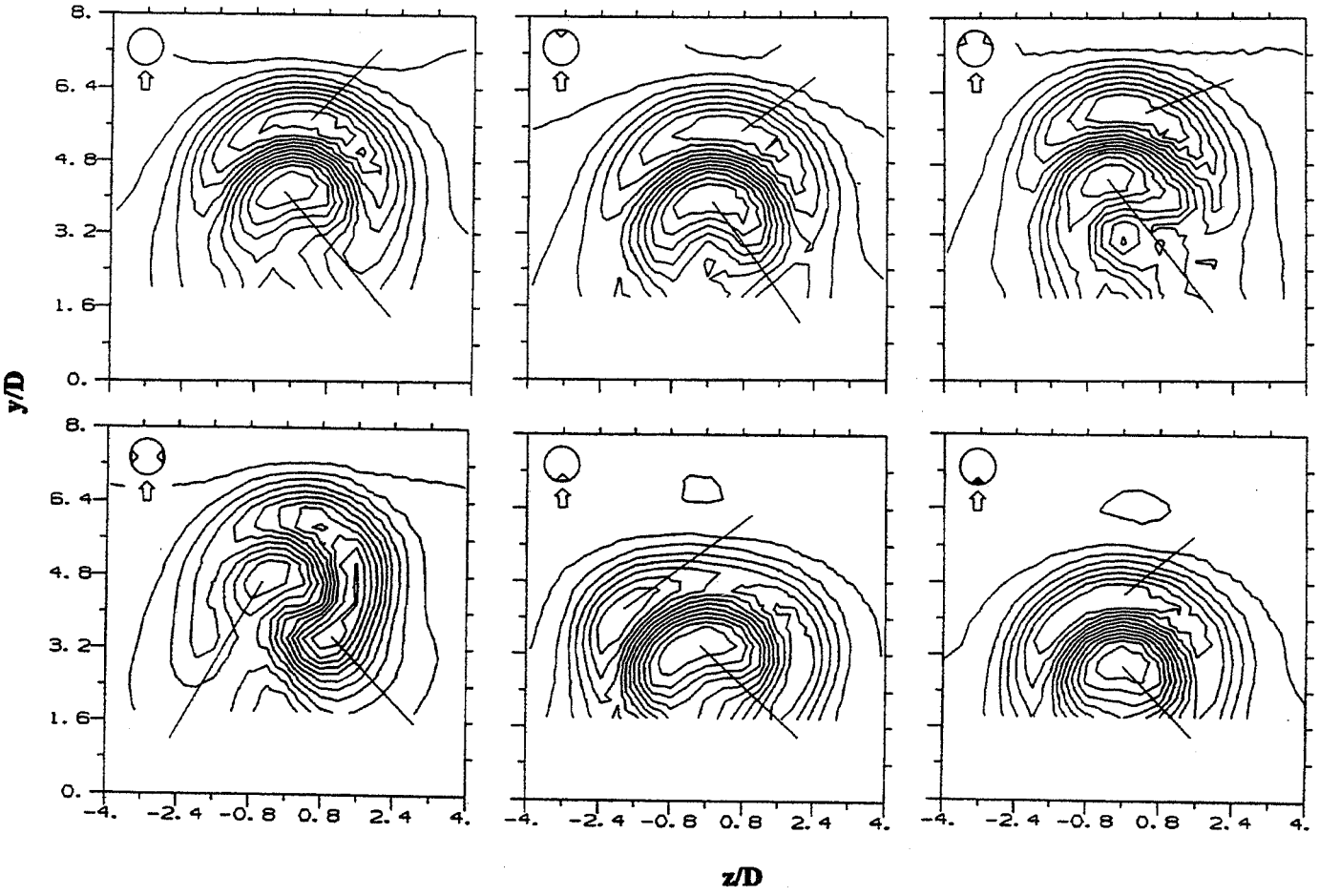

STATIC PRESSURE DISTRIBUTION NEAR THE NOZZLE EXIT

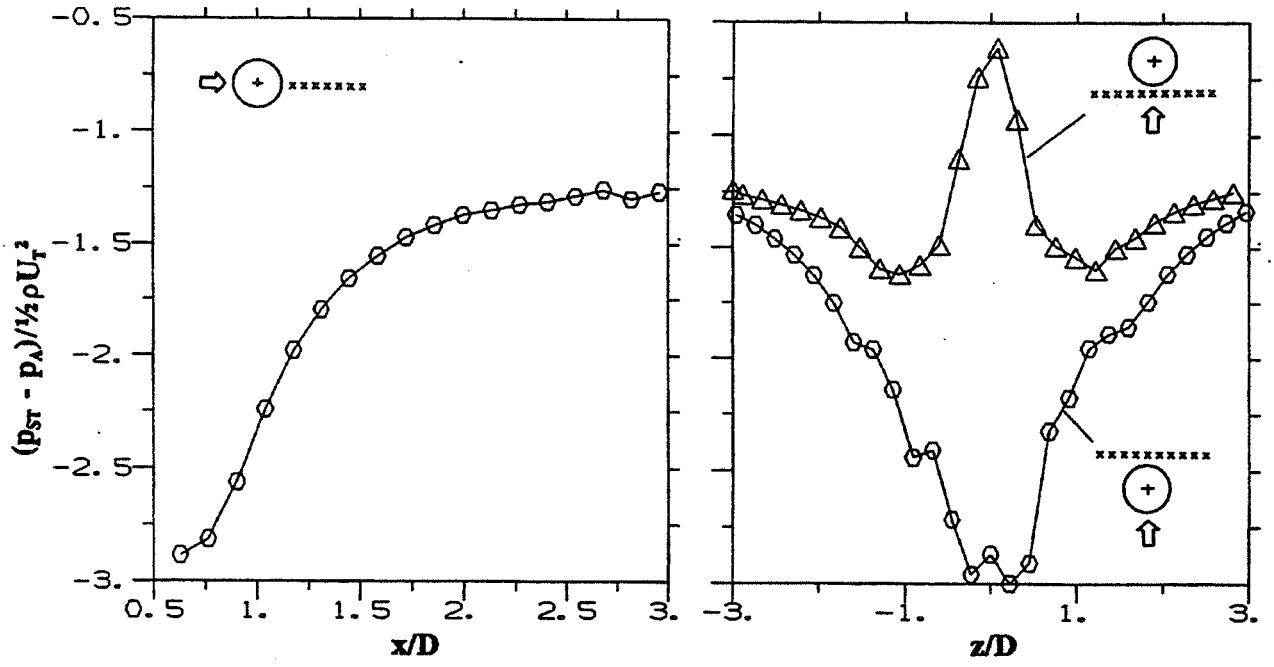

$$\frac{1}{\rho}\frac{\partial p}{\partial z} = \nu\frac{\partial \omega_x}{\partial y}$$

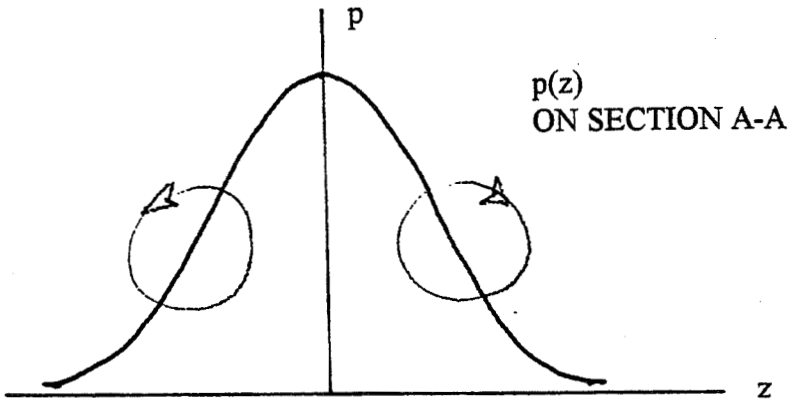

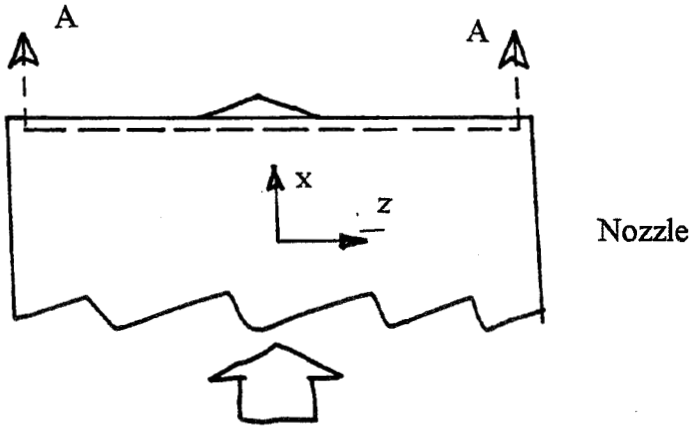

MEAN VELOCITY (TOP) AND STREAMWISE VORTICITY (BOTTOM) DISTRIBUTIONS, J=21

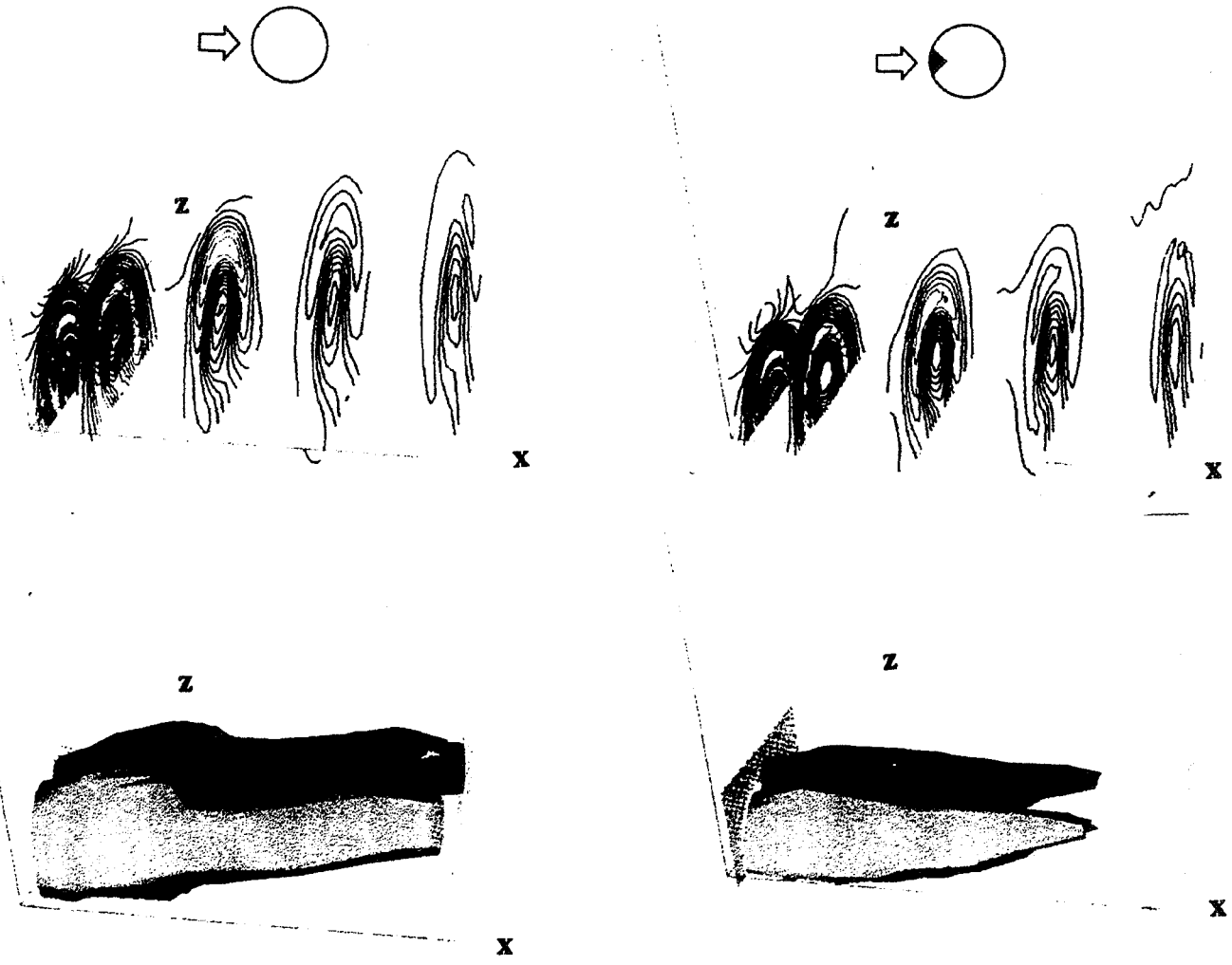

POSSIBLE INVESTIGATION FOR FILM COOLING APPLICATION

THE FACT THAT A TAB PLACED ON THE WINDWARD SIDE REDUCES JET PENETRATION IS OF INTEREST IN FILM COOLING APPLICATION. WE WOULD LIKE TO PURSUE THIS FURTHER THROUGH EXPERIMENTS INCLUDING:

(1) BASIC STUDIES ON TAB GEOMETRY OPTIMIZATION (LOW 'J', ANGLED JET, ARRAY OF JETS).

(2) HEAT TRANSFER.

(3) TESTS FOR TURBINE BLADES AND OTHER APPLICATIONS.

FILM-COOLING HEAT-TRANSFER MEASUREMENTS USING LIQUID CRYSTALS

Steven Hippensteele
NASA Lewis Research Center
Cleveland, Ohio

The Transient Liquid-Crystal Heat-Transfer Technique

2-D Film-Cooling Heat-Transfer on an AlliedSignal Vane

Effects of Tab Vortex Generators on Surface Heat Transfer Downstream of a Jet in Crossflow

Transient Heat Transfer Technique

Based on 1-D heat conduction out of a semi-infinite wall:

$$\theta = 1 - e^{\beta^2} erfc\,\beta$$

$$\theta = \frac{T_i - T_{LC}}{T_i - T_R}$$

$$\beta = \frac{h\sqrt{t}}{\sqrt{\rho c k}}$$

erfc β = complimentary error function
i=initial, LC=liquid crystal, R=recovery
ρ=wall density, c=specific heat, k=thermal conductivity

Transient Liquid-Crystal Heat-Transfer Technique

Vane surface coated with thermochromic liquid crystals

Initially heated in oven to a uniform temperature and cooled during the test (see oven sketch and photo)

Isotherms (revealed by the liquid crystals) are video taped and used to solve the 1-D conduction problem in the semi-infinite test surface

By operating the coolant and air at a constant room temperature, only the hydrodynamic effects will be included the heat transfer coefficients

By varying the coolant temperature, the cooling effectiveness can be determined (ref. Vedula & Metzger)

Results: high-resolution heat-transfer and film-cooling effectiveness maps of the surface downstream of the film cooling holes

Test Section Oven

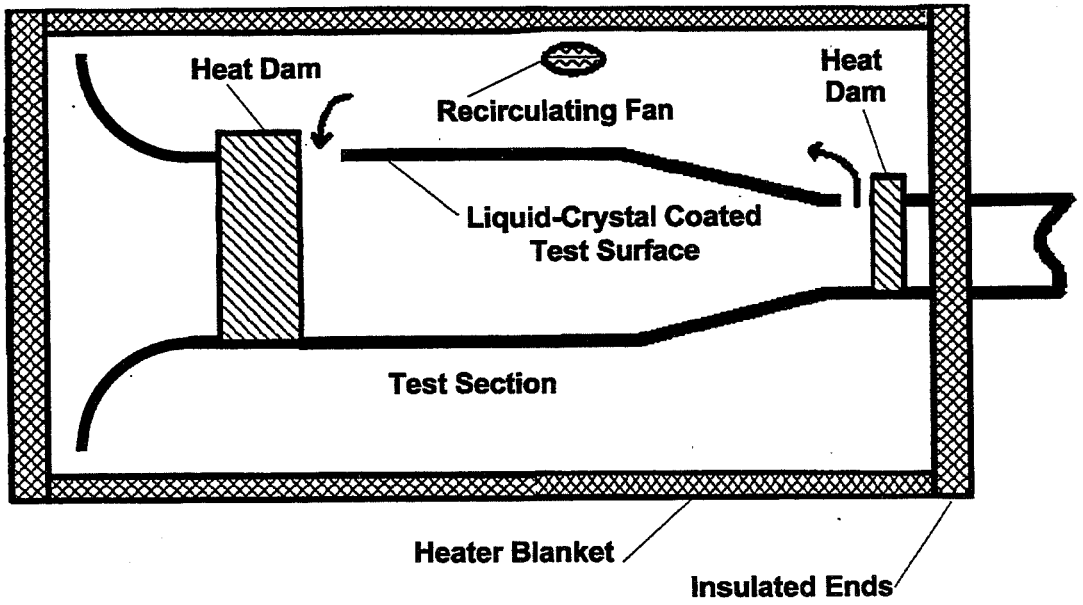

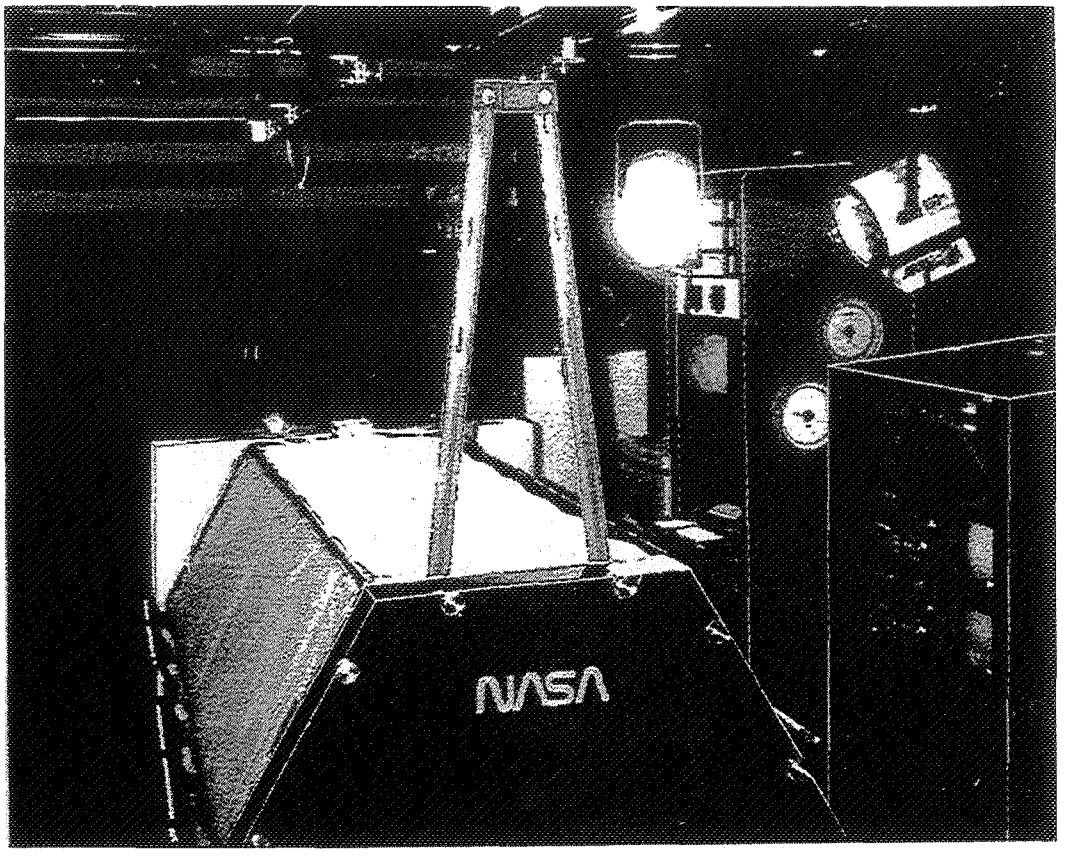

2-D Film-Cooling Heat-Transfer on an AlliedSignal Turbine Vane

The unwrapped midspan geometry of the AlliedSignal TFE 1042-70A high pressure turbine first stage vane has been offered for detailed heat transfer studies and Lewis. This vane contains 12 rows of film cooling holes. A linear cascade will be fabricated using this vane geometry for the experimental study of surface heat transfer using the transient liquid-crystal heat-transfer technique. The vane size will be about 4 times actual size so that both the exit Mach number and the exit Reynolds number can be maintained. The coolant will be SF_6 so that the coolant-to-gas density ratio can be maintained and changed. The test vane surface will be coated with thermochromic liquid crystals and initially heated in an oven. The isotherms revealed by the liquid crystals, that result from the cooling during the test period, are video taped and used to solve the 1-D conduction problem in the semi-infinite test surface. By operating the coolant and air at a constant room temperature, only the hydrodynamic effects will be included the heat transfer coefficients. By varying the coolant temperature, the cooling effectiveness can be determined. From this comes high-resolution heat transfer and film cooling effectiveness maps of the surface downstream of the film cooling holes.

2-D Film-Cooling Heat-Transfer on an AlliedSignal Vane

Detailed heat transfer studies to validate film cooling HT models (Garg)

Using the transient liquid-crystal heat-transfer technique

The Vane Cascade

AlliedSignal offered the unwrapped midspan geometry of their TFE 1042-70A high pressure turbine first-stage vane for study and non-proprietary reporting (Winstanley)

- Contains 12 rows of film cooling holes
- 4 times actual size stereo-lithographic model (see photo)
- Real exit Mach number and Reynolds number will be tested
- Coolant will be SF_6 so real coolant-to-gas density ratio can be tested

A linear cascade of vanes will be used for the experimental study (heat transfer, cooling effectiveness, hot-wire surveys, & velocity surveys with high free-stream turbulence (Ames))

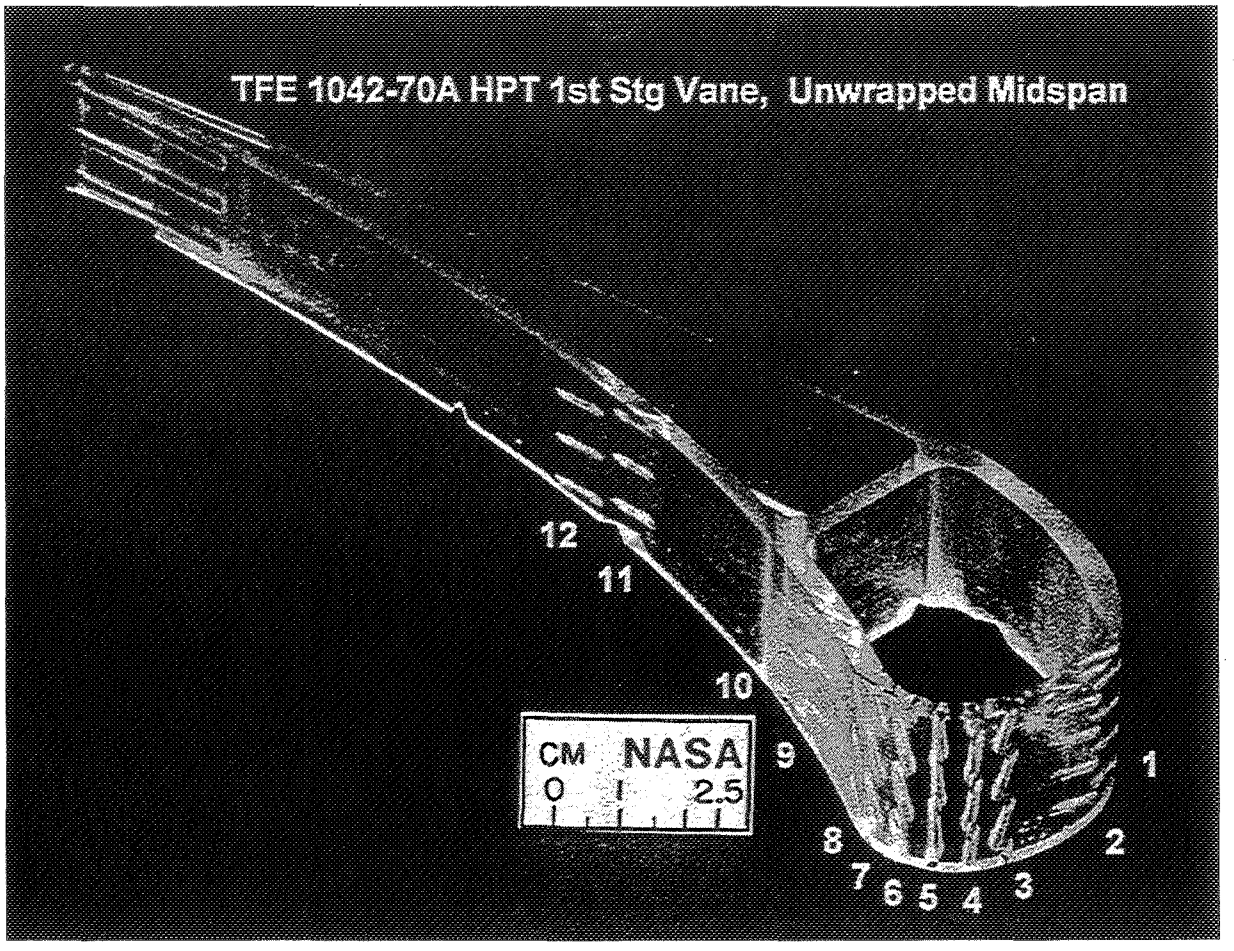

Effects of Tab Vortex Generators on Surface Heat Transfer Downstream of a Jet in Crossflow

Tab-type vortex generators located on the windward side of a jet in crossflow have shown considerable effect on the downstream flow (Zaman and Foss). The tab-generated vorticity reduces the penetration of the jet which may be significant in film cooling applications. For this reason experimental measurements have been initiated using the transient liquid-crystal heat-transfer technique in which an acrylic test surface containing an air jet coated with thermochromic liquid crystals. From this comes high-resolution heat transfer maps of the surface downstream of the jet (or film cooling) hole. Initial data will be presented that has only very recently been taken.

Effects of Tab Vortex Generators on Heat Transfer Downstream of a Jet in Crossflow

Tab vortex generators (windward side of a jet in a crossflow) have shown considerable aerodynamic effects on the downstream flow (Zaman and Foss)

The tab-generated vorticity reduces jet penetration which may be significant in film cooling applications

Therefore, experimental measurements have started using the transient liquid-crystal heat-transfer technique (see facility sketch and photo)

High-resolution heat-transfer maps will be made for the surface downstream of the jet (and eventually for film cooling holes) (see 2 isothermal/h maps)

Initial data, as available (shown in video)

Transient Liquid-Crystal Heat Transfer Facility

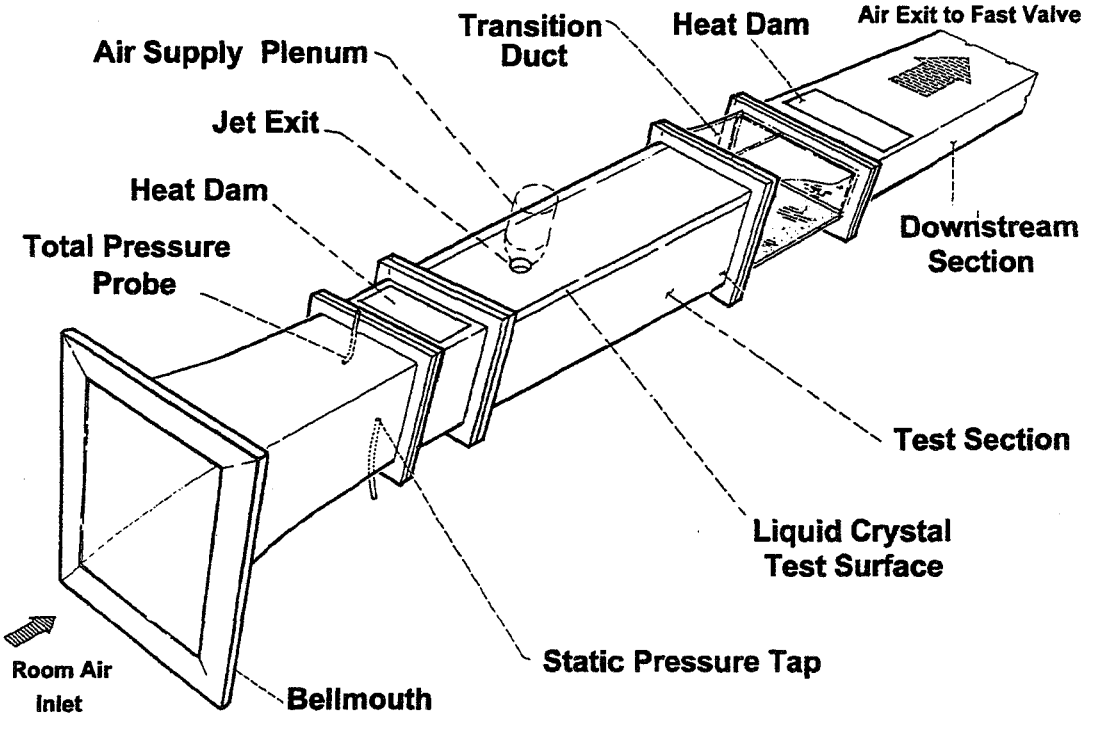

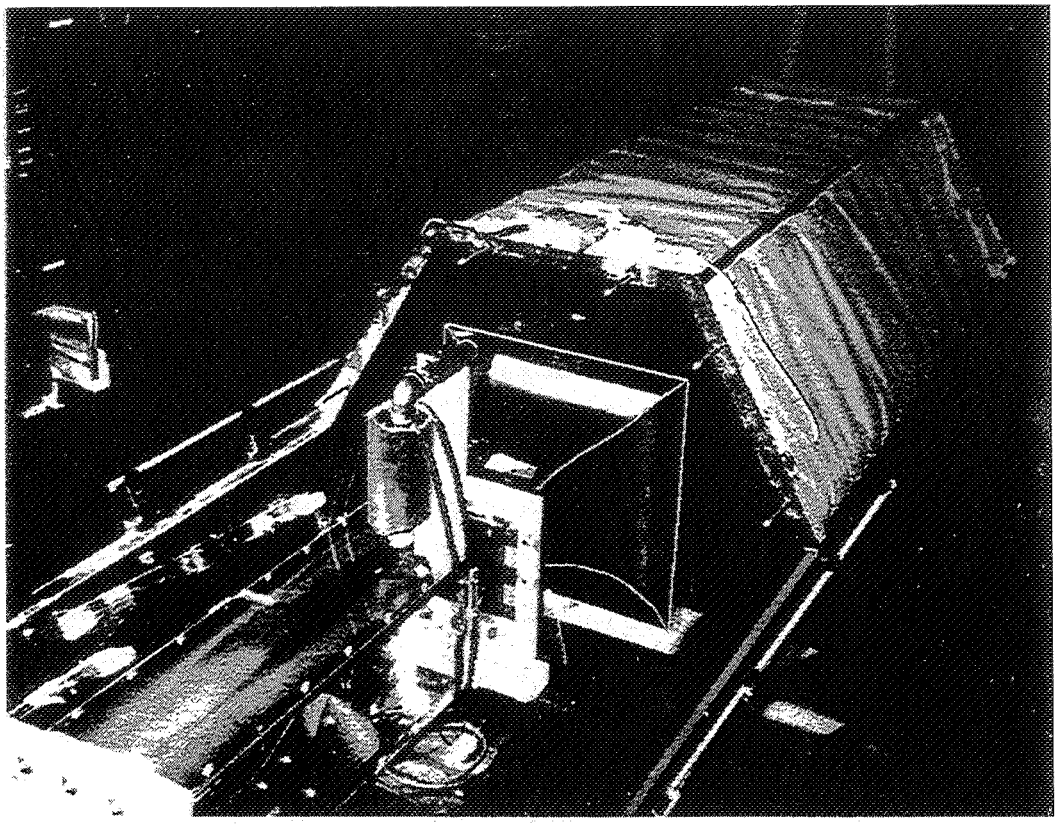

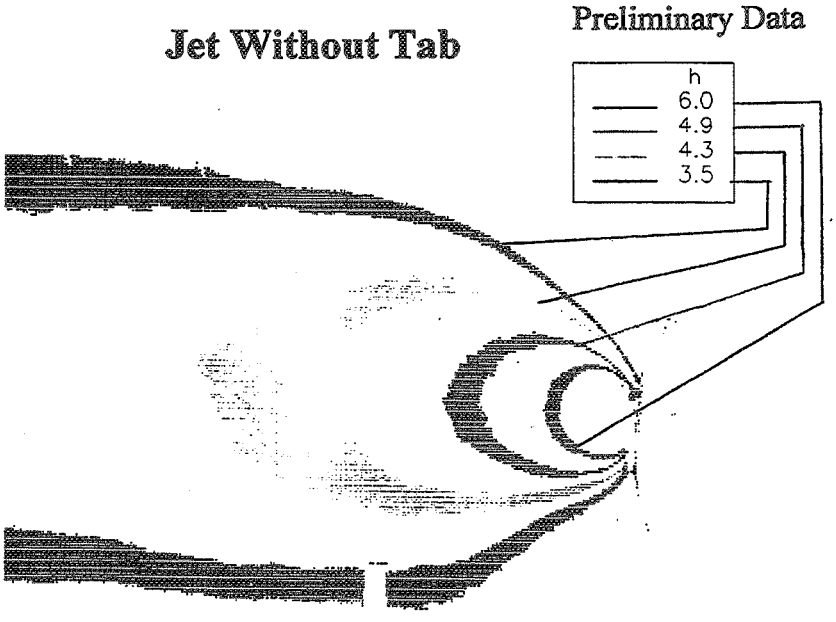
Jet Without Tab
Preliminary Data
h
6.0
4.9
4.3
3.5

Jet With Tab

Preliminary Data

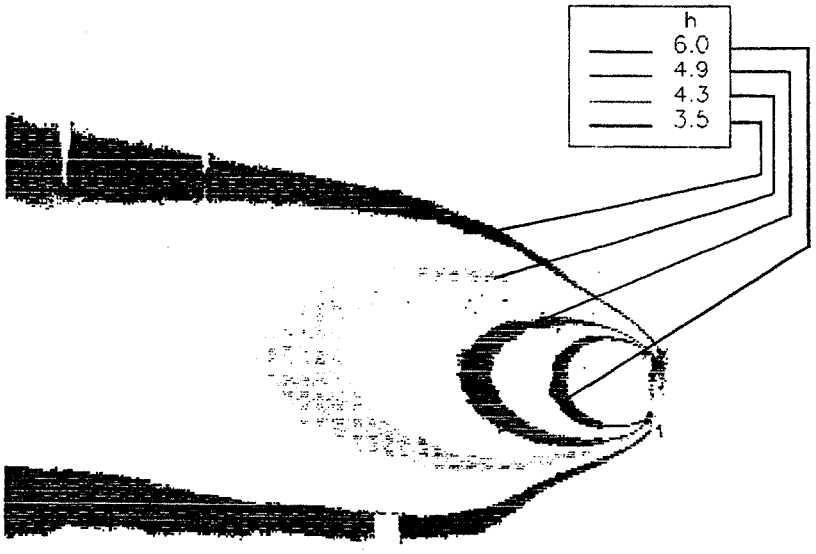

TURBINE VANE HEAT TRANSFER, FILM COOLING, AND TURBULENCE EXPERIMENTS

Forrest E. Ames
Allison Engine Company
Indianapolis, Indiana

PRESENTATION OVERVIEW

I. Introduction
   - o Motivation
   - o Objectives

II. Experimental Apparatus and Approach

III. Experimental Results
   - o Suction Surface Film Cooling Comparisons
   - o Pressure Surface Film Cooling and Velocity Profiles
   - o Suction Surface Heat Transfer with Film Cooling
   - o Pressure Surface Heat Transfer with Film Cooling

IV. Conclusions and Thoughts for Future Work

INTRODUCTION

I. Several years ago a test was run at Allison on an advanced film cooled vane design.
   - o The tests indicated we were overpredicting film cooling protection on the pressure side.
   - o Results suggested we were underpredicting surface heat transfer downstream from the pressure surface film cooling.

II. The current study was undertaken to improve our understanding of the film cooled pressure surfaces with high inlet turbulence.

III. Study's objectives were:
   - o Examine influence of high inlet turbulence on vane film cooling
   - o Document local heat transfer rate and BL with jet injection

EXPERIMENTAL APPROACH

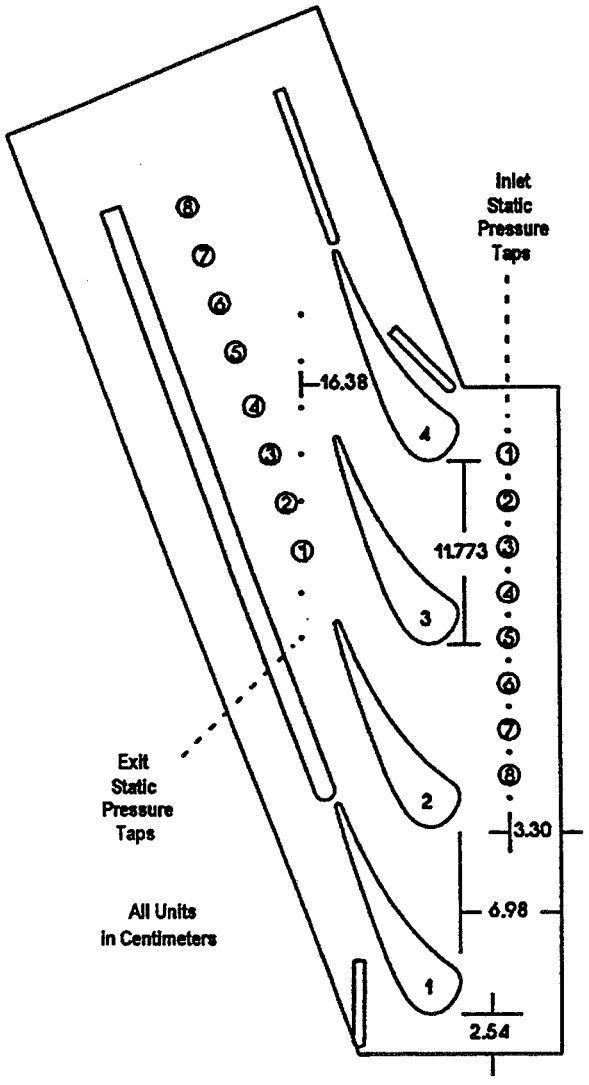

Schematic of four vane C3X cascade

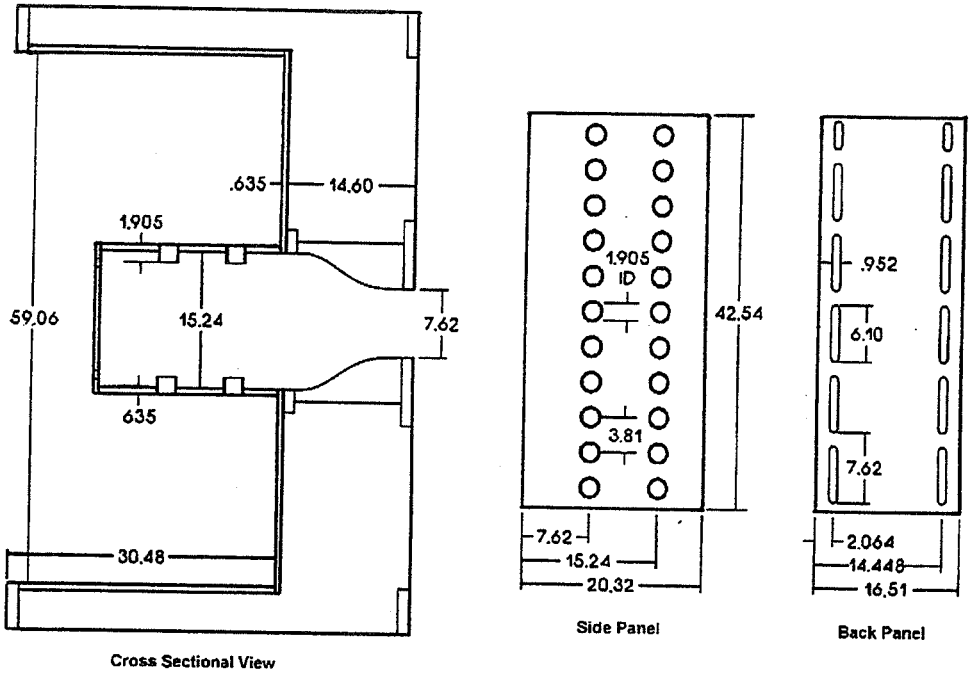

Schematic of mock combustor turbulence generator

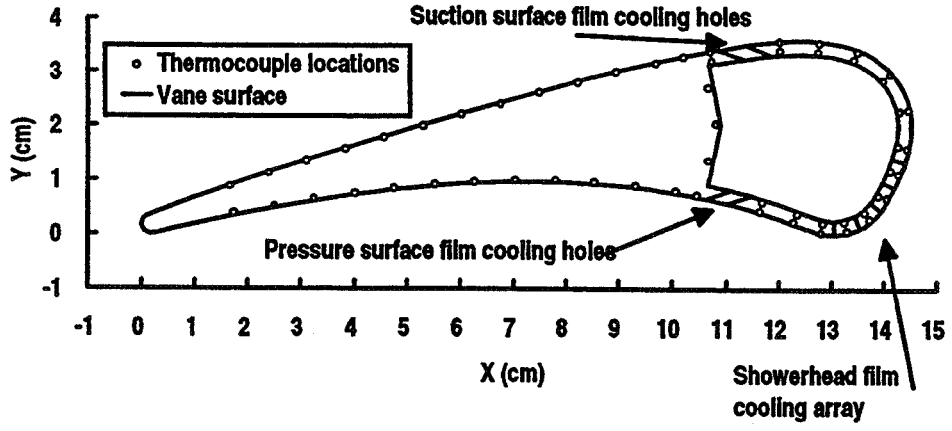

C3X film cooled vane thermocouple positions

FILM COOLING RESULTS

- Comparison between L'Ecuyer correlation and data show good agreement both in level and in trends.

- Agreement both suggests suction surface film cooling is comparable to flat plate data and gives confidence in experimental method.

- Data show higher near hole effectiveness levels for low velocity ratios but lower protection downstream.

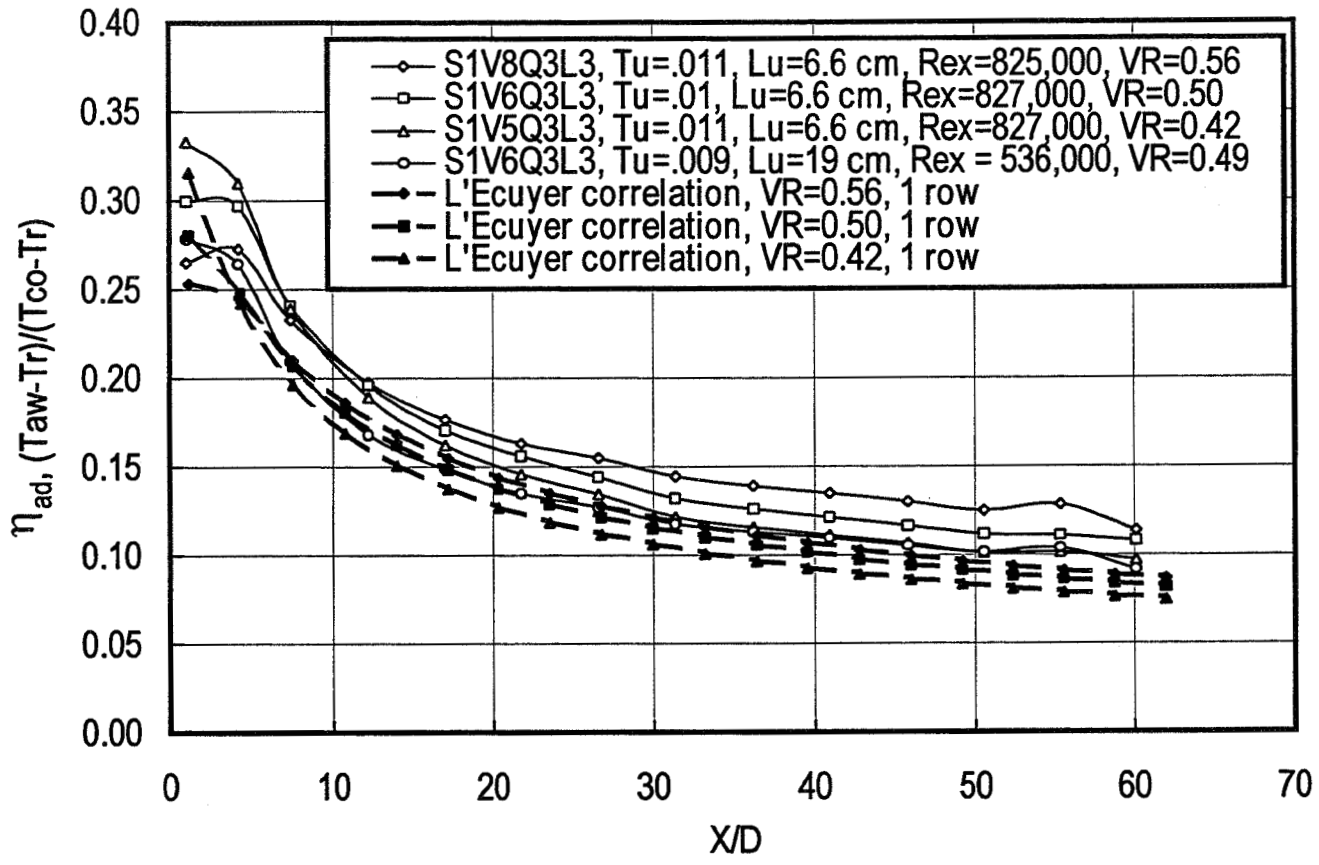

Suction surface film cooling with low turbulence

- Typical range of velocity ratios for first stage vane suction surface is quite narrow due to low Pc/Pt, low local Ps, high Tg/Tco, and hole discharge loss.

- Very high acceleration appears to cause large rise in near hole η (VR=.5, Tu=.01) and significant reduction in the far field.

- Data show large reduction in η with Tu

- Near hole data have a large uncertainty due to corrected η based on 2-D conduction analysis. Low Tu condition for low VR has largest σ.

- Conduction correction for X/D > 8 is very small.

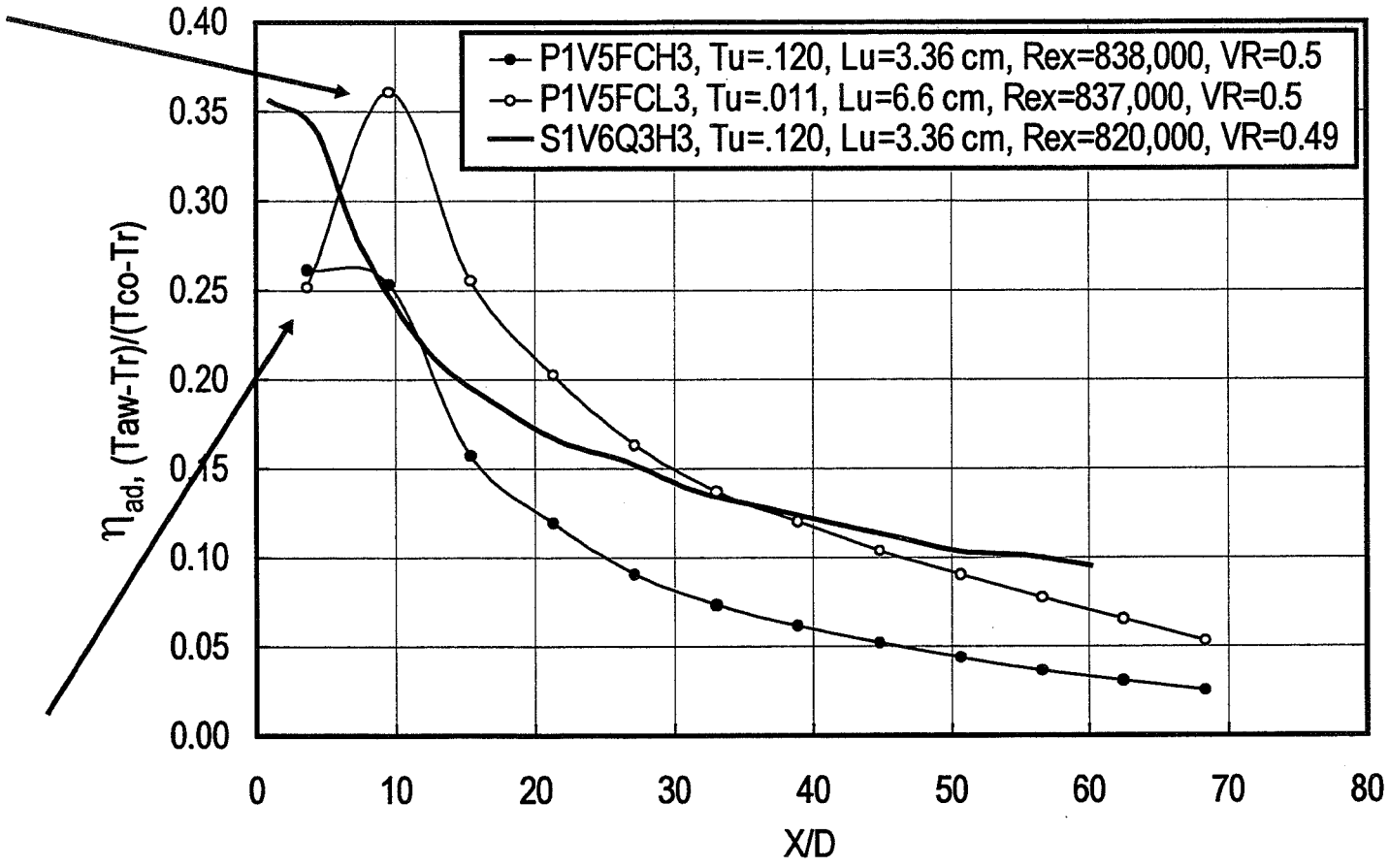

Pressure surface film cooling, low & high turbulence, single row, VR = 0.5

o Overall result of combination of high turbulence level and high acceleration is very low effectiveness level on the PS.

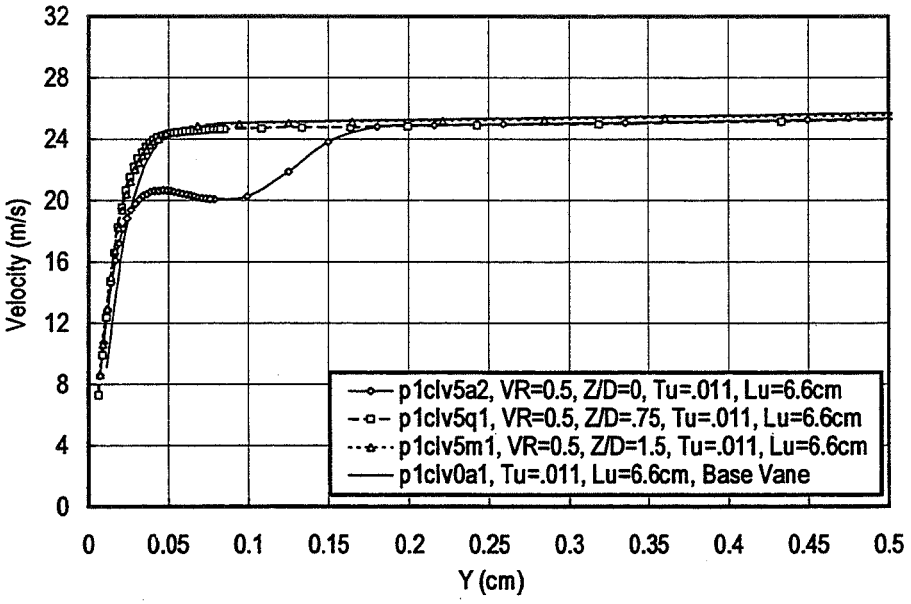

Low turbulence PS velocity profile, VR = 0.5, one row

- Low turbulence PS boundary layer shows a large velocity deficit downstream from jet but little effect on the profiles taken at Z/D's of 0.75 and 1.5.
- Turbulence level in jet moderate in intensity (6%) peaks in shear layer (7%) and low in between.
- Dissipation moderate in jet very high in shear layer.

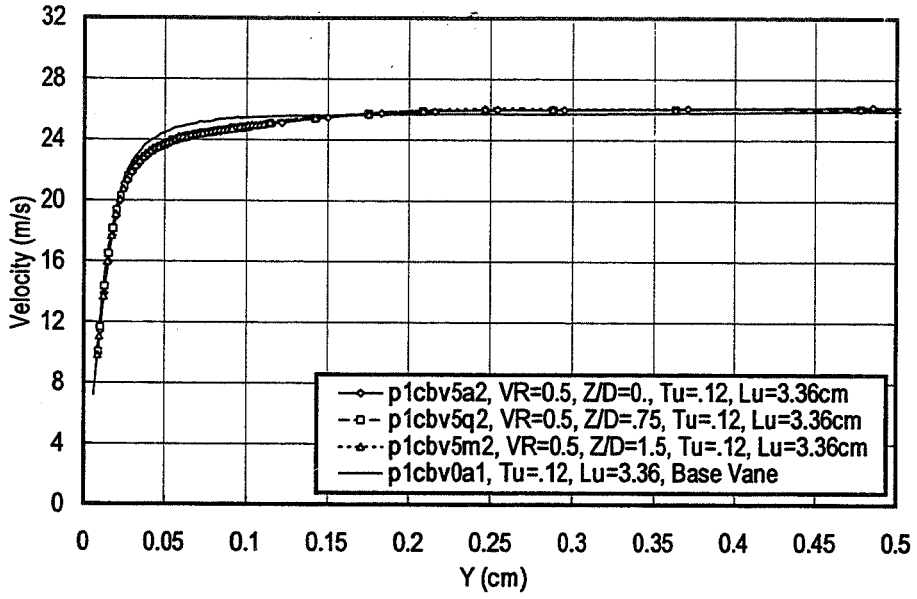

High turbulence PS velocity profile, VR = 0.5, one row

- Time averaged high turbulence PS boundary layer shows excellent uniformity across entire span by an X/D of 10.
- Turbulence level is uniformly high for all spanwise conditions
- Dissipation level 50% higher than basevane at .1 cm

- Data for two rows of holes on the PS at low and high turbulence are compared to one row data superposed at a velocity ratio of 0.5 .

- Comparison of low and high turbulence data show a substantial reduction in η due to turbulence.

- Double row and superposed single row comparison for high Tu indicates no benefit from staggered row due to extra blockage effect.

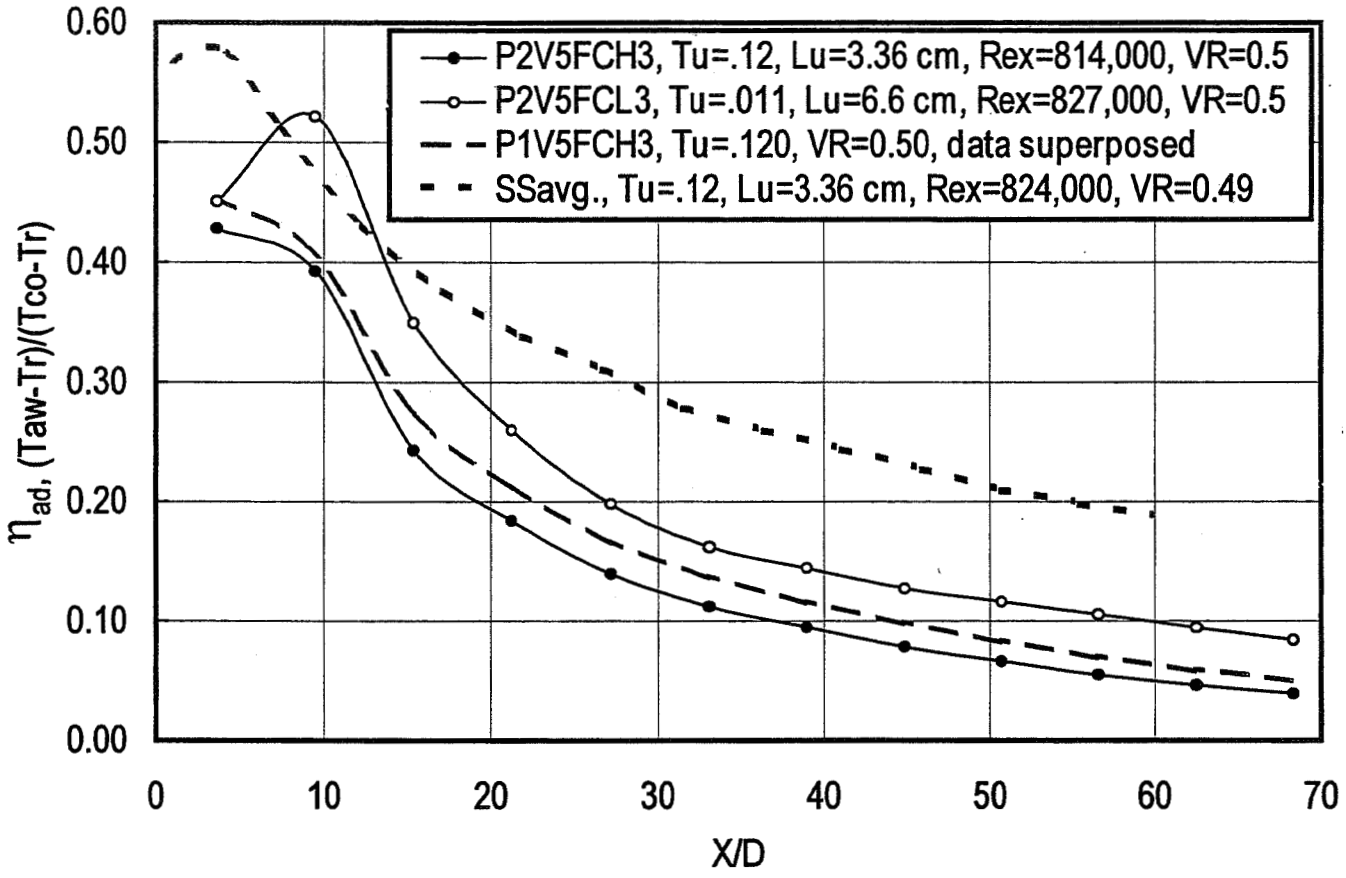

Comparison of double row with superposed single row data, pressure surface

o Similar to the single row data, combination of turbulence mixing and high acceleration produces very low effectiveness level on PS compared to SS.

- Data for two rows of holes on the PS at higher VRs show higher η values than superposed values from one row.

- For low turbulence, higher blockage from the double staggered row substantially reduces penetration of the downstream jet for VR = 1.5.

- Velocity profiles also show less liftoff for the upstream jet.

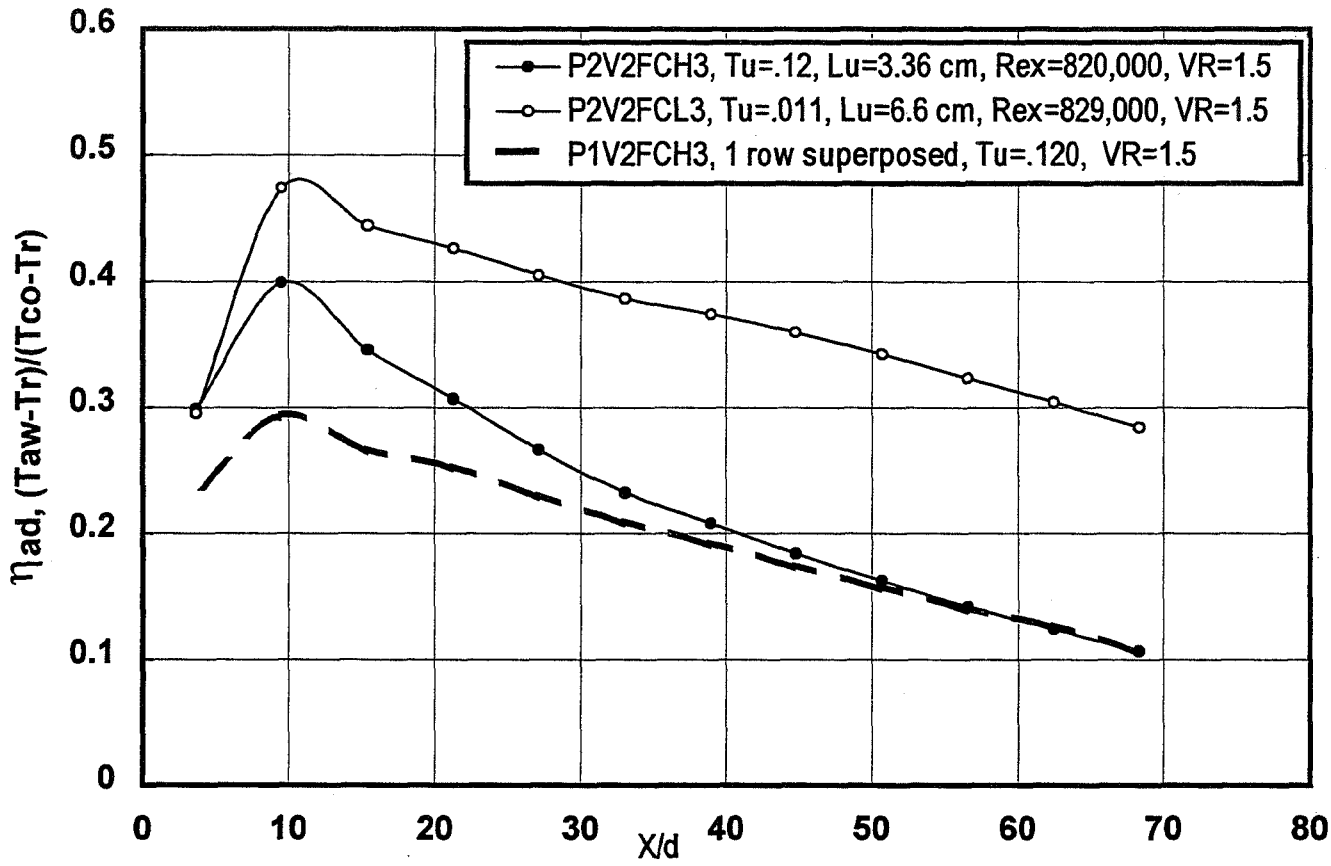

Pressure surface effectiveness, 2 rows, 30° holes, VR = 1.5, DR=0.94

- While the staggered row arrangement produces a substantial enhancement to film cooling on the PS, turbulent mixing from high local turbulence levels produce substantial reductions in effectiveness.

- The data for two rows can be compared for low and high turbulence by ratioing η for similar conditions.

- The average ratio of the four conditions decreases with X/D indicating how turbulent mixing gradually but increasingly reduces η.

- Generally, all the ratios of η decrease with increasing X/D. Near hole ratios for a VR of one show higher η values at an X/D of four for the high turbulence case.

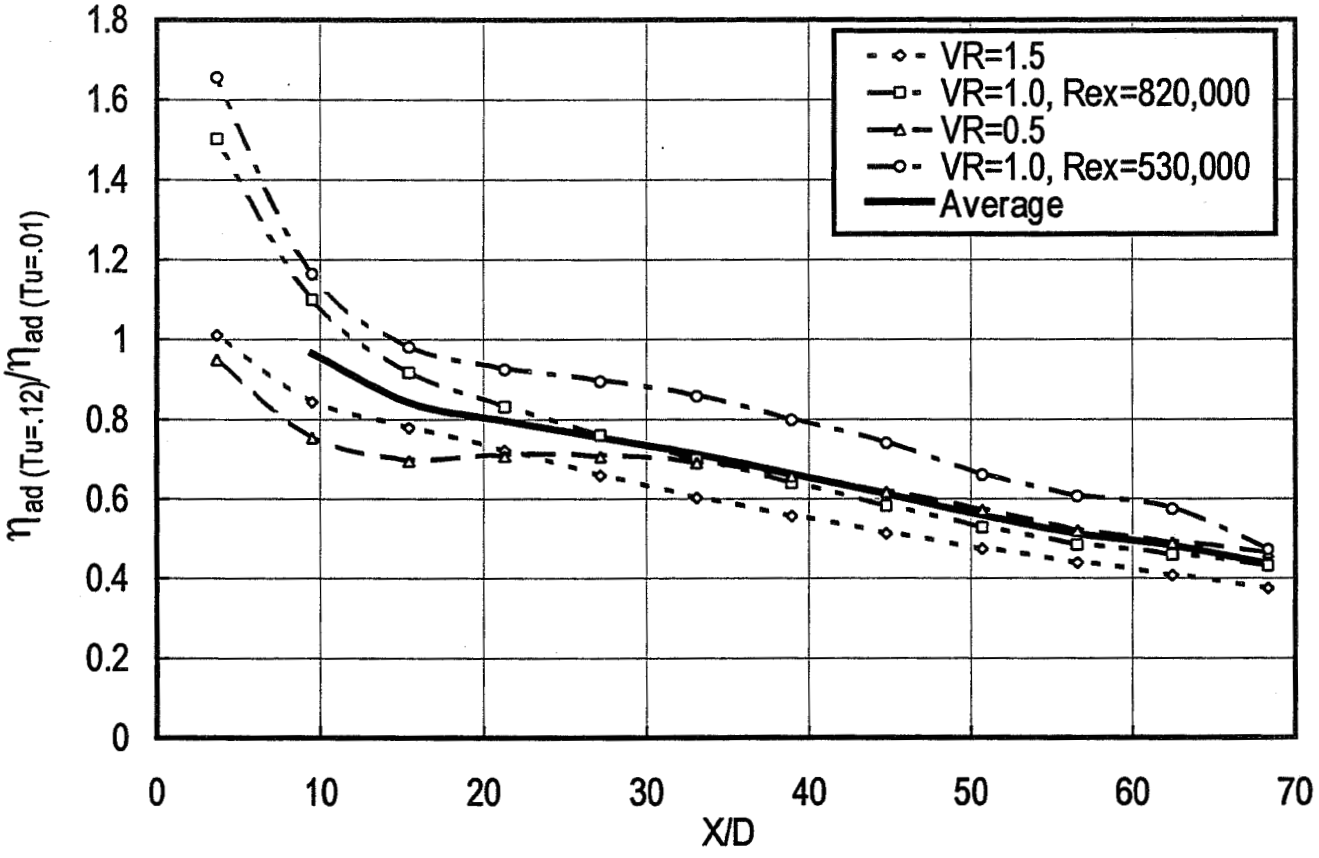

Ratio of high and low turbulence effectiveness, PS, 2 rows, 30° holes, DR=0.94

- High turbulence η values may benefit from enhanced turbulent mixing in the near hole region. η values in the near hole region are also more uncertain due to conduction effects.

HEAT TRANSFER RESULTS

- Two staggered rows of film cooling produce an average augmentation peak of about 18 percent above the turbulent baseline.
- The heat transfer quickly decays to the base level.
- The low turbulence case produced a comparable level of augmentation.
- A single row of holes produced an augmentation ratio of about 1.11 for both high and low turbulence levels.

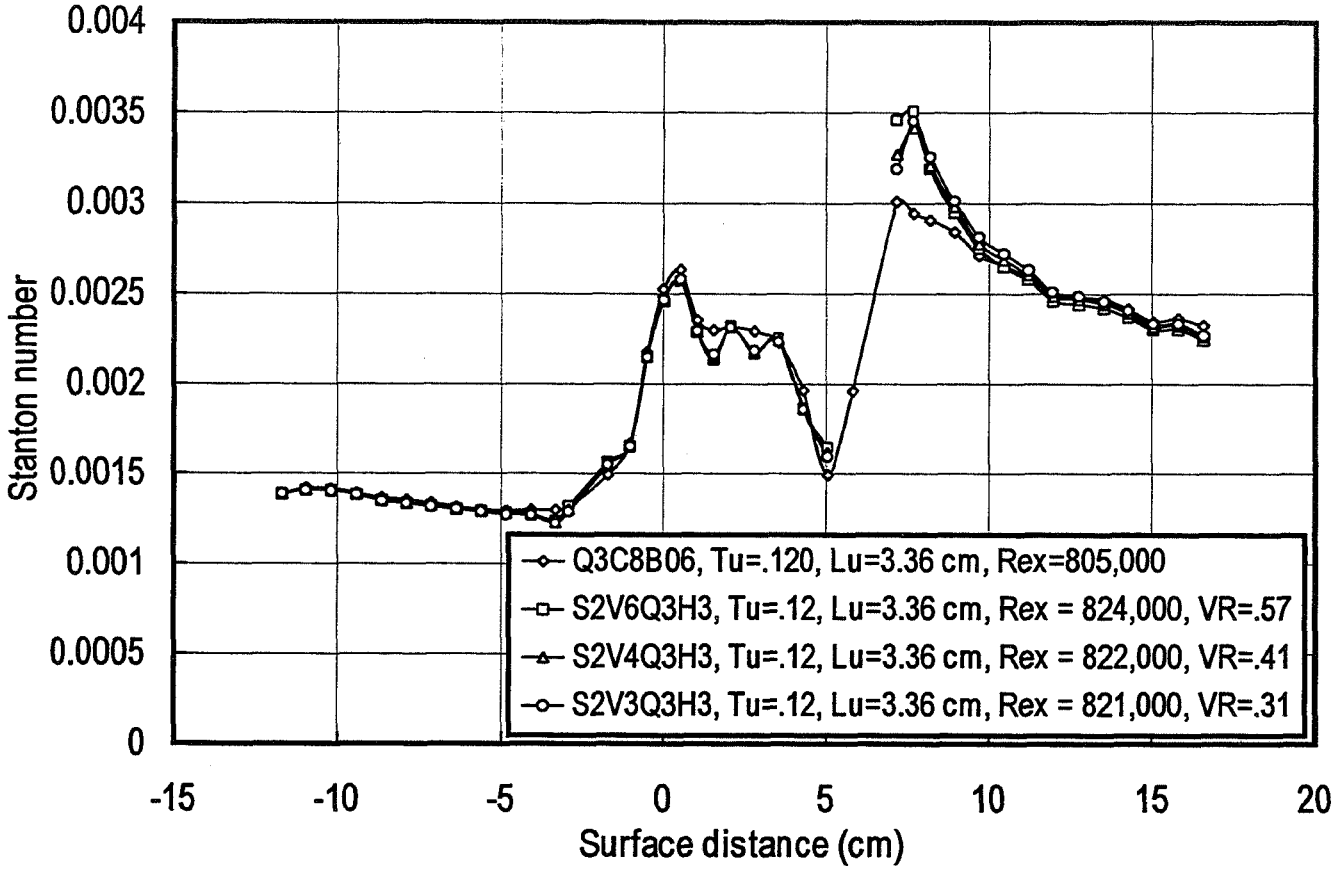

Suction surface heat transfer, 2 rows, 30° holes, high turbulence

- The level of augmentation was found to be reasonably consistent over the range of velocity ratios investigated for either one or two rows. The heat transfer increase for the showerhead array was also low past transition.

- In spite of an augmentation level of 60 percent above the low turbulence case, the heat transfer was increased by up to an additional 46 percent over the base case for a VR of 1.5.
- Generally, heat transfer augmentation ratio scaled on velocity ratio.
- Similar to the augmentation on the suction surface boundary layer, the effect of the jet quickly dissipated in the downstream direction.

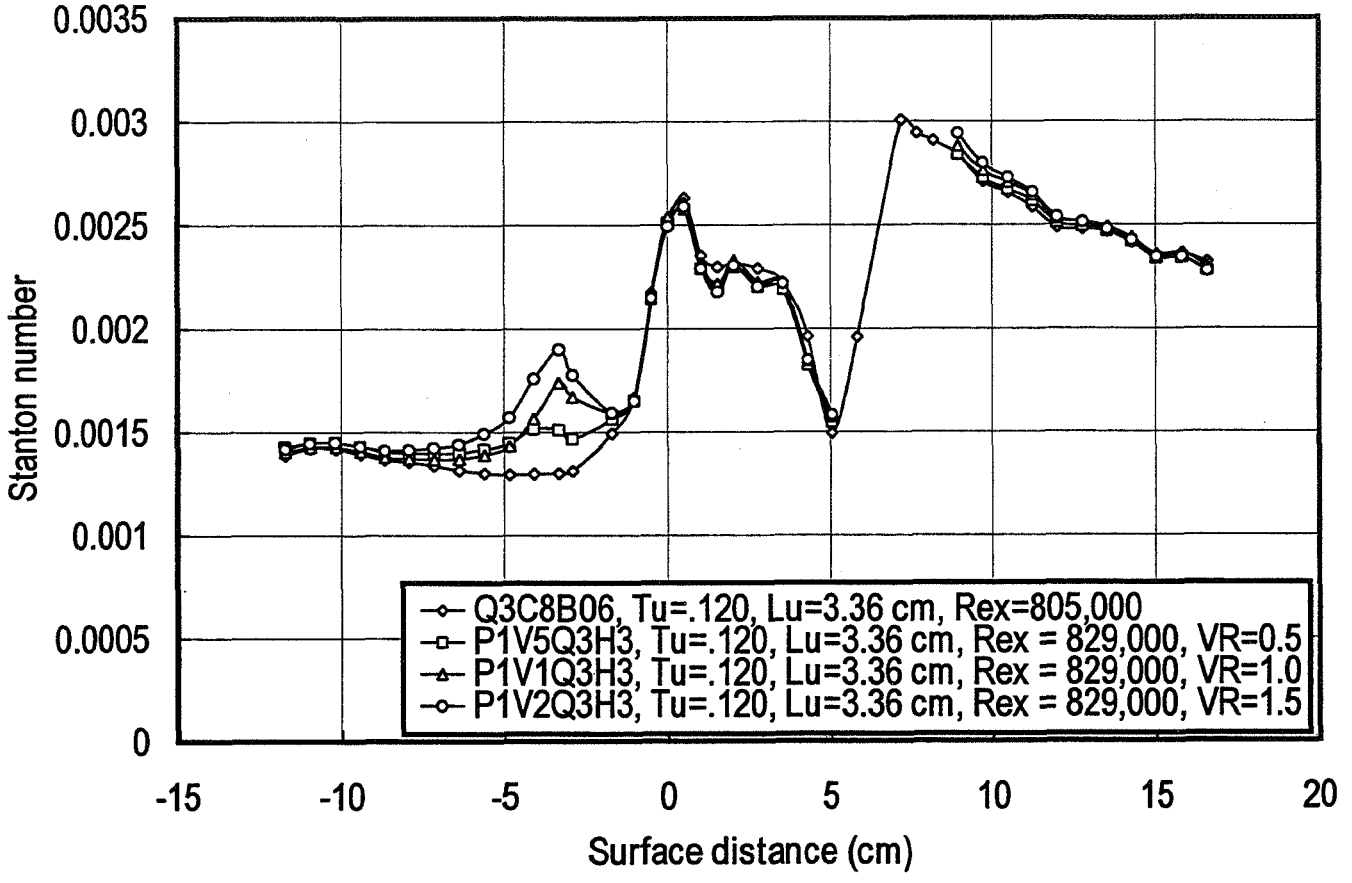

Pressure surface heat transfer, 1 row, 30° holes, high turbulence

- The peak augmentation on the pressure surface for the single row at a velocity ratio of 0.5 was about 16 percent compared to a peak of 11 percent on the suction surface for a single row and a comparable velocity ratio.

- The augmentation curves for velocity ratios of 1.0 and 1.5 were very similar in form.
- The augmentation curve for a velocity ratio of 0.5 had a delayed peak and a slower decay.
- The delayed peak level and decay were believed due to the shear layer that formed and caused an increased production of turbulence.
- At an X/D of 9, dissipation rates for velocity ratios of 0.5 and 1.0 were close.

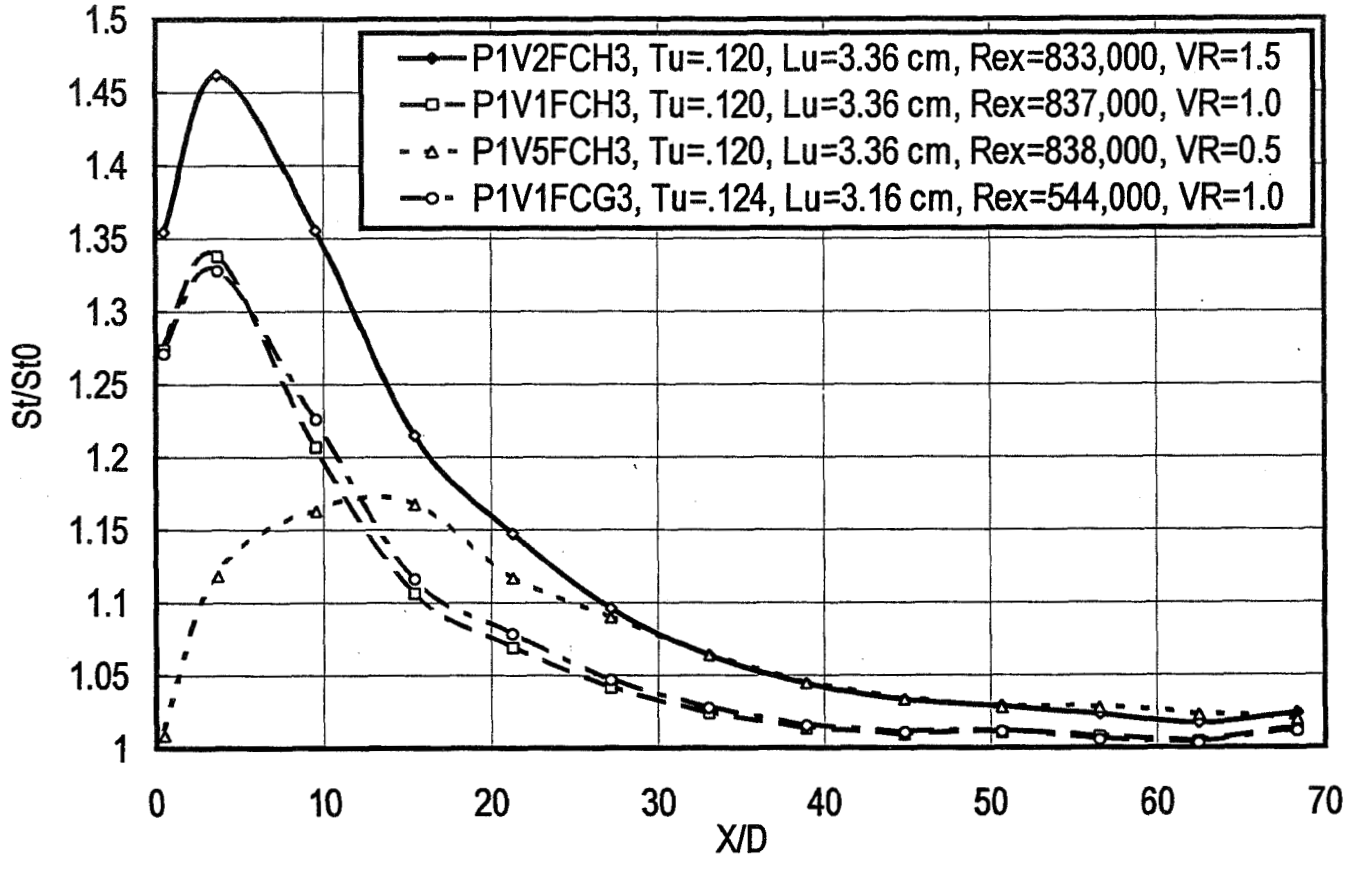

Pressure surface heat transfer, 1 row, 30° holes, high turbulence

- The dissipation level at Y of 0.1 cm for a VR of 1.5 was about three times the level determined for a VR of 1.0 and about 3.5 times higher than for a VR of 0.5 indicating no simple relationship between dissipation and augmentation.

HEAT TRANSFER RESULTS

- Two rows of holes produce about twice the increase in peak heat transfer as a single row.

- The augmentation curves look quite similar with the curves for a single row.

- The decay rate for a double row is quicker than the rate of decay in augmentation for a single row.

- The augmentation curve for the velocity ratio of 0.5 has a different shape and decay rate than the higher VR data

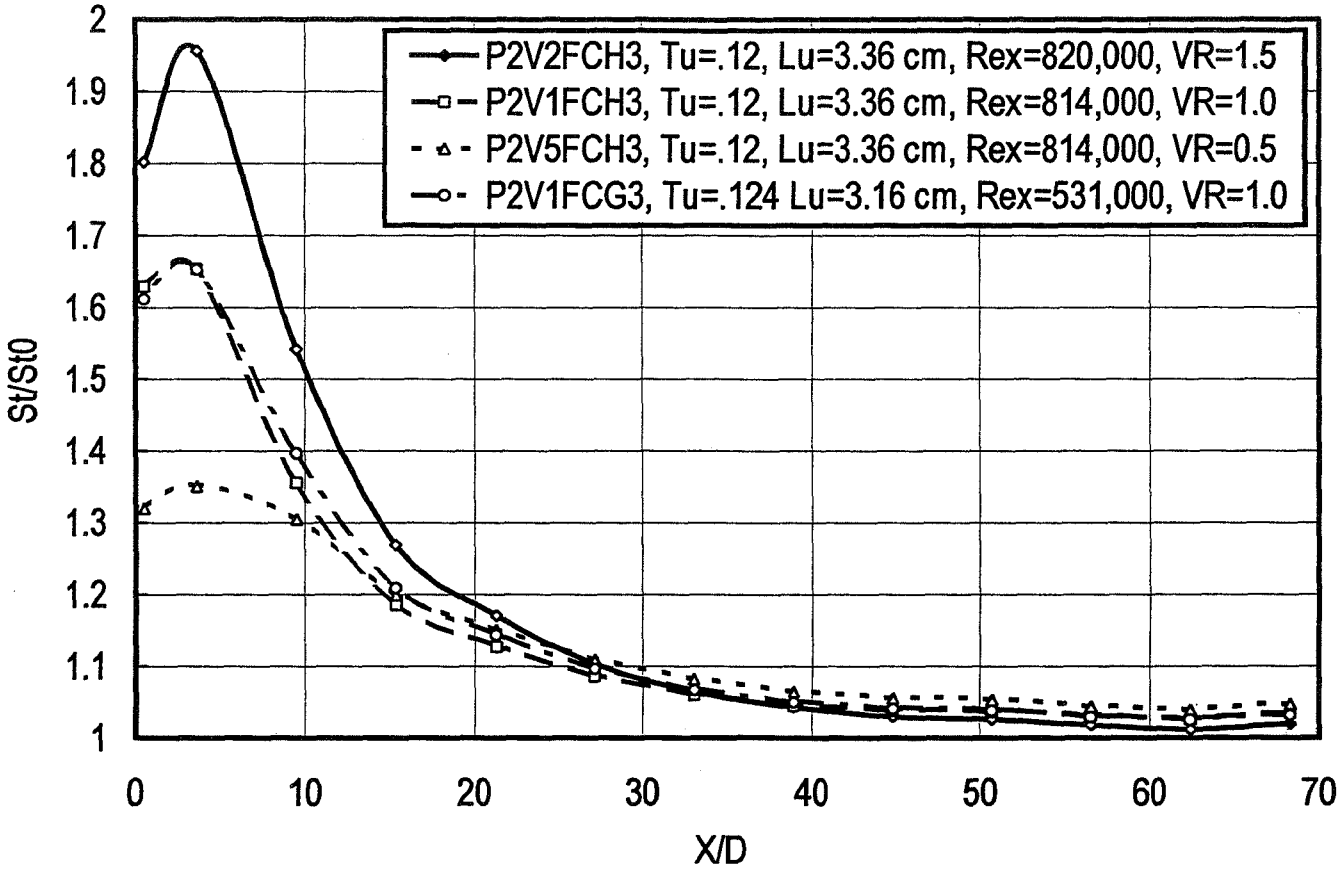

Pressure surface heat transfer, 2 rows, 30° holes, high turbulence

- The dissipation levels at Y of 0.1 cm for VR's of 0.5 and 1.0 are noticeably higher than single row values as measured at X/D of 9. The dissipation levels determined for the VR of 1.5 are comparable to single row data.

CONCLUSIONS

- For this C3X vane, suction surface film cooling produced levels of η similar to a flat plate configuration for the low Tu case.
- High pressure surface acceleration raised near hole η over suction surface but η level diminished with continued velocity increase.
- High relative level of turbulence on PS caused rapid and continuing depletion of film cooling coverage.
- Two staggered rows of film cooling produced substantial enhancements over a single row for high VR's.
- Peak heat transfer augmentation for suction surface was about 11 percent for one row and 18 percent for two for both turbulence levels.
- PS augmentation scaled on VR and number of rows with peak augmentation levels of up to 95 percent over high turbulence base for two staggered rows at a VR of 1.5.

- Flows with strong continuous acceleration need to be studied at various Tu levels. (different positions along a vane PS)
- Effect of relative hole size on augmentation also needs to be evaluated.

INVESTIGATION OF ROTOR WAKE EFFECTS ON FILM COOLING

James D. Heidmann
NASA Lewis Research Center
Cleveland, Ohio

Outline

- **Motivation and goals**
- **Experimental study**
- **Computational study**
- **Wake–affected film cooling model**
- **Conclusions and recommendations**

Motivation and Goals

- **Effect of wake passing on film cooling is not well understood**
- **Lack of understanding may result in excess coolant usage**
- **Focus on showerhead cooling due to sensitivity to wake passing**
- **Temporal, spanwise, and chordwise resolution of test data**
- **Seeking physics–based model to account for wake passing effect**
- **Model should be applicable over a broad range of parameters**

Rotor–Wake Turbine Facility Test Section

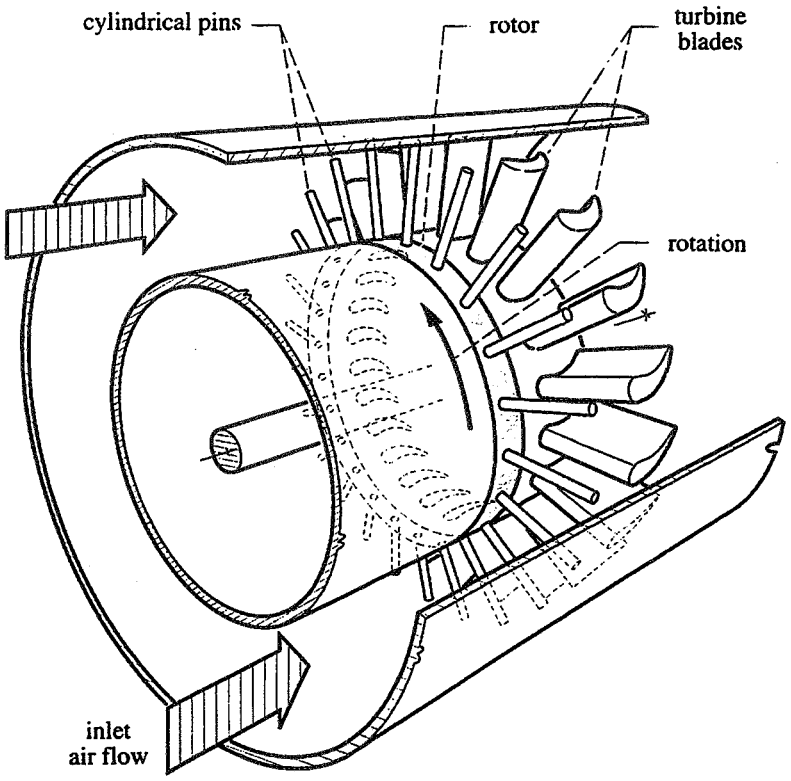

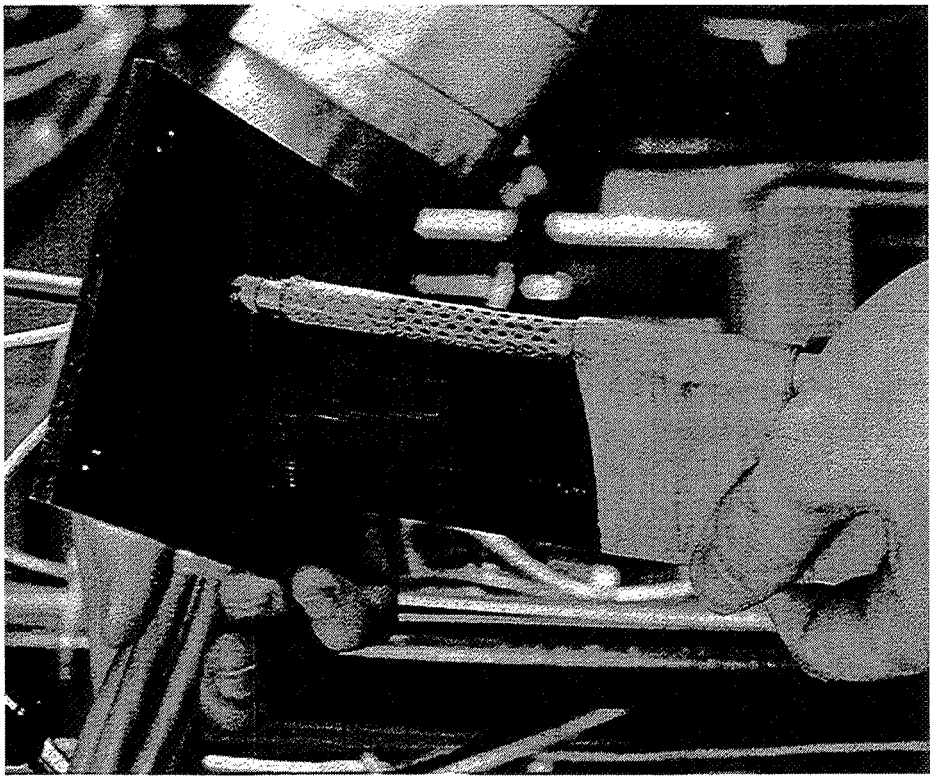

Experimental Span–Average Film Effectiveness

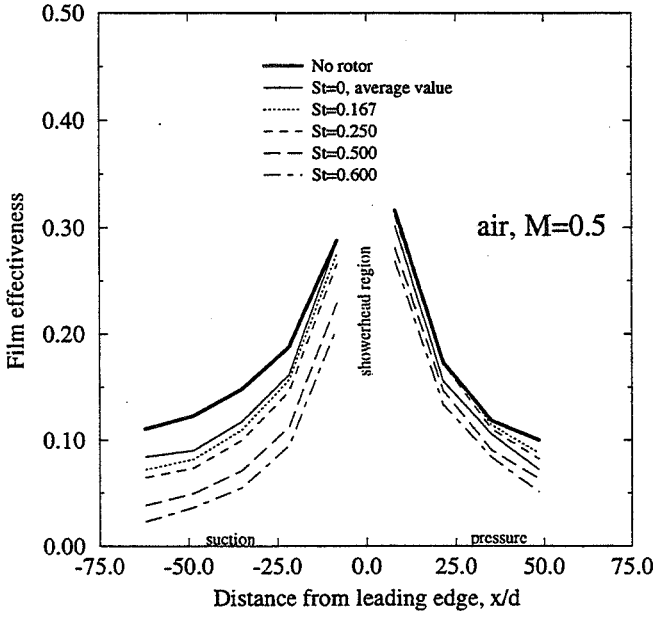

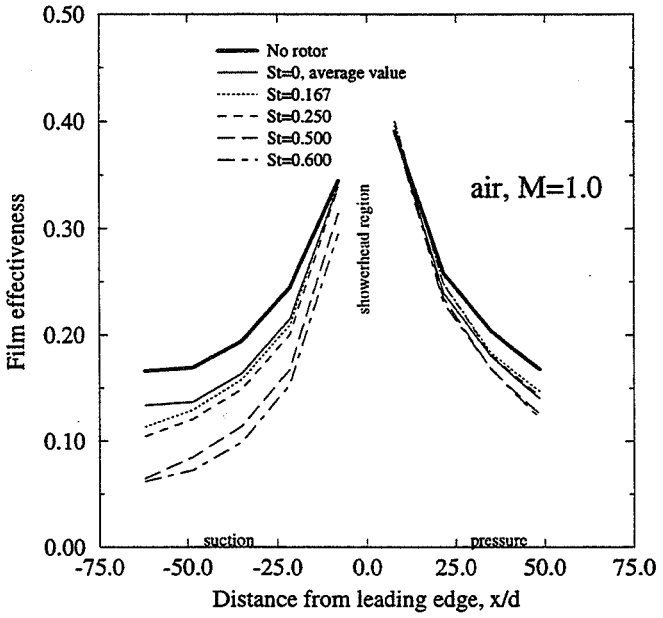

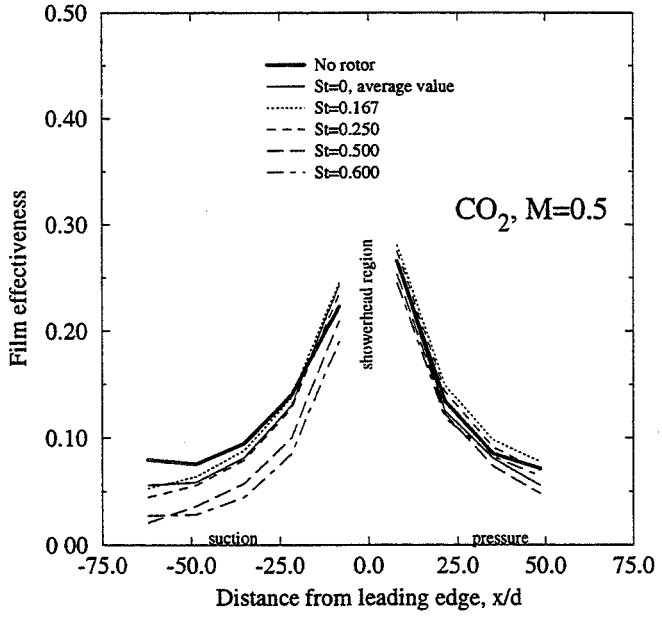

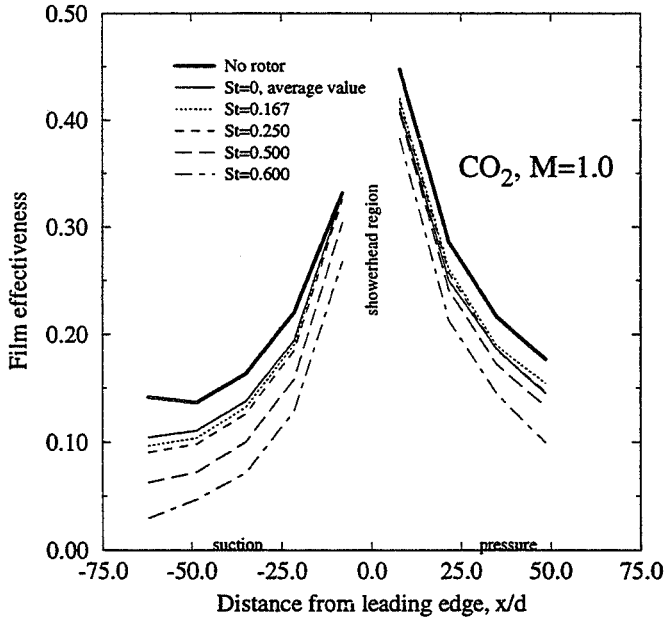

Nickel Thin Film Gauge Array

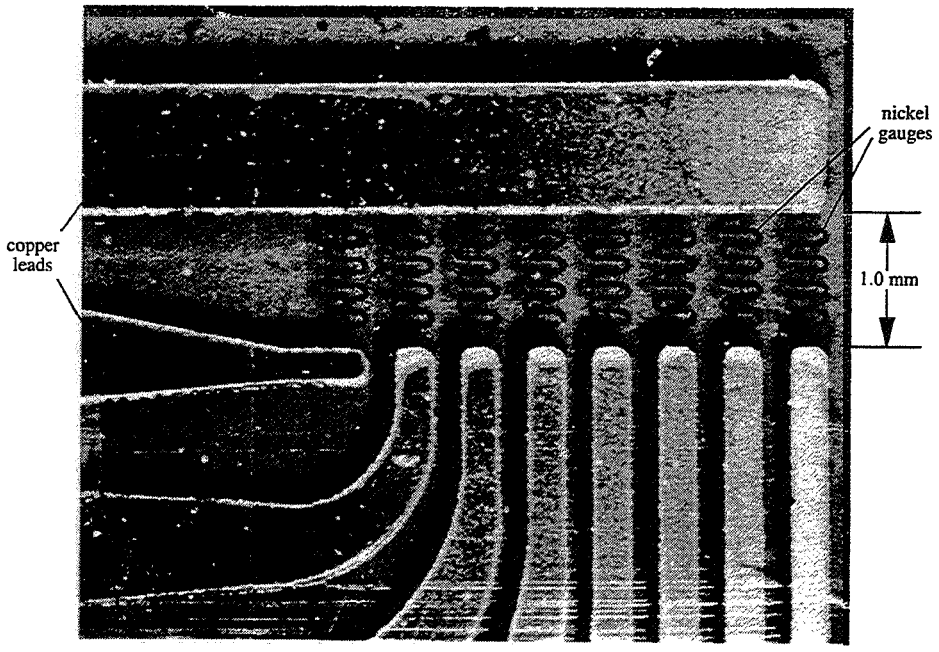

Experimental Span–Resolved Film Effectiveness

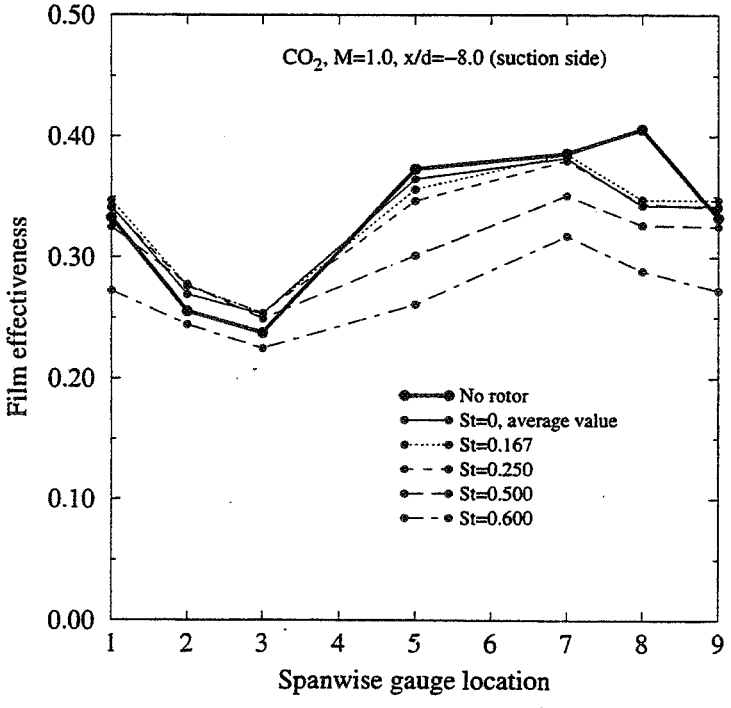

Experimental Stationary Rotor Film Effectiveness

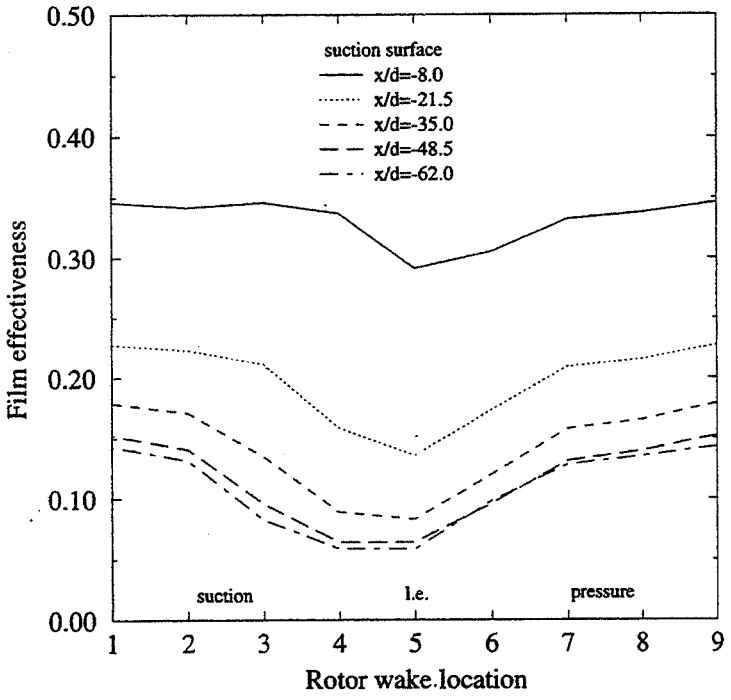

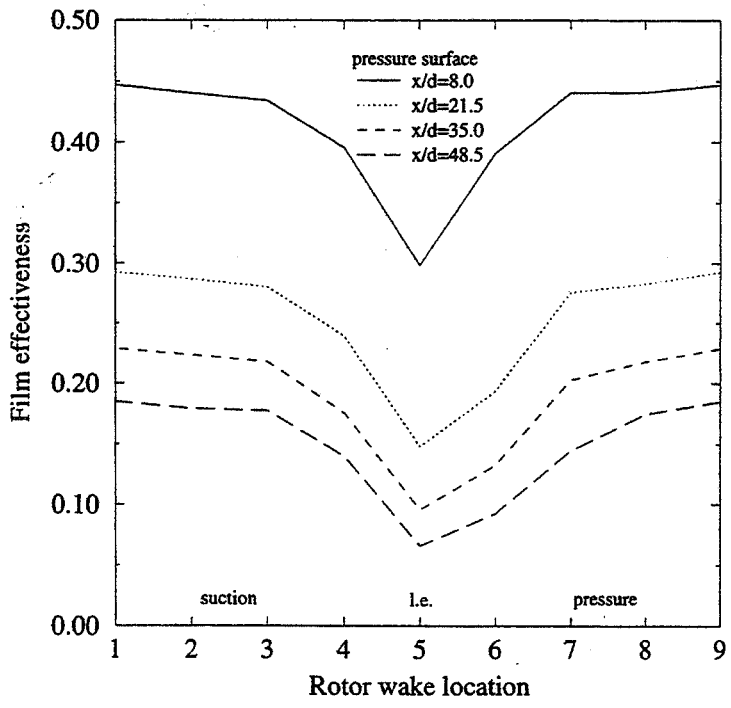

Blade–to–Blade Computational Grid

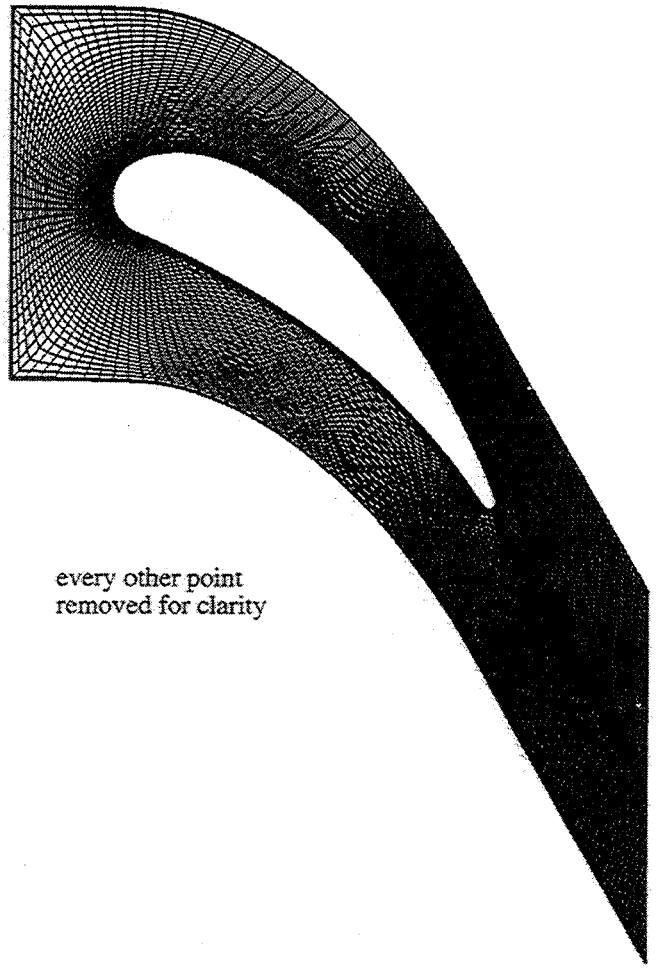

Blade–to–Blade Computational Grid

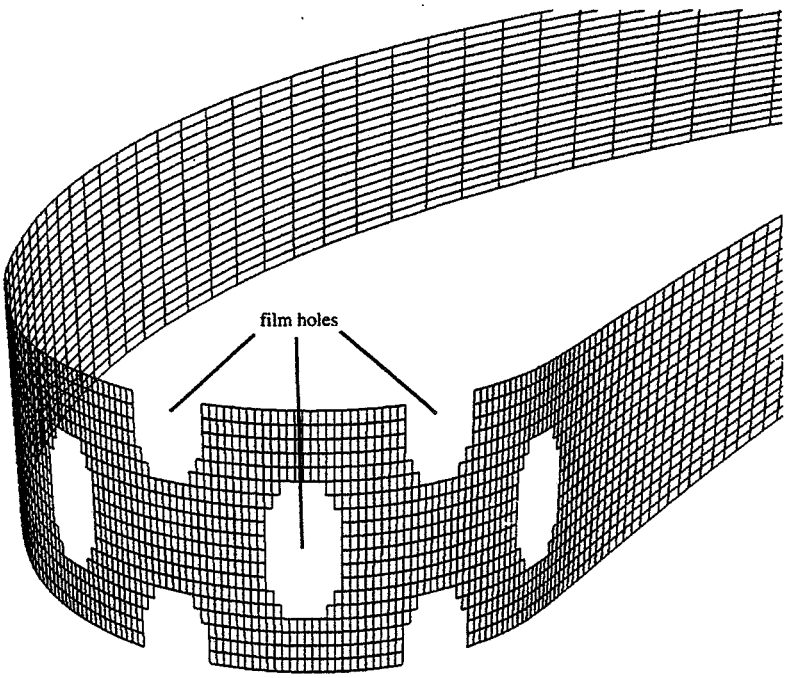

Instantaneous 2–D Entropy Contours

$\phi = 0$

$\phi = \pi/2$

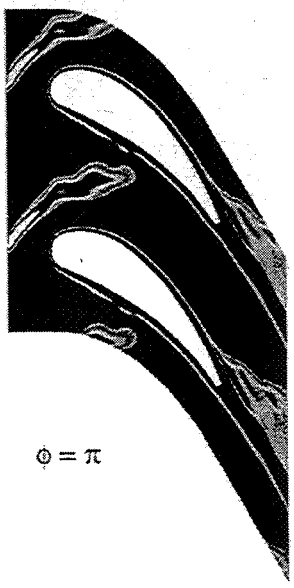

$\phi = \pi$

$\phi = 3\pi/2$

Perturbation Velocity Colored by Perturbation Stagnation Temperature

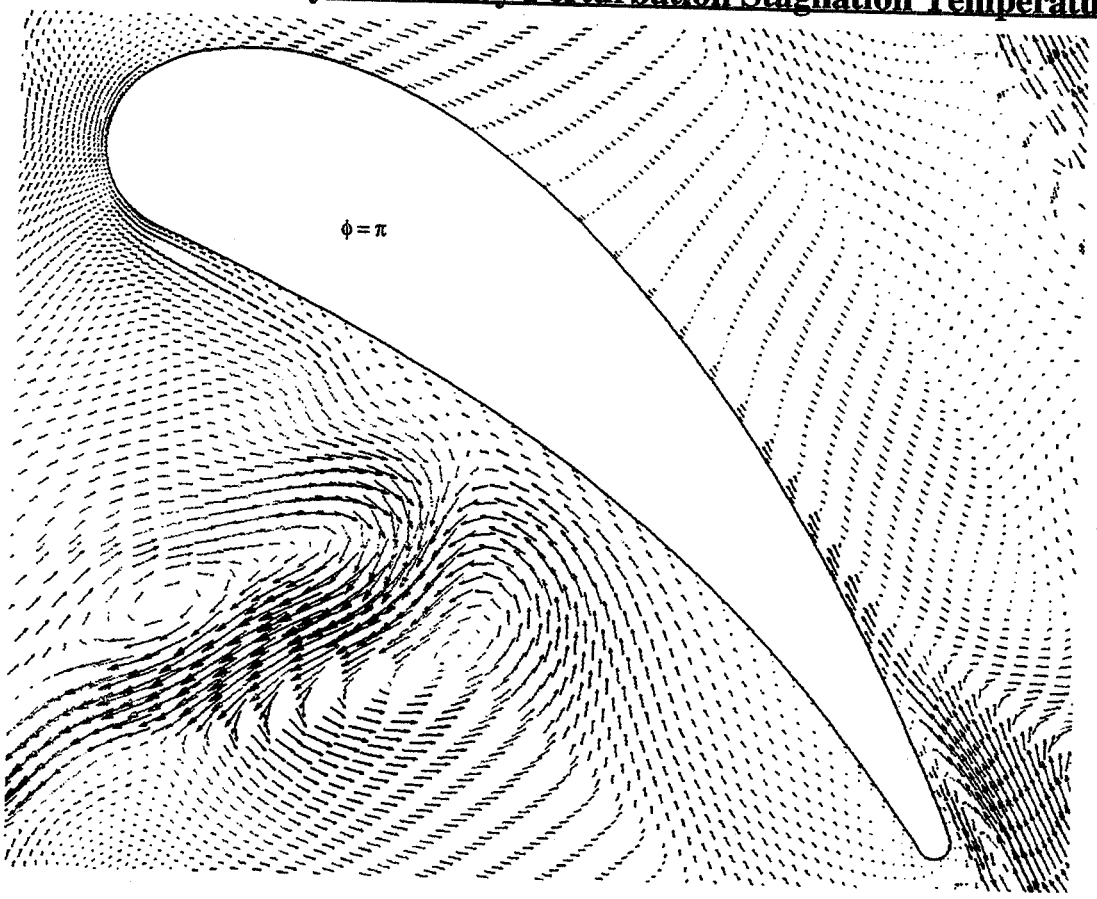

Instantaneous Film Effectiveness

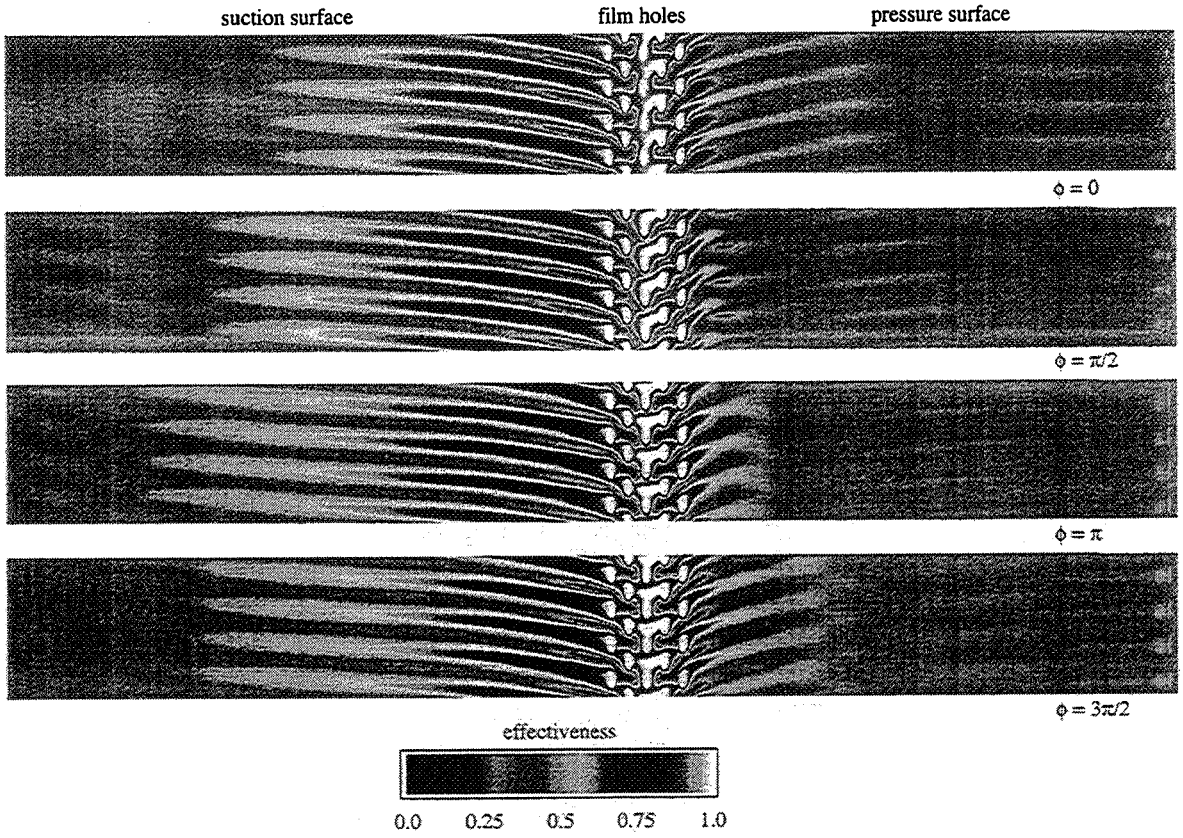

Time–Average Unsteady Stagnation Temperature

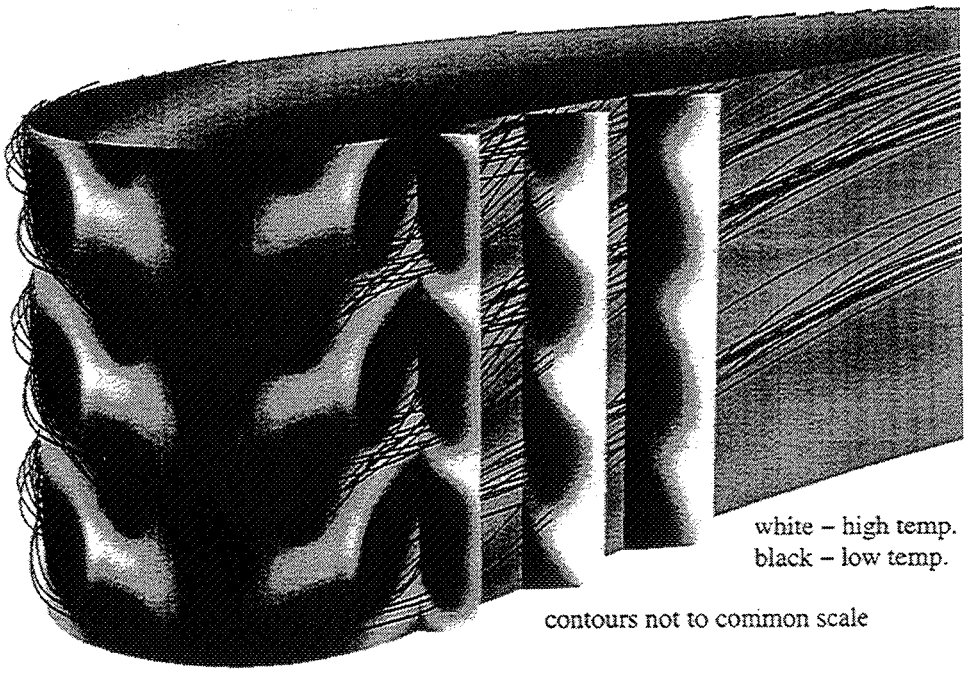

Exp./Calc. Comparison – Injectant Condition Effect

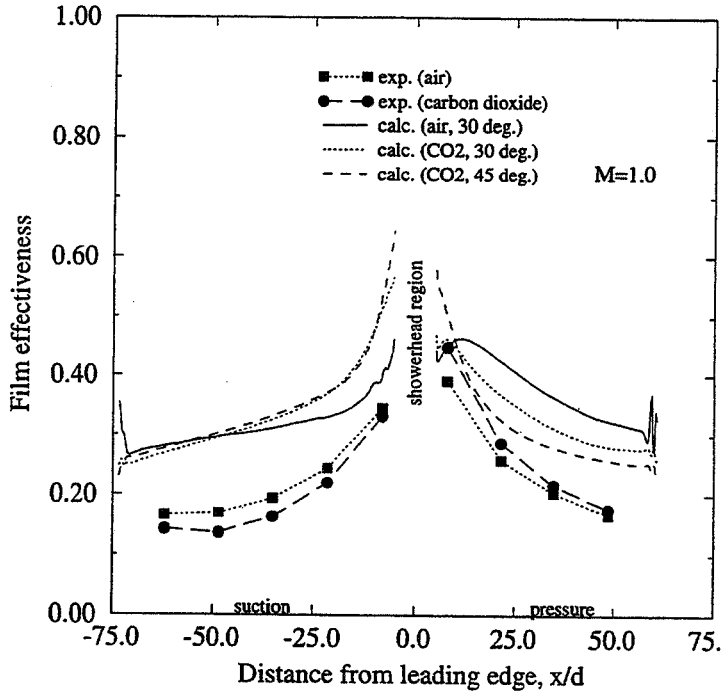

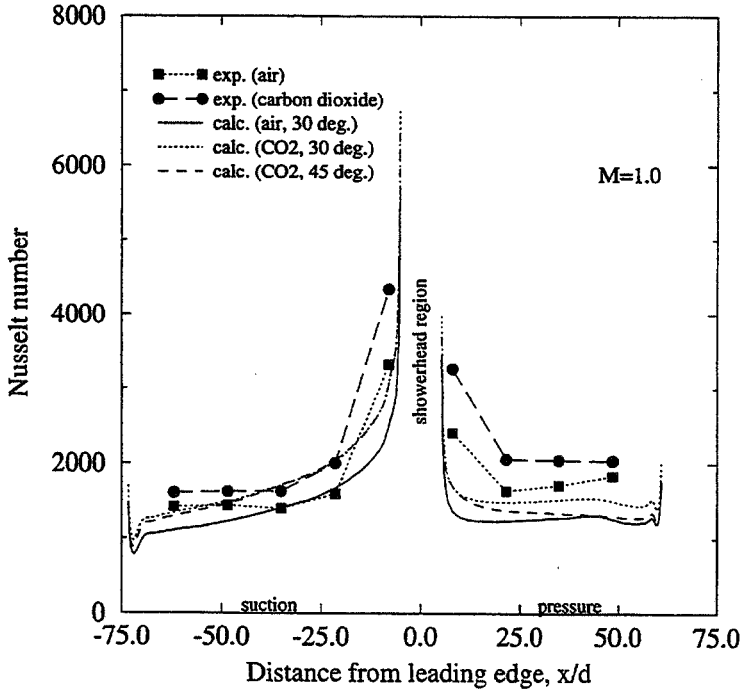

Best-Fit Equations for Air and CO_2

Air:

$$\eta = \frac{0.761}{1.0 + \left(\frac{0.054x}{MS(1.0 \pm 0.139M \pm 0.286St)}\right)^{0.792 \pm 0.033}} - 0.093St$$

$$\Delta\eta_{rms} = 0.0068$$

CO_2:

$$\eta = \frac{0.948}{1.0 + \left(\frac{0.094x}{MS(1.0 \pm 0.241M \pm 0.144St)}\right)^{0.762 \pm 0.014}} - 0.095St$$

$$\Delta\eta_{rms} = 0.0074$$

Correlated Span–Average Film Effectiveness

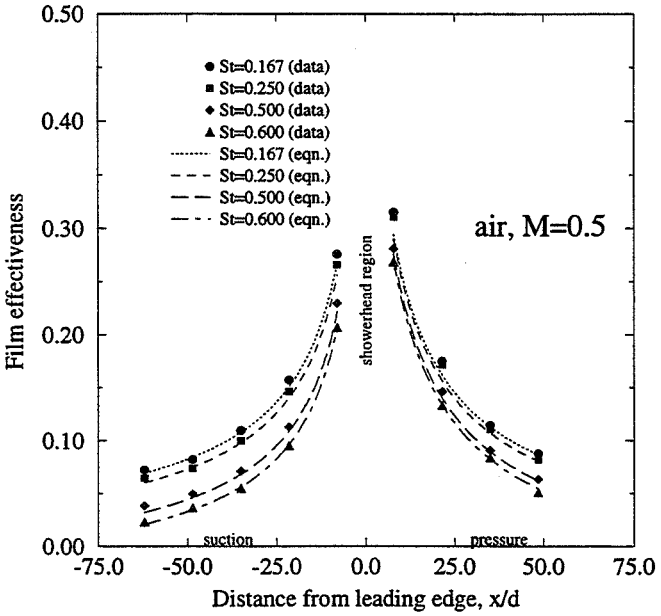

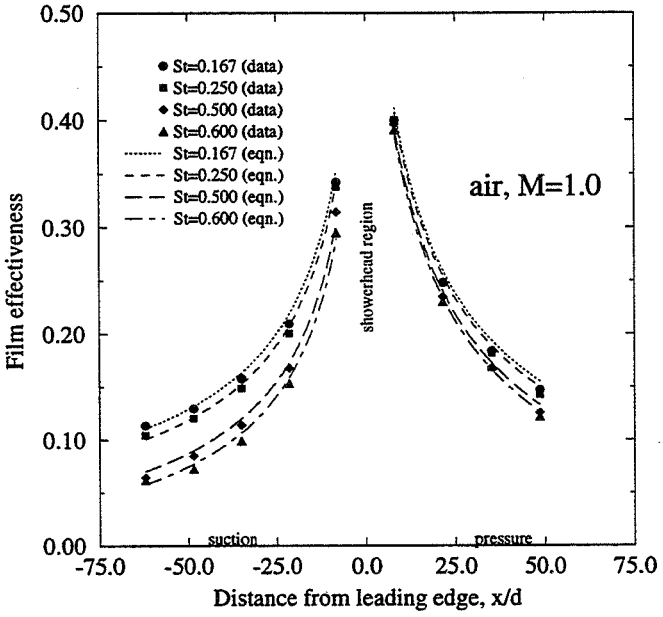

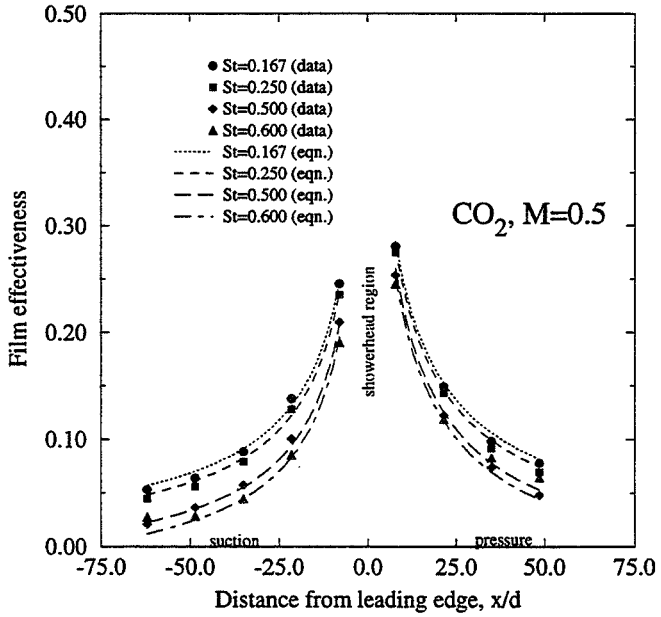

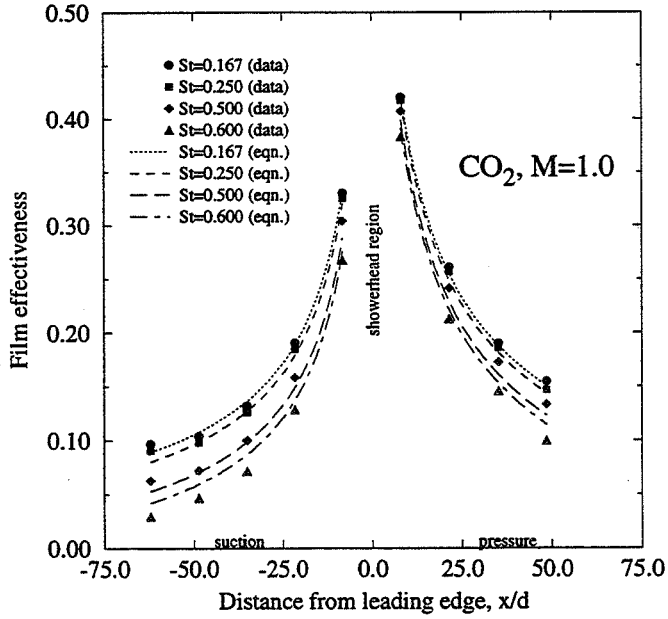

Conclusions and Recommendations

- **Primary wake effect is linear reduction in η with St**
- **Secondary wake effect is skewing of suction/pressure side cooling**
- **Steady computations match experimental Nu, but overpredict η**
- **Unsteady computations elucidate wake/film interaction**
- **Model may be used to estimate wake passing effect**
- **Need boundary layer and full stage experiments**
- **Need resolved film hole and full stage unsteady computations**
- **Need validated turbulence models for film cooling**

UNSTEADY HIGH TURBULENCE EFFECT ON TURBINE BLADE FILM COOLING HEAT TRANSFER PERFORMANCE USING A TRANSIENT LIQUID CRYSTAL TECHNIQUE

H. Du, S.V. Ekkad, and J.C. Han
Texas A&M University
College Station, Texas

OBJECTIVES

To study detailed distributions of heat transfer coefficients and film effectiveness for a gas turbine blade, including film cooling hole region, under the effects of upstream flow conditions:

- **Free stream turbulence**
- **Unsteady wakes**
- **Unsteady wakes with trailing edge coolant ejections**

and the effects of film cooling injections with air and CO_2 as coolants:

- **Blowing ratios**
- **Coolant-to-mainstream density ratios**
- **Advanced film hole shapes.**

Sketch of Test Section

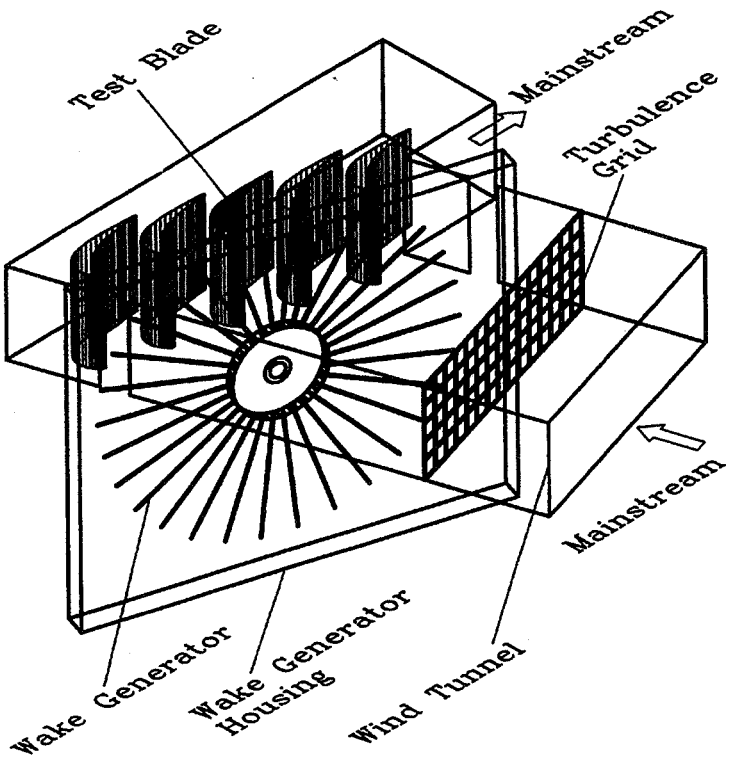

Camera Arrangement

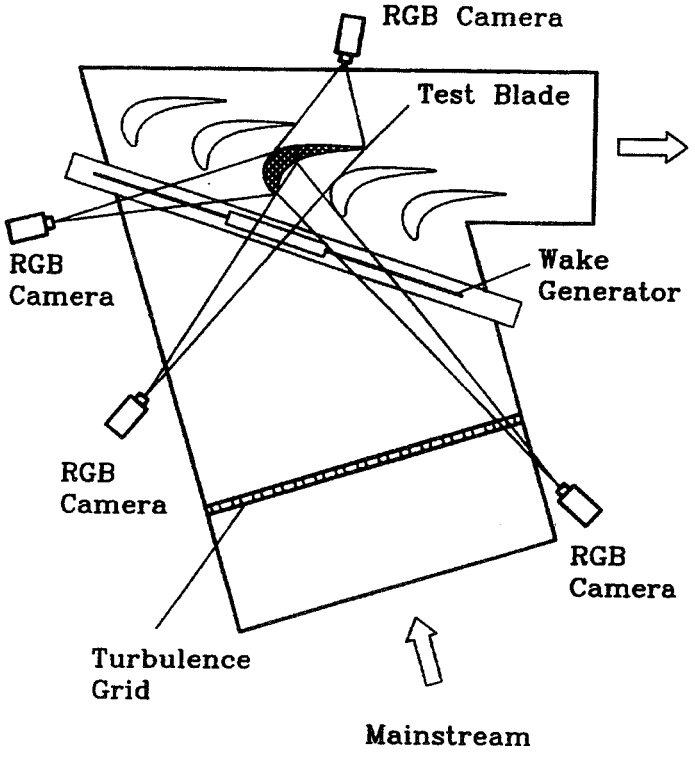

Geometries of the Test Blade with Film Holes

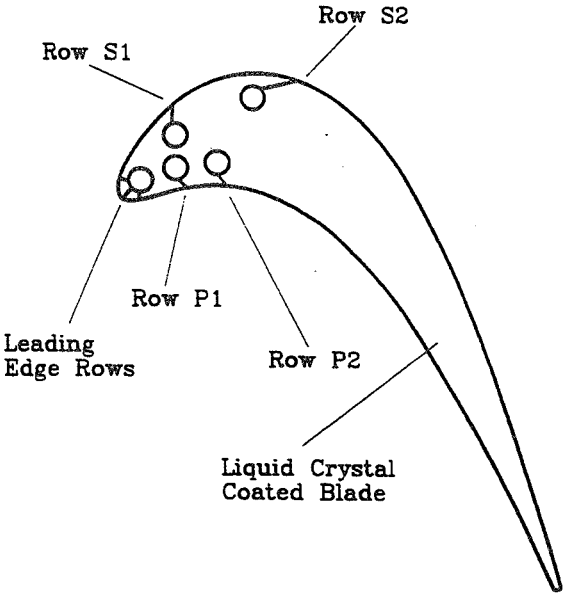

Film Hole Location	P/D	L/D	Axial Angle	Radial Angle	Tangential Angle
LE	7.31	2.7	90°	27°	—
S1	4.13	7.6	—	90°	45°
S2	5.71	12.8	—	90°	30°
P1	6.79	4.2	—	32°	55°
P2	5.00	6.7	—	35°	50°

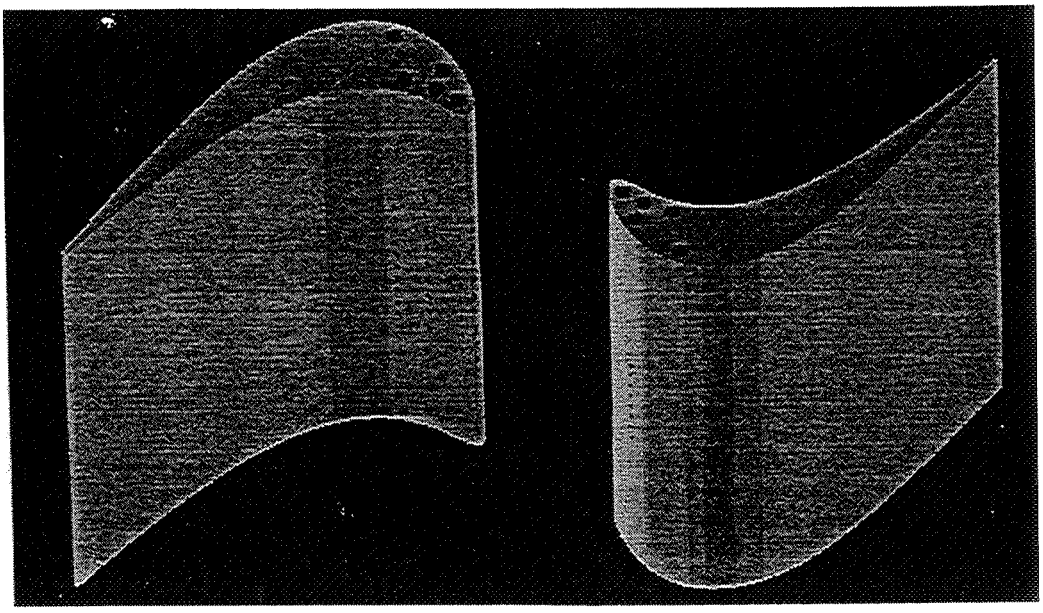

APPROACH

- **A transient liquid crystal technique has been developed for this study.**
- **In the experiments, the liquid crystal coated blade is heated to a uniform temperature, and then suddenly exposed to a pre-set mainstream flow condition.**
- **A Color Frame Grabber system, through the RGB cameras, is used to record the time of the color change of the liquid crystal on the blade surface.**
- **The color change times are related to heat transfer coefficients and film effectiveness based on the solution of a 1-D semi-infinite transient conduction model with a convective boundary conditions.**

THEORY

ONE-DIMENSIONAL SEMI-INFINITE SOLID ASSUMPTION:

$$k\frac{\partial^2 T}{\partial x^2} = \rho c_p \frac{\partial T}{\partial t}$$

Initial condition:

$$at\ t=0,\quad T=T_i$$

Boundary conditions:

$$at\ x=0,\quad -k\frac{\partial T}{\partial x} = h(T_w - T_m);\ as\ x\to\infty,\quad T=T_i$$

Solution at x=0:

$$\frac{T_w - T_i}{T_m - T_i} = 1 - exp(\frac{h^2 \alpha t}{k^2}) erfc(\frac{h\sqrt{\alpha t}}{k})$$

FILM COOLING CONCEPT

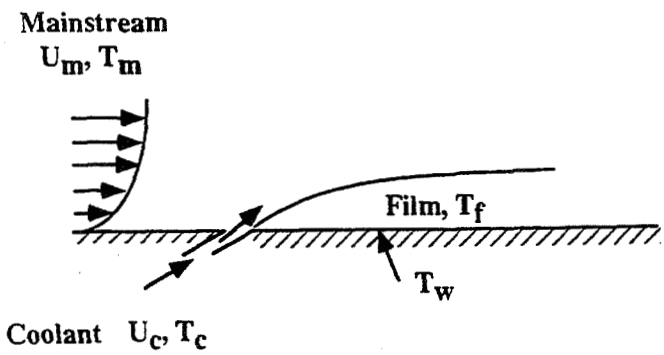

$$q''_0 = h_0(T_m - T_w) \quad \textit{with no film cooling}$$

$$q'' = h(T_f - T_w) \quad \textit{with film cooling}$$

$$\eta = \frac{T_m - T_f}{T_m - T_c}, \quad \textit{film effectiveness}$$

$$\frac{q''}{q''_0} = \frac{h}{h_0}\frac{T_f - T_w}{T_m - T_w}$$

For Film Cooling Case: $T_m = T_f$

Solution:

$$\frac{T_w - T_i}{T_f - T_i} = 1 - exp(\frac{h^2 \alpha t}{k^2}) erfc(\frac{h\sqrt{\alpha t}}{k})$$

where T_f = local film temperature

$$T_f = \eta(T_c - T_m) + T_m = \eta T_c + (1 - \eta) T_m$$

η= local film effectiveness

Solution:

$$T_w - T_i = [1 - exp(\frac{h^2 \alpha t}{k^2}) erfc(\frac{h\sqrt{\alpha t}}{k})][\eta T_c + (1 - \eta) T_m - T_i]$$

Measured Region on Liquid Crystal Coated Blade

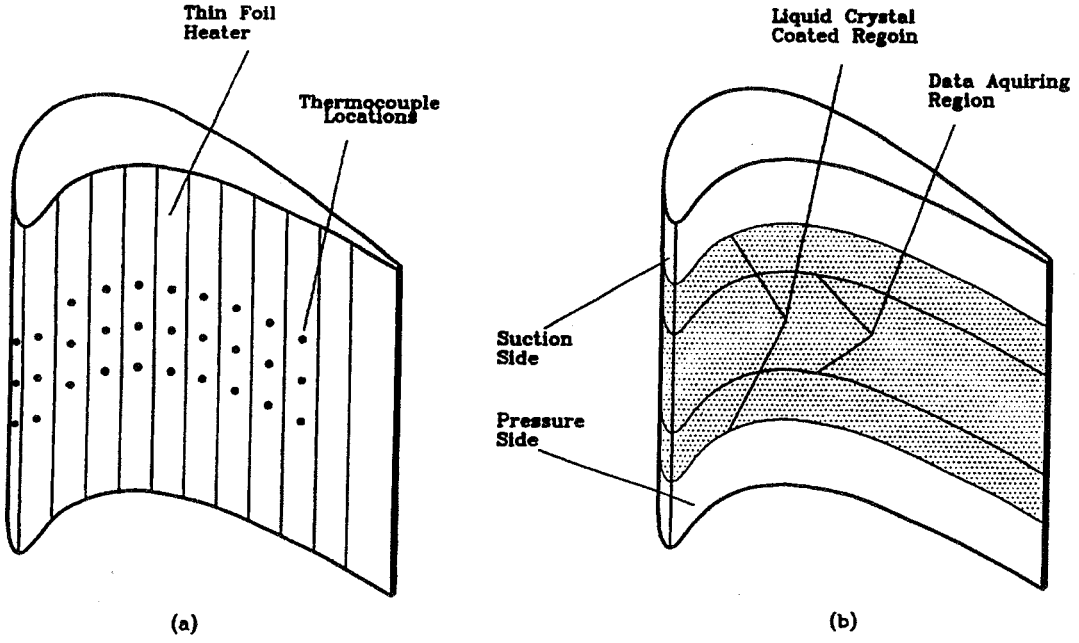

Heater Box Cross Section

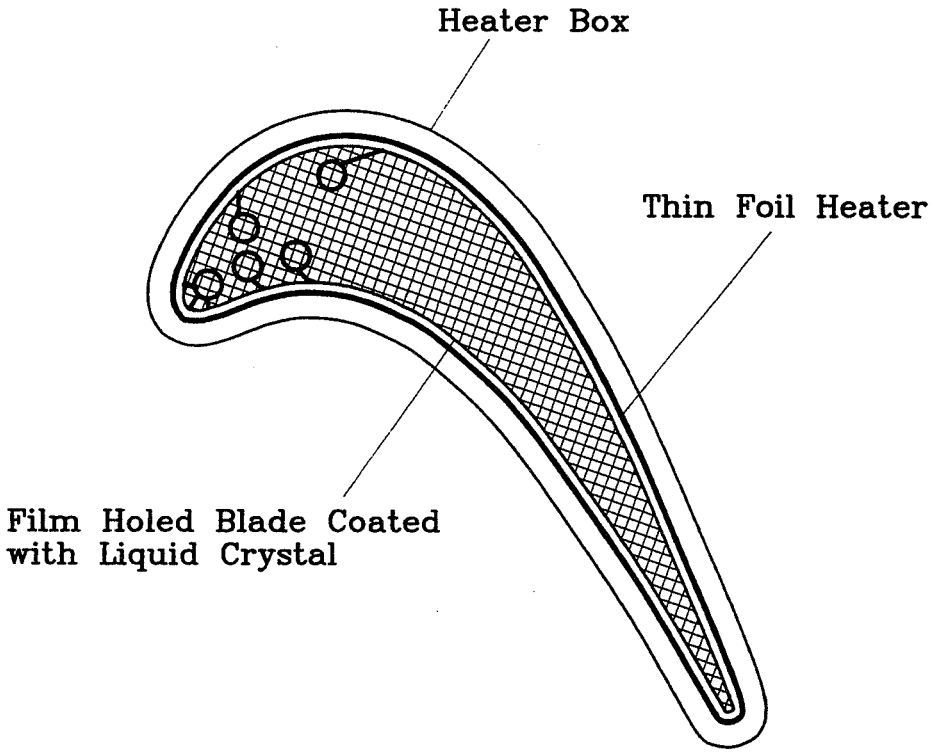

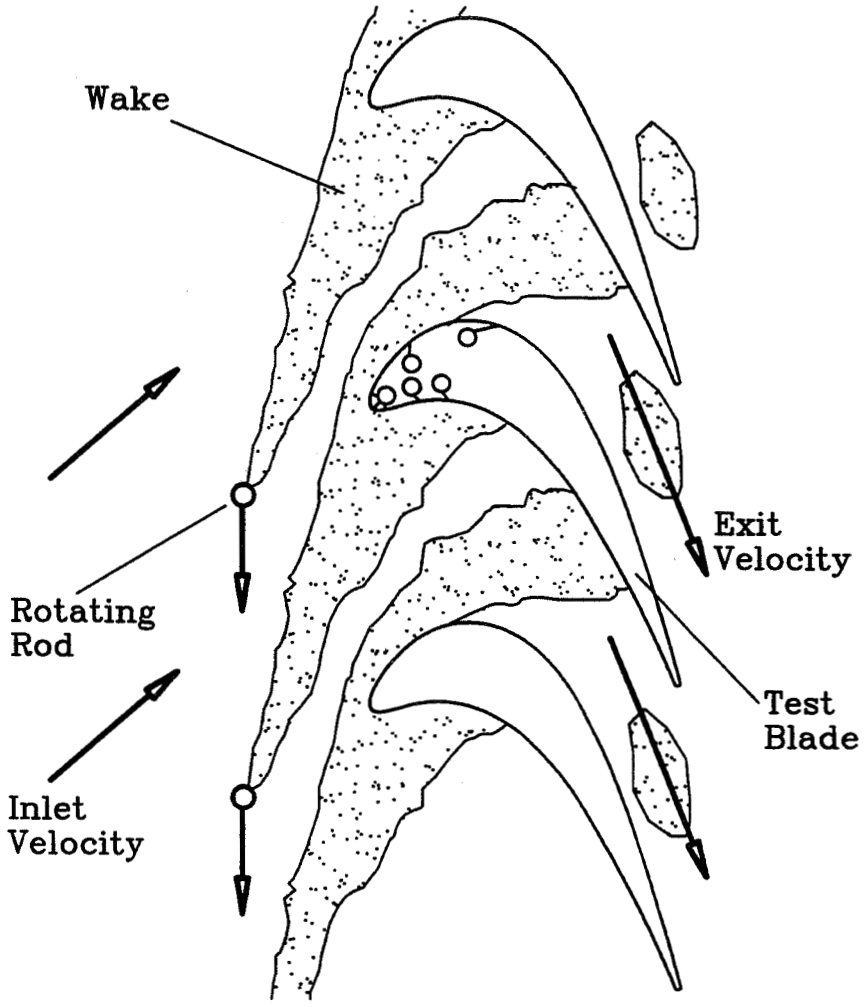

Conceptual View of Unsteady Wake Effect on Blade

$$Re = \frac{V_1 C_x}{\nu}$$

$$S = \frac{2\pi Nnd}{V_1}$$

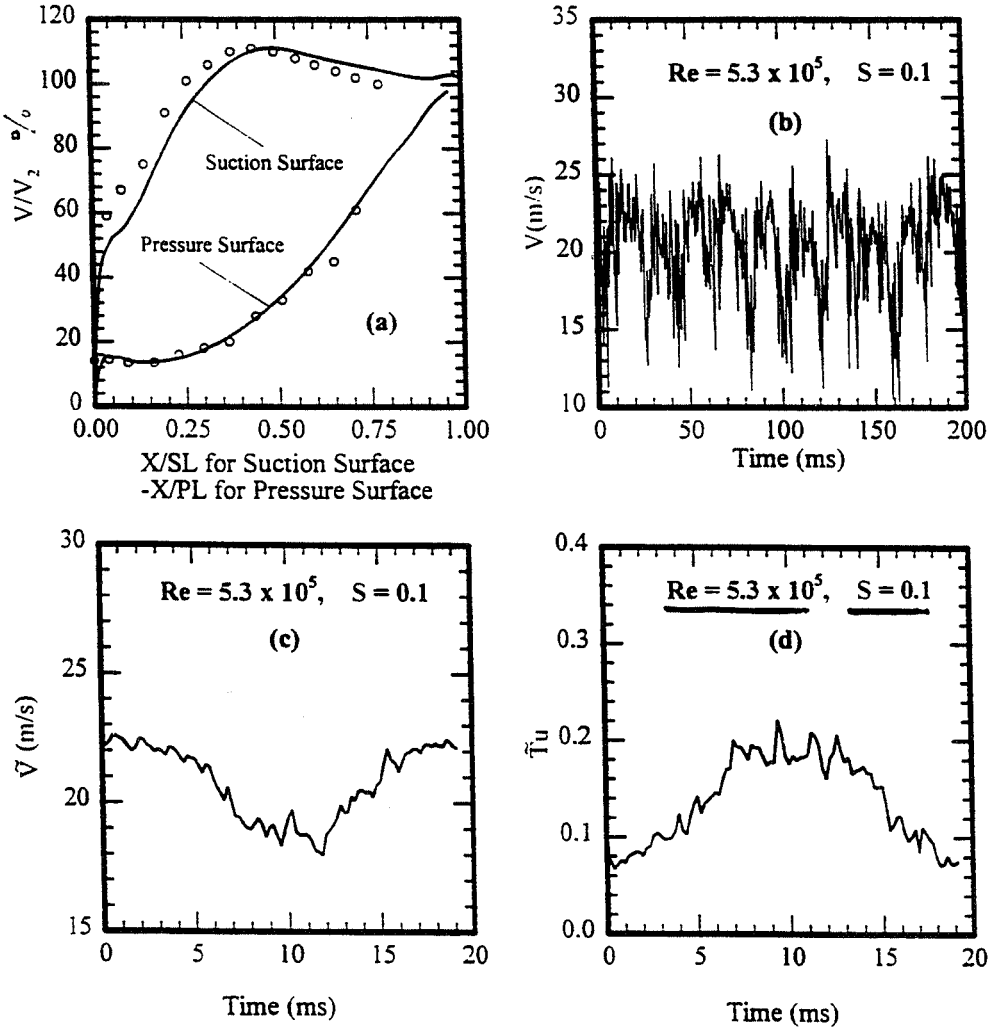

Local-to-exit velocity ratio (V/V_2) distributions on the test blade, profiles for V(t), $\tilde{V}$, $\tilde{T}u$, under wake effect at cascade inlet

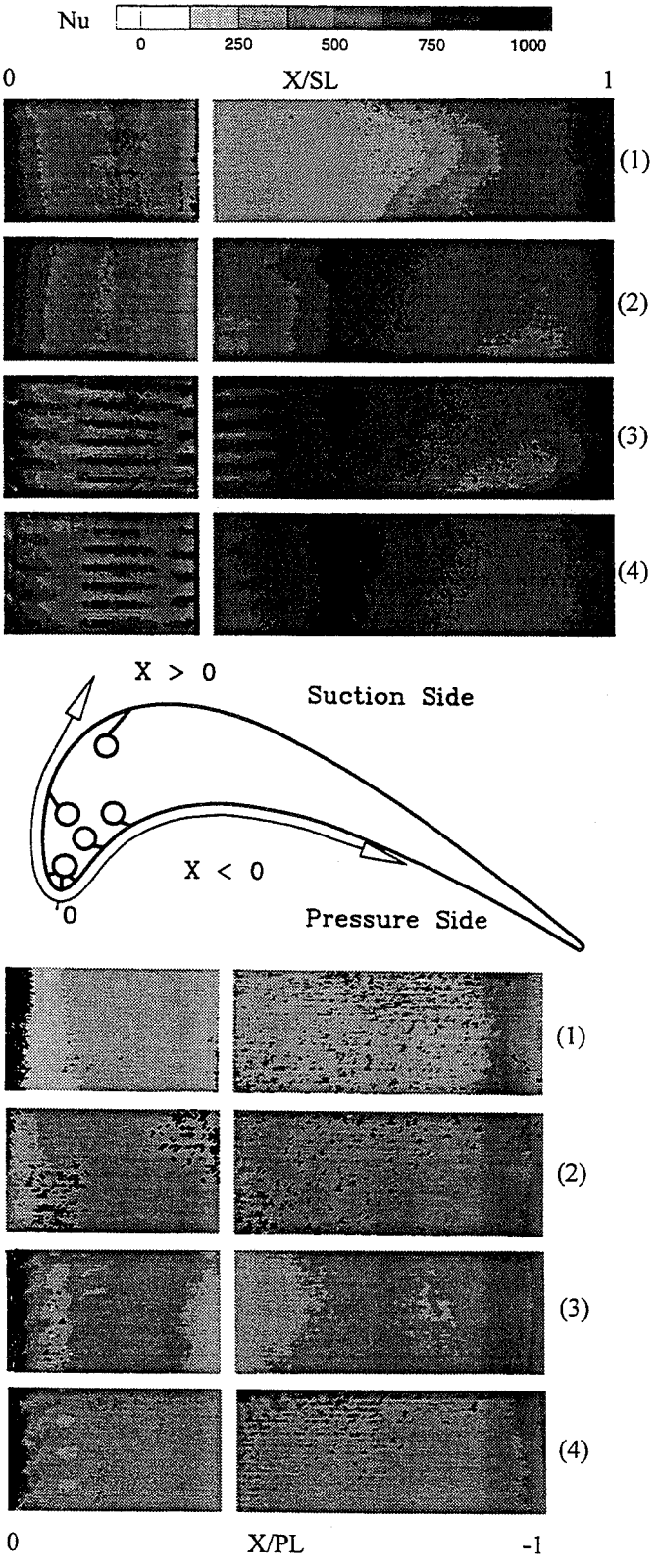
Nu
0
250
500
750
1000
0
X/SL
1
(1)
(2)
(3)
(4)
X > 0
Suction Side
X < 0
0
Pressure Side
(1)
(2)
(3)
(4)
0
X/PL
-1

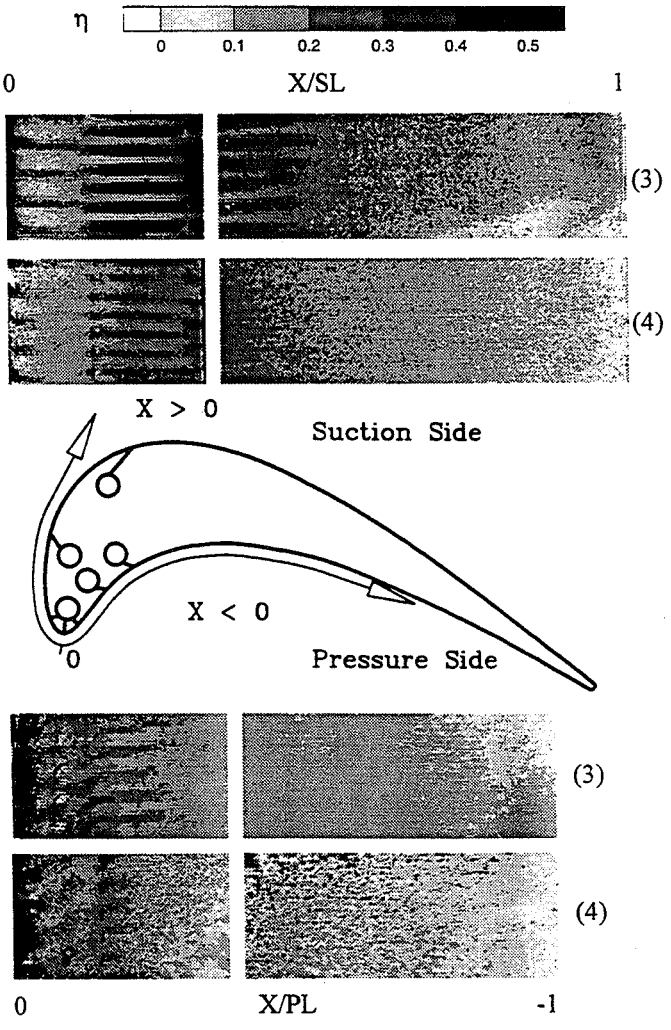
η
0
0.1
0.2
0.3
0.4
0.5
0
X/SL
1
(3)
(4)
X > 0
Suction Side
X < 0
0
Pressure Side
(3)
(4)
0
X/PL
-1

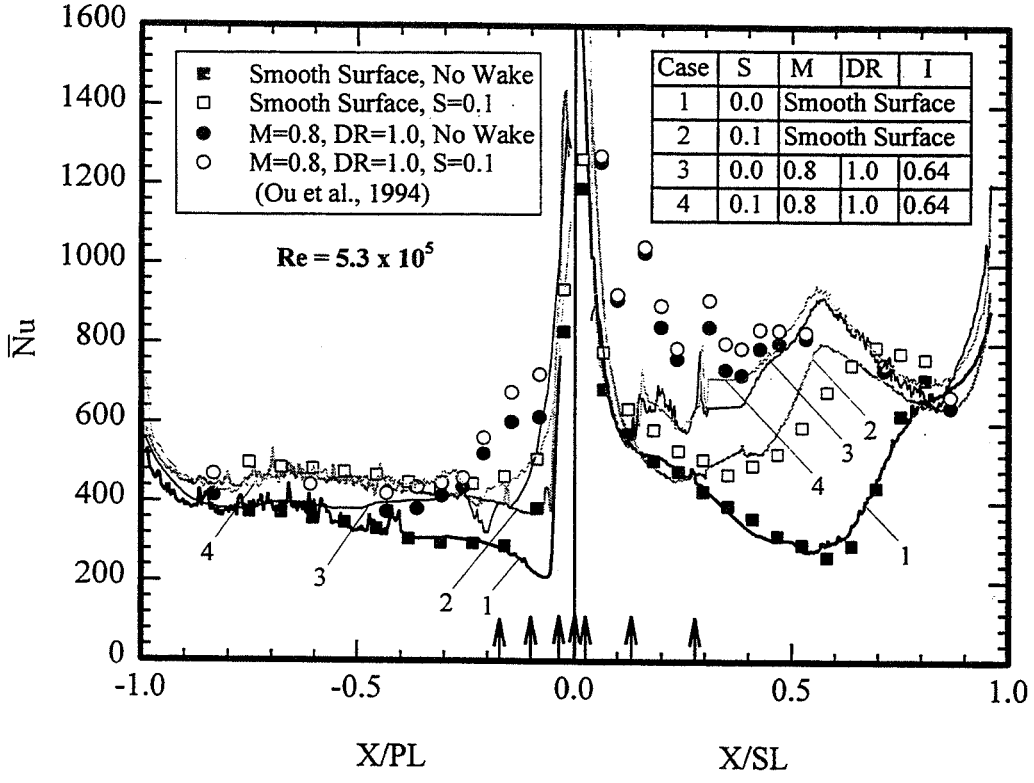

Effect of Unsteady Wake on Spanwise-Averaged Nusselt Number

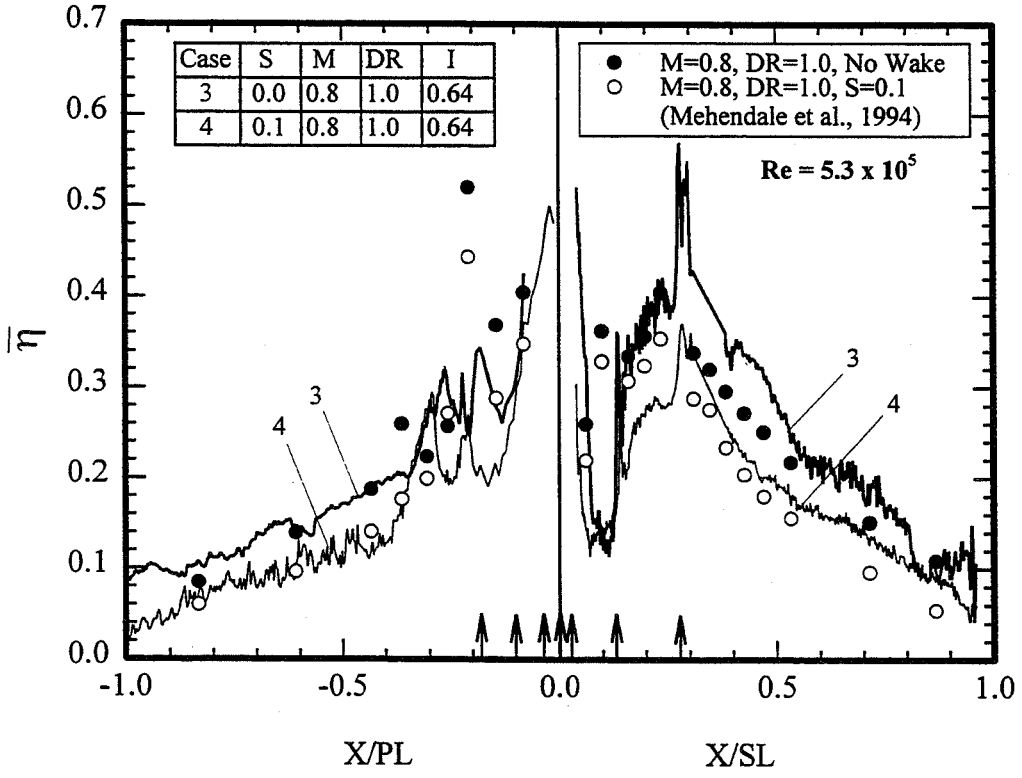

Effect of Unsteady Wake on Spanwise-Averaged Film Effectiveness

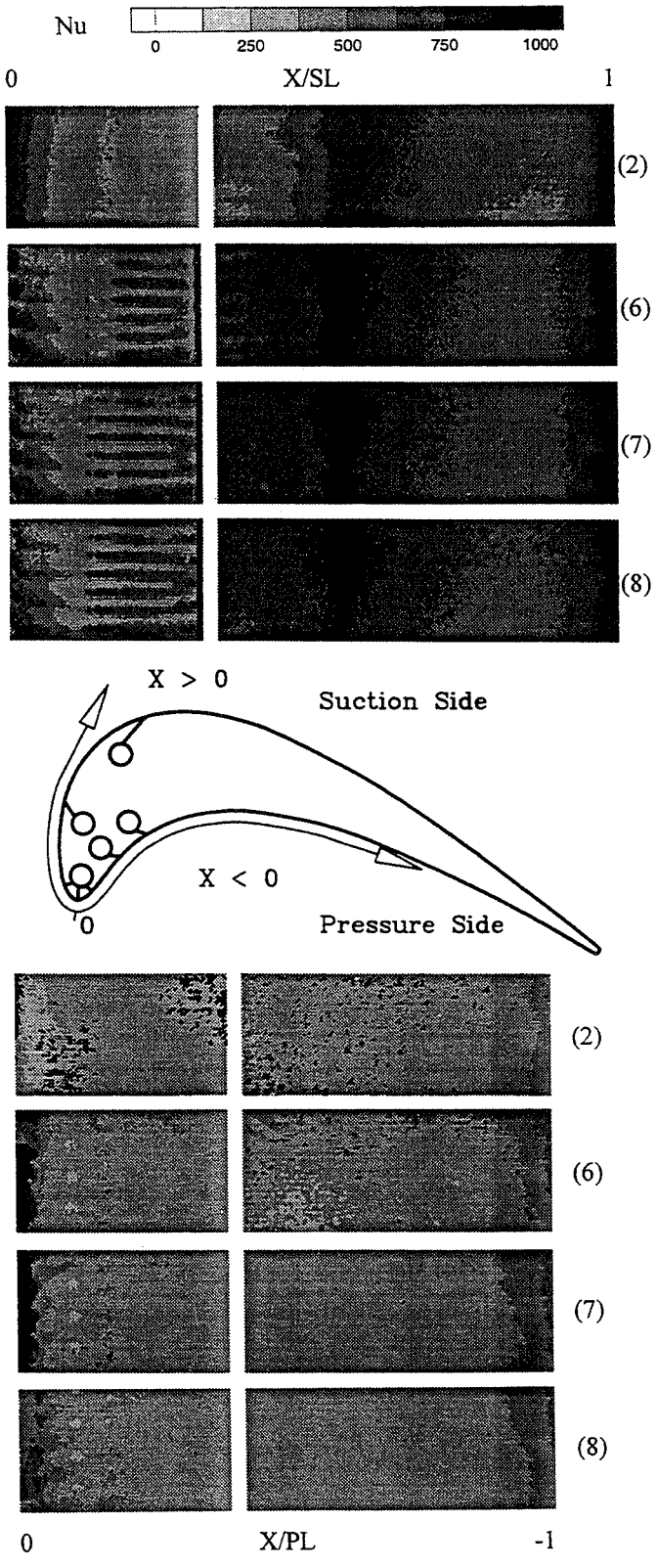
Nu
0
250
500
750
1000
0
X/SL
1
(2)
(6)
(7)
(8)
X > 0
Suction Side
X < 0
0
Pressure Side
(2)
(6)
(7)
(8)
0
X/PL
-1

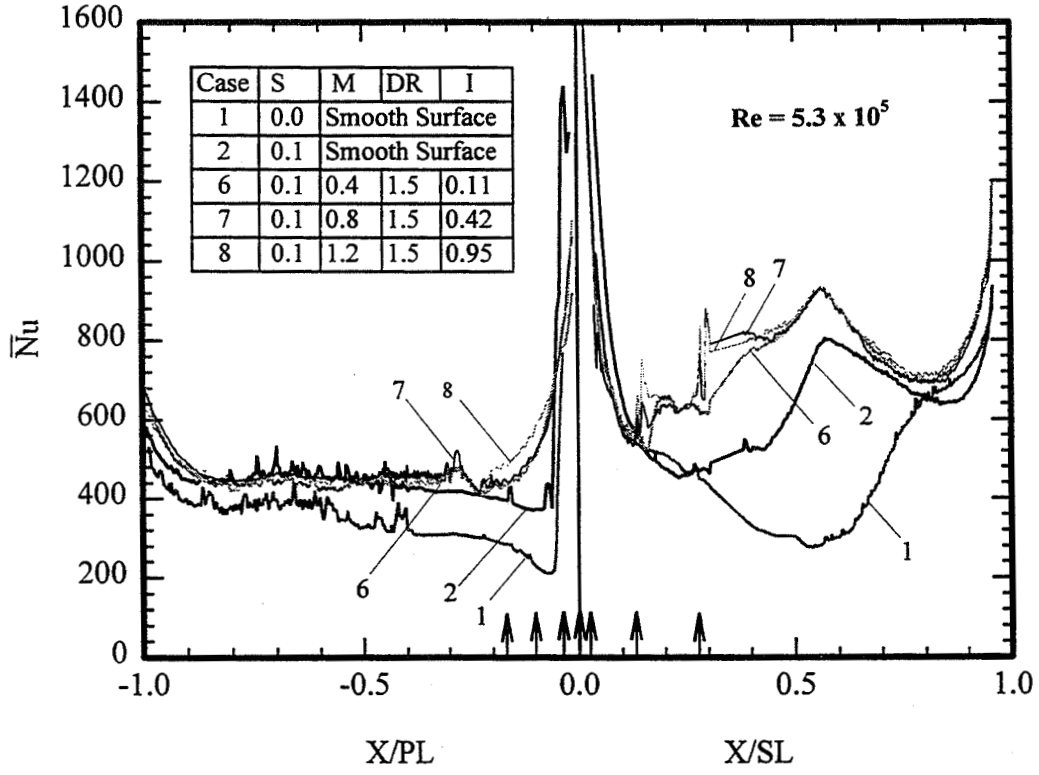

Blowing Ratio Effect on Spanwise-Averaged Nusselt Number at Given Wake Condition

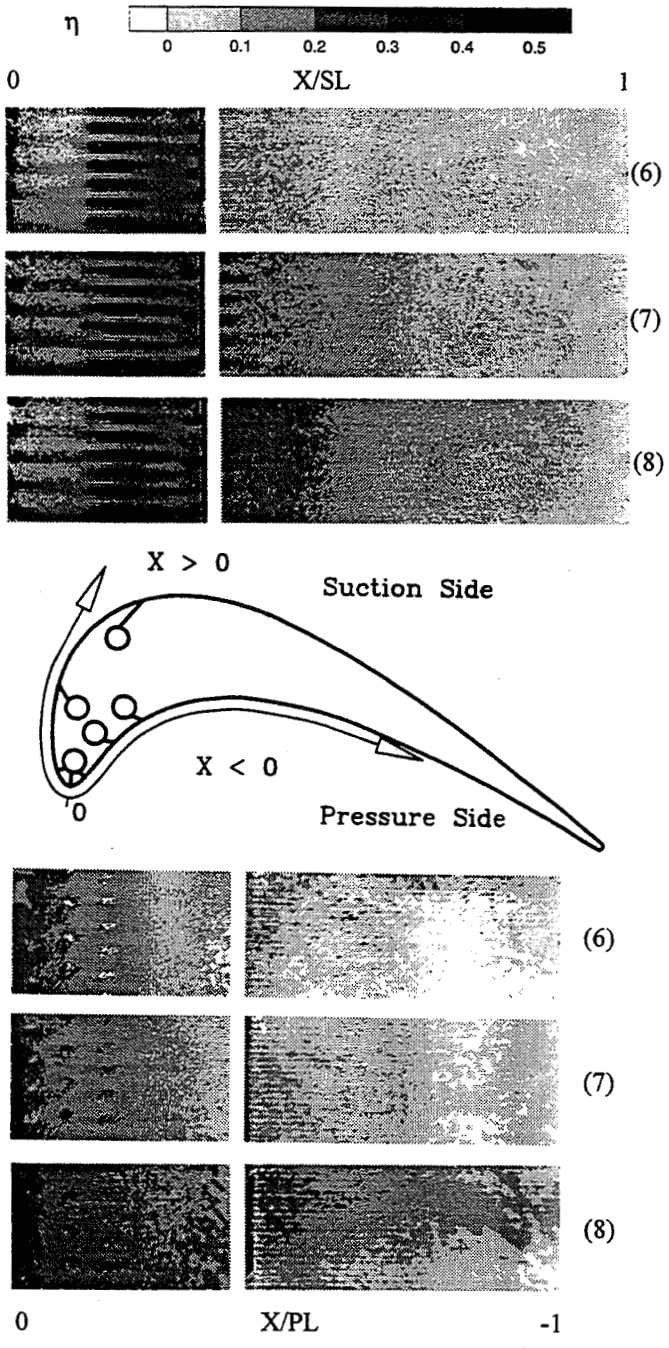
η
0
0.1
0.2
0.3
0.4
0.5
0
X/SL
1
(6)
(7)
(8)
X > 0
Suction Side
X < 0
0
Pressure Side
(6)
(7)
(8)
0
X/PL
-1

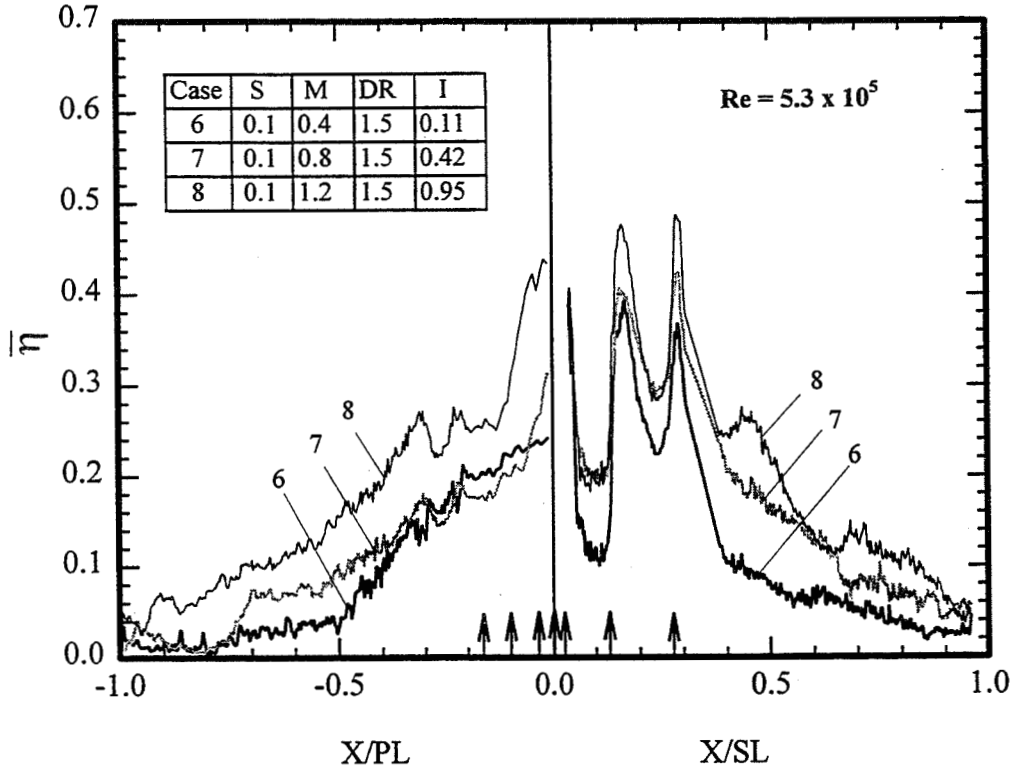

Blowing Ratio Effect on Spanwise-Averaged Film Effectiveness at Given Wake Condition

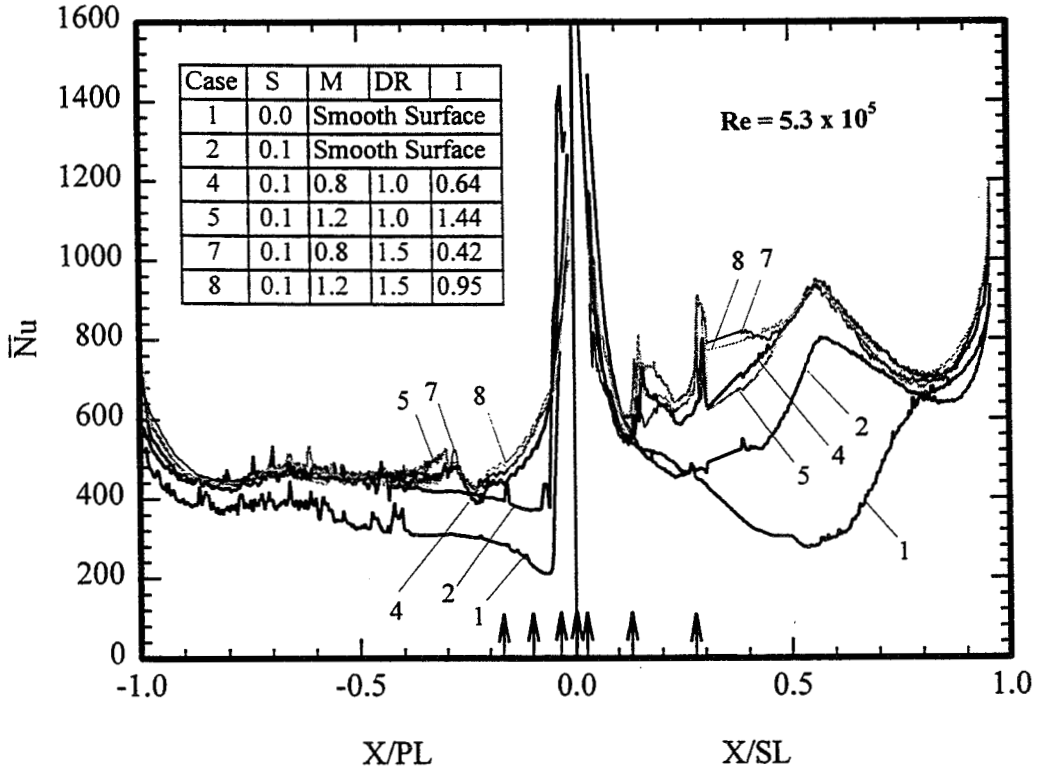

Density Ratio Effect on Spanwise-Averaged Nusselt Number at Given Wake Condition

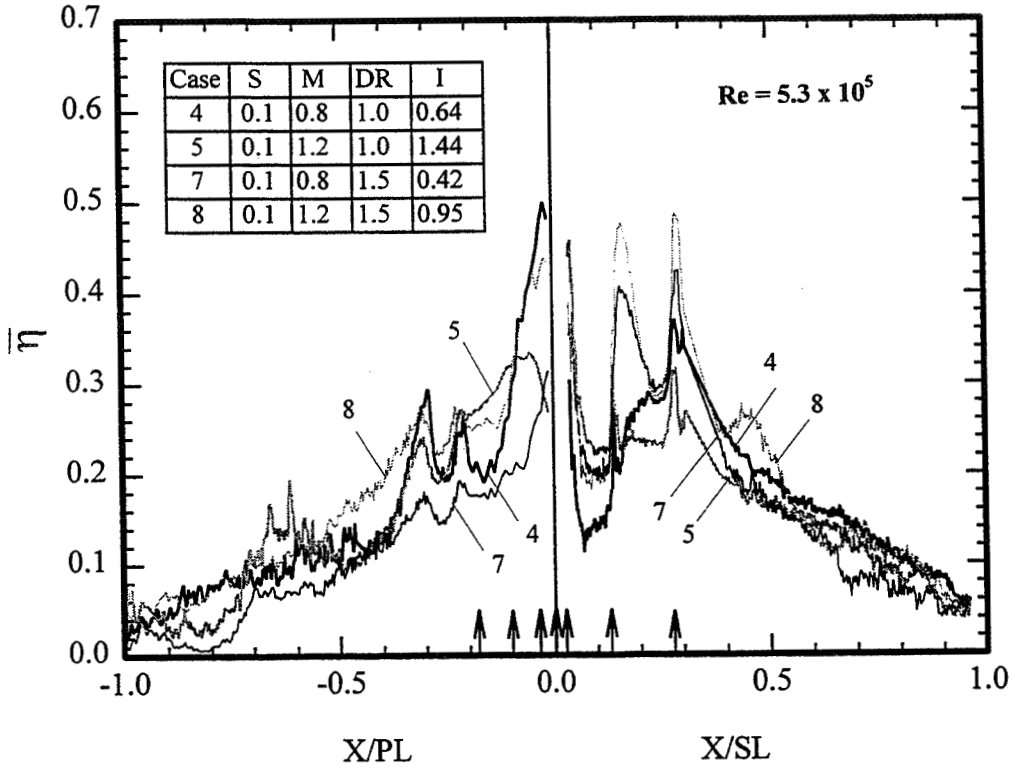

Density Ratio Effect on Spanwise-Averaged Film Effectiveness at Given Wake Condition

Conceptual View of Effect of Unsteady Wake with Trailing Edge Ejection

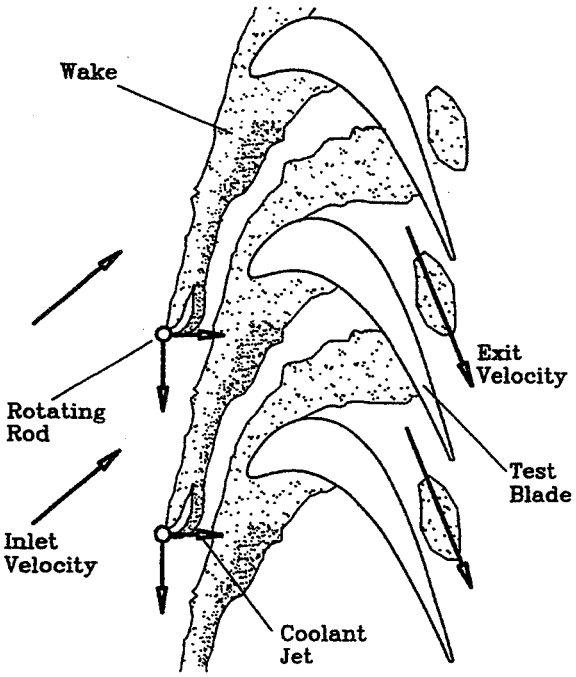

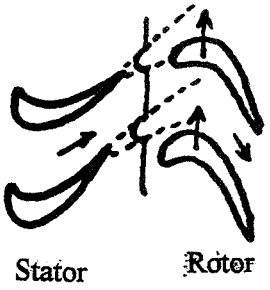

Sketch of Rotating Rod with Ejection Holes

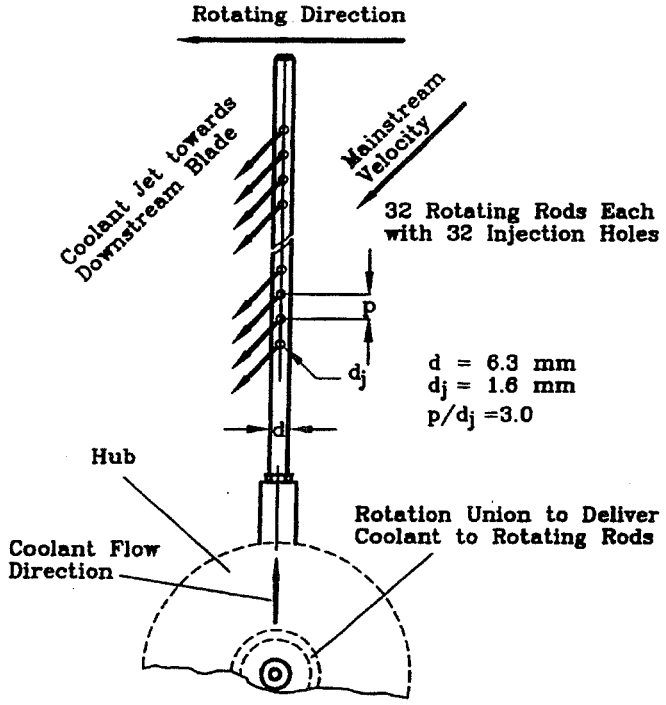

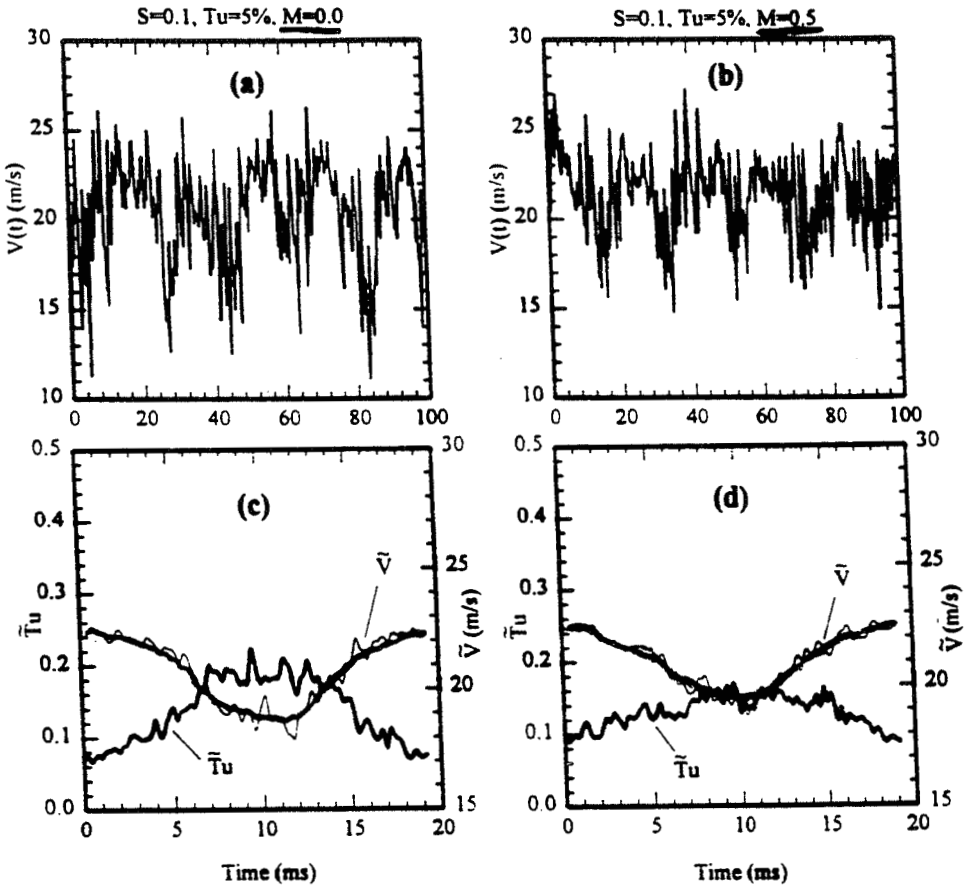

Instantaneous Velocity V(t), Ensemble-Averaged Velocity $\tilde{V}$, and Ensemble-Averaged Turbulence Intensity $\tilde{Tu}$

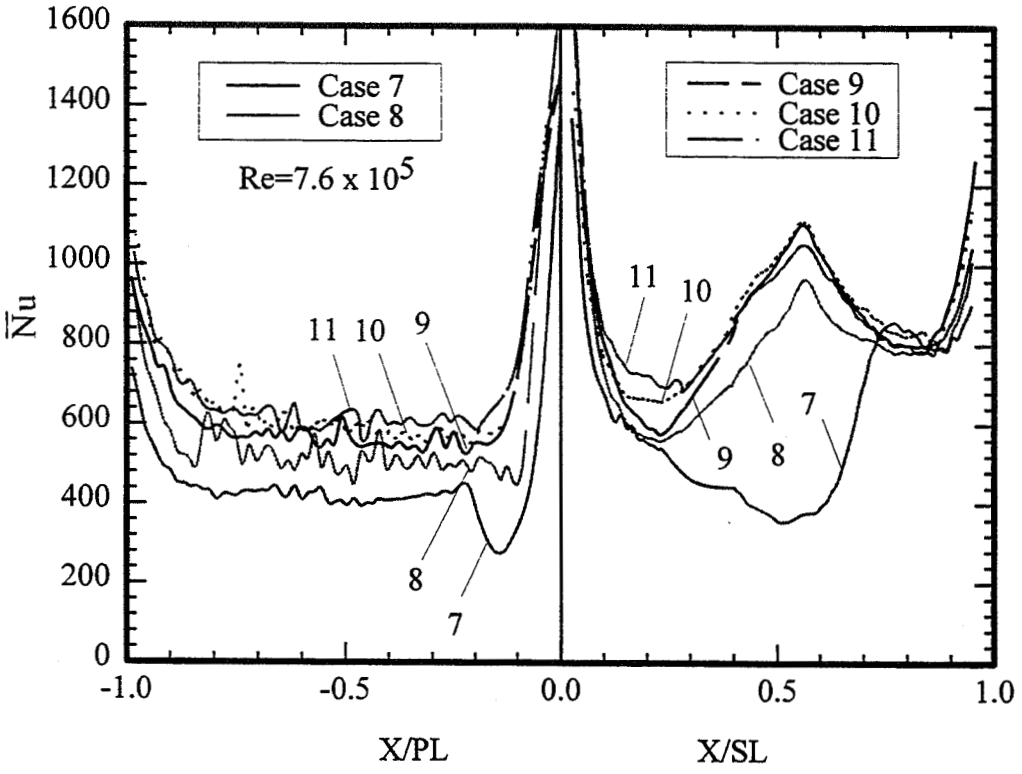

Combined Effect of Unsteady Wake, Free-Stream Turbulence and Coolant Ejection on Spanwise-Averaged Nusselt Number for $Re = 7.6 \times 10^5$

MILESTONE

The effects of upstream flow conditions and film cooling injections have been studied. The tasks for the coming year are:

- **To design and fabricate a test blade with several rows of shaped film holes. These advanced film hole shape designs will be decided after consulting with GE for the optimum shapes.**

- **To measure detailed heat transfer coefficients and film effectiveness for the blade with shaped film cooling holes under the combined effects of free-stream turbulence, unsteady wake and unsteady wake with coolant ejection.**

RESULTS

- **Nusselt numbers increase with an increase in free-stream turbulence level, and also increase with the addition of unsteady wakes. Adding grid-generated turbulence to unsteady wakes further increases Nusselt numbers on the downstream blade surface.**
- **The trailing edge ejection is to increase Nusselt numbers on the front parts of both the blade suction and pressure surfaces.**
- **Film injection promotes earlier laminar to turbulent boundary layer transition on the suction surface and also greatly enhances local Nusselt numbers.**
- **Unsteady wakes slightly enhance Nusselt numbers but significantly reduce film effectiveness on a film-cooled blade compared with a film-cooled blade without unsteady wakes.**
- **An increase in blowing ratio increases Nusselt numbers for both coolants. Film effectiveness is highest at a blowing ratio of 0.8 for air injection and at a blowing ratio of 1.2 for CO_2 injection.**

GROUP DISCUSSION - December 12, 1996

SESSION II. FILM COOLING

Ray Gaugler - Facilitator Nirm Nirmalan - Scribe

We have new detail computational methods. That is not our end product. Vision in my mind is to have something that can be used by designers. Final Goal: we are trying to find out what is going on. NASA Role & Vision.

Terry Simon

Are shaped holes all product specific? Are they better left inside the company?

Ray Gaugler

NASA, under AST, is working with an AlliedSignal vane that has shaped holes.

Terry Simon

Who decided the shape?

Ray Gaugler

AlliedSignal did.

Yong Kim

From A/F contract, the shaped hole. Film cooling (FC) hole shape depends where on the vane it is to be located.

Ray Gaugler

Lots of shaped holes in upcoming papers in the IGTI. It is product specific in the AST program.

Bob Bergholz

AST has both product and non-product specific. Testing will occur and will be shared within the AST community.

Phil Ligrani

Free stream turbulence & wake passing	}	Work is being done.
Shock Interactions		Anything going?
Flow Interactions	}	
Relative Importance		Oxford: Martin Oldfield
Shock Wave	}	We are interested, but it is difficult.
Shaped Holes	}	Need to study with curvature.

Luzeng Zhang

Shock waves. Interested but they are very difficult to study.
Also in shaped holes, you need to consider acceleration and curvature influences.

Ray Gaugler

There are shaped hole data.

J. C. Han

We are trying to find optimum shaped holes. P&W has the most.

Boris Glezer

What are the shape of holes? One good for one airfoil is not the same for another airfoil. Need to address this effect of curvature.

Jim Heidmann

Is it the curvature effect along with the pressure gradient effect?

Ron Bunker

On the AlliedSignal blade the shaped hole looks almost standard. Pretty good!

Younes Makki

P&W (maybe) showed improved effectiveness.

Joel Wagner

Testing in Florida. All kinds of shaped holes. Manufacturing (EDM) is very expensive.

Younes Makki

Recast and EDM are expensive.

Bob Simoneau

Recall of Steve Papell cusp shaped FC holes to produce vorticity. P&W took it and got data. They looked at it and other shaped holes. Looked good.

Ming-King Chyu

Manufacturing is an issue. Variability of shaped holes are vast. Leylak has done some modeling. Need to stay with a hole. Should standardize their shape for study.

Luzeng Zhang

Lot of data in the 70's. Shaped holes 1) reduces the exit blowing ratio (BR), 2) improves spanwise spreadability, and 3) improves exit vorticity and therefore the stickability. Our test shows no difference between shaped and round holes. At high BR there is a difference.

Bob Simoneau

[To Terry Simon] Are you planning to look at FC inlet air at 90 degrees to the hole?

Terry Simon

Yes, we have that test section installed now. The flow startes to turn streamwise even before it leaves the FC hole. Taking data in the hole is hard and using a hot wire is uncertain. May need to use LDA. We would like to work on compound and shaped holes.

Yong Kim

[To Terry Simon] Flow was measured but pressure drop (CD) was not.

Terry Simon

We did not measure pressure drop. We metered the flow. Velocity is not too high.
[To Karen Thole] You were involved in an experiment where you had a recirculating flow?

Karen Thole

CDs were different. Tests were done in Germany. Hole shape does not help diffusing very much. Inlet direction does matter in shaped holes (CFD).

Terry Simon

We should do CD.

Yong Kim

Shaped holes are valuable.

Karen Thole

Measured static pressure around the hole: there is variation.

Terry Simon

Thanks.

J. C. Han

Can anyone comment on how do you compare shaped and compound holes?

Luzeng Zhang

Bogard has a paper on comparing holes.

Karen Thole

Bogard did compound hole.

Khairul Zaman

Measuring pressure drop in the tunnel is too difficult because it is too small. Need to use an orifice to meter the flow.

Terry Simon

That is what we do. But I need to measure static pressure for CD. Measure from inlet total (plenum) pressure to external static pressure.

Chi-Rong Wang

Upstream recirculation effects on incoming flow.

J. C. Han

We have some data. No data to compare with. Could be a problem.

Ming-King Chyu

Liquid crystal heat transfer is not good near film cooling holes: 1D conduction does not work. Check on data reduction method.

Joel Wagner

3D conduction is going on in and around the film cooling hole. No work done yet.

Luzeng Zhang

Goldstein has a paper. 1993 Turbine Conference (ASME , Orlando)?

Ming-King Chyu

Liquid crystal is a work horse. Napthalene will change shape.

J. C. Han

1D conducton will take care of it.

Simon

We did not see recirculation zone with a 30 degree angled hole. Acharya was able to see it because it was a 90 degree angled hole.

Unknown

Literature on jets and nozzles. There are shapes. Any consideration of this.

Khairul Zaman

Jets spread but film cooling holes should not.

Simon

Forrest Ames showed mixing improved the sticking effect of film cooling flow

Forrest Ames

No.

Yong Kim

Liquid crystal heat transfer: if temp. is periodic, the solution is wrong. I had a problem with it.

Satish Ramadhyani

Plenums in experiments are smooth. Will it have trips and augmentors in it?

Ray Gaugler

Any answers?

Bob Bergholz

Maybe.

Sai Lau

Film cooling, rotation?

Luzeng Zhang

Mitsubishi started work.

Ed North

Lots of problems with it (rotation data). Rotation data is vague and difficult, rare.

Sai Lau

What are general shapes? Flat plate? Rotation and buoyancy effects?

Boris Glezer

Avoid film cooling in rotating parts.

Joel Wagner

We studied with SF_6. Blade, Mike Blair: density, buoyancy effects. On pressure side, strong effects. Suction side do not remember. Had a single hole.

Robert Norton

In a low speed rig, is it applicable to a real engine, like A/F, MIT or Mike Dunn?

Joel Wagner

Dust conditions give good flow visualization.

Satish Ramadhyani

What about studying physics. A rotating cone: Coriolis, buoyancy? Will that help?

Ray Gaugler

[To Vijay Garg] Can you simulate density difference?

Vijay Garg

Can put in temperature to simulate density difference. ACE rotor: some holes were choked. When CFD group looks at data, lots of questions. For 2 equation model: Ali Ameri does not know what is coming out of holes.

Rob Norton

Why not do a parametric study to see the effects.

Vijay Garg

It only makes a difference very near the holes: have some effects (Tu & Scale), but there is no data very near the holes.

Bob Simoneau

Comments about Satish Ramadhyani's cone idea: will people find it useful? Is it an academic exam?

Joel Wagner

That may be the way to get the effect of curvature.

Boris Glezer

Maybe sometimes.

Ray Gaugler

Adjourn.

Session III

Coolant Flow Integration & Optimization

MULTIDISCIPLINARY OPTIMIZATION OF COOLED TURBINE DESIGN USING 3-D CFD ANALYSIS*

Aditi Chattopdhyay, John N. Rajadas,
and Shashishekara Talya S.
Arizona State University
Tempe, Arizona

OBJECTIVES

Minimize turbine blade temperature and optimize coolant flow management using Multiobjective, Multidisciplinary Optimization Procedure

Design parameters used in optimization

* **Blade shape**
* **Coolant path geometry**
* **Film cooling parameters**

DESIGN VARIABLES

Blade chord length

Surface geometry parameters

- **Number of splines**
- **Spline parameters**

Coolant path configuration

- **Coolant hole geometry parameters**

* Presented at the conference by Yong Kim, AlliedSignal Aerospace.

DESIGN VARIABLES (contd)

Film cooling parameters

- Position of holes on blade surface
- Shape and size of holes
- Angle(s) of injection
- Injection rate

OPTIMIZATION FORMULATION

Minimize

Maximum blade temperature (T_{max})

Subject to constraints on

Aerodynamic performance

Average temperature ($T_{ave} \leq T_{all}$)

Blade thickness

Trailing edge angle

Throat width

BLADE MODEL

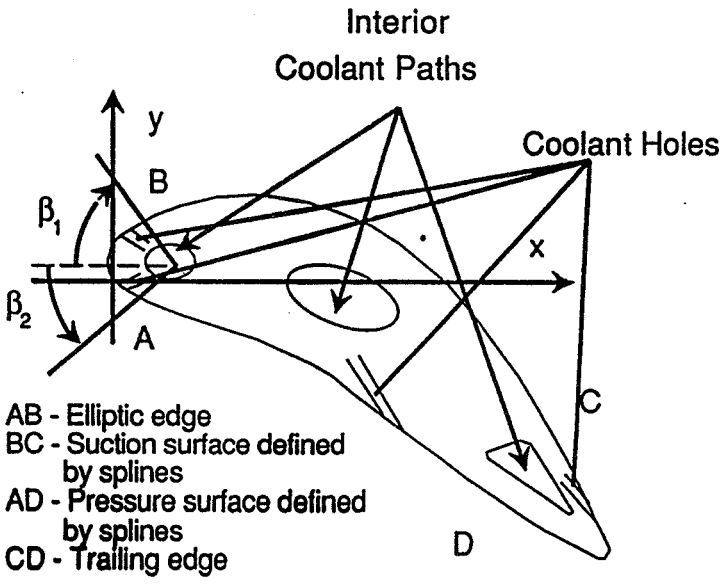

ANALYSIS

* **CFD for flow field**
  - **RVC3D / RVCQ3D (NASA Lewis Research Center)**
* **Heat transfer**
  - **Finite element analysis in blade interior (ASU)**
* **Multiobjective, Multidisciplinary Optimization Procedure (ASU)**
  - **Kreisselmeier - Steinhauser (K-S) function approach**
  - **Multilevel format**

CFD/EXPERIMENTS TO OPTIMIZE FILM-COOLING HOLE SHAPE DESIGN TOOLS

Yong Kim
AlliedSignal Aerospace
Phoenix, Arizona

Advanced Subsonic Technology
Area of Interest: 7 Affordable Turbine Cooling Technology

Goal:

- Reduce DOC by 3 to 5% by Increased TRIT of 100 to 200 Degrees F Without Excessive Increase in Cooling Flow

Approach:

- Produce Benchmark 3-D Unsteady Film Cooling Heat Transfer Measurements
- Validate 3-D CFD Models to Benchmark Data. Increase Film Cooling Effectiveness with Advanced Hole Shape
- Initiate Multidisciplinary Optimization (MDO) Applicable to Airfoil Cooling

Milestones:

- Complete Benchmark Measurements 3Q99
- Complete Film Cooling 3-D CFD Model Validation 4Q99
- Complete Initial MDO of Turbine Airfoils 4Q99

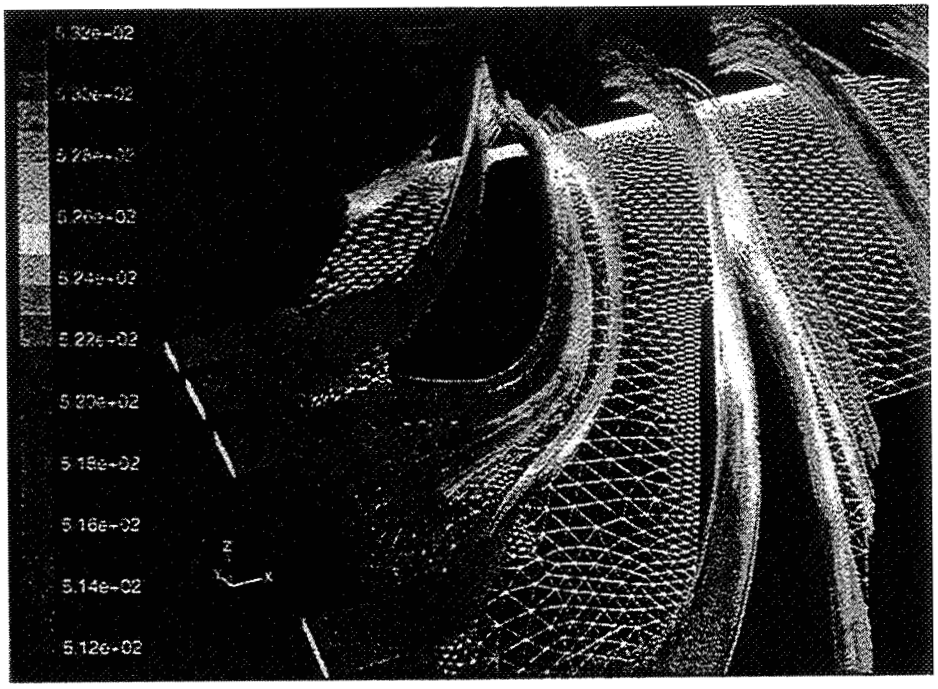

NASA AST Area of Interest 7 - Program Block Background

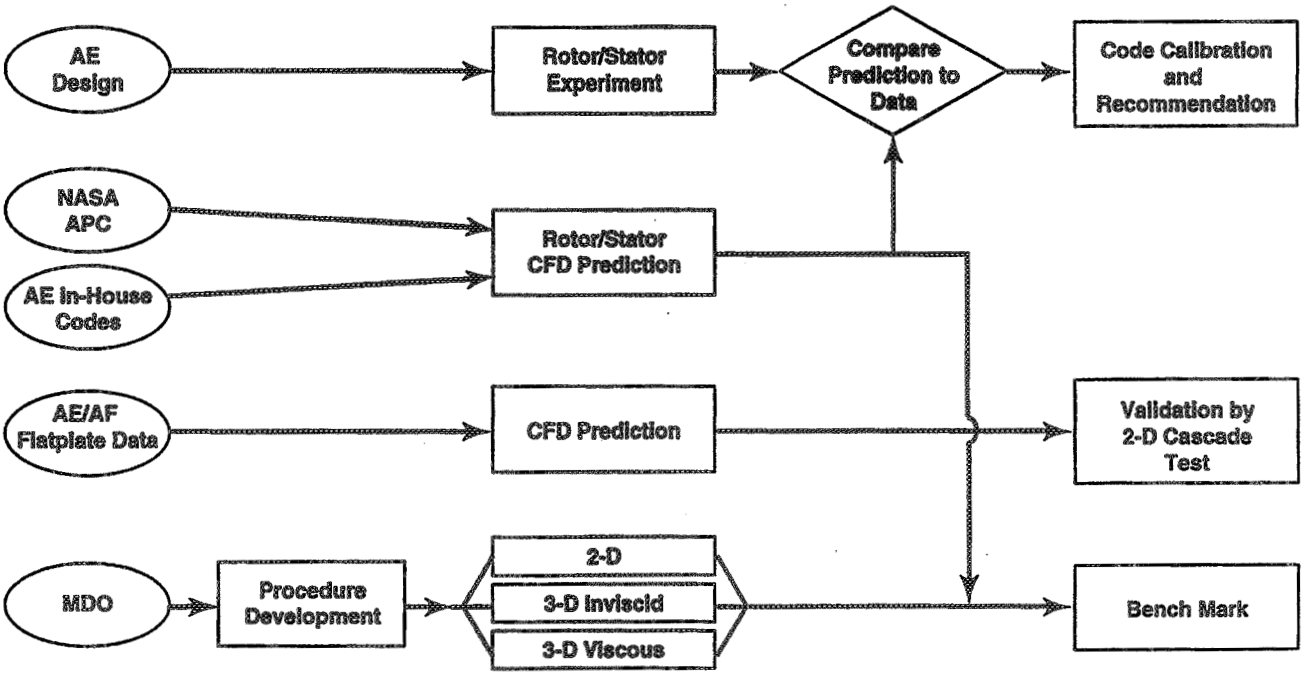

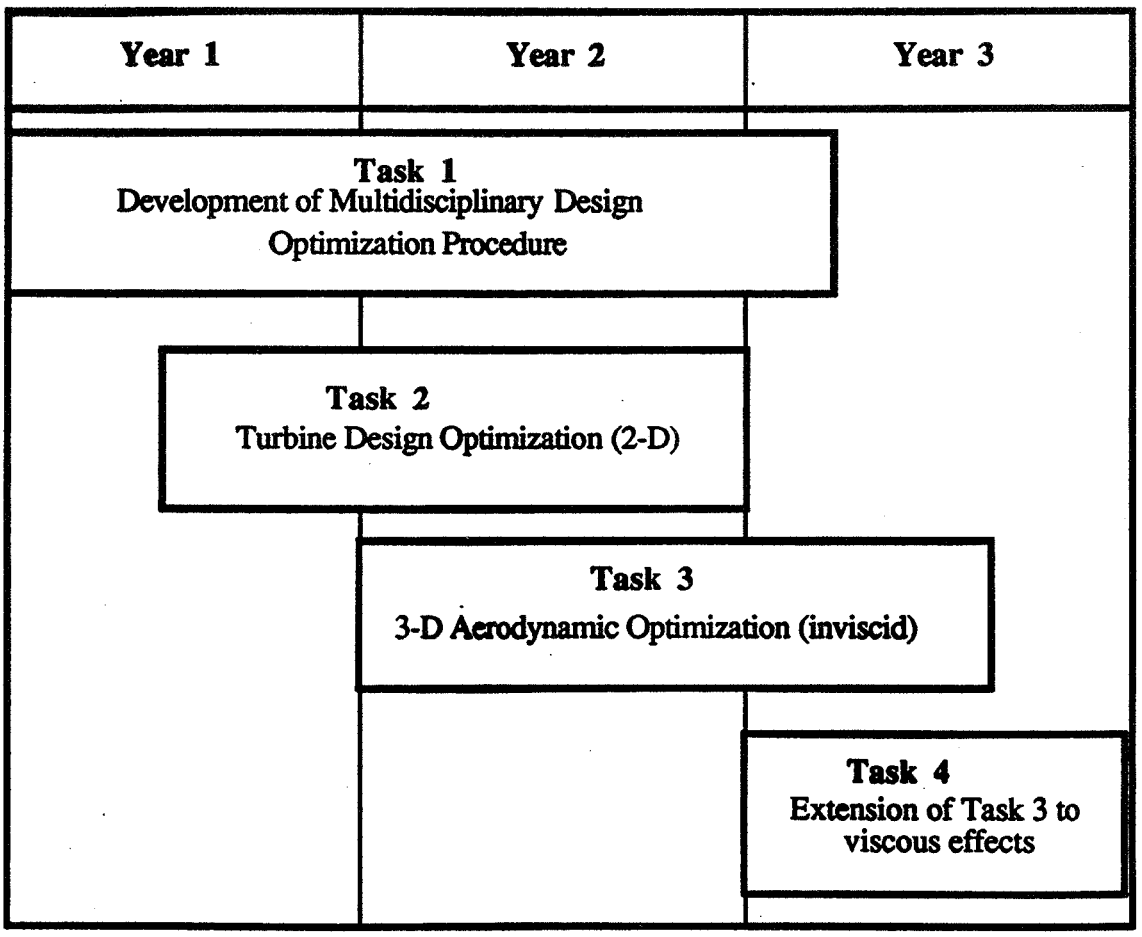

CFD AS A FILM-COOLING DESIGN TOOL

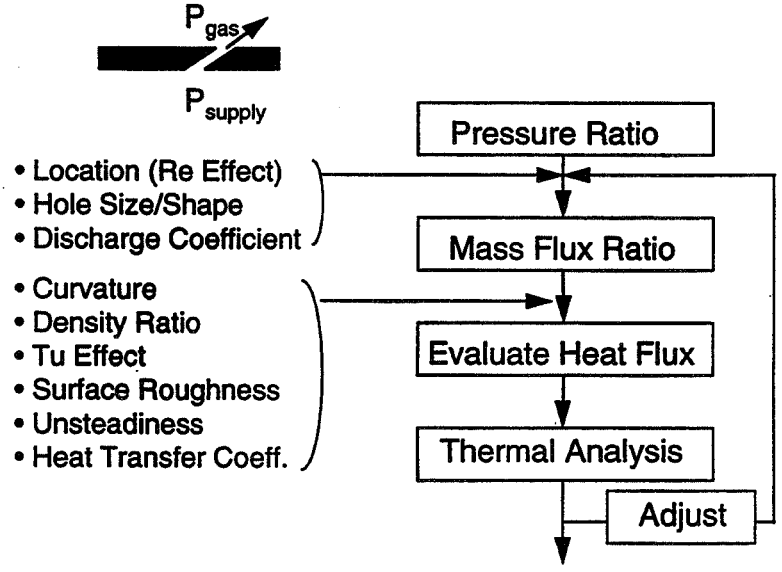

APPROACH

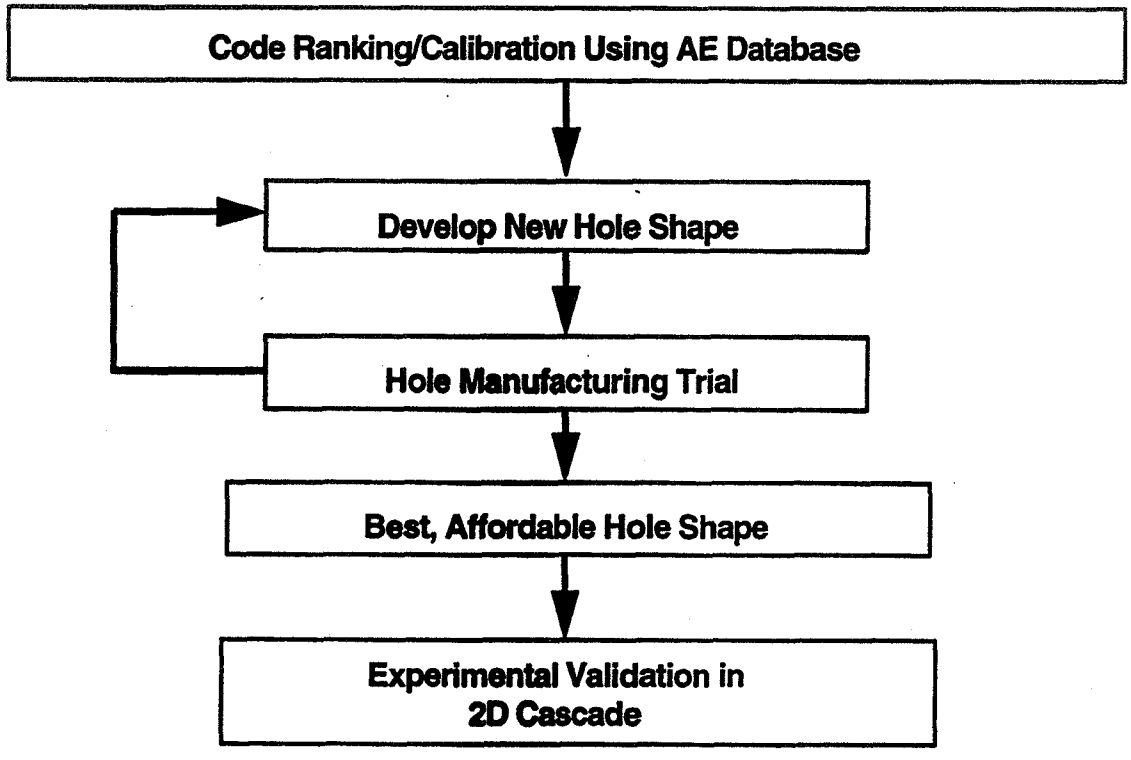

CODE RANKING/CALIBRATION PROCESS

Code Selection Based on:

- Availability
- Reliability
- Efficiency

Turbulence Model/Near-wall Treatment Selection Based on:

- Available Database

Result:

Fluent/uns Using RNG k-ε with Two-layer (Low-Re) Near-wall Model and Tetrahedral Cells

COMPUTATIONAL DOMAIN

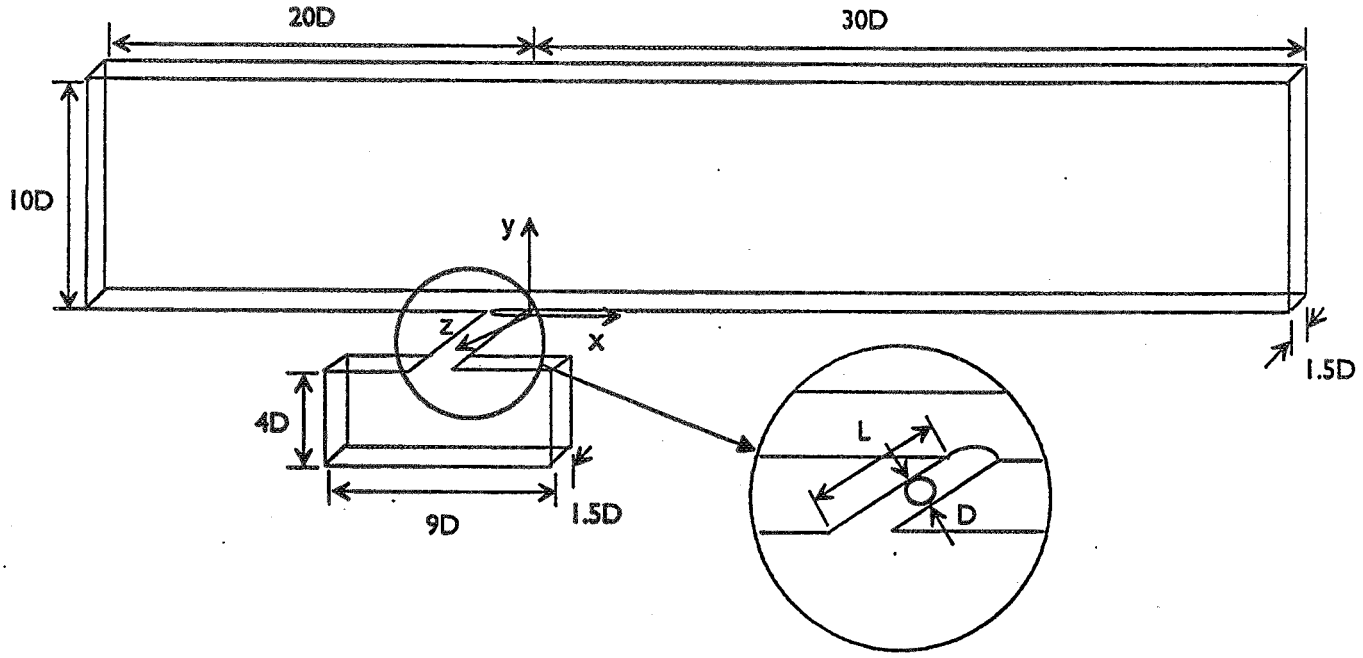

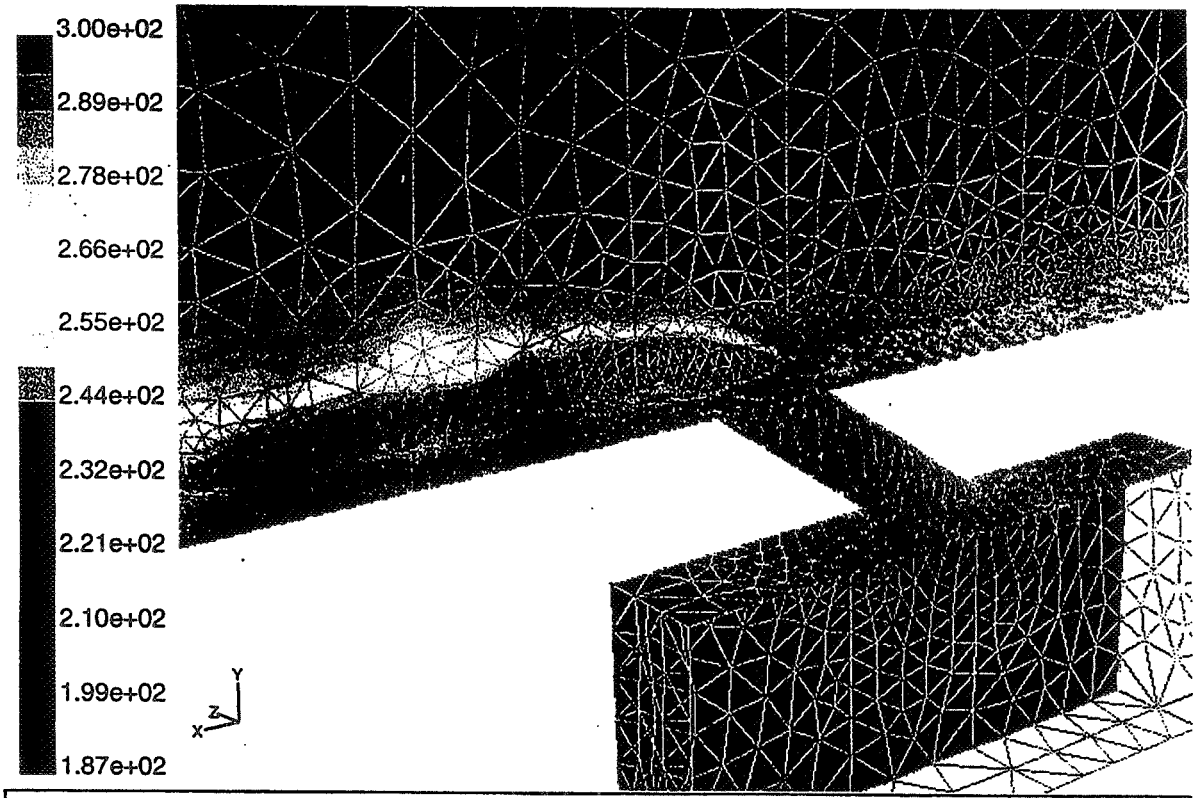

Contours of Total Temperature (k)

Fluent/UNS 4.1 (3d, rngke)
Mon Nov 04 1996
Fluent Inc.

COMPARISON WITH EXPERIMENTAL DATA (M=0.6 CASE)

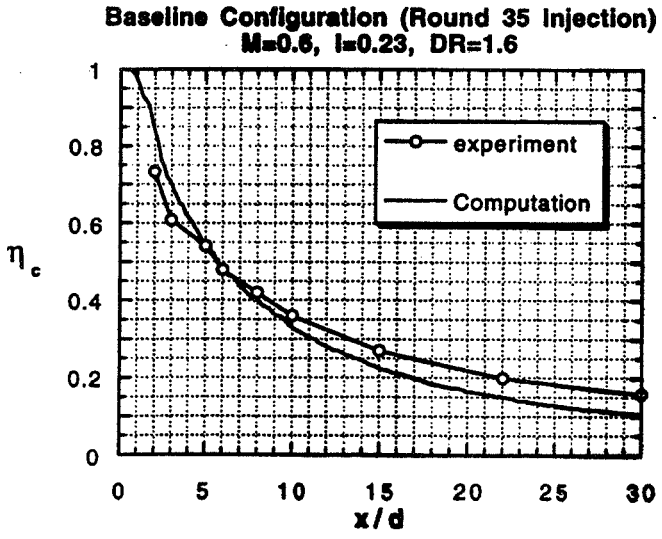

Centerline Effectiveness

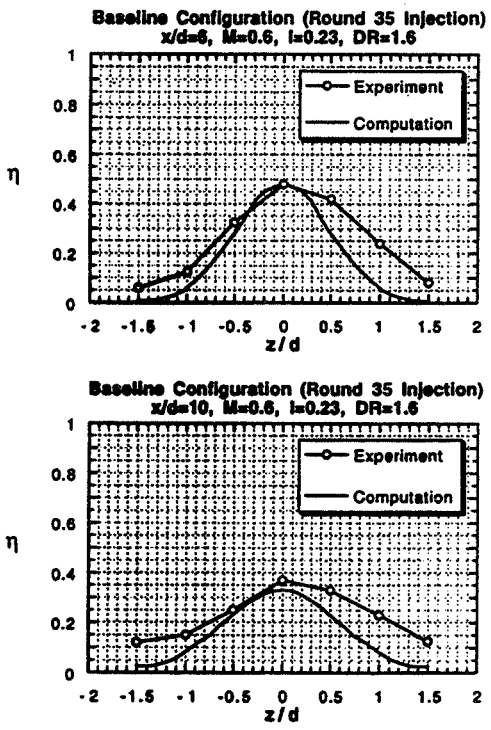

Local Effectiveness

COMPARISON WITH EXPERIMENTAL DATA (M=1.0 CASE)

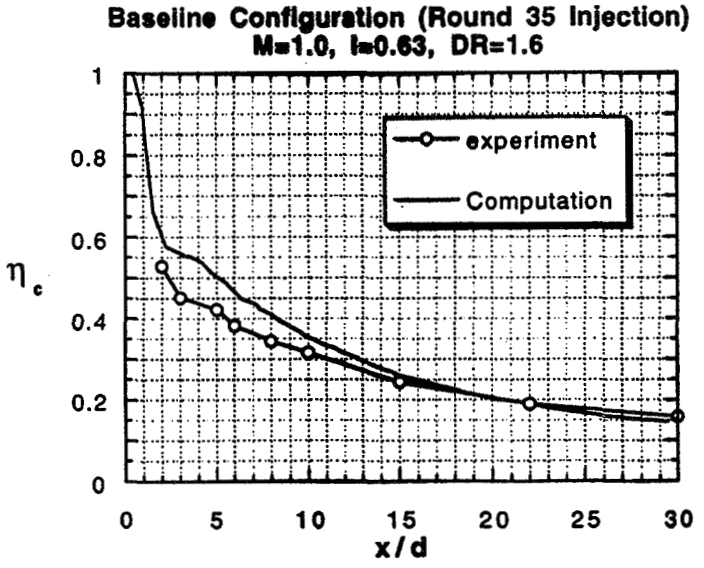

Centerline Effectiveness

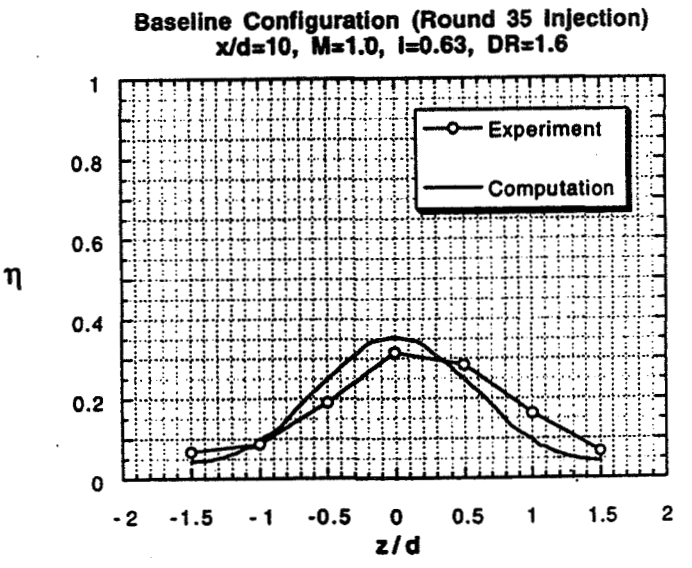

Local Effectiveness

COMPARISON BETWEEN ROUND AND NEW SHAPE HOLE RESULTS

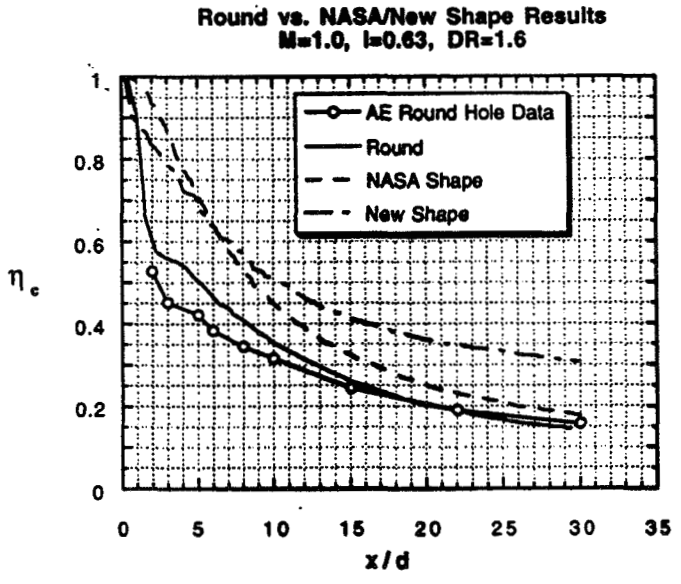

Centerline Effectiveness

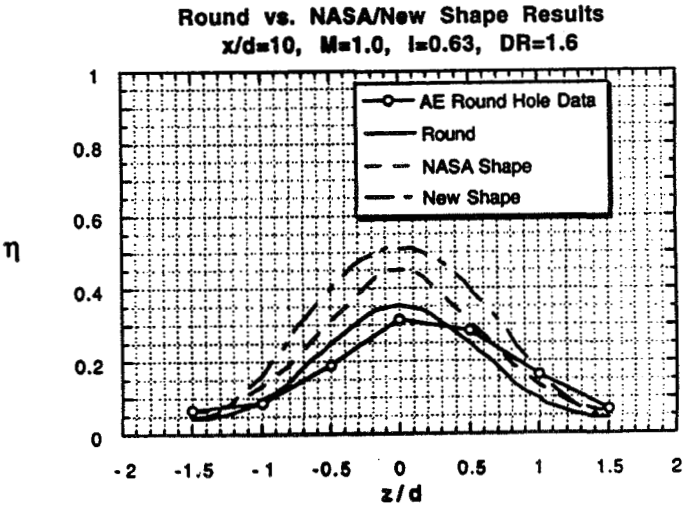

Local Effectiveness

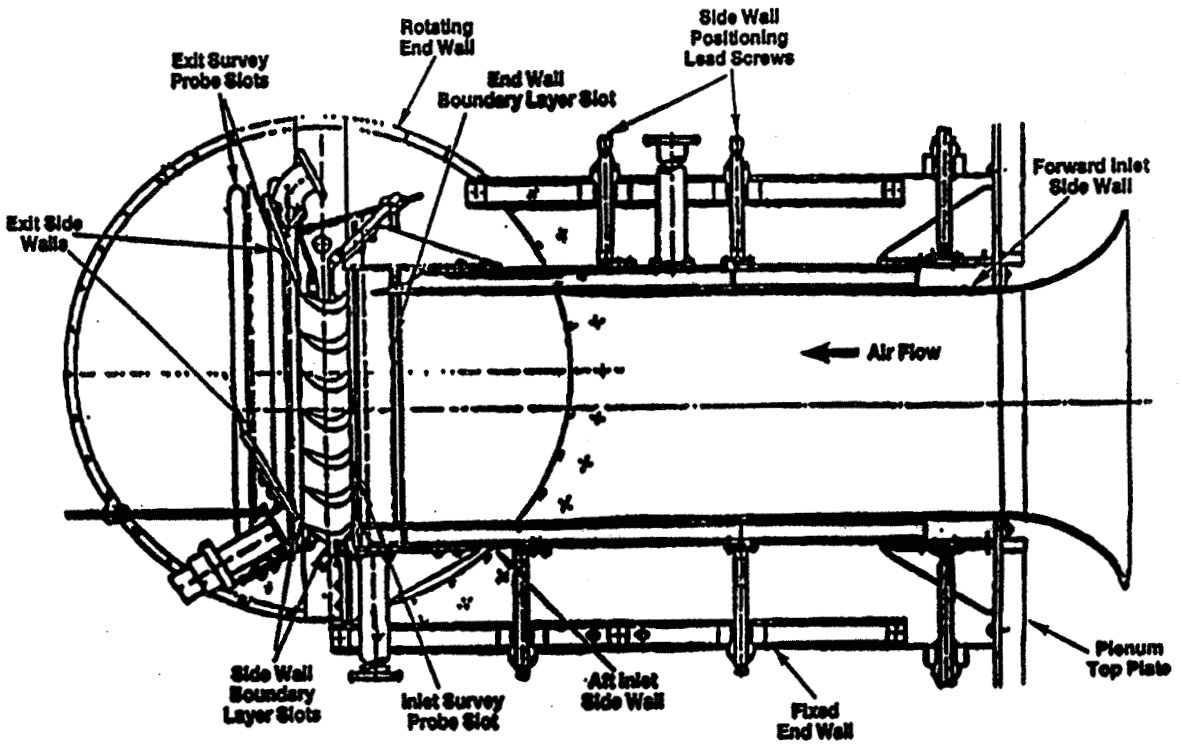

Linear Cascade Rig

TRACER-GAS TECHNIQUE TO MEASURE LOCAL FILM COOLING EFFECTIVENESS

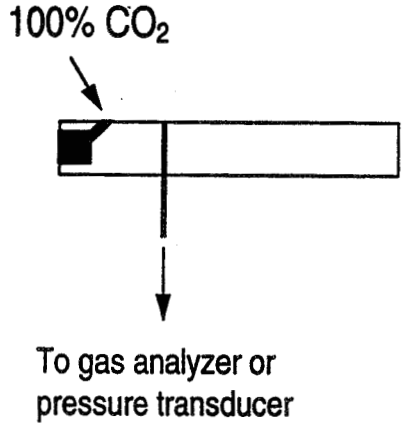

- Relies on heat-mass transfer analogy
- Heavy gas to match density ratio(up to1.5)
- Sampling taps can also be used as press. taps

CLOSURE

INTERIM RESULTS

- New hole shape developed which meets program goal of increasing TRIT by 100 - 200 °F
- 3-D CFD is an effective design tool for film cooling prediction

FUTURE MILESTONES

- Develop affordable manufacturing method
- Experimental validation of new hole shape

TURBINE AIRFOIL FILM COOLING—DESIGN INTEGRATION

Robert Bergholz
General Electric Aircraft Engines
Cincinnati, Ohio

AGENDA

- **Turbine Airfoil Film Cooling - Design Integration**
- **GEAE Single-Passage Cascade Facility**
- **GE CR&D Transient Cascade Facility**
- **Turbine Airfoil Film Cooling Design Issues**

Turbine Airfoil Film Cooling - Design Integration

Objectives

- Maximize coolant heat capacity utilization.
- Focus on overall heat flux management via film and thermal barrier technologies to control structural thermal gradients.
- Optimize overall film effectiveness distribution.
- Customize film hole geometries for improved effectiveness with lower blowing ratios.

Approach

- Acquire film effectiveness and external heat transfer coefficient data on promising film cooling configurations.
- Apply optimization and computational DOE methods to quantify and rank design payoffs.
- Use unstructured grid CFD tools to predict film hole and external flowfields, local heat transfer effects, and customized film hole geometries.

Results

- GEAE Single-Passage Cascade
  - Gas concentration / mass-transfer method.
  - η_f results for several airfoil geometries.
- GE CR&D Transient Cascade
  - Both η_f and h measurement capability.
  - Data acquired for full-scale vane geometries.
- GE CR&D Water Tunnel
  - PLIF measurement technique.
  - Full-coverage, discrete-hole film cooling applicable to combustor liners.

Milestones

- **1996**
  - Single-Passage Cascade
    - Engine airfoil support tests.
  - Transient Cascade
    - GEAE / CR&D IR&D film tests.
- **1997 - 99**
  - Single-Passage Cascade
    - Engine blade / vane, showerhead, ...
  - Transient Cascade
    - AST film tests.

GEAE Single-Passage Cascade

Fred Buck (GE Aircraft Engines)

BACKGROUND -- FILM COOLING TESTS AT GEAE

- **Past History**
  - The current airfoil film cooling data base at GE Aircraft Engines was obtained using full annular cascades, sector cascades or 2-D linear cascades run at different mainstream and coolant temperatures.
  - For large aircraft engine turbine airfoils (e.g., GE90, CF6-80 and CFM56), these tests require large amounts of airflow (e.g., for an annular cascade ~ 40 kg/sec) and significant manpower and financial resources.
- **Current Reality**
  - Resource reductions mandated by the current business climate have reduced the available opportunities to run such test programs.

A more economical and efficient test method was required to continue to obtain the required η design data base.

SINGLE PASSAGE RIG CONCEPT

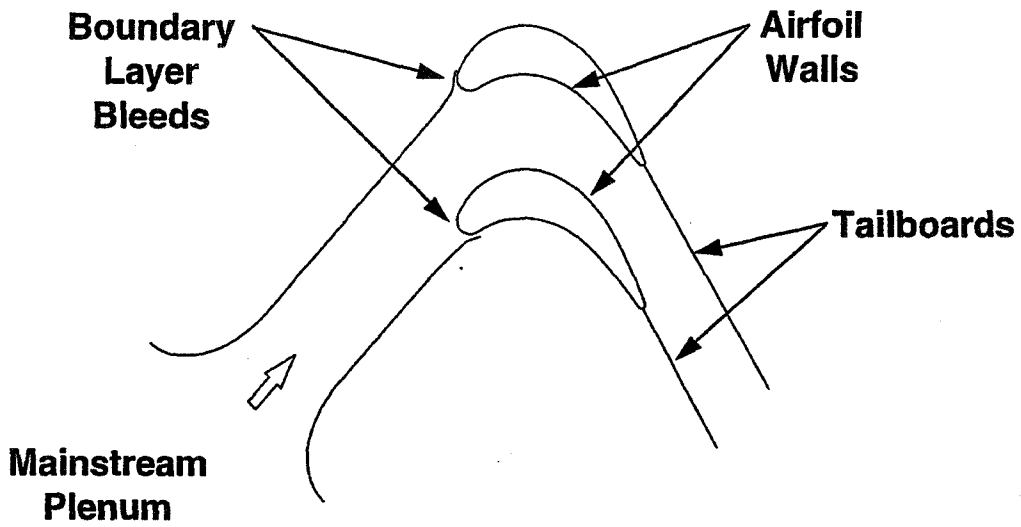

Modelling a single passage would significantly reduce the mainstream flow required to match engine Mach and Reynolds numbers.

FILM COOLING EFFECTIVENESS MEASUREMENTS MADE USING MASS TRANSFER/GAS ANALYSIS

- **For thermal film cooling effectiveness measurements:**
  - **Tests are run with mainstream and coolant flows at different temperatures. Mainstream and/or coolant temperature should be set to match engine coolant-to-mainstream density ratio.**

$$T_g/T_{cool} = \rho_{cool}/\rho_g$$

  - **Effectiveness measurements made from wall and flow temperatures using**

$$\eta = (T_{rec} - T_{aw,c})/(T_{rec} - T_{cool})$$

Wall temperatures in most cases will be measured using embedded thermocouples.

  - **Corrections may be required to account for nonadiabatic wall conditions (e.g., conduction within the cooled wall and/or radiation).**

MASS TRANSFER/GAS ANALYSIS TECHNIQUE (CONTINUED)

- **For gas analysis film cooling effectiveness measurements:**
  - **Tests are run using a foreign gas or a mixture of gases as the coolant. The engine coolant-to-mainstream density ratio should be matched.**
  - **Film cooling effectiveness measurements are made using foreign gas concentrations measured at the wall**

$$\eta = (C_g - C_{wall})/(C_g - C_{cool})$$

  - **In this test, the wall gas concentrations were measured using static pressure taps installed downstream of the film injection site. Multiple spanwise tap locations were required to determine the average spanwise film cooling effectiveness.**
  - **The rate at which the wall samples are extracted should be controlled.**

Film cooling effectiveness measurements made using gas analysis would permit testing with ambient mainstream flow.

SCHEMATIC OF TEST

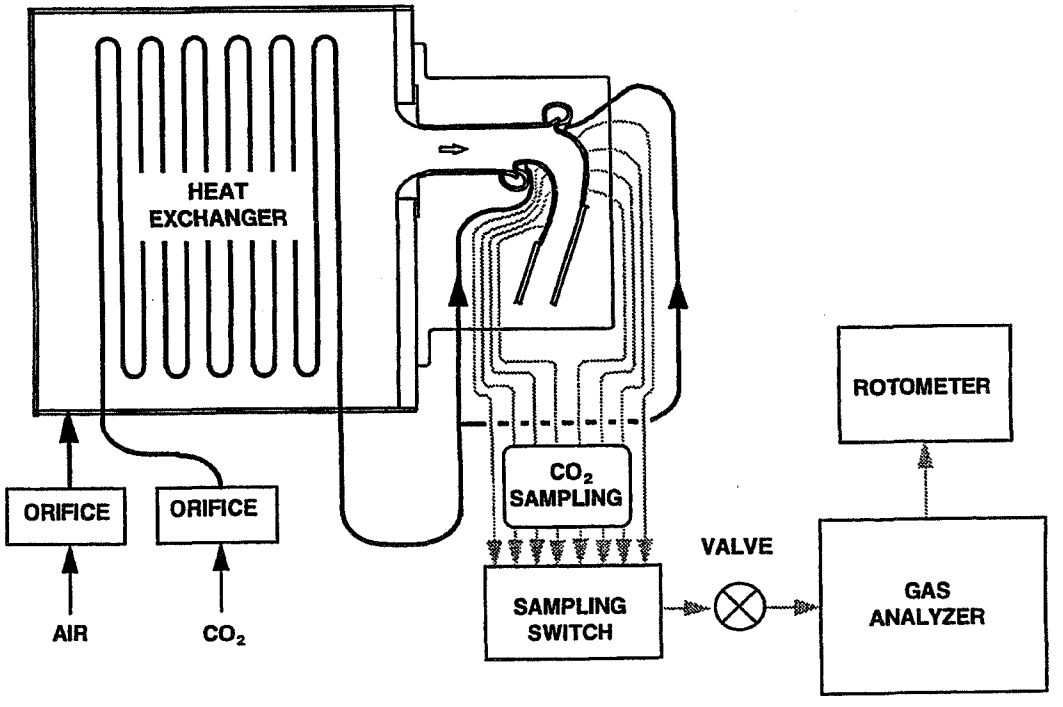

TEST MODEL CROSS-SECTION

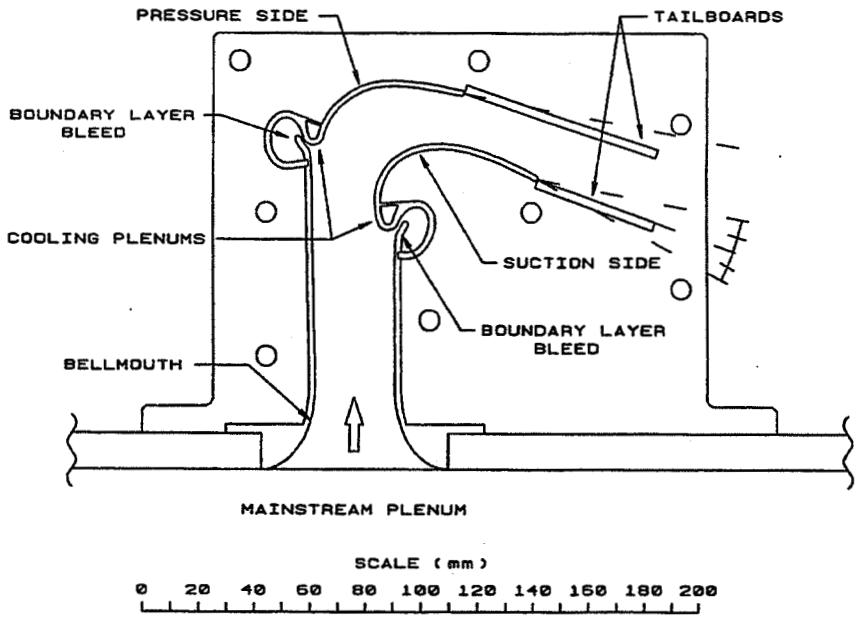

The test model consisted of 2-D components which were sandwiched between two slotted endwalls.

FILM HOLE GEOMETRY AND TEST MODEL INSTRUMENTATION

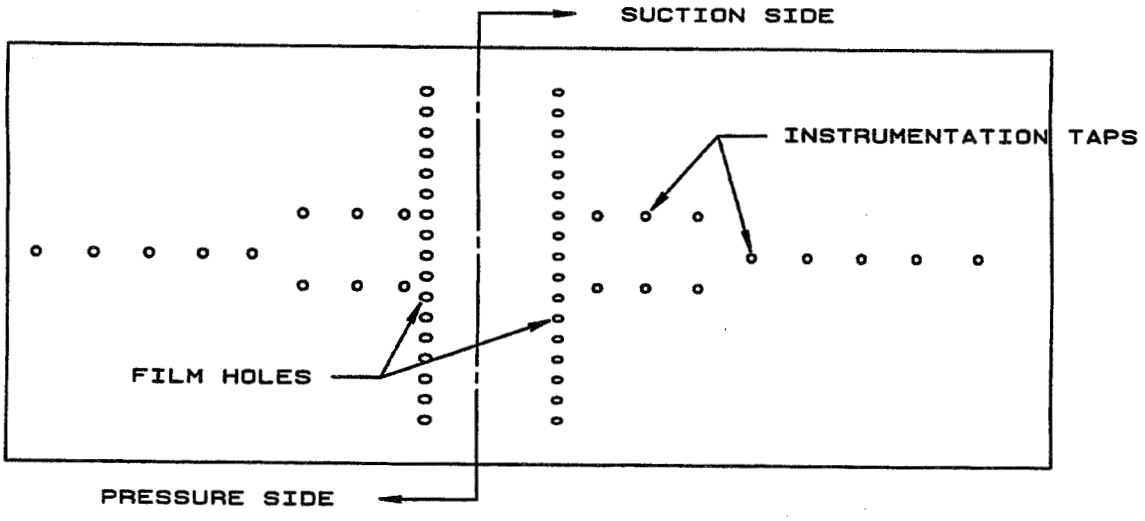

LOCAL PRESSURE DISTRIBUTION -- COMPARISON WITH DESIGN INTENT

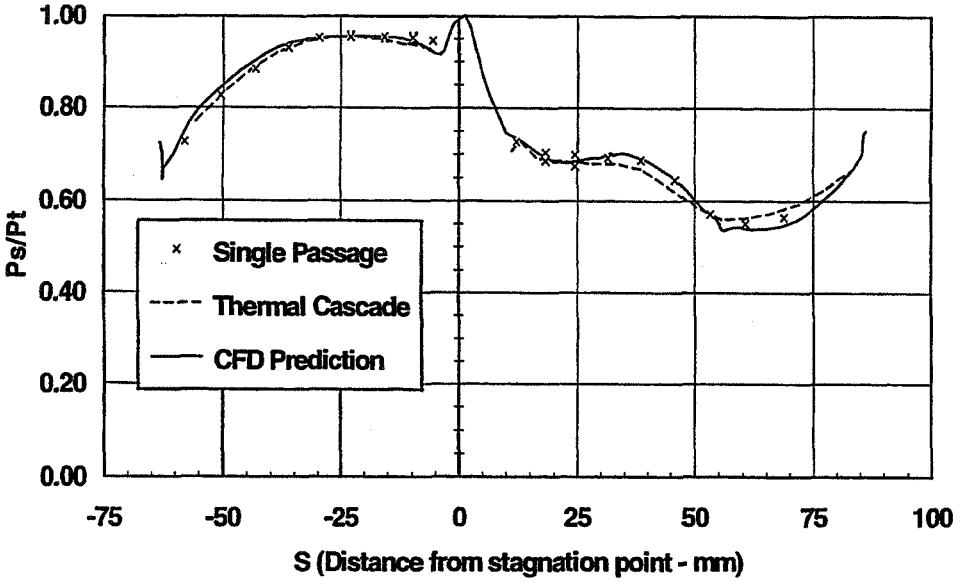

The cascade pressure distribution was matched over the entire single passage datum surface.

LOCAL RESULTS - PRESSURE SIDE m ~ 1.0

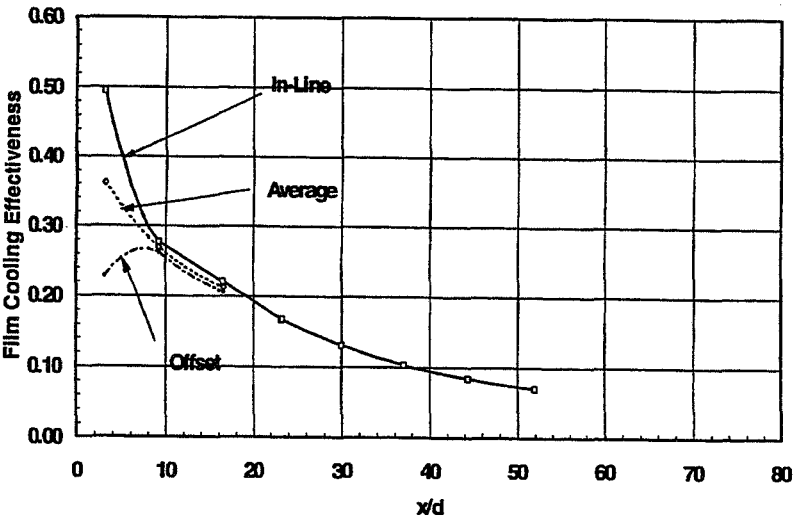

On pressure side for x/d > 10, In-Line and Offset η were approximately equal.

LOCAL RESULTS - SUCTION SIDE
m ~ 1.0

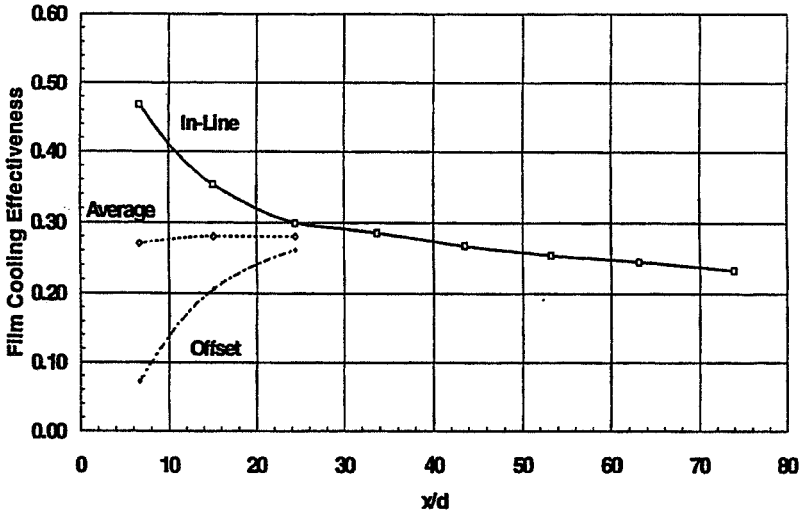

On suction side at x/d ~ 25, In-Line and Offset η still were measurably different.

GE CR&D Transient Cascade

Ron Bunker (GE CR&D)

Objective

- Measure Both Heat Transfer Coefficients and Film Cooling Effectiveness Values in Linear Airfoil Cascades Under Pressure and Temperature Conditions which Simulate Engine Non-Dimensional Parameters (Reynolds Numbers, Mach Numbers, Coolant-to-Gas Density Ratios, Inlet Turbulence Intensities)
- Build and Operate a Transient Test Facility Similar to the One Used by Lander, Fish and Suo (J. Aircraft, 1972)

Transient Test Methodology

- Adiabatic Film Effectiveness
- $$\frac{T_{rec} - T_{aw}}{T_{rec} - T_{co}}$$
- Heat Transfer Rate (Lander, Fish, Suo, 1972)
- $$q_c = h_f(T_{aw} - T_w) = \rho l c_p \frac{dT_w}{dt}$$

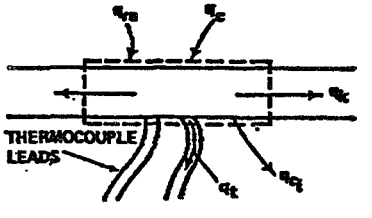

Transient Test Methodology

- Curve Fitted Equation from Measured Temperatures and Times

$$\frac{T_w(\text{steadystate}) - T_w(t)}{T_w(\text{steadystate}) - T_w(t=0)} = e^{-\frac{h_f t}{\rho l c_p}}$$

Schematic of Test Facility

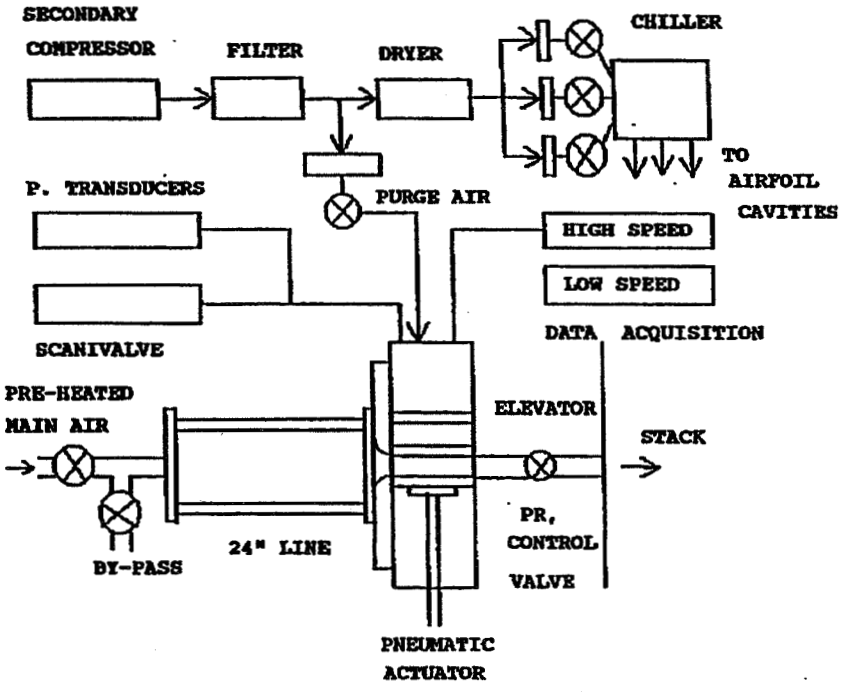

Schematic of Cascade Test Section

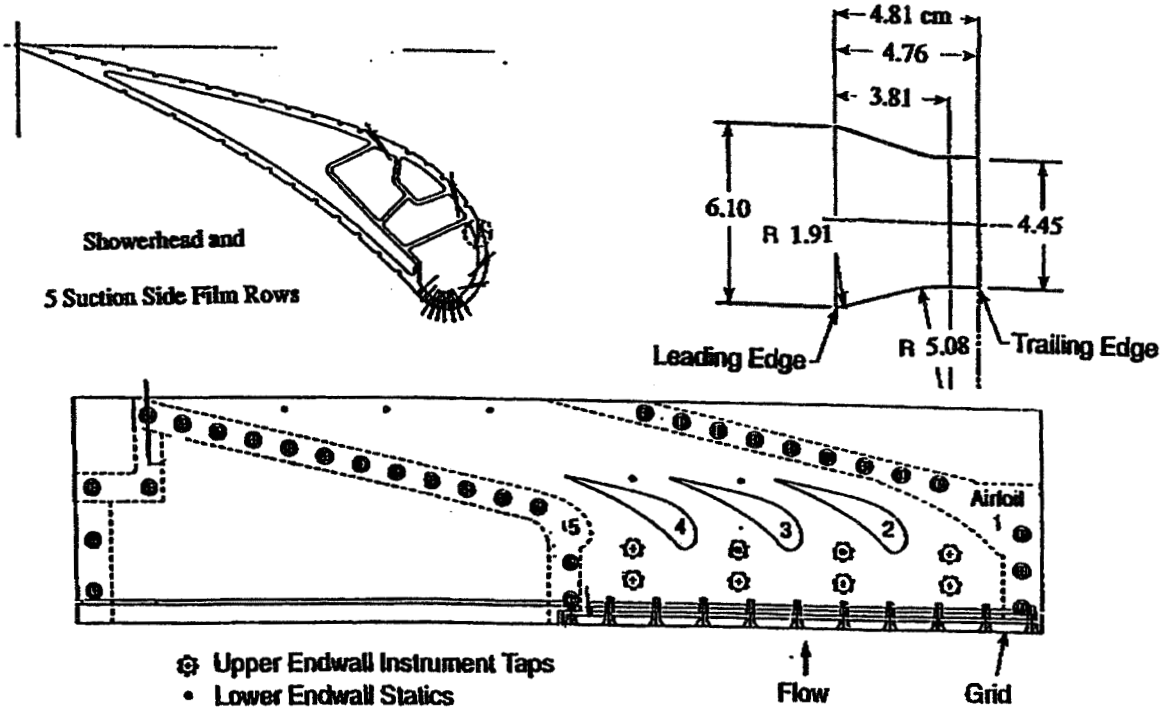

Airfoil Temperature and Film Cooling Effectiveness

Reynolds Number=517,000 (Based on Inlet conditions and Chord Length)

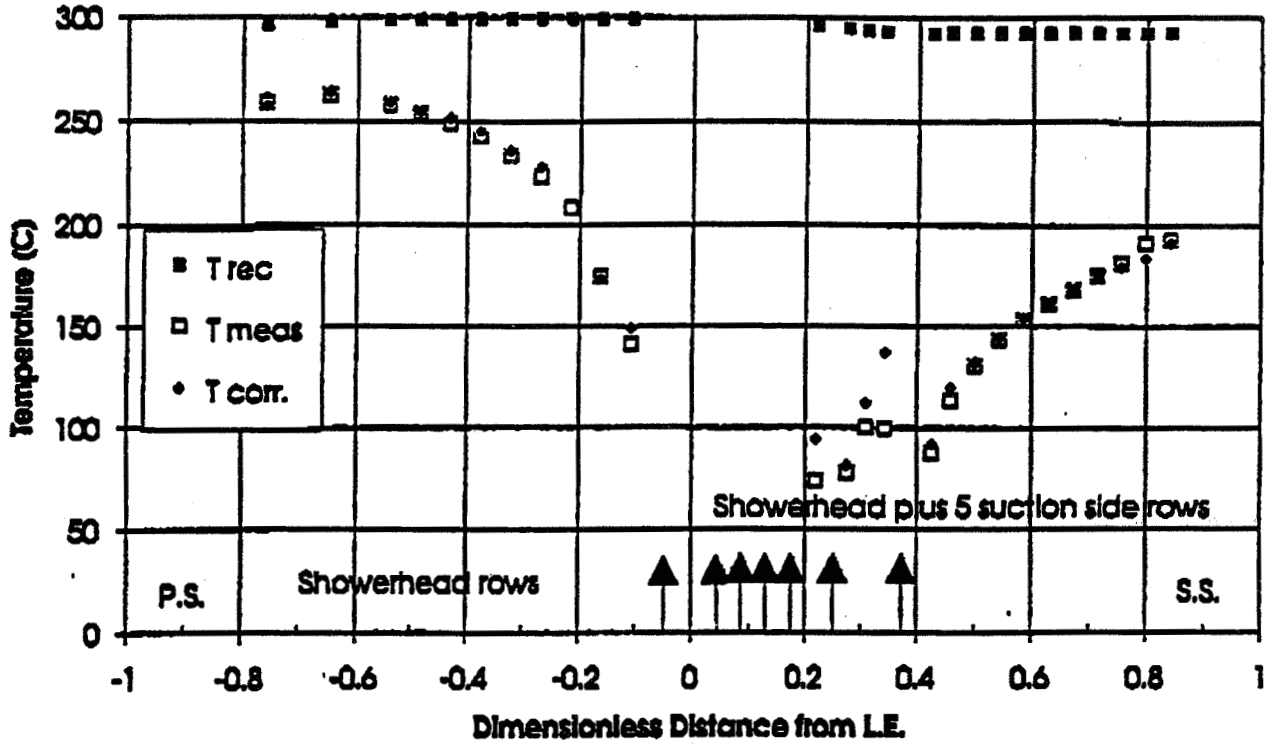

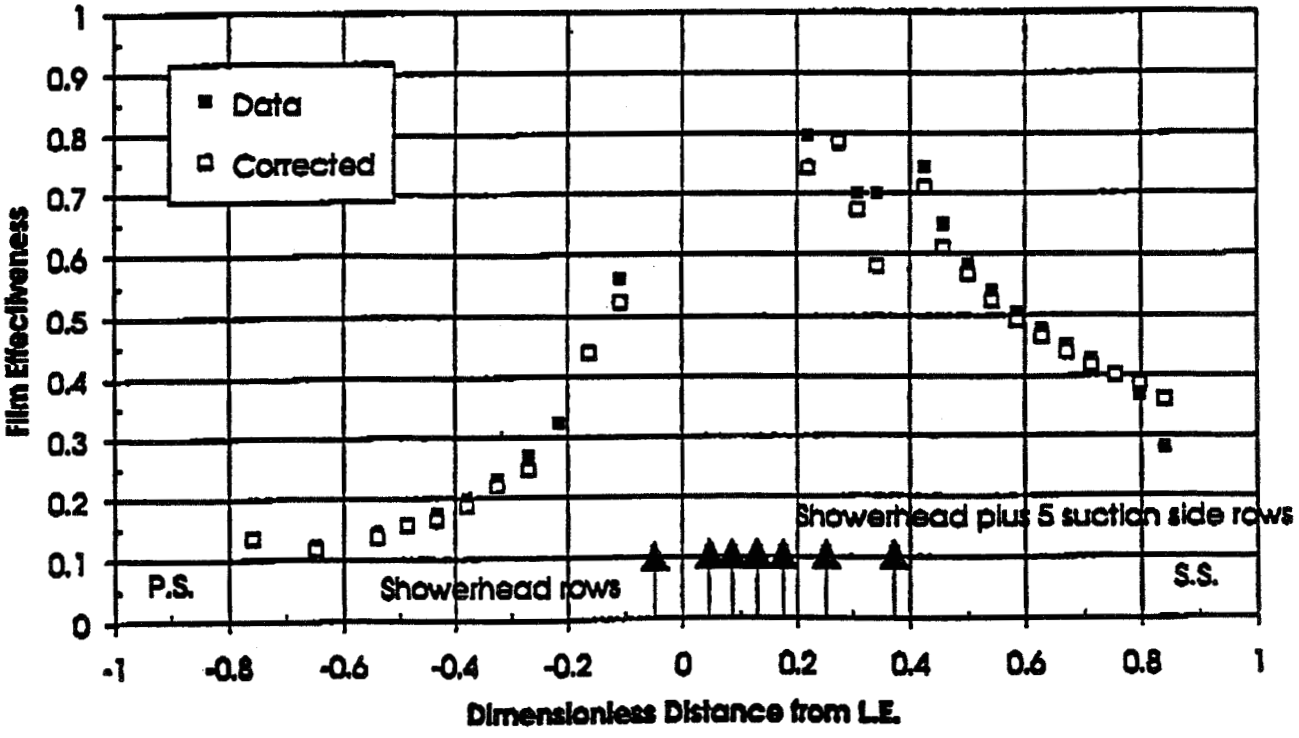

Summary and Conclusions

- Transient Test Facility Built to Determine Both Heat Transfer and Film Effectiveness in Linear Airfoil Cascades
  - Steady-state Operation Provides Film Effectiveness
  - Transient Operation Provides Both
- Base Line Tests Conducted with Cylinders In Cross Flow - Stagnation Point Heat Transfer Agrees with Established Correlations
- Linear Airfoil Cascade Tests Show;
  - Mach Number Distributions Agree with Inviscid Code Predictions
  - Airfoil Heat Transfer Coefficients Measured with Plugged Film Holes Follow Boundary Layer Code Predictions
  - Film Injection Increases Heat Transfer Levels both on Pressure and Suction Sides

Turbine Airfoil Film Cooling Design Issues

- **Expand the current film cooling database to cover a broader range of engine-level conditions for both blades and vanes ...**
  - Reynolds number
  - Blowing ratio
  - Density ratio
  - Roughness
- **Develop small-scale transducers for direct measurement of heat flux in high-temperature environments.**
- **Focus on enhanced cooling designs for "edges" - tips, trailing edges.**
- **Apply CFD technology to screen film hole geometries.**
  - Interior hole flow
  - Film jet vortex - wall interaction
  - Shear-layer / wall-layer dynamics
- **Understand relative film-TBC-convection payoffs for different design requirements.**
  - Optimization targets
    - Min Wc at constant life
    - Max SFC (Fn / Weight) at constant part life
    - Max life (min LCF) at constant WC
    - Min life-cycle cost - component / system
  - Inverse cooling configuration design for prescribed mechanical / cooling constraints
- **Create flexible design systems responsive to increasingly rapid engine development cycles.**

AN INITIAL MULTI-DOMAIN MODELING OF AN ACTIVELY COOLED STRUCTURE

Erlendur Steinthorsson
ICOMP
Cleveland, Ohio

OUTLINE

- Introduction
- Objectives of current research
- Methodology for coolant flow simulations
  - key components
  - key advantages
- Multiblock/Multigrid scheme - sample results
- Future research
- Summary

INTRODUCTION – The TRAF3D.MB Code

A computer code designed for simulating flow and heat transfer in turbo-machinery:

- Based on the TRAF3D code (Arnone, et al., 1992),
- finite volume discretization (second order accurate),
- multigrid convergence acceleration,
- multi-block grids for complex geometries,
- Algebraic and two-equation turbulence models.

INTRODUCTION – The TRAF3D.MB Code

Code has been applied to several turbomachinery flows, including

- turbine blade and blade tip heat transfer (Ameri, et al., 1995, 1996),
- study of heat transfer on recessed tips (squealer tips, Ameri, et al., 1997)
- study of heat transfer in serpentine passages and channels with ribs and bleed holes (Rigby, et al., 1996, 1997),
- simulations of flow and heat transfer within the "branched duct" coolant passage model (Steinthorsson, et al., 1996, 1997)

Why is the TRAF3D.MB code designed the way it is?

What is the rationale behind the main code-design choices,

...to use multi-block grid systems for complicated geometries,

and

...to use multigrid convergence acceleration.

OBJECTIVES

- Develop a methodology for 3-D numerical simulations of flow and heat transfer in turbomachinery that is
    - capable of delivering *accurate results,*
    - computationally *efficient,*
    - capable of handling *complicated geometries,*
    - efficient in terms of human effort,
    - useful as a platform for evaluating turbulence models, film-cooling flow models and other models for turbine cooling flows.
- Demonstrate the effectiveness of the methodology by simulating benchmark flows and by computing flow and heat transfer in gas turbine engines at realistic operating conditions.

DEVELOPMENT OF METHODOLOGY

Key issues:

- Accuracy,
- efficiency,
- modularity.

Constraint:

- Must be applicable to flows in complicated geometries.

METHODOLOGY FOR 3-D NUMERICAL SIMULATIONS

Key issues that determine *Accuracy* and *Efficiency*:

Accuracy:

- discretization of the governing equations
- quality of grid system
- resolution of the flow field

Efficiency:

- automation of grid generation
- choice of algorithms
- optimization of computer codes (vectorization, parallelization)
- structure of grid system
- judicious use of grid points.

TRAF3D.MB

Key Design Choices:

- Use multi-block grid systems.
- Use multi-grid convergence acceleration.
- Use finite volume discretization.

MULTI–BLOCK GRID SYSTEMS

Globally unstructured:

- "Unstructured" assembly of blocks,
- great flexibility for modeling complicated geometries.

Locally structured:

- Each block is a "body-fitted" structured grid,
- grid lines are at least C^1 continuous at block boundaries.

WHY USE MULTI–BLOCK STRUCTURED MESHES?

For reasons of *accuracy*:

- well suited for viscous boundary layers,
- high-order schemes can be implemented "easily."

For reasons of *efficiency*:

- simple array data structures are applicable,
- high level of optimization on computers,
- low memory overhead,
- regular cell-to-cell connectivity allows effective application of implicit schemes, multigrid schemes and other convergence acceleration techniques.

GENERATION OF MULTI–BLOCK GRIDS

Current "state of the art":

- Commercial grid generator is available.
- Grid generation is "semi-automatic";
  - shape of blocks and grid point distribution is optimized,
  - topology needs to be specified.
- Human effort is greatly reduced compared to older structured grid generation technology.
- Can be fully automated for specific classes of geometries.

TRAF3D.MB - Ability to Handle Complicated Geometries

- Completely general multiblock capability:
  - no limitation on number of blocks
  - no limitation on connectivity between blocks
- Writes blocks to files (SSD) if memory is limited
- Ability to handle block interfaces with discontinuous grid lines across branch cuts.
- Automatically detects periodic block interfaces
  - linear (e.g., linear cascades)
  - annular (requires rotation of velocity vectors upon transfer across the interface).

SAMPLE GEOMETRY HANDLED BY TRAF3D.MB

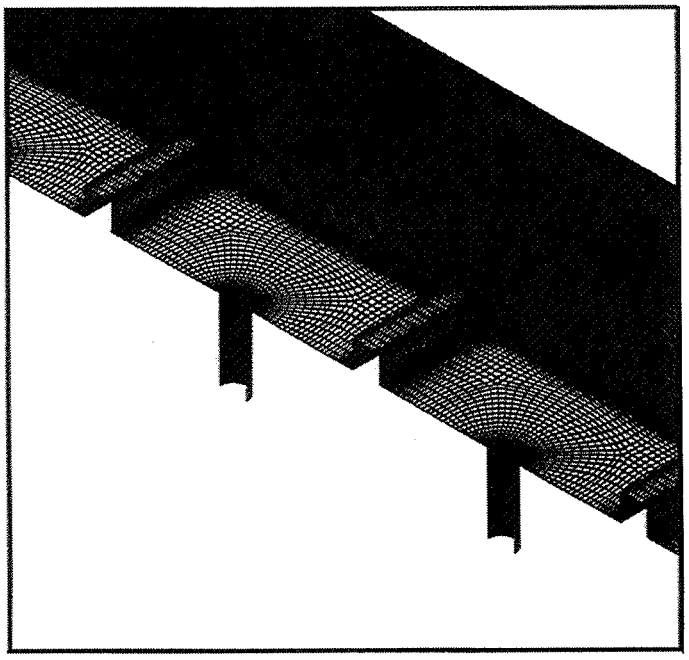

MULTIGRID CONVERGENCE ACCELERATION

- Makes convergence rates essentially independent of grid resolution.
- Reduces required CPU time by an order of magnitude or more.
- Leads to at most 20% increase in memory
- Especially useful for simulations requiring high resolution of the flow field.
- Small increase in code complexity (same routines can be used for smoothing on all levels).

TRAF3D.MB - OVERVIEW

- Full, compressible Navier-Stokes equations.
- Baldwin - Lomax and k-ω turbulence models.
- Rotating reference frames (Chima and Yokota, 1990).
- Discretization (2nd order accurate in space):
  - cell-centered finite volume discretization
  - central differencing (Swanson and Turkel, 1987)
  - central differencing for diffusion terms
- Runge-Kutta time integration with local time stepping and implicit residual smoothing (Jameson, et al. 1981, 1983, 1988),
- Multigrid scheme (FAS, FMG; Brandt, 1977, Jameson, 1983).

TRAF3D.MB - Ability to Handle Complicated Geometries

- Completely general multiblock capability:
  - no limitation on number of blocks
  - no limitation on connectivity between blocks
- Automatic arrangement of blocks into files if memory is limited.
- Writes blocks to files (SSD) if memory is limited
- Ability to handle block interfaces with discontinuous grid lines across branch cuts.
- Automatically detects periodic block interfaces
  - linear (e.g., linear cascades)
  - annular (requires rotation of velocity vectors upon transfer across the interface)

TRAF3D.MB Sample Results

Flow and heat transfer on squealer tips:

- E3 turbine blade.
- Results obtained using k-ω turbulence model.

Flow and Heat transfer in "branched duct" geometry.

- Nominal Reynolds number: Re = 335,000.
- Results obtained using Baldwin-Lomax turbulence model.
- Results obtained using k-ω turbulence model.

Flow and Heat Transfer on E3 Rotor Blade with Squealer Tip

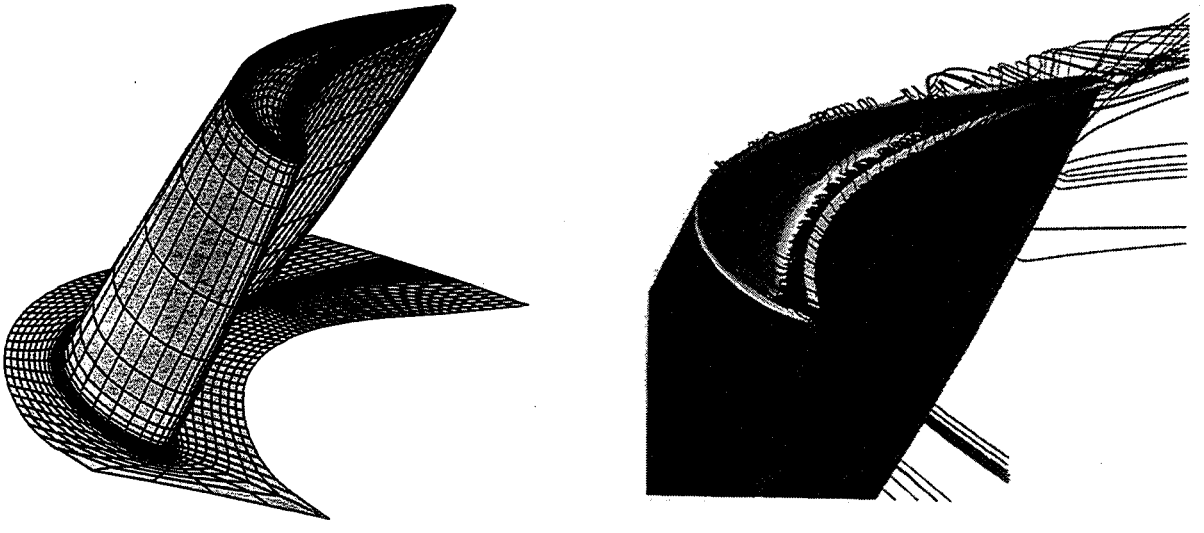

Branched Duct – Grid System

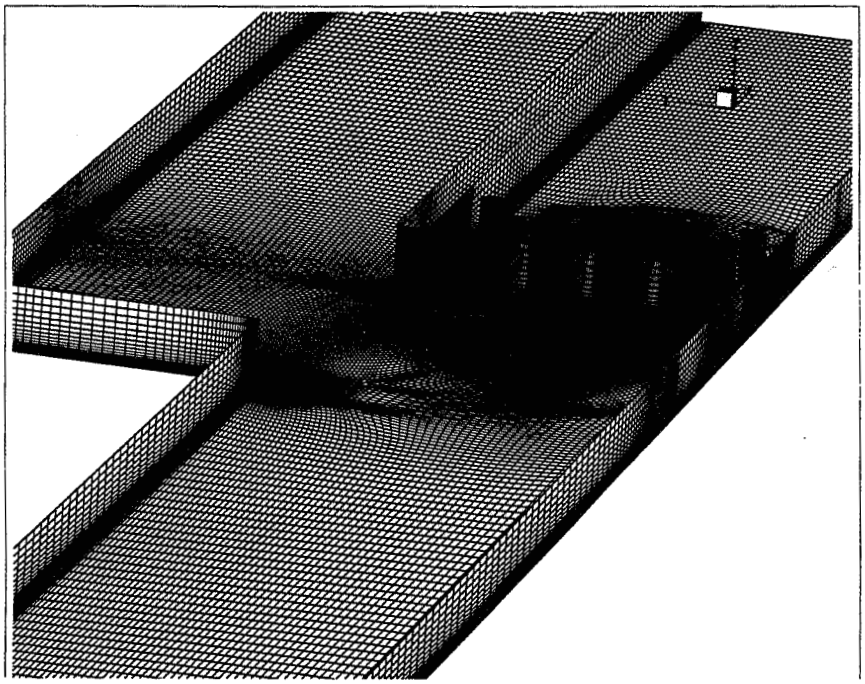

Branched Duct – Velocity Field

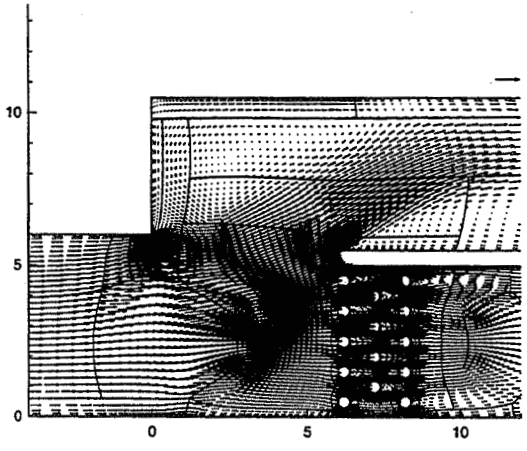

Symmetry plane

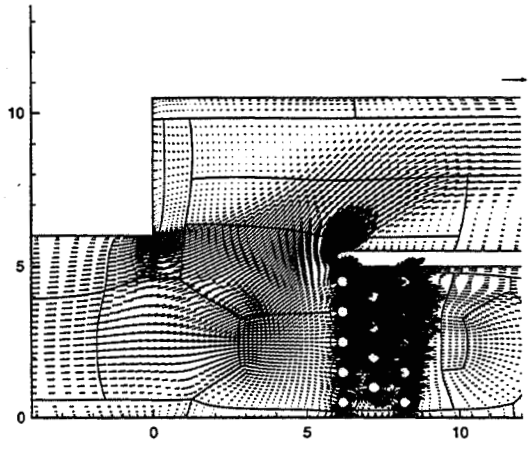

Near Wall
(vectors magnified 25 times)

Branched Duct – Heat Transfer (Re=335,000)

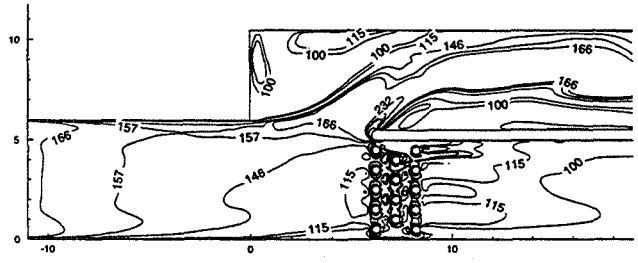

(a)

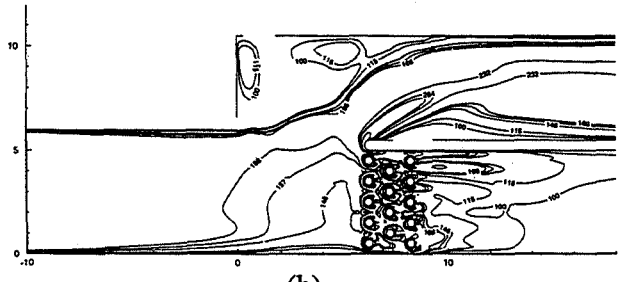

(b)

(a) Results obtained with Baldwin-Lomax Turbulence model.

(b) Results obtained with k–ω Turbulence model.

(c) Experimental results (NASA TM 106189, AIAA-93-1797).

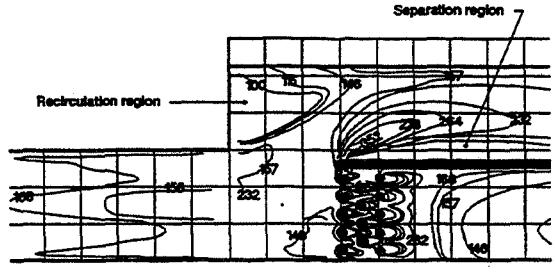

(c)

FUTURE RESEARCH

- Implement additional turbulence models.
- Add parallel computing capability.
- Study methods to improve rate of convergence to steady state for multi-block grids containing large number of blocks.
- Implement improved convergence acceleration schemes, e.g, pre-conditioning methods.
- Implement solution adaptive refinement capability.
- Implement heat conduction module for conjugate heat transfer studies.

SUMMARY

- A methodology for the simulation of turbine cooling flows is being developed.
- The methodology seeks to combine numerical techniques that optimize both accuracy and computational efficiency.
- Key components of the methodology include the use of *multiblock grid systems* for modeling complex geometries, and *multigrid convergence acceleration* for enhancing computational efficiency in highly resolved fluid flow simulations.
- The use of the methodology has been demonstrated in several turbomachinery flow and heat transfer studies.
- Ongoing and future work involves implementing additional turbulence models, improving computational efficiency, adding AMR.

AERO-THERMO-STRUCTURAL OPTIMIZATION OF COOLED TURBINE BLADES*

George Dulikravich
Pennsylvania State University
University Park, Pennsylvania

OBJECTIVES:

Develop a design system for constrained optimization of 3-D cooled turbine blades.

Provide industry with a modular design optimization tool that will take into account interaction of the hot gas flow field, heat transfer in the blade material and the internal coolant flow field, and stress/deformation field in the blade .

EXPECTED BENEFITS:

1. **fully 3-D analysis and design capability instead of 2-D or quasi 3-D capability,**
2. **simultaneous account of heat transfer, aerodynamics, and elasticity instead of aerodynamics alone,**
3. **maximum use of the existing flow-field analysis software,**
4. **optimized aerodynamic blade shape for minimum total pressure loss and maximum torque,**

* Presented at the conference by Joe Gladden, NASA Lewis Research Center.

5. ability to specify geometric, elasticity, flow field and thermal constraints,

6. optimization of hot surface heat flux and temperature distributions,

7. minimized number of coolant flow passages inside the blade,

8. minimized coolant mass flow rate as a result of minimized integrated blade surface heat flux,

9. minimized coolant pressure drop due to the resulting smooth wall coolant flow passages,

10. reduced need for manufacture of small holes for blade film cooling,

11. reduced need for elaborate pattern of pins and fins on cooling passage walls, and

12. minimized design cycle time.

PRESENT STATUS:

We have already developed and tested the following software:

1) **Inverse design of single coolant passage shapes in 3-D coated & uncoated turbine blades,**

2) **Inverse determination of temperatures, heat fluxes, and convective heat transfer coefficients on 3-D coolant passage walls or on blade hot surface,**

3) **3-D finite element thermo-elasticity dynamic analysis of unsteady stresses and deformations,**

4) **A hybrid constrained optimizer incorporating:**
gradient search,
genetic algorithm, and
simulated annealing.

5) **Non-Iterative Inverse Determination of Temperature-Dependent Thermal Conductivities.**

WORK IN PROGRESS:

1) **Optimization of thicknesses of the blade wall and multiple internal struts.**

AERODYNAMICS

Conic Section Design Variables and Turbine Blade Definition

Uses conic curves connected between control points

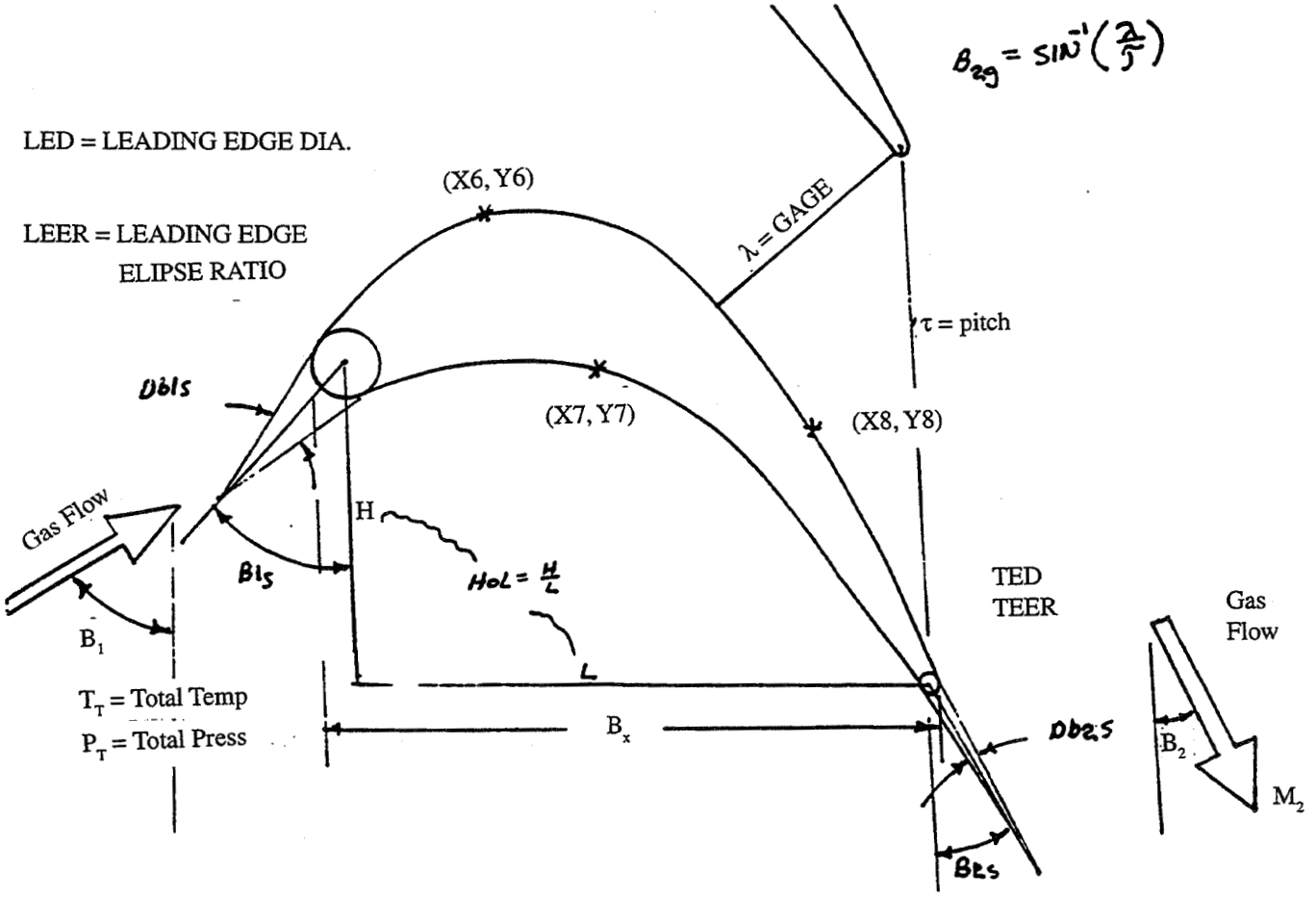

2D turbine airfoil definition using conic sections and control points

Constraint Functions

inequality and equality constraints

$$g_k(\mathbf{x}) \leq 0 \qquad h_k(\mathbf{x}) = 0$$

Perimeter

Cross-sectional Area

Chord Angle

Moment of Inertia

Airfoil Thickness

Platform

Leading Edge

Trailing Edge

Axial Chord

Throat Area

GENERIC TURBINE ROTOR BLADE

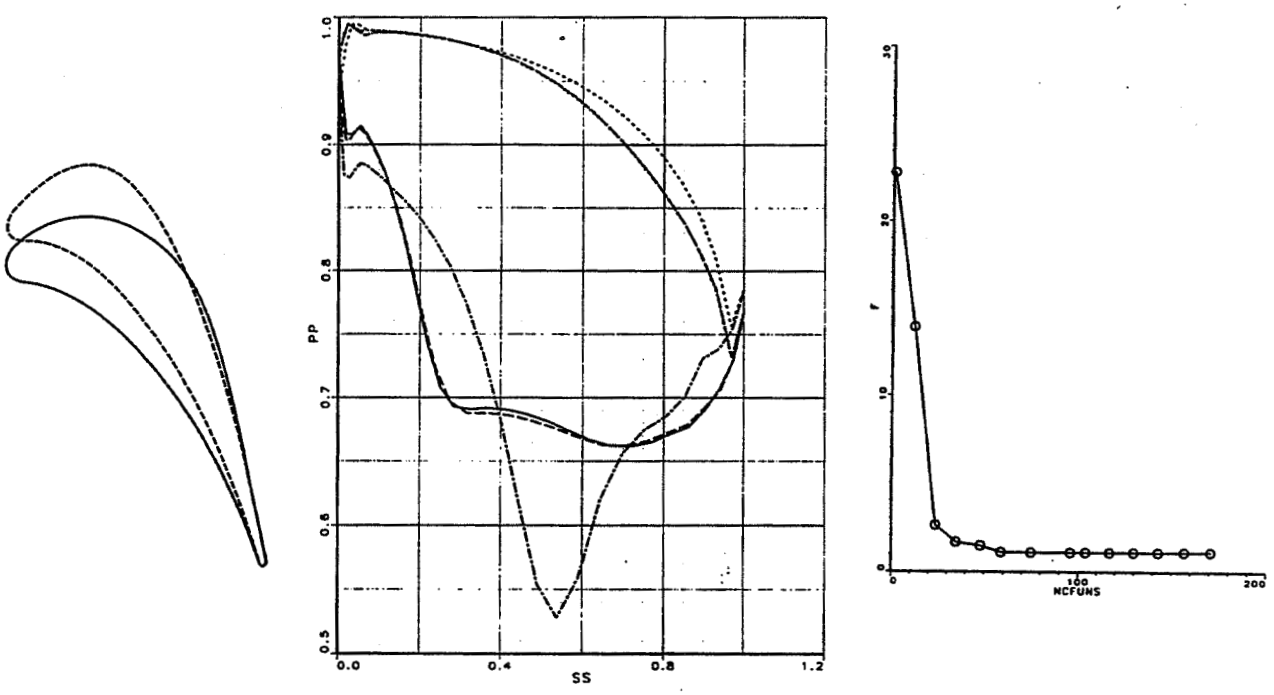

Aerodynamic shape design of generic turbine rotor airfoil using conic section design variables and target pressure distribution function.

SHAPE OPTIMIZATION OF 3-D COOLANT FLOW PASSAGES

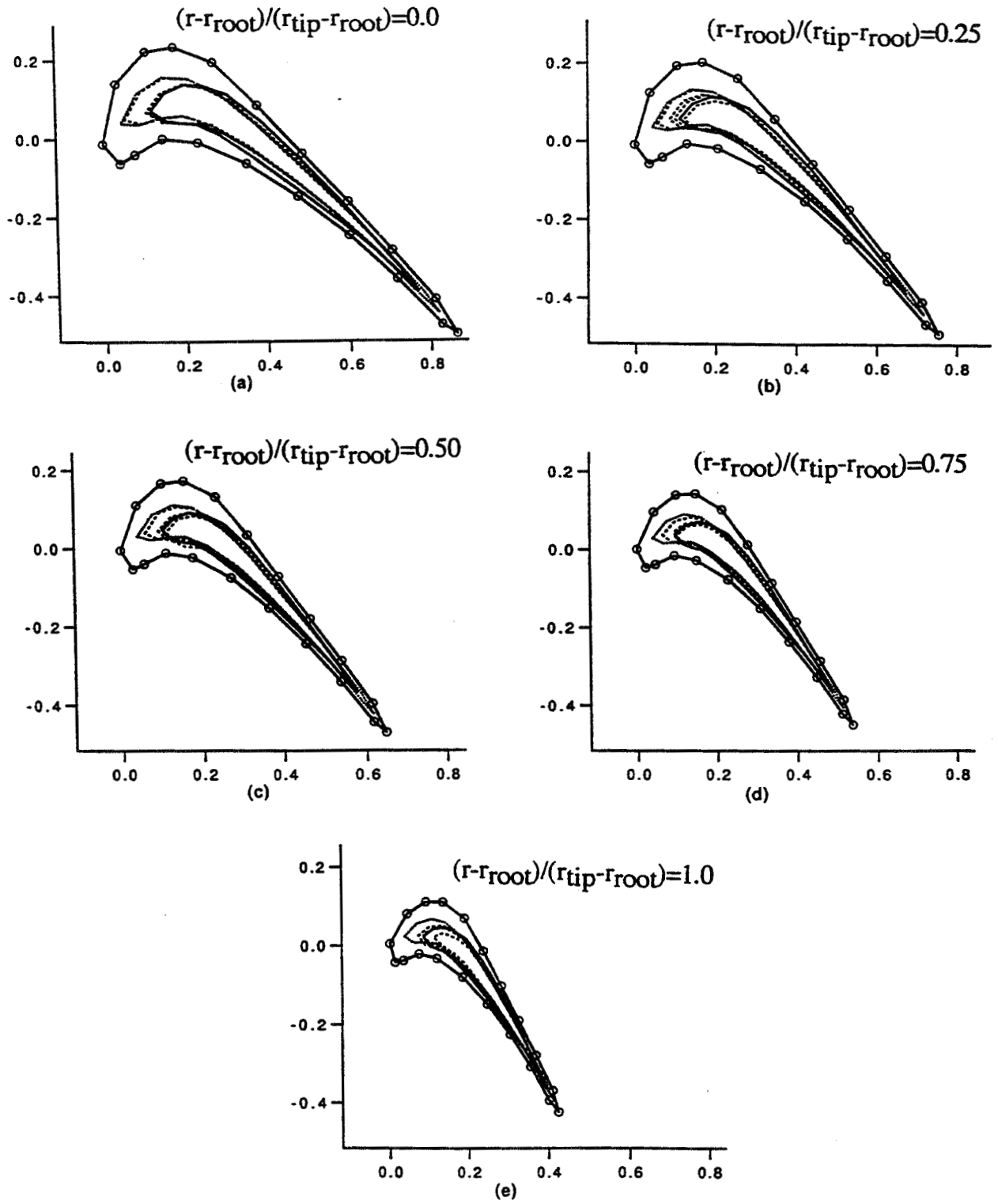

Geometric evolution of thickness distributions on individual cross-sections of the three-dimensional blade.

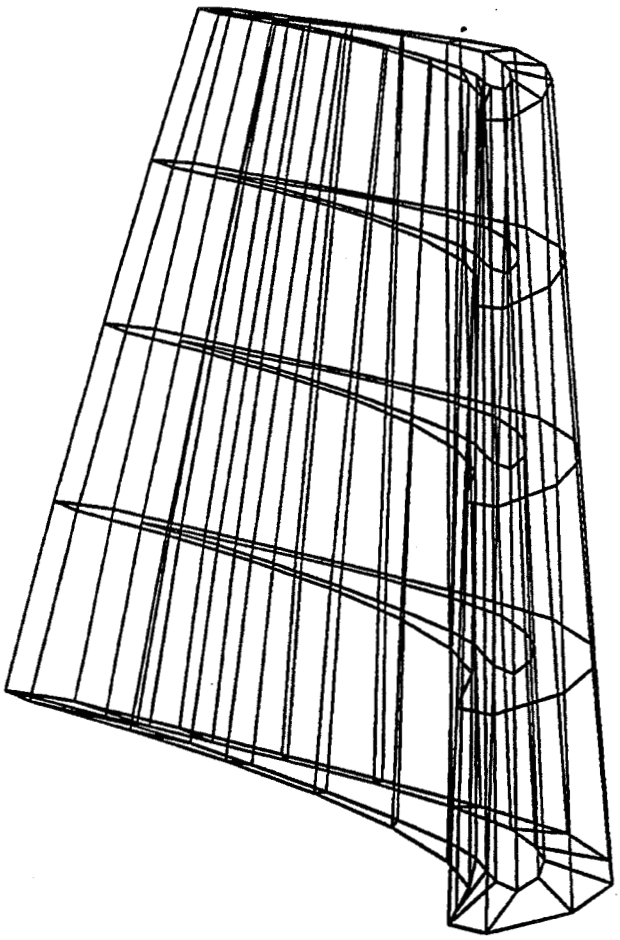

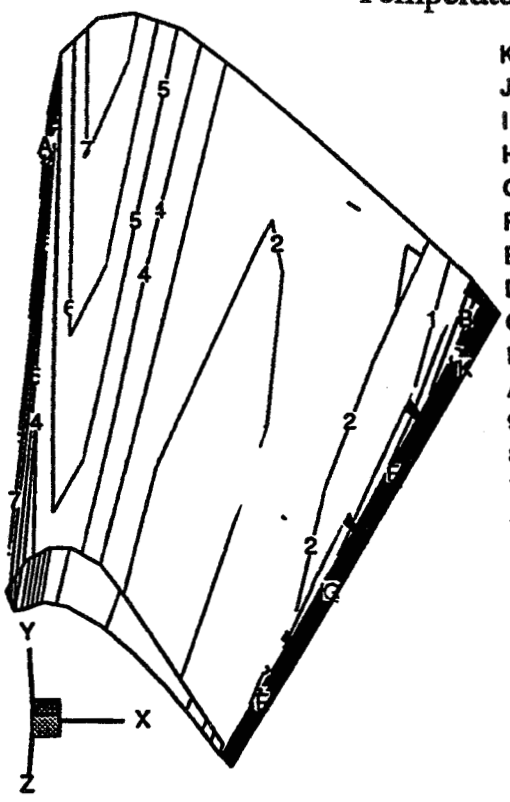

$$t(s) \approx \sum_{j=1}^{n} c_j P_{j-1}(s) - \frac{c_1}{2}$$

where the Chebyshev coefficients are

$$c_j = \frac{2}{n} \sum_{k=1}^{n} t\left[\cos\left(\frac{\pi(k-1/2)}{n}\right)\right] \times \cos\left(\frac{\pi(j-1)(k-1/2)}{n}\right)$$

and

$$P_j(s) = \cos(j \arccos s)$$

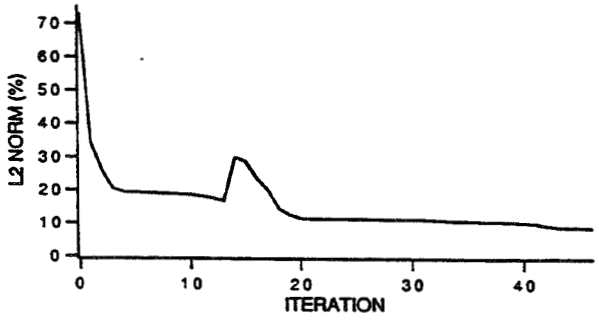

Convergence history of the objective function for the three-dimensional turbine blade wall thickness optimization.

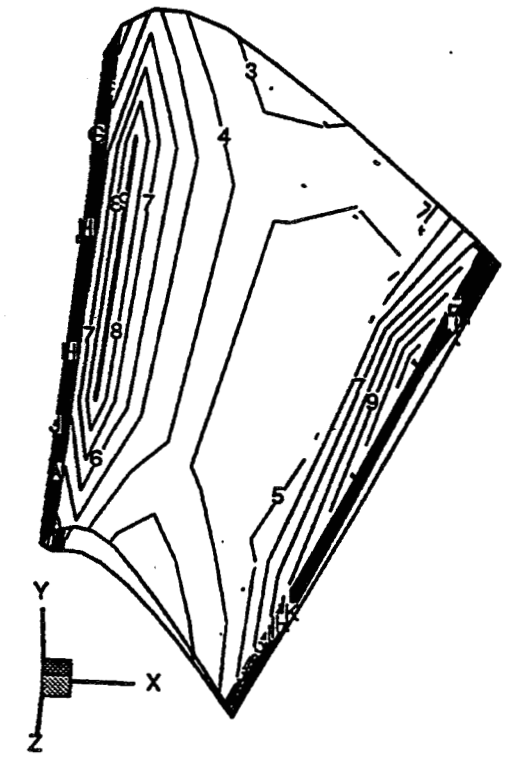

HEAT TRANSFER

WHAT IS INVERSE HEAT CONDUCTION?

DETERMINE

Temperatures, Heat Fluxes and Convective Heat Transfer Coefficients on Unknown, Inaccessible Surfaces

GIVEN OVER-SPECIFIED INFORMATION

Interior Temperature and Temperature Gradient Measurements

Over-Specified Thermal Boundary Conditions on Accessible Surfaces (Temperature and Heat Flux)

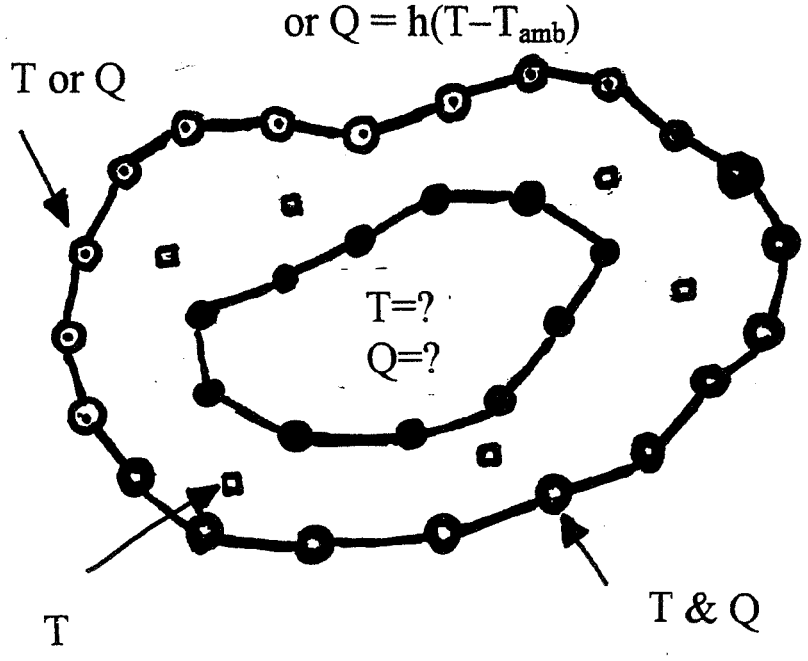

APPROACHES

ITERATIVE

Sum of Least Squares Minimization

Errors are Magnified

Requires Regularization and Smoothing of Extrapolated Heat Fluxes

DIRECT (IMPLICIT)

Forms a Singular Solution Matrix

Discard Eigenvalues That Amplify Errors

Uses SVD

APPLY BOUNDARY CONDITIONS

Example

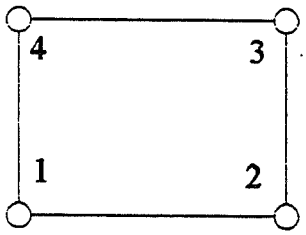

$u = \bar{u}_1$ & $q = \bar{q}_2$ $\qquad$ $u = \bar{u}_2$ & $q = \bar{q}_2$

BEM Solution Set

$$\begin{bmatrix} h_{11} & h_{12} & h_{13} & h_{14} \\ h_{21} & h_{22} & h_{23} & h_{24} \\ h_{31} & h_{32} & h_{33} & h_{34} \\ h_{41} & h_{42} & h_{43} & h_{44} \end{bmatrix} \begin{Bmatrix} \bar{u}_1 \\ \bar{u}_2 \\ u_3 \\ u_4 \end{Bmatrix} = \begin{bmatrix} g_{11} & g_{12} & g_{13} & g_{14} \\ g_{21} & g_{22} & g_{23} & g_{24} \\ g_{31} & g_{32} & g_{33} & g_{34} \\ g_{41} & g_{42} & g_{43} & g_{44} \end{bmatrix} \begin{Bmatrix} \bar{q}_1 \\ \bar{q}_2 \\ q_3 \\ q_4 \end{Bmatrix}$$

Collected Unknowns on the Right-Hand Side

$$\begin{bmatrix} h_{13} & -g_{13} & h_{14} & -g_{14} \\ h_{23} & -g_{23} & h_{24} & -g_{24} \\ h_{33} & -g_{33} & h_{34} & -g_{34} \\ h_{43} & -g_{43} & h_{44} & -g_{44} \end{bmatrix} \begin{Bmatrix} u_3 \\ q_3 \\ u_4 \\ q_4 \end{Bmatrix} = \begin{bmatrix} -h_{11} & g_{11} & -h_{12} & g_{12} \\ -h_{21} & g_{21} & -h_{22} & g_{22} \\ -h_{31} & g_{31} & -h_{32} & g_{32} \\ -h_{41} & g_{41} & -h_{42} & g_{42} \end{bmatrix} \begin{Bmatrix} \bar{u}_1 \\ \bar{q}_1 \\ \bar{u}_2 \\ \bar{q}_2 \end{Bmatrix}$$

Near-Singular or Ill-Conditioned Systems of Linear Algebraic Equations

$$[A]\{X\} = \{F\}$$

Annular Disk with an Arbitrary Heat Source Function

$$g(r,\theta) = g_0 \sin\left[\frac{r - r_a}{r_b - r_a}\right] \sin\theta$$

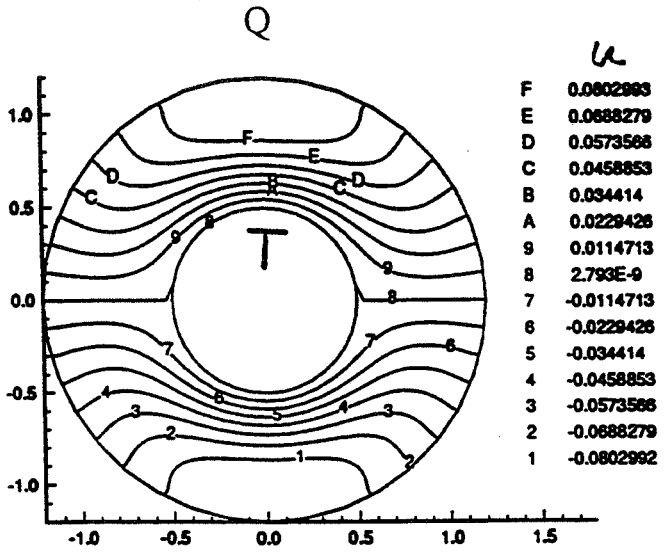

Forward (Well-Posed) Isotherms

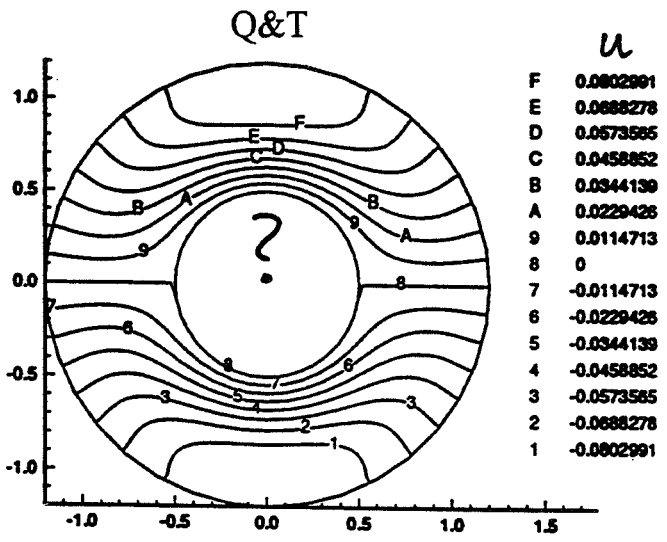

Inverse (Ill-Posed) Isotherms

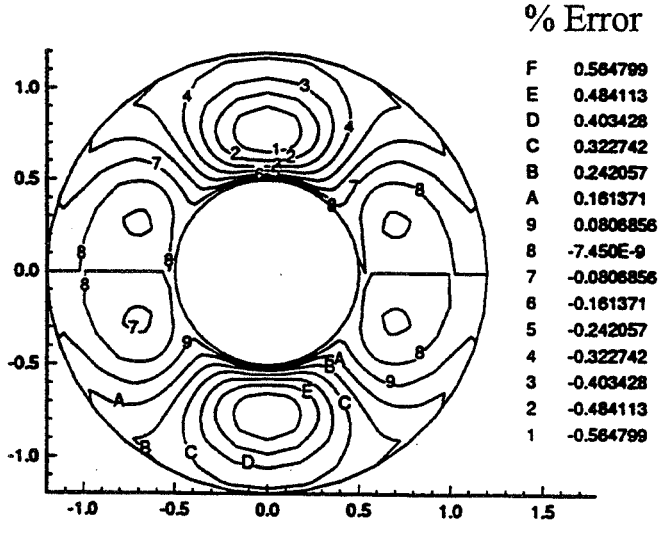

Error in Forward BEM

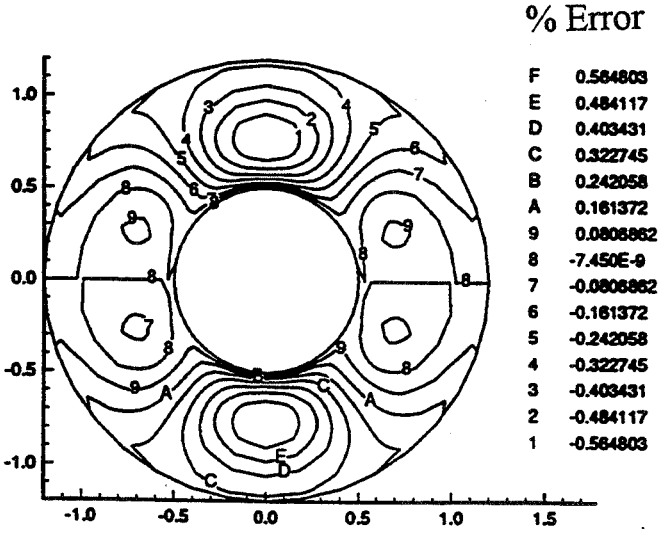

Error in Inverse BEM

Annular Disk With Interior Temperature Measurements

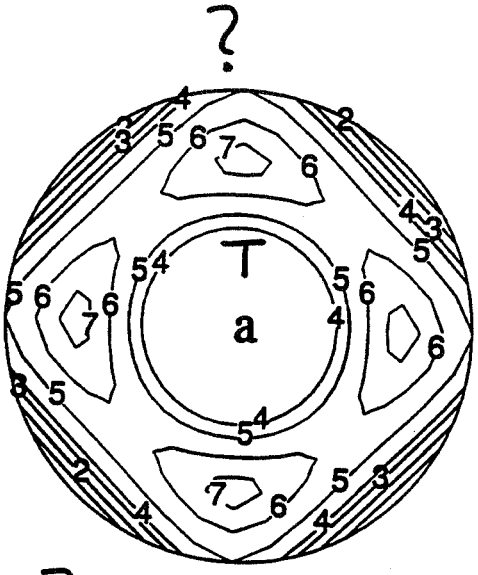

Non-dimensional temperature

7	0.054344
6	0.043368
5	0.0223428
4	1E-12
3	-0.0123143
2	-0.0296428
1	-0.0469714

76 Equations
108 Unknowns

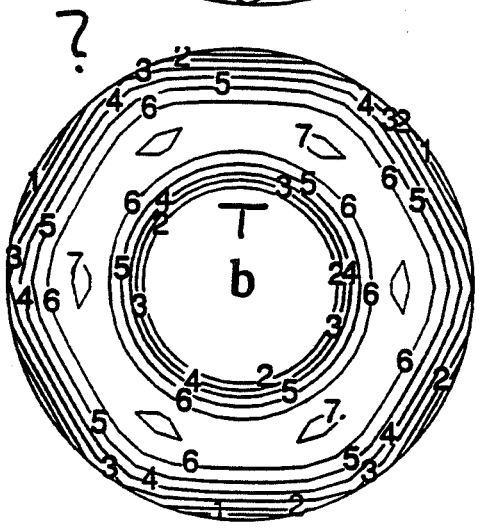

Non-dimensional temperature

7	0.0593573
6	0.0485429
5	0.0367857
4	0.0250286
3	0.0132714
2	1E-12
1	-0.0102429

78 Equations
108 Unknowns

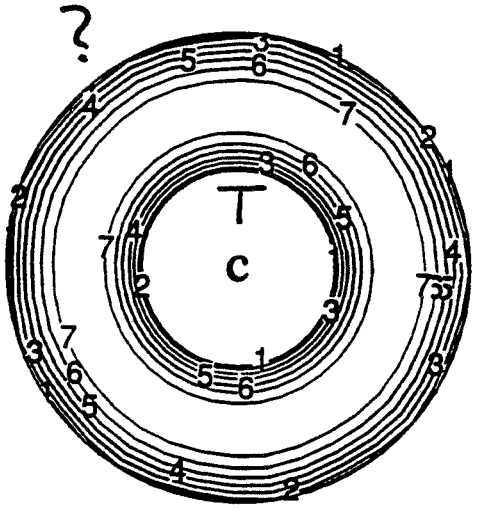

Non-dimensional temperature

7	0.0525
6	0.0431
5	0.0337
4	0.0243
3	0.0149
2	0.0055
1	1E-12

81 Equations
108 Unknowns

Isotherms Predicted With the Inverse BEM When Temperatures Were Specified at 4, 6 and 9 Equidistantly Spaced Interior Points

Cube-Within-A-Cube

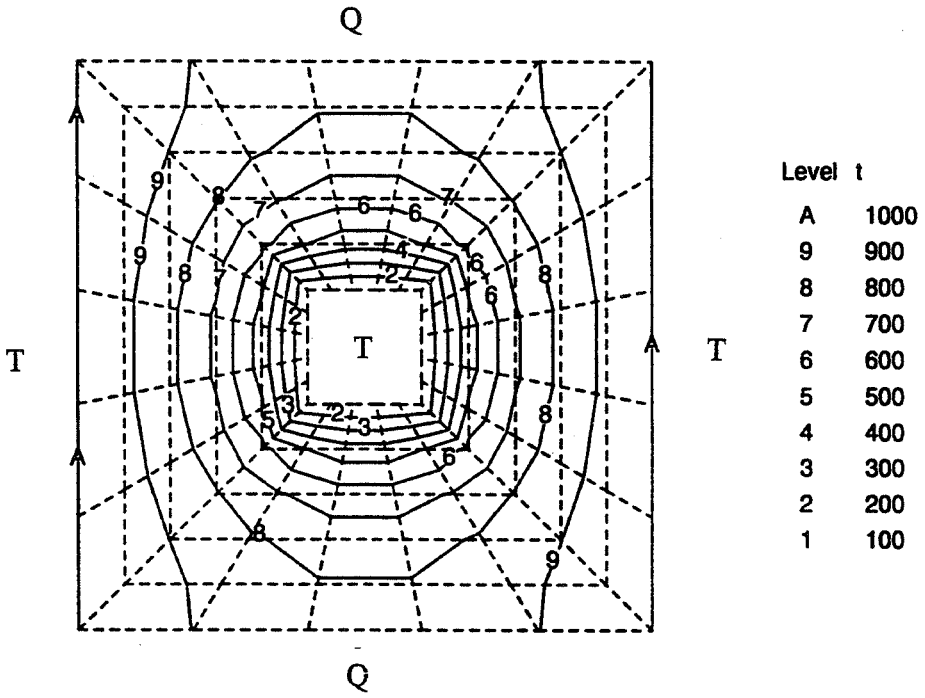

Isotherms on a Slice Through Center of the Cube Predicted by the Forward BEM

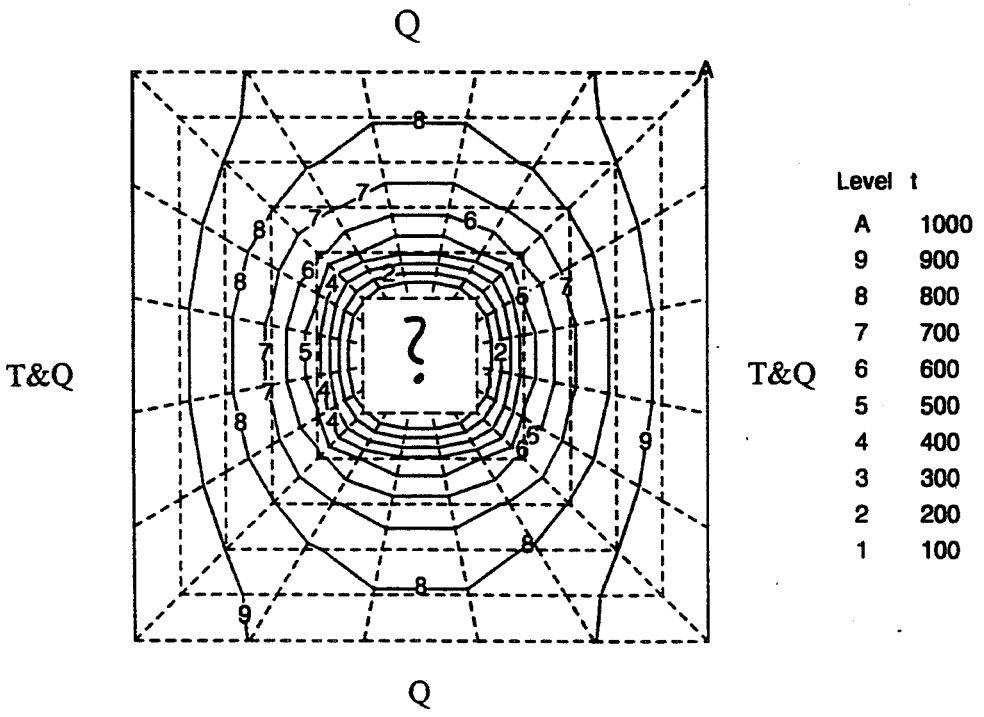

Isotherms on a Slice Through Center of the Cube Predicted by the Inverse BEM

Three-Dimensional Rocket Nozzle Wall Section

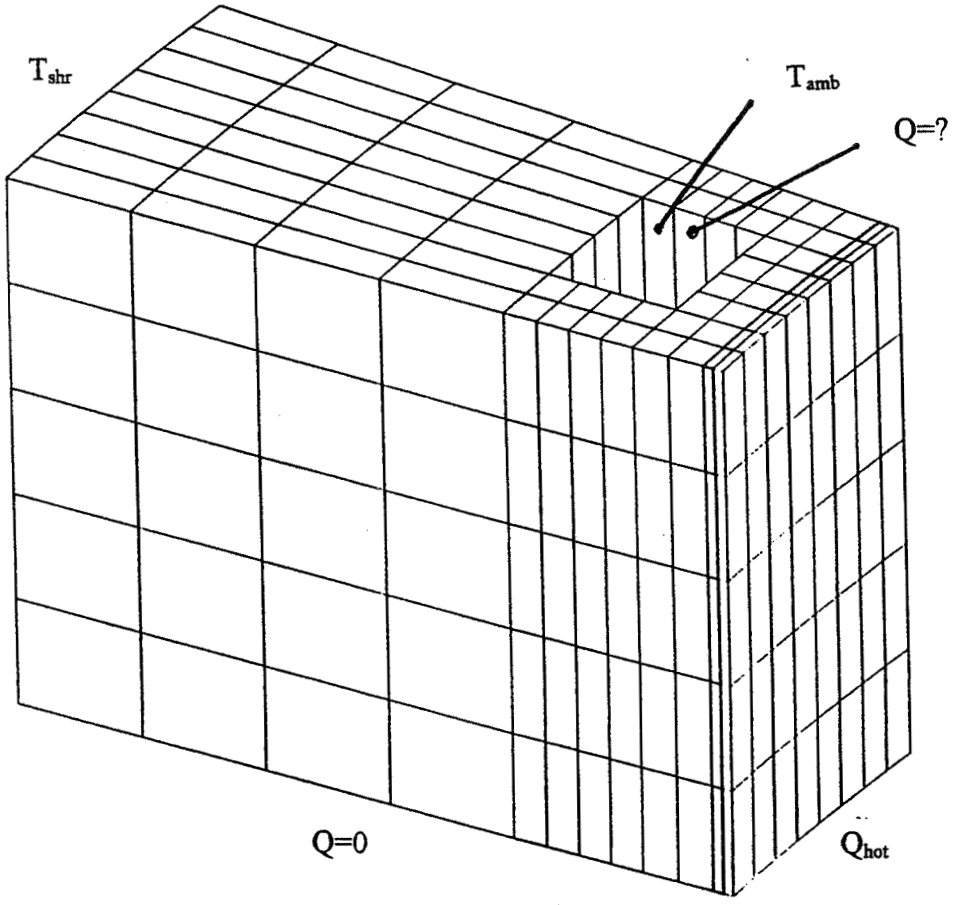

Surface Grid of a Rocket Nozzle Wall Section Composed of Four Materials and Having a Finned Coolant Passage

	Zirconium Oxide	Nickel-chromium	Copper	Copper closeout
k (W/m K)	8.0	23.0	378.0	385.0

Table. Thermal Conductivities of Different Material Layers

$T_{shroud} = 140$ K
$Q_{hot} = -100 \times 10^6$ W/m^2
$T_{amb} = 50$ K
$h_{conv} = 1 \times 10^5$ W/m^{2}K

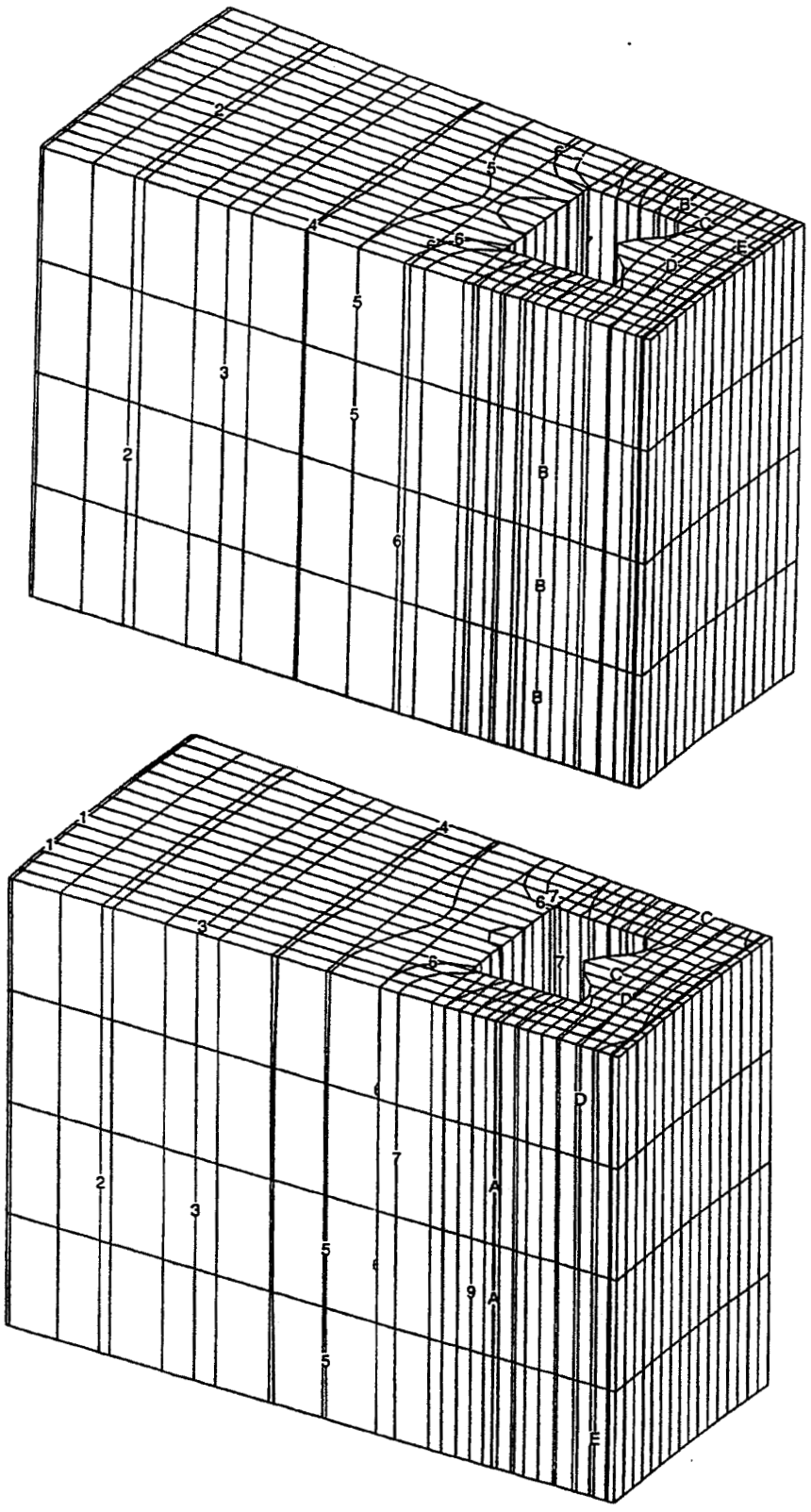

Level	θ
F	1923.5
E	826.567
D	746.781
C	669.452
B	552.454
A	491.619
9	437.355
8	384.202
7	326.679
6	306.872
5	276.419
4	251.383
3	217.076
2	177.857
1	141.466

Level	θ
F	1923.5
E	826.567
D	746.781
C	669.452
B	552.454
A	491.619
9	437.355
8	384.202
7	326.679
6	306.872
5	276.419
4	251.383
3	217.076
2	177.857
1	141.466

Isotherms Predicted by the Well-Posed and Ill-Posed BEM for a Three-Dimensional Segment of a Rocket Thrust Chamber Wall with a Finned Coolant Passage

Cooling of a Three-Dimensional Electronic Chip Package

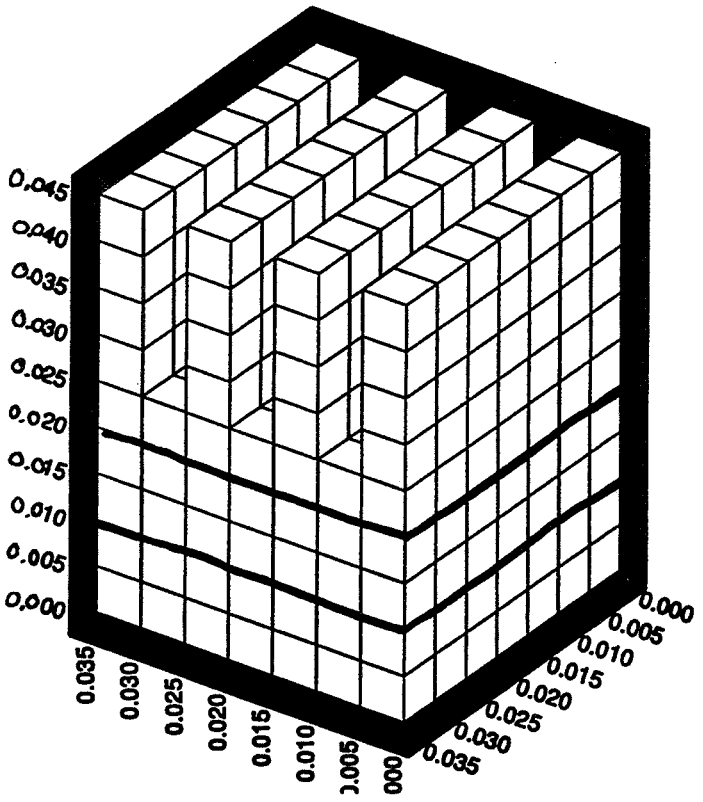

Computational Surface Grid for a Cooled Electronic Chip Package

	Tungsten Heat Sink	Silica Heat Spreader Plate	Silica Substrate	Silicon Chip
k (W/m K)	137.0	1.39 W/m K	1.39 W/m K	102.0

$h_{conv} = 3000$ W/m^2 K

$T_{amb} = 300$ K

$g = 100{,}000$ W/m^3

Isotherms (Solid Lines) Surface Grid (Dashed Lines)

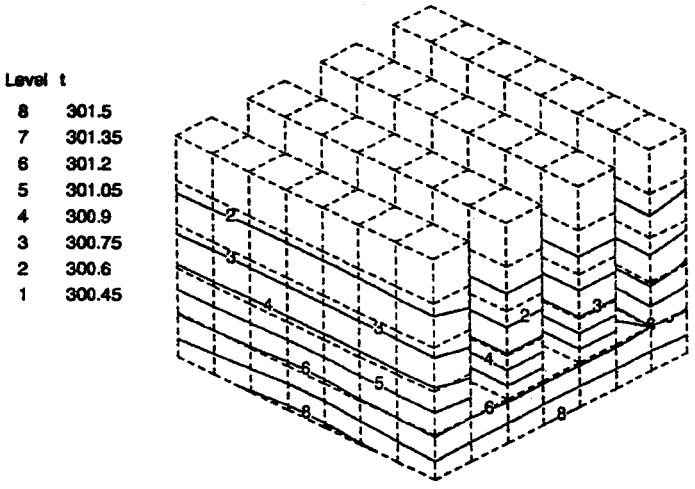

Isotherms on the Finned Heat Sink
Predicted by Forward BEM

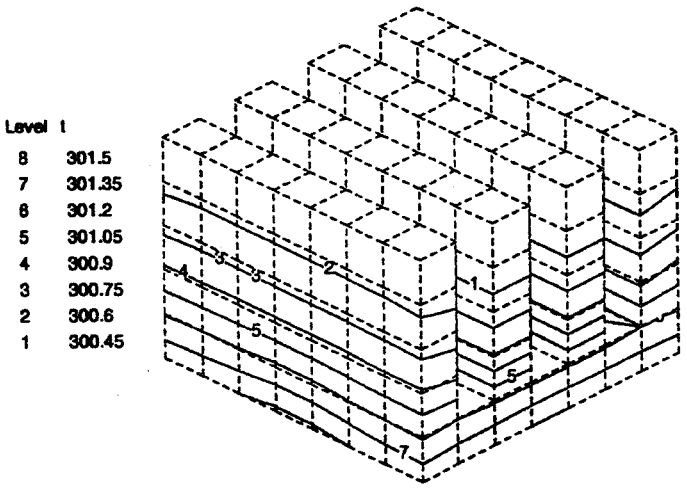

Isotherms on the Finned Heat Sink
Predicted by the Inverse BEM

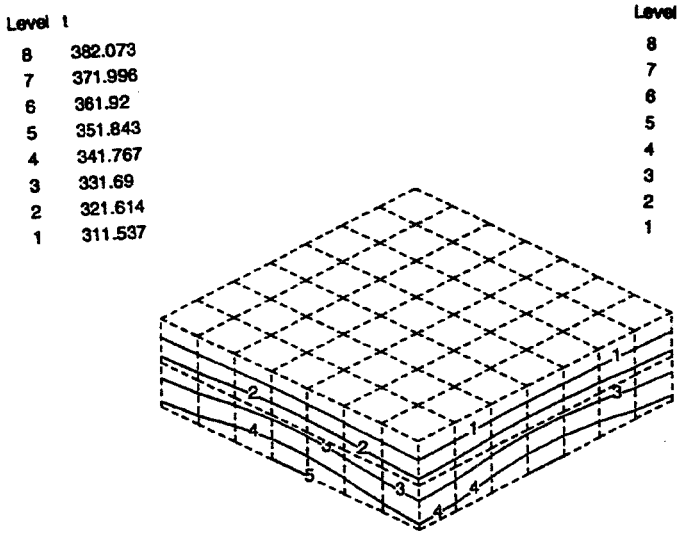

Isotherms on the Heat Spreader
Predicted by the Forward BEM

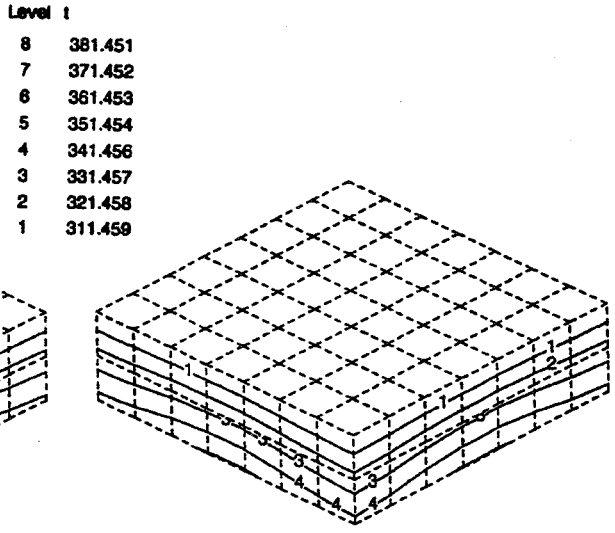

Isotherms on the Heat Spreader
Predicted by the Inverse BEM

Isotherms (Solid Lines) Surface Grid (Dashed Lines)

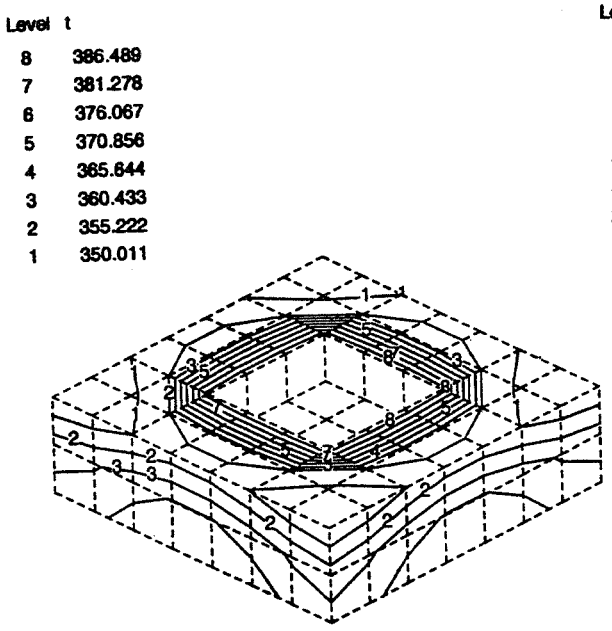

Isotherms on the Substrate Plate Predicted by Forward

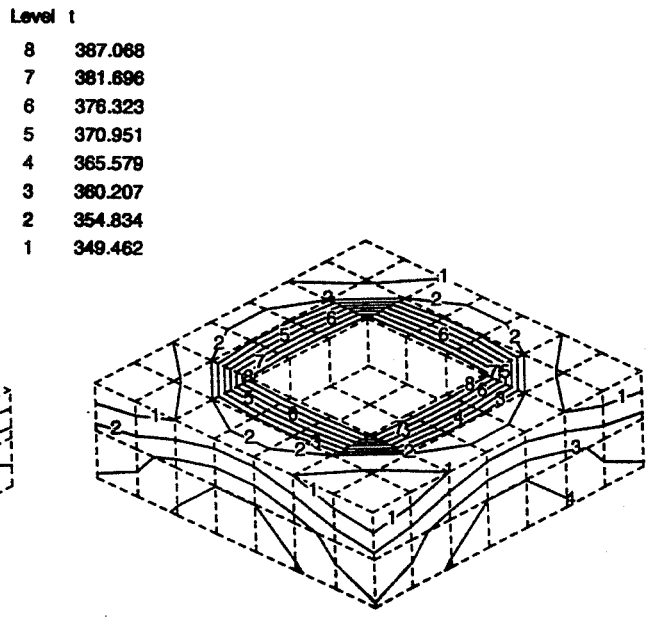

Isotherms on the Substrate Plate Predicted by the Inverse BEM

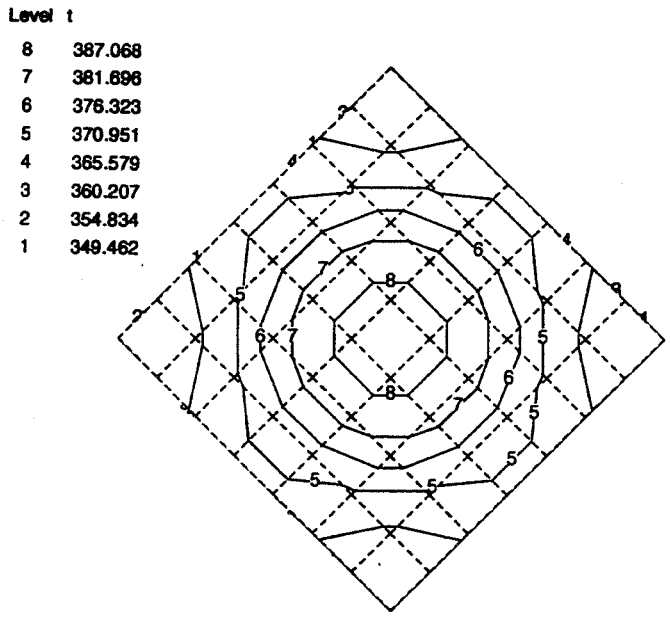

Isotherms on the Bottom Surface Predicted by the Forward BEM

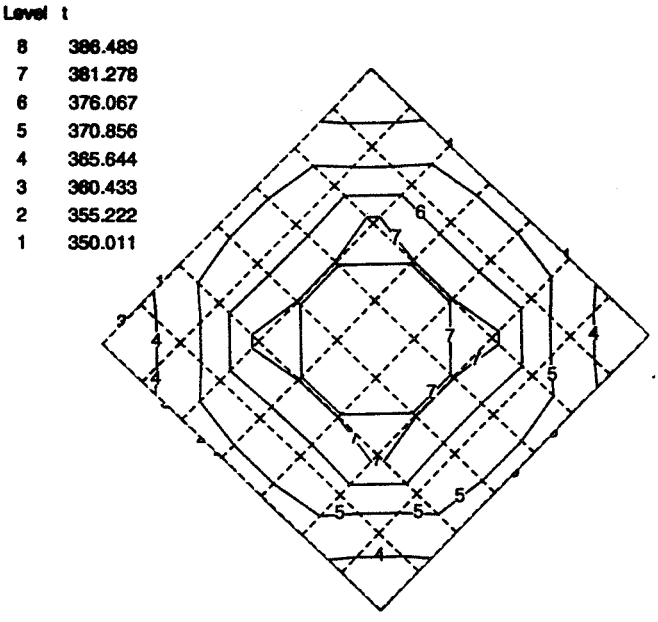

Isotherms on the Bottom Surface Predicted by the Inverse BEM

Level	t
8	392.127
7	391.814
6	391.5
5	391.187
4	390.873
3	390.56
2	390.246
1	389.933

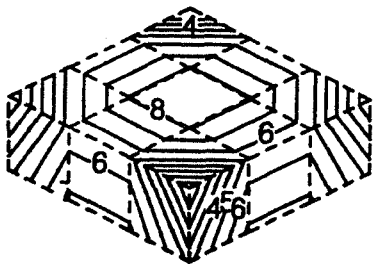

Isotherms on the Surface of Chip
Predicted by the Forward BEM

Level	t
8	391.399
7	391.098
6	390.797
5	390.496
4	390.194
3	389.893
2	389.592
1	389.291

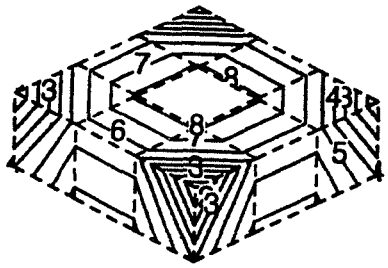

Isotherms on the Surface of Chip
Predicted by the Inverse BEM

Conjugate Thermal Entry Problem

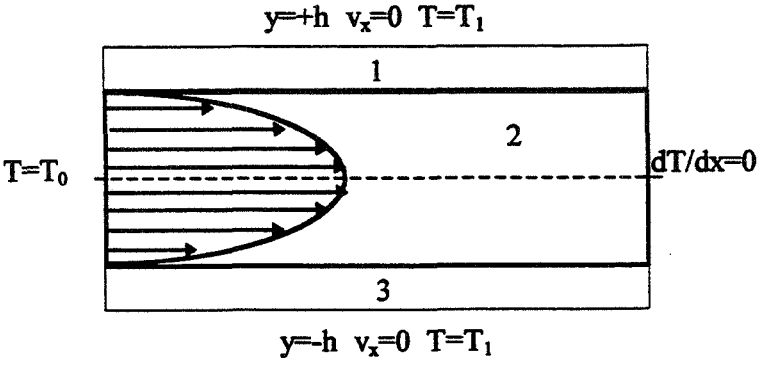

Region 1: Solid with conductivity k_S

Region 2: Fluid with conductivity k_F and known velocity profile $v_x(y)$

Region 3: Solid with conductivity k_S

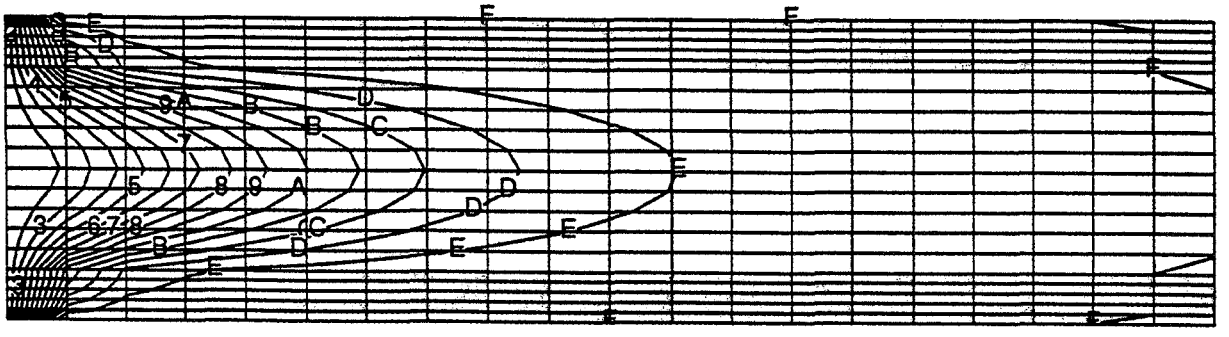

Level	t
F	1
E	0.9285715
D	0.8571429
C	0.7857143
B	0.7142857
A	0.6428572
9	0.5714286
8	0.5
7	0.4285715
6	0.3571429
5	0.2857143
4	0.2142857
3	0.1428571

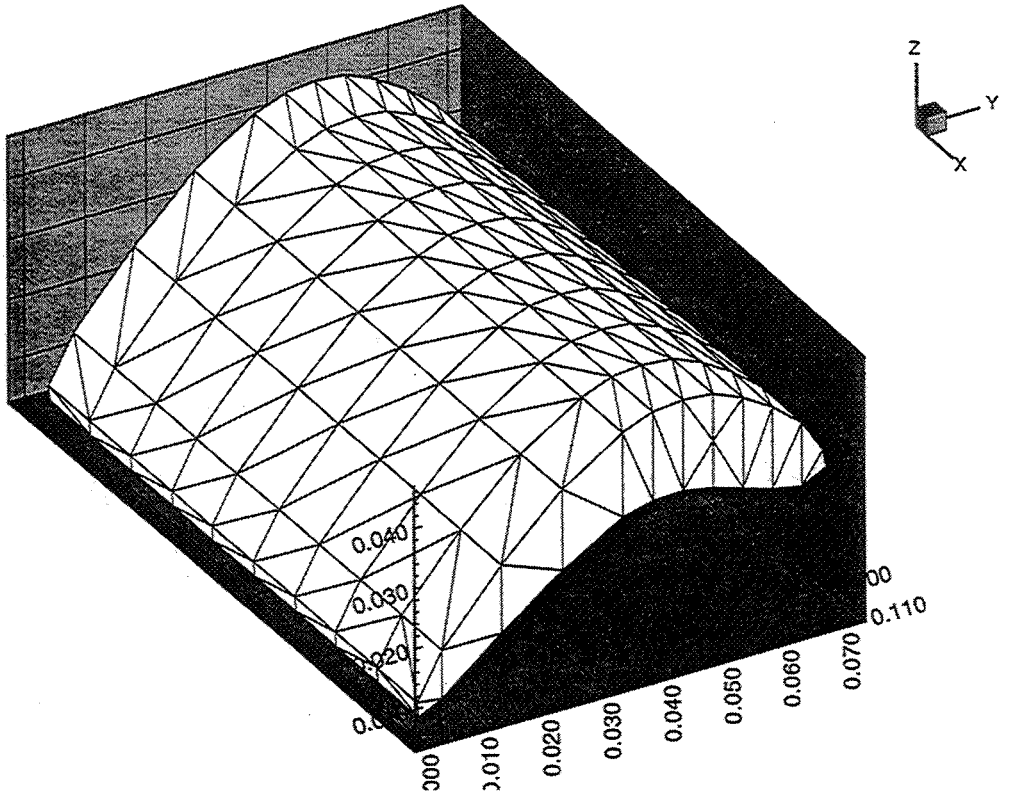

Figure 1: Tetrahedron mesh of a solid turbine blade.

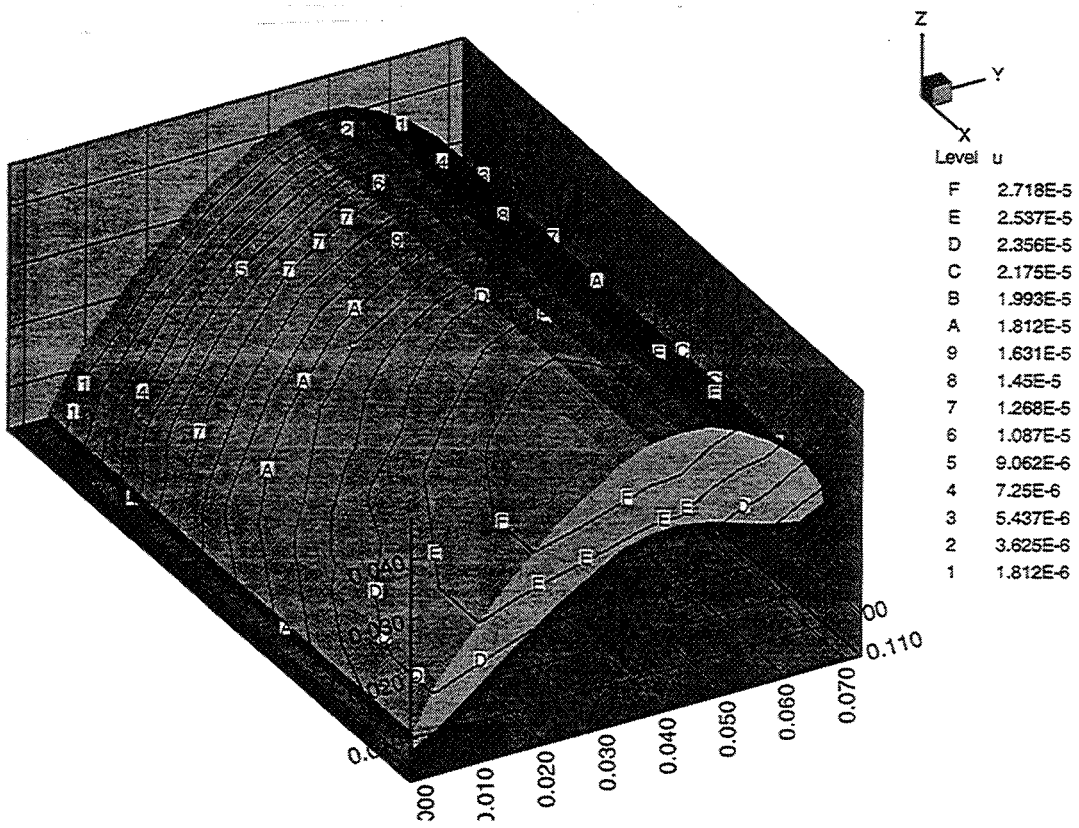

Figure 2: Axial displacements(u) in meters.

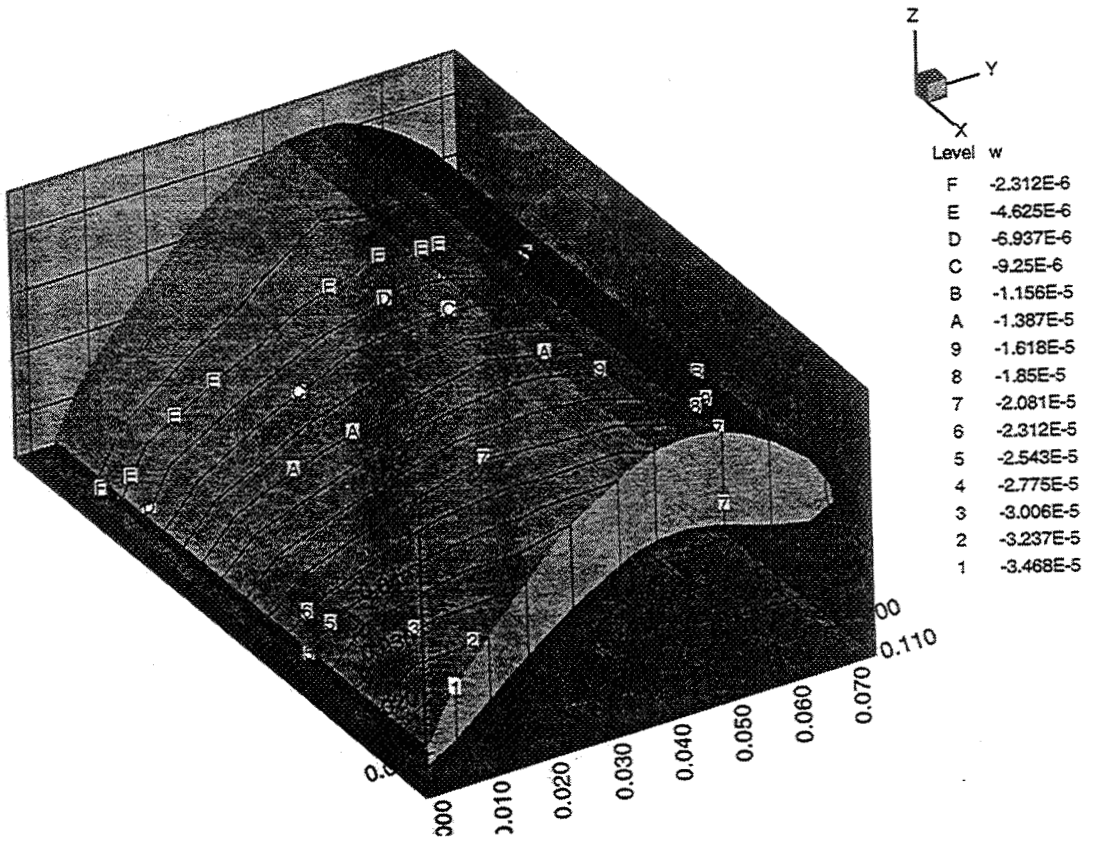

Figure 3: Transverse displacements(w) in meters.

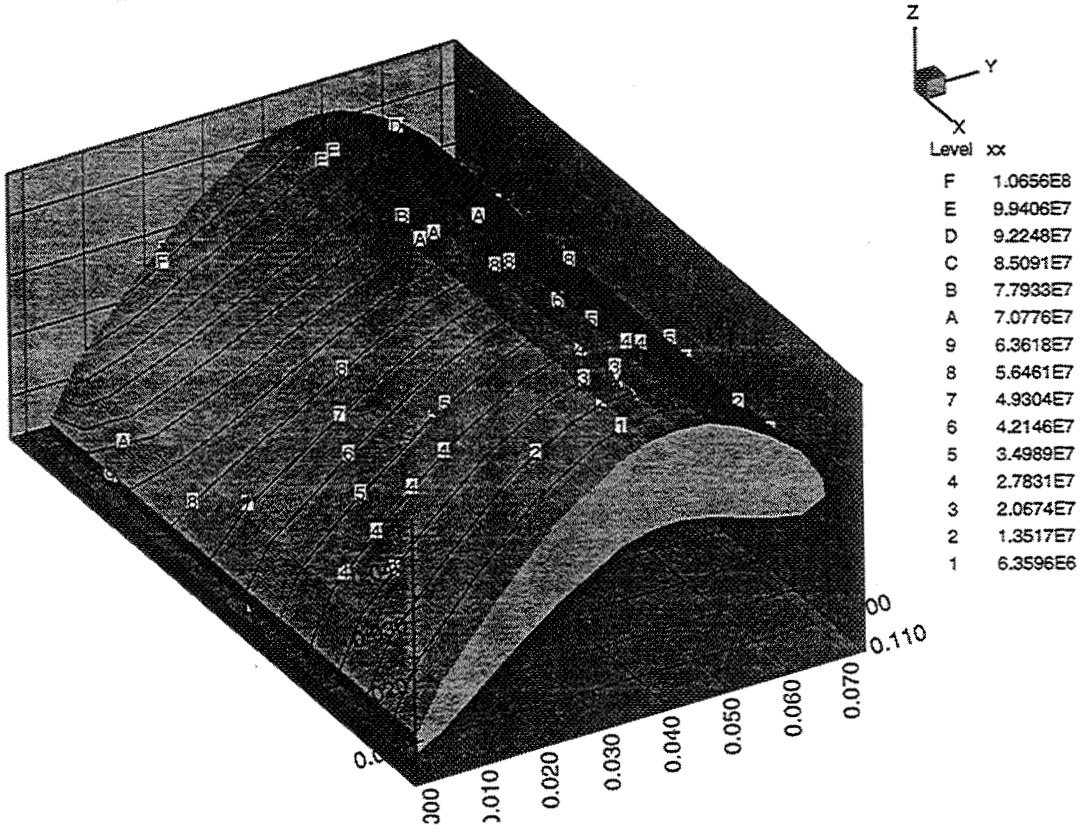

Figure 4: Axial stress(xx) in Pa.

GROUP DISCUSSION - December 12, 1996

SESSION III. COOLANT FLOW INTEGRATION AND OPTIMIZATION

Bob Simoneau - Facilitator Jim Heidmann - Scribe

Nirm Nirmalan to give review of work at Allison.

Peer Review by industry told NASA to take a leadership in interdisciplinary/ multidisciplinary design analysis methods - a system that couples the internal cooling system through the film cooling holes to the external aerodynamics (1993).

Industry was telling NASA to "stay out of" industry design systems, but to provide tools.

Early work used quasi, 3D, invicid programs (TSONIC) on the external side and network nodal analysis with correlations on the inside.

Bob Simoneau knows of no system to tie the whole problem together.

Joel Wagner

People still use meanlines and streamlines to correlate results. There is a blurring of the lines between primary and secondary flow paths. He doesn't see 3D driving the design, but inputting information.

Rob Norton

Need to look at effect of variations in shapes of pedestals, pins, etc. to study sensitivity to small changes in manufacturing tolerances. Look at trade-offs.

Nirm Nirmalan

Allison - cost modeling of airfoils. Designer should be able to estimate cost of design early in design process. Most cost is decided in early design - detailed design has only a small influence. Would like to put this info into design codes. Get data from experimental cascades, etc. Getting heat transfer designer to think about manufacturing (especially casting) is difficult.

Bob Simoneau

Asked if thermal design is equally important to aero in design?

Bob Bergholz

Seeing less emphasis on narrow specialization, particularly in gas path - aero designer considers heat load. "Aerothermal" is becoming unified. More of this in future.

Rob Norton

Agrees with above point. Need to look strongly at manufacturing because that is where the big costs are.

Boris Glezer

"Inter-discipline" is key word. Small companies learned this early. EPS showing more signs of interaction in industry: e.g. endwall cooling, combustion interaction, materials, and cooling penalties (discharging air requires full engine testing). Working with universities.

Bob Bergholz

Manufacturing - more tools that can demonstrate real payoff - "Can we build it?" Quantitative answers. Casting technology has improved through identified payoffs. More willing to invest in a process if there is an identified payoff.

Nirm Nirmalan

Manufacturing is very uncertain process. Payoff - difficult to identify low NO_x payoff.

Ed North

Dollar value on NO_x - it's a "go - no go" value. No compromises! It can't meet NO_x standards, you can't fly. Limited by flame temperature.

Bob Simoneau

Steady increase in industry use of CFD for design decisions. We are pushing the envelope, lower tolerances - is that the right direction? What about fidelity and resolution on the big scale?

Ron Bunker

When marketing a power turbine with a combined cycle efficiency of 60%, reaching the goal efficiency is highly important.

Bob Simoneau

So high fidelity resolution on the big scale is important, right?

Ron Bunker

Yes, integrating aerodynamics, heat transfer, performance, mechanical, life, materials, and manufacturing are all important; especially, in steam power turbines.

Rob Norton

Question for Yong Kim - Did you compare heat transfer predictions? Answer - No, because of tetrahedral elements, but I'm waiting for future improvements in resolution.

Bob Simoneau

Have we run out of ideas?

Bud Lakshminarayana

New data coming from Europe - detailed measurements of FC effectiveness. We should utilize this data. Need to simulate Re, M, Ro, curvature, etc. All have effect on film cooling. CFD is bringing Aero and HT committees together. Aerodynamics, manufacturing, and life coming together have a long way to go! 3D, Coriolis effects need to be looked at. Need coupled plenum, hole, external flow computations to develop models. More experiments in rotating rig. What about Wisler's rig at GE? It's not being used for film cooling.

Dave Rigby

Why don't we look at slots or wide holes approaching slots? Less lift-off.

Boris Glezer

Structural problem - trailing edge to approach this geometry - it may be possible on pressure or suction side. Easy if a simple shape.

Luzeng Zhang

Limited cooling air - constrained in spanwise direction. Round hole acts as a meter - a slot would not. Laser cannot drill slot.

Nirm Nirmalan

Manufacturing process matters - Allison casts holes - slots may be better in a cast blade, but it depends on the initial manufacturing process, which is decided by the Aero preliminary design.

Ed North

Endwall cooling - don't have high pattern factors in steam turbines - endwalls are difficult to cool. Need cooperation with aircraft engine designer. Can't afford empirical endwall cooling - need to be smart.

Boris Glezer

On board:

Heat Transfer occupies a region inside
a triangle whose vertices are:
$/HP, Efficiency, and Life.

"Interdisciplinary"

J. C. Han

Endwall cooling - would linear cascade be sufficient? (to Ed North)

Ed North

Need to talk to aerodynamicist.

Luzeng Zhang

Can get some info. with 2D cascade since endwall is 3D, but not all.

Bud Lakshminarayana

RAE has some data on endwall cooling - cascade must have right velocity profile entering - can't simulate rotor endwall flow in cascade due to rotation, but can simulate stator - Bob B. agrees. Does industry have concepts which will do away with film cooling?

Ed North

Closed loop cooling is coming for industrial turbines (for ground power) along with combined cycle efficiency improvements. Thermal barrier coatings need to be viable for long periods of time. CLC is secret to high performance - no film cooling - difficult, but rewards are high.

Luzeng Zhang

We aren't "looking for" film cooling - sometimes we "need" film cooling. They are necessities.

Bob Bergholz

Heat flux reduction is critical. Don't look at max. temp. - gradients are important. FC controls heat flux in blade. A high performance FC design may be bad due to thermal gradients. How to control heat flux in part.

Bob Simoneau

Good points on what is important in experiments - not much discussion on integration. Why?

J. C. Han

It is important, but very difficult to specify appropriate external conditions. Need "real" turbine passage for rotating film cooling. These are very difficult experiments, but you need integration between the FC and inside supply flow for reliable results.

Bob Simoneau

We agree that it is important, then.

Yung Kim

Problem is formidable. Codes require a lot of issues - network problem - don't have good database for film cooling discharge coef., need each problem to be subroutine for integration of parts.

Joe Gladden

ASU and PSU are working on optimization programs. We may optimize to zero coolant.

Ray Gaugler

Thanks to all of you for participating in this Workshop and to OAI (especially Karen Balog) for hosting it.

Adjourn.

Registered Attendees

(Did not attend*)

Coolant Flow Management Workshop
December 12-13, 1996

(Work phone listed first)
(FAX No. listed second)

Abhari, Reza*
Ohio State University
Gas Turbine Laboratory
2300 West Case Road
Columbus, OH 43235
(614) 292-5524 or 8453
(614) 292-5552
abhari.1@osu.edu

Acharya, Sumanta
Louisiana State University
Mechanical Engineering Department
Baton Rouge, LA 70803
(504) 388-5809
(504) 388-5924
acharya@ me.lsu.edu

Ameri, Ali
AYT
Mail Stop 5-11
21000 Brookpark Road
Cleveland, OH 44135
(216) 433-8346
(216) 433-5802
ameri@lerc.nasa.gov

Ames, Forrest
Allison Engine Company
P.O. Box 420/SC T10B
Indianapolis, IN 46206-0420
(317) 230-2476
(317) 230-6514
iefea@agt.gmeds.com

Ashpis, David
NASA Lewis Research Center
21000 Brookpark Road
Mail Stop 5-11
Cleveland, OH 44135
(216) 433-8317
(216) 433-5802
ashpis@lerc.nasa.gov

Bergholz, Bob
General Electric Aircraft Engines
One Neumann Way
Cincinnati, OH 45215-6301
(513) 243-7332
(513) 243-0971
robert.f.bergholz@ae.ge.com

Boyle, Bob
NASA Lewis Research Center
21000 Brookpark Road
Mail Stop 5-11
Cleveland, OH 44135
(216) 433-5889
(216) 433-5802
aeboyle@lerc.nasa.gov

Bui, Trong
M.S. 5-11
21000 Brookpark Road
NASA Lewis Research Center
Cleveland, OH 44135
(216) 433-5639
(216) 433-5802
bui@lerc.nasa.gov

Bunker, Ron
General Electric Company
Corporate Research and Development
P.O. Box 8
Schenectady, NY 12301
(518) 387-5086
(518) 387-7258
bunker@crd.ge.com

Chima, Rod
NASA Lewis Research Center
Mail Stop 77-6
21000 Brookpark Road
Cleveland, OH 44135
(216) 433-5919
(216) 433-3918
fsrod@lerc.nasa.gov

Chyu, Ming-King
Carnegie Mellon University
Department of Mechanical Engineering
Schenly Park
Pittsburgh, PA 15213-3890
(412) 268-3658
(412) 268-3348
mc47@andrew.cmu.edu

Civinskas, Kaz
NASA Lewis Research Center
21000 Brookpark Road
Mail Stop 77-6
Cleveland, OH 44135
(216) 433-5890
(216) 433-3918
kestutis.c.civinskas@lerc.nasa.gov

Dulikravich, George*
Penn State University
Department of Aerospace Engineering
233 Hammon
University Park, PA 16802
(814) 863-0134
(814) 865-7092
gsd@ecL.psu.edu

Dutta, Sandip
University of South Carolina
300 Main Street/Mechanical Engr.
Columbia, SC 29205
(803) 777-8013
(803) 777-0106
dutta@engr.engr.sc.edu

Fant, Daniel
Clemson University
South Carolina Energy R&D Center
386-2 College Avenue
Clemson, SC 29634-5180
(864) 656-2267
(864) 656-0142
dfant@clemson.edu

Foss, Judith
NASA Lewis Research Center
Mail Stop 5-11
21000 Brookpark Road
Cleveland, OH 44135
(216) 433-3587
(216) 433-5802
judith.k.foss@lerc.nasa.gov

Garg, Vijay
AYT
Mail Stop 5-11
21000 Brookpark Road
Cleveland, OH 44135
(216) 433-6788
(216) 433-5802
fsgarg@oz.lerc.nasa.gov

Gaugler, Ray
NASA Lewis Research Center
21000 Brookpark Road
Mail Stop 5-11
Cleveland OH 44135
(216) 433-5882
(216) 433-5802
raymond.e.gaugler@lerc.nasa.gov

Giel, Paul
NYMA Inc.
Mail Stop NYMA
3000 Aerospace Parkway
Brook Park, OH 44142
(216) 977-1340
(216) 977-1269
pwgiel@lerc.nasa.gov

Gladden, Joseph (retired)
NASA Lewis Research Center
21000 Brookpark Road
Mail Stop 5-11
Cleveland, OH 44135

Glezer, Boris
Solar Turbines Inc.
2200 Pacific Hwy
San Diego, CA 92101
(619) 544-5454
(619) 544-2682

Gorla, Rama
Cleveland State University
Department of Mechanical Engineering
1960 E. 24th Street
Cleveland, OH 44115
(216) 523-7276

Hale, Charles
Purdue University
1288 Mechanical Engineering
West Lafayette, IN 47907-1288
(317) 494-1540
(317) 494-0530
chale@ecn.purdue.edu

Han, J. C.
Texas A&M University
Dept of Mechanical Engineering
College Station, TX 77843-3123
(409) 845-3738
(409) 862-2418
jch2187@acs.tamu.edu

Heidmann, James
NASA Lewis Research Center
21000 Brookpark Road
Mail Stop 77-6
Cleveland, OH 44135
(216) 433-3604
(216) 433-3918
toheid@hoops.lerc.nasa.gov

Hendricks, Robert
NASA Lewis Research Center
21000 Brookpark Road
Mail Stop 301-5
Cleveland, OH 44135
(216) 977-7507
(216) 977-7500
robert.c.hendricks@lerc.nasa.gov

Hippensteele, Steven
NASA Lewis Research Center
21000 Brookpark Road
Mail Stop 5-11
Cleveland, OH 44135
(216) 433-5897
(216) 433-5802
steven.a.hippensteele@lerc.nasa.gov

Ibrahim, Mounir
Cleveland State University
Department of Mechanical Engineering
1960 E. 24th Street
Cleveland, OH 44115
(216) 687-2580
(216) 687-9280
ibrahim@csvaxe.csuohio.edu

Kao, Kai-Hsiung
Ohio Aerospace Institute/ICOMP
Mail Stop 5-11
21000 Brookpark Road
Cleveland, OH 44135
(216) 433-2432
(216) 433-5802
fskao@figment.lerc.nasa.gov

Kim, Chan
NASA Lewis Research Center
21000 Brookpark Road
Mail Stop 77-6
Cleveland, OH 44135
(216) 433-8715
(216) 433-3918
tokim@prostar.lerc.nasa.gov

Kim, Yong
AlliedSignal Engines
Dept 93-32 MS 301-120
P. O. Box 52181
111 S. 34th Street
Phoenix, AZ 85072-2181
(602) 231-2166
(602) 231-3018
ywkim.phx@alliedsignal.com

Kohler, Steven (day 2)*
Rolls-Royce
c/o Westinghouse Electric Corp.
4400 Alafaya Trail MC205
Orlando, FL 32826-2399
(407) 249-7536
(407) 281-5633

Kwon, Okey
Allison Advanced Development Co.
P.O. Box 7162
Speed Code X13
Indianapolis, IN 46206-7162
(317) 230-4954
(317) 230-3009
ieokk@agt.gmeds.com

Lakshminarayana, B.
Penn State University
Department of Aerospace Engineering
233 Hammon
University Park, PA 16802
(814) 865-5551
(814) 865-7092
b1Laer@engr.psu.edu

Lau, Sai
Texas A&M University
Dept of Mechanical Engineering
College Station, TX 77843-3123
(409) 845-0171
(409) 862-2418
slau@mengr.tamu.edu

Ligrani, Phillip
University of Utah
Department of Mechanical Engineering
MEB 3209
Salt Lake City, UT 84112
(801) 581-4240
(801) 585-9826
ligrani@stress.mech.utah.edu

Liou, William
Ohio Aerospace Institute/ICOMP
Mail Stop OAI
22800 Cedar Point Road
Cleveland, OH 44142
(216) 962-3152
(216) 962-3200
fswwl@icomp01.lerc.nasa.gov

Lucci, Barb
NASA Lewis Research Center
21000 Brookpark Road
Mail Stop 5-11
Cleveland, OH 44135
(216) 433-5902
(216) 433-5802
Lucci@cw22.lerc.nasa.gov

Makki, Younes
Williams International
2280 West Maple Road
Walled Lake, MI 48088
(810) 624-5200 x1884
(810) 669-1577

Mockler, Ted
NASA Lewis Research Center
21000 Brookpark Road
Mail Stop 77-2
Cleveland, OH 44135
(216) 977-7057
(216) 977-7008
mockler@lerc.nasa.gov

Nenni, Joseph
NYMA Inc.
2001 Aerospace Parkway
Brook Park, OH 44142
(216) 977-1339

Nirmalan, Nirm
Allison Engine Company
P.O. Box 420/SC W16
Indianapolis, IN 46206-0420
(317) 230-3052
(317) 230-5600
ievn0@agt.gmeds.com

North, Ed
Westinghouse Electric Corp.
4400 Alafaya Trail MC205
Orlando, FL 32826-2399
(407) 281-2477
(407) 281-5633
north.we@wec.com

Norton, Robert
Allison Engine Company
P.O. Box 420/SC T10B
Indianapolis, IN 46206-0420
(317) 230-3725
(317) 230-6514
aerjn@agt.gmeds.com

Plesniak, Michael
Purdue University
Mechanical Engineering
West Lafeyette, IN 47907-1288
(317) 494-1537
(317) 494-0530
plesniak@ecn.purdue.edu

Poinsatte, Phil
NASA Lewis Research Center
21000 Brookpark Road
Mail Stop 5-11
Cleveland, OH 44135
(216) 433-5898
(216) 433-5802
poinsatte@lerc.nasa.gov

Poulos, Earnest
Cleveland State University
24th and Euclid Avenue
Cleveland, OH 44115
(216) 687-2406

Ramadhyani, Satish
Purdue University
1288 Mechanical Engineering
West Layfayette, IN 47907-1288
(317) 494-5701
(317) 494-0530
ramadhy@ecn.purdue.edu

Reddy, D. R.
NASA Lewis Research Center
21000 Brookpark Road
Mail Stop 5-11
Cleveland, OH 44135
(216) 433-8133
(216) 433-5802
dreddy@lerc.nasa.gov

Rigby, David
NYMA, Inc.
Mail Stop NYMA
3000 Aerospace Parkway
Brook Park, OH 44142
(216) 433-5416
(216) 433-5802
rigby@lerc.nasa.gov

Rohde, John
NASA Lewis Research Center
21000 Brookpark Road
Mail Stop 11-3
Cleveland, OH 44135
(216) 433-3949
(216) 433-5100
j.rohde@lerc.nasa.gov

Shih, Tom
Carnegie Mellon University
Department of Mechanical Engineering
Schenly Park
Pittsburgh, PA 15213-3890
(412) 268-2503
(412) 268-3348
ts2k@andrew.cmu.edu

Simon, Fred (retired)
NASA Lewis Research Center
21000 Brookpark Road
Mail Stop 5-11
Cleveland, OH 44135

Simon, Terry
University of Minnesota
Mechanical Engineering Department
111 Church Street SE
Minneapolis, MN 55455-0111
(612) 625-5831
(612) 624-5230
tsimon@me.umn.edu

Simoneau, Robert
Carnegie Mellon University
Department of Mechanical Engineering
Schenly Park
Pittsburgh, PA 15213-3890
(412) 268-1108
(412) 268-3348
simoneau@andrew.cmu.edu

Sirbaugh, James
NYMA, Inc.
2001 Aerospace Parkway
Brook Park, OH 44142
(216) 433-8653
(216) 433-2184
tosirb@dumbo.lerc.nasa.gov

Steinthorsson, Erlendur
17325 Euclid Avenue
Cleveland, OH 44112-1290
(216) 531-3000, ext. 2442
(216) 531-0038
esteinthorsson@parker.com

Thole, Karen
University of Wisconsin
Mechanical Engineering Department
1513 University
Madison, WI 53706-1572
(608) 262-0923
(608) 265-2316
thole@engr.wisc.edu

Thurman, Doug
NASA Lewis Research Center
21000 Brookpark Road
Mail Stop 5-11
Cleveland, OH 44135
(216) 433-6573
(216) 433-5802
drthurman@lerc.nasa.gov

Tse, David
Scientific Research Associates Inc.
P.O. Box 498
Glastonbury, CT 06033
(860) 659-0333 x227
(860) 633-0676
dgt@mach4.srai.com

VanFossen, James
NASA Lewis Research Center
21000 Brookpark Road
Mail Stop 5-11
Cleveland, OH 44135
(216) 433-5892
(216) 433-5802
jvanfossen@lerc.nasa.gov

VanOverbeke, Thomas
NASA Lewis Research Center
Mail Stop 5-11
21000 Brookpark Road
Cleveland, OH 44135
(216) 433-5867
(216) 433-5802
aevano@thesis.lerc.nasa.gov

Wagner, Joel
United Technologies Research Center
Silver Lane
East Hartford, CT 06108
(860) 610-7151
(860) 610-7656
wagnerjh@utrc.utc.com

Wang, Chi-Rong
NASA Lewis Research Center
21000 Brookpark Road
Mail Stop 5-11
Cleveland, OH 44135
(216) 433-5865
(216) 433-5802
aewang@nexus.lerc.nasa.gov

Zaman, Khairul
NASA Lewis Research Center
Mail Stop 5-11
21000 Brookpark Road
Cleveland, OH 44135
(216) 433-5888
(216) 433-5802
khairul.b.zaman@lerc.nasa.gov

Zhang, Luzeng
Solar Turbines Inc.
2200 Pacific Hwy
San Diego, CA 92101
(619) 544-5928
(619) 544-2682

REPORT DOCUMENTATION PAGE

Form Approved
OMB No. 0704-0188

1. AGENCY USE ONLY (*Leave blank*)	2. REPORT DATE	3. REPORT TYPE AND DATES COVERED
	August 1997	Conference Publication

4. TITLE AND SUBTITLE

1996 Coolant Flow Managment Workshop

5. FUNDING NUMBERS

WU–523–26–13

6. AUTHOR(S)

7. PERFORMING ORGANIZATION NAME(S) AND ADDRESS(ES)

National Aeronautics and Space Administration
Lewis Research Center
Cleveland, Ohio 44135–3191

8. PERFORMING ORGANIZATION REPORT NUMBER

E–10761

9. SPONSORING/MONITORING AGENCY NAME(S) AND ADDRESS(ES)

National Aeronautics and Space Administration
Washington, DC 20546–0001

10. SPONSORING/MONITORING AGENCY REPORT NUMBER

NASA CP–10195

11. SUPPLEMENTARY NOTES

Responsible person, Steven A. Hippensteele, organization code 5820, (216) 433–5897.

12a. DISTRIBUTION/AVAILABILITY STATEMENT

Unclassified - Unlimited
Subject Category 34

This publication is available from the NASA Center for AeroSpace Information, (301) 621–0390.

12b. DISTRIBUTION CODE

13. ABSTRACT ***(Maximum 200 words)***

The following compilation of documents includes a list of the 66 attendees, a copy of the viewgraphs presented, and a summary of the discussions held after each session at the 1996 Coolant Flow Management Workshop held at the Ohio Aerospace Institute, adjacent to the NASA Lewis Research Center, Cleveland, Ohio on December 12–13, 1996. The workshop was organized by H. Joseph Gladden and Steven A. Hippensteele of NASA Lewis Research Center. Participants in this workshop included Coolant Flow Management team members from NASA Lewis, their support service contractors, the turbine engine companies, and the universities. The participants were involved with research projects, contracts and grants relating to: (1) details of turbine internal passages, (2) computational film cooling capabilities, and (3) the effects of heat transfer on both sides. The purpose of the workshop was to assemble the team members, along with others who work in gas turbine cooling research, to discuss needed research and recommend approaches that can be incorporated into the Center's Coolant Flow Management program. The workshop was divided into three sessions: (I) Internal Coolant Passage Presentations, (II) Film Cooling Presentations, and (III) Coolant Flow Integration and Optimization. Following each session there was a group discussion period.

14. SUBJECT TERMS	15. NUMBER OF PAGES
Turbine cooling; Film cooling; Convection cooling; Serpentine passage; Rotation; Heat transfer; Turbulence; Turbomachinery; Gas turbine engine; Experimental; CFD (Computational Fluid Dynamics) Codes	353
	16. PRICE CODE: A16

17. SECURITY CLASSIFICATION OF REPORT	18. SECURITY CLASSIFICATION OF THIS PAGE	19. SECURITY CLASSIFICATION OF ABSTRACT	20. LIMITATION OF ABSTRACT
Unclassified	Unclassified	Unclassified	